LA-11735-MS

Bowen 1990

Elio 6899

Los Alamos Climatology

IS-4 REPORT SECTION

REPRODUCTION COPY

C.3

3 9338 00321 2023

7301

Cover design by Ruth E. Holt, Group IS-12

LA-11735-MS

UC-902
Issued: May 1990

Los Alamos Climatology

Brent M. Bowen

3 9338 00321 2023

Los Alamos National Laboratory
Los Alamos, New Mexico 87545

Los Alamos Climatology

by

Brent M. Bowen

Technical Assistance	**William A. Olsen and I-li Chen**
Editorial Assistance	**Beverly Talley**
Composition	**Kathy Derouin**

Contents

Preface xiii
Acknowledgments xv
Abstract xvii

1 Introduction 1

1.1 Background 1
1.1.1 Geography 1
1.1.2 Large-Scale Atmospheric Flow 2
1.2 Los Alamos Climatology Summary 3
1.2.1 Temperature 3
1.2.2 Precipitation 5
1.2.3 Surface Winds 8
1.2.4 Humidity 10
1.2.5 Insolation (Sunshine) 10
1.2.6 Severe Storms 11
1.2.7 Atmospheric Pressure 11
1.2.8 Atmospheric Dispersion 12
1.3 Observation Network 13
1.4 Meteorological Units of Measurement 13

2 Surface Air Temperatures and Moisture Content 15

2.1 Monthly Mean Temperatures 15
2.2 New Mexico Monthly Mean Temperatures 16
2.3 Hourly Temperatures and Humidity 17
2.4 Temperature Probabilities 48
2.5 Design Temperatures 49
2.6 Vertical Temperature Profiles 49
2.7 Degree Days 52
2.7.1 Heating-Degree Days 52
2.7.2 Cooling-Degree Days 53
2.8 Growing-Season Data 59
2.9 Freeze-Thaw Data 66
2.10 Apparent and Wind-Chill-Equivalent Temperatures 68
2.11 Daily Mean High and Low Temperatures 71

3 Precipitation, Including Snowfall 75

3.1 Precipitation 75
3.1.1 Monthly Precipitation Means 75
3.1.2 Hourly Precipitation Means and Frequencies 76
3.1.3 Precipitation Probabilities 77
3.1.4 Specified Daily Precipitation Amounts 77
3.1.5 Precipitation Network Data 77
3.2 Snowfall 80

3.2.1 Monthly Snowfall Means 80
3.2.2 Monthly Snowfall Probabilities 85
3.2.3 Specified Daily Snowfall Amounts 86

4 Wind **89**

4.1 Wind Roses 89
4.2 Mean Wind-Direction Frequencies and Wind Speeds 93

5 Atmospheric Pressure **123**

5.1 Monthly and Daily Pressure 123
5.2 Los Alamos Pressure Adjustment 125
5.3 Hourly Pressure 126
5.4 Air Density 127
5.5 Atmospheric Composition 128

6 Insolation (Sunshine) **131**

6.1 Monthly Insolation 131
6.2 Hourly Insolation 133
6.3 Sunrise, Sunset, and Twilight 133
6.3.1 Sunrise and Sunset 133
6.3.2 Twilight 135

7 Other Weather Phenomena **139**

7.1 Tornadoes and Dust Devils 139
7.2 Thunderstorms, Lightning, and Hail 139
7.3 Floods 140
7.4 Winter Storms 141
7.5 Ice 141
7.6 Heavy Snow Loading 141
7.7 Wind 142
7.8 Dust, Haze, and Smoke 142
7.9 Fog 143
7.10 Drought 143
7.11 Heat Waves 144
7.12 Cold Waves 144
7.13 Optical Phenomena 145

8 Historical Climate Trends **147**

8.1 Los Alamos 147
8.2 White Rock 151

9 Extremes 153

9.1 Extreme Value Analysis 153
9.1.1 Precipitation 154
9.1.2 Snowfall 156
9.1.3 Maximum Wind Gusts 157
9.1.4 Minimum Temperatures 158
9.2 Daily Weather Extremes 160

10 Turbulence and Dispersion 173

10.1 Turbulence (by Wind Direction) 173
10.2 Vertical Profiles of σ_θ and σ_ϕ 176
10.3 Dispersion 179
10.4 Comparison of Stability Class Methods 181

11 Wind Persistence 187

11.1 Wind-Speed Persistence 187
11.1.1 Explanation 187
11.1.2 Discussion 192
11.1.3 Persistence Tables 196
11.2 Wind-Direction Persistence 196
11.2.1 Explanation 196
11.2.2 Discussion 198
11.2.3 Persistence Tables 204

Appendixes 207

A Historical Locations of Weather Stations 207
B Future Plans 209
C Data Quality and Accuracy 211
D Unit Conversion Factors 215
E Psychometric Charts 227
F Wind-Chill-Equivalent Temperature Charts 231

Glossary 233

References 253

Figures

1.1 Regional location of Los Alamos 1
1.2 Aerial view looking west across the Pajarito Plateau toward the Jemez Mountains 2
1.3 Los Alamos normal weather (monthly temperature, precipitation, and snowfall) 4
1.4 Regional up-valley and down-valley winds 9
1.5 Map showing meteorological tower locations and site numbers 14

2.1 Monthly mean maximum and minimum temperatures at Los Alamos and White Rock 15
2.2–2.15 New Mexico locator map and temperature maps showing monthly and annual mean temperatures in New Mexico 19
2.16 Hourly mean temperatures, relative humidity, and wet-bulb and dew-point temperatures for January, April, July, and October 34
2.17 Mean temperature vertical profiles for January, April, July, and October 54
2.18, 2.19 Annual mean heating-degree and cooling-degree days in New Mexico 60

3.1 Los Alamos and White Rock monthly mean precipitation 75
3.2 Hourly precipitation amounts and frequencies at three sites (TA-59, East Gate, and Area G) during January, June, July, and August 78
3.3 Summer and annual mean precipitation at Los Alamos 84
3.4 Los Alamos monthly normal snowfall 85

4.1 Annual day, night, and total wind roses at Los Alamos 90
4.2–4.5 Day and night wind roses at Los Alamos for January, April, July, and October 94
4.6–4.9 Total wind roses at Los Alamos for January, April, July, and October 102
4.10–4.13 Day, night, and total wind roses at TA-59 for January, April, July, and October 107
4.14 Annual (1980–1987) day, night, and total wind roses at TA-59 111
4.15–4.18 Hourly wind-direction frequencies and mean wind speeds at TA-50, East Gate, and Area G for January, April, July, and October 112
4.19 Hourly wind-direction frequencies and mean wind speeds at TA-59 for January, April, July, and October 120

5.1 Monthly mean atmospheric pressure at Los Alamos 123
5.2 Hourly mean atmospheric pressure at Los Alamos during January, April, July, and October 126

6.1 Daily mean and maximum possible insolation at TA-59 and Area G, plotted by month 132
6.2 Hourly mean and maximum possible insolation at TA-59 and Area G for January, April, July, and October 134

7.1 Monthly normal thunderstorm days at Los Alamos....140
7.2 Monthly mean number of fog days at Los Alamos over a 27-year period....143

8.1 Los Alamos historical annual mean temperatures....147
8.2 Los Alamos historical annual precipitation....147
8.3 Los Alamos historical seasonal snowfall....148

9.1 Annual extreme precipitation analyses for Los Alamos and White Rock....153
9.2 Daily extreme precipitation values for Los Alamos and White Rock....154
9.3, 9.4 Shorter-period extreme precipitation values for Los Alamos (TA-59) and Area G (TA-54)....155
9.5 Seasonal extreme snowfall analyses for Los Alamos....157
9.6 Monthly and daily extreme snowfall values for Los Alamos....158
9.7 Extreme snow-depth values for Los Alamos....159
9.8 Extreme instantaneous wind-gust values for Los Alamos....159
9.9 Extreme minimum-temperature values for Los Alamos and White Rock....160

10.1 Horizontal wind-direction standard deviation (15-minute-averaged σ_θ) at TA-59 and Area G....174
10.2 Vertical wind-direction standard deviation (15-minute-averaged σ_ϕ) at TA-59 and Area G....175
10.3 Vertical profiles of σ_ϕ and σ_θ at TA-50 for different stability categories....177
10.4 Vertical profiles of wind speeds at TA-50 for different stability categories....178
10.5 Calculated horizontal- and vertical-dispersion coefficients (σ_y,σ_z) based on TA-50 values....182

11.1 Winter and summer persistence probabilities at TA-59 of wind-speed classes by directional quadrant....188
11.2 Winter and summer persistence probabilities at Area G of wind-speed classes by directional quadrant....190
11.3 Winter and summer persistence probabilities at TA-50 of wind-speed classes by directional quadrant....192
11.4 Winter and summer persistence probabilities at TA-59 of wind directions ±1 direction....198
11.5 Winter and summer persistence probabilities at Area G of wind directions ±1 direction....200
11.6 Winter and summer persistence probabilities at TA-50 of wind directions ±1 direction....202

Tables

1.1 Normals, means, and extremes (1911–1988) 6
1.2 Sites and meteorological data 14

2.1 Monthly mean temperatures at Los Alamos and White Rock 16
2.2 Site listing for New Mexico locator map (Fig. 2.2) 18
2.3–2.14 Tables for January through December, showing hourly temperature, wet-bulb temperature, and relative humidity, with dew point, mixing ratio, and absolute humidity given for every 3 hours 36
2.15, 2.16 Los Alamos and White Rock temperature probabilities 50
2.17 Winter and summer design temperatures at TA-59 and Area G 52
2.18, 2.19 Los Alamos and White Rock monthly heating-degree days for various temperature bases (°F) 56
2.20, 2.21 Los Alamos and White Rock monthly heating-degree days for 65°F temperature base 58
2.22, 2.23 Los Alamos and White Rock monthly cooling-degree days for various temperature bases (°F) 62
2.24, 2.25 Los Alamos and White Rock monthly cooling-degree days for 65°F temperature base 64
2.26, 2.27 Los Alamos and White Rock growing-season data 66
2.28, 2.29 Los Alamos and White Rock freeze-thaw days 68
2.30, 2.31 July and January extreme and mean apparent temperatures at Los Alamos 70
2.32 January extreme and mean wind-chill-equivalent temperatures at Los Alamos 71
2.33, 2.34 Los Alamos and White Rock daily mean high and low temperatures 72

3.1 Los Alamos and White Rock monthly and annual precipitation means and medians 75
3.2, 3.3 Los Alamos and White Rock precipitation probabilities 80
3.4, 3.5 Los Alamos and White Rock mean number of days of precipitation for specified amounts, maximum number of days in which precipitation exceeded the specified amount, and latest year the maximum occurred 82
3.6 Los Alamos monthly and annual snowfall means and medians 85
3.7 Los Alamos snowfall probabilities 86
3.8 Los Alamos mean number of days of snowfall for specified amounts, maximum number of days in which snowfall exceeded the specified amount, and latest year maximum occurred 87

5.1 Monthly atmospheric pressure, means, and extremes 124
5.2 Monthly mean atmospheric density at Los Alamos 128
5.3 Proportions of gases composing dry air in lower atmosphere (up to 80 km) 129

6.1 Monthly insolation statistics 133
6.2 Los Alamos sunrise and sunset times and twilight durations 136

8.1 Los Alamos annual mean temperatures, precipitation, snowfall, and seasonal snowfall 150
8.2 Los Alamos annual temperature, precipitation, snowfall, and seasonal snowfall statistics 151
8.3 White Rock annual mean temperatures and precipitation 152

9.1 Precipitation for various return periods and time periods at Los Alamos (TA-59) and Area G (TA-54)/White Rock 156
9.2–9.13 Los Alamos weather extremes for the months January through December 161

10.1 Estimation of Pasquill-Gifford (P-G) stability categories based on σ_ϕ ranges 176
10.2 Key to objective method used to determine P-G stability categories 183
10.3 Percentage of time of P-G–derived versus σ_ϕ–derived stability categories at Los Alamos (TA-59) 184
10.4 Percentage of time of P-G–derived versus σ_ϕ–derived stability categories at Area G 185

11.1, 11.2 Winter and summer wind-speed persistence 196
11.3 Wind-direction persistence for a single direction 204
11.4 Wind-direction persistence for a centered direction ±1 direction 205

A.1 Historical weather station locations (for temperature and precipitation) 208

D.1 Length conversion factors 216
D.2 Temperature, lapse rate, and atmospheric-pressure conversion factors 217
D.3 Energy (radiation) flux and energy per area conversion factors 218
D.4 Temperature conversion chart 219
D.5 Wind-speed conversion chart 220
D.6 Wind-direction conversion chart 221
D.7 Atmospheric-pressure conversion chart 222
D.8 Sea-level (adjusted to) atmospheric-pressure conversion chart 224
D.9 Vertical insolation flux (radiation flux) conversion chart 226

E.1 Relative humidity psychometric chart 228
E.2 Dew-point psychometric chart 229

F.1 Wind-chill-equivalent temperatures 232

Preface

This report was written for a wide audience of readers, from engineers and scientists to individuals just wanting to know about Los Alamos weather. For this reason, and because English units are still the standard in National Oceanic and Atmospheric Administration (NOAA) reporting and publications, familiar English units are primarily used in this report. In most tables and graphs, data are presented in English units, such as degrees Fahrenheit (°F), inches (in.), and miles per hour (mph). However, metric units, such as degrees Celsius (centigrade) (°C), centimeters (cm), and meters per second (m/s), are also displayed on second ordinates of most graphs. Only metric units are given for some variables, such as insolation and atmospheric density. In the sections on turbulence and wind persistence, wind speed is given in meters per second because this unit is standard in dispersion meteorology.

The Los Alamos National Laboratory's Environmental Protection Group (HSE-8) is responsible for monitoring effects of Laboratory operations on the environment. The Air Quality and Meteorology Section in HSE-8 is responsible for operating a meteorological monitoring network and providing guidance during a possible emergency response resulting from an atmospheric release of toxic pollutants. Meteorological data are also used for routine environmental assessment, Clean Air Act compliance, atmospheric-dispersion research, weather forecasting, and engineering design. The tower and monitoring network are maintained to fulfill U.S. Department of Energy (DOE) environmental guidelines (DOE Orders 5480.1 and 5400.xy) and U.S. Environmental Protection Agency (EPA) guidelines (On-Site Meteorological Program Guidance for Regulatory Modeling Applications).

Acknowledgments

I thank Bill Olsen (Environmental Protection Group, HSE-8), who, besides running the best meteorological network I have seen, helped review several drafts of this report and made many useful contributions. Thanks, also, to I-li Chen (A-1), who helped develop software for the meteorology program, and to Celeste Bender and Margaret Salazar for contributions in data analysis. Cindy Boone (IS-12) did an excellent job of creating and developing many of the illustrations. Eric Vigil (IS-12) also helped with graphics, and Joyce Martinez (IS-5) prepared tables in Appendix D. Gratitude is expressed to Jean Dewart (HSE-8) for reviewing this document and for her efforts in making the meteorology program a success, and to Greg Stone (SST-7) for reviewing the report and for his many comments and suggestions that helped strengthen the report.

Thomas C. Gunderson (Deputy Division Leader of the Health, Safety, and Environment Division) is credited with seeing the need for a climate report and assigning the task during his tenure as HSE-8 Group Leader in 1985. Special appreciation is expressed to Kenneth M. Hargis (HSE-8 Environmental Protection Group Leader) and Craig Eberhart (HSE-8 Air Quality and Meteorology Section Leader) for their support for completing the report.

Beverly Talley edited the report and is responsible for its readability and appearance, and Kathy Derouin deserves credit for the report's composition. Beverly and Kathy are important reasons why I am proud to be associated with this report.

Rainmaker*

First day in August, last rain was in May,
When the rainmaker came to Kansas,
In the middle of a dusty day.
The rainmaker said to the people,
"Tell me what you are prepared to pay,"
The rainmaker said to the people,
"Well, I'll conjure up a rain today."
Ninety degrees in the breeze where it's shady,
A hundred and ten in the hot sun,
Heat from the street burns the feet of the ladies . . . ,
See how they run.

Call down the lightnin' by a mystical name,
Then the rainmaker called on the thunder,
And suddenly it began to rain,
Then the rainmaker passed his hat to the people,
But the people all turned away,
Then the rainmaker's eyes and the Kansas skies,
Both became dark with rain.

First day in August, last rain was in May,
When the rainmaker came to Kansas,
In the middle of a dusty day.
The rainmaker smiled as he hitched up his wagon,
And without a word he rolled away,
And the people of the town at the sound of his laughter,
They knew the rain had come to stay.
Rain rain, go away, come again another day,
Rain, rain, go away, come again another day.
R a i n, r a i n, r a i n.

Harry Nilsson and Bill Martin

* © 1964 Tickson Music (BMI)/Unichappell Music (BMI).
Used by permission. All rights reserved.

Abstract

This report presents Los Alamos climate data and analyses of basic meteorological variables beginning in late 1910 and continuing into 1989. The first section summarizes Los Alamos climate. Temperature, humidity, and precipitation analyses are given in the next few sections, with daily temperature and precipitation records listed and analyzed from late 1910. More-detailed records of temperatures and humidity, as well as winds, pressure, insolation, and other weather phenomena, are analyzed and discussed in later sections for the years 1980–1988, followed by a section on historical climate trends in Los Alamos. The last part of the report is directed to readers desiring more technical information. One section is devoted to weather extremes, another presents climate records and variability, and two others deal with topics important in air-pollution meteorology: (1) dispersion, and (2) wind persistence and turbulence. The appendixes include a section on historical locations of weather stations, one on future plans of the Laboratory's Meteorology Section, and one on data quality and accuracy. Unit conversions and psychometric tables are listed in Appendixes D and E, followed by wind-chill-equivalent temperature charts in Appendix F. Finally, a glossary of weather terms is given at the end of the report.

1 Introduction

1.1 Background

1.1.1 Geography

The Los Alamos National Laboratory and the communities of Los Alamos and White Rock are located in Los Alamos County in north-central New Mexico. By air, the Laboratory is located approximately 60 miles (100 km) north-northeast of Albuquerque and 25 miles (40 km) northwest of Santa Fe (Fig. 1.1). Much of Los Alamos County is located on the Pajarito Plateau on the eastern flanks of the Jemez Mountains. The plateau slopes downward to the east-southeast, covering a distance of more than 15 miles (24 km) from the base of the Jemez Mountains (approximately 7800 ft [2380 m] above sea level [ASL]) to a location just above the Rio Grande River Valley (~6200 ft [1890 m] ASL). Numerous alternating "finger" mesas and canyons run along the plateau slope line (see Fig. 1.2). The canyons are 150–300 ft (46–91 m) deep and 300–600 ft (91–183 m) wide. The Sangre de Cristo Mountains lie nearly 40 miles (64 km) to the east. The Rio Grande Valley runs north-northeast to south-southwest between the two mountain ranges.

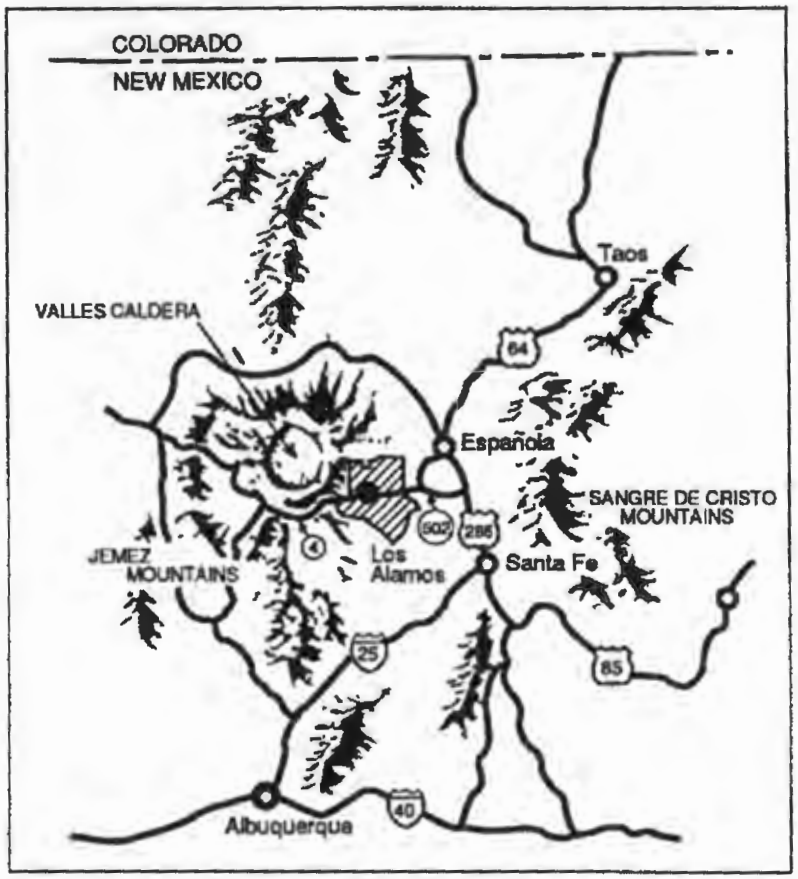

Fig. 1.1. Regional location of Los Alamos.

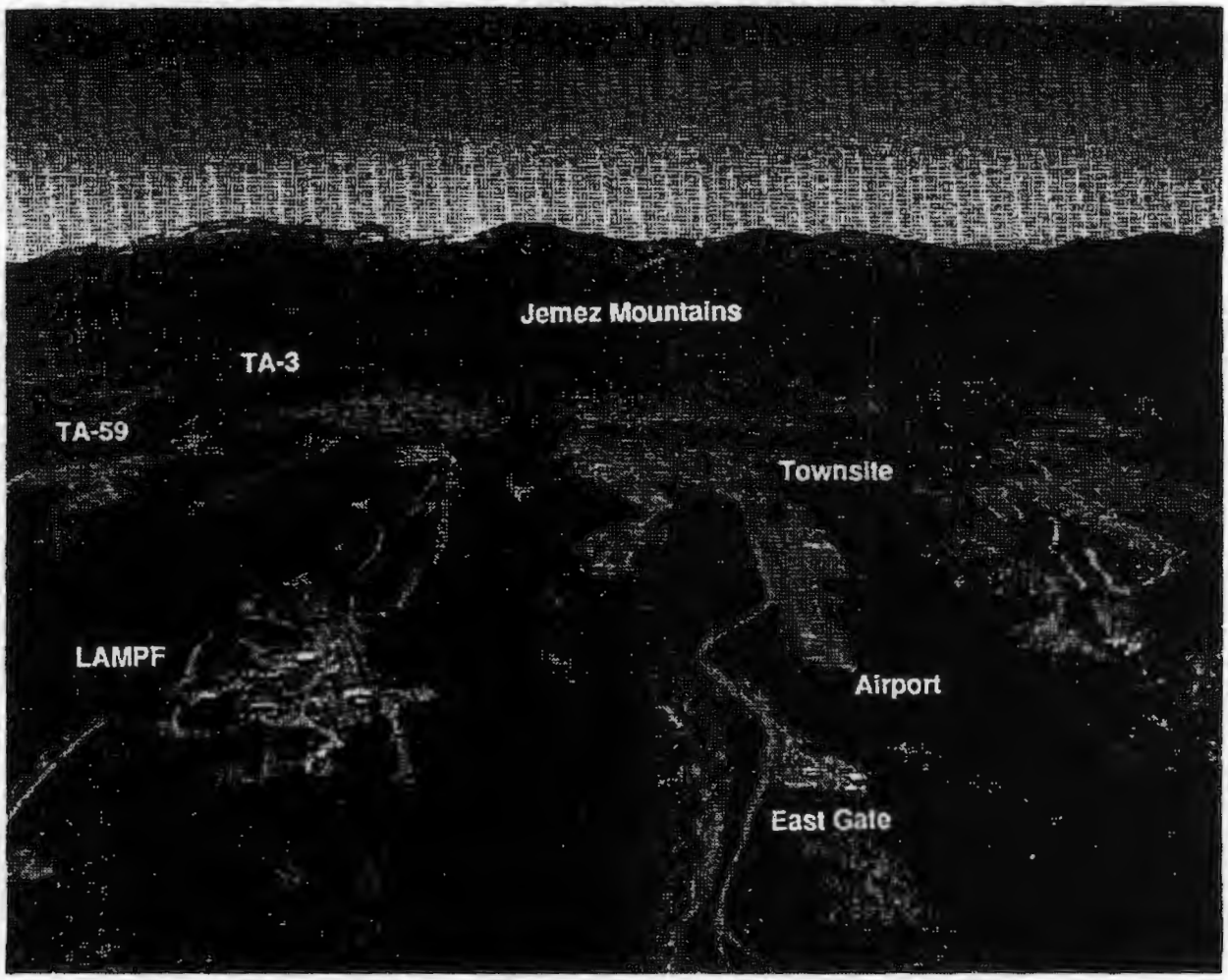

Fig. 1.2. Aerial view looking west across the Pajarito Plateau toward the Jemez Mountains. Los Alamos townsite is in the center, the main Laboratory Technical Area (TA-3) and the Environmental Protection Group (HSE-8) Air Quality and Meteorology Section site (TA-59) are shown in the middle left, and the airport and East Gate entrance to Los Alamos are shown at the bottom (east of the townsite). The large technical area at the lower left is the Los Alamos Meson Physics Facility (LAMPF) at TA-53.

1.1.2 Large-Scale Atmospheric Flow

Moisture is transported to north-central New Mexico from the Gulf of Mexico (800 miles [1300 km] to the southeast) and from the Pacific Ocean (800 miles [1300 km] to the west and 650 miles [1050 km] to the southwest). Moisture is transported readily from the Gulf of Mexico because the terrain is relatively smooth and low over most of the distance toward north-central New Mexico. Subtropical moisture from the Pacific Ocean is also transported to north-central New Mexico at times, although the route is over mountains and high terrain. This terrain in southern California and northern

Arizona squeezes out and obstructs much of the moisture transported from the Pacific Ocean lying to the west. Similarly, moisture transported from the Pacific from the southwest toward New Mexico must pass over the long fetch of mountainous and rough terrain in that direction. Finally, moisture in the westerly flow is also squeezed out by the Jemez Mountains as it reaches Los Alamos.

Los Alamos and northern New Mexico are located on the southern edge of the usual storm track or jet stream. During the cold season (autumn through spring), west-to-east–moving storms often bring clouds and precipitation. Storms that move through New Mexico can produce heavy rain and snow at times, and storms that pass just to the north of New Mexico can cause strong winds, especially during the spring. Upper low-pressure systems occasionally break off or cut off from the primary jet stream and establish themselves over the southwest United States. These "cutoff lows" also can produce heavy snows and rains over New Mexico, especially when a cold air mass is located over the state.

Occasionally, the jet stream is directed due southward toward New Mexico during winter, bringing frigid arctic or even Siberian air masses to the state. The jet stream is displaced northward to the extreme northern United States and southern Canada during the summer. A high-pressure system is often located over the eastern United States or the western Atlantic (the "Bermuda" high), resulting in a weak southeasterly flow from the Gulf of Mexico toward New Mexico. This monsoon pattern provides Los Alamos with frequent thundershowers during the summer, especially during July and August.

1.2 Los Alamos Climatology Summary

Los Alamos has a semiarid, temperate mountain climate. Normal temperatures, precipitation, and snowfall are plotted in Fig. 1.3 and are shown in Table 1.1. Means and extremes of these and other climate variables are also found in Table 1.1.

1.2.1 Temperature

Despite Los Alamos' relatively far southern location, temperatures are cool at the nearly 7400-ft (2255-m) ASL elevation. Mean temperatures vary with altitude, averaging 5°F (3°C) higher in and near the Rio Grande Valley (6500 ft [1980 m] ASL) and 5°F to 10°F (–3°C to –5.5°C) lower in the nearby Jemez Mountains (8500–10 000 ft [2600–3050 m] ASL).

Winter temperatures typically range from 15°F to 25°F (–9°C to –4°C) during the night and from 30°F to 50°F (–1°C to 10°C) during the day. Cold arctic air masses occasionally invade the Los Alamos area from the north and east, but often the shallow layer of coldest air is dammed to the east by the Sangre de Cristo Mountains. Occasionally, Los Alamos temperatures drop to nearly 0°F (–18°C) or below. The coldest nights occur with a cold-air mass over the area, fresh snow on the ground, light winds, and clear skies. During these conditions, overnight temperatures are even lower toward the valley. Many winter days are sunny with light winds, so the strong sunshine

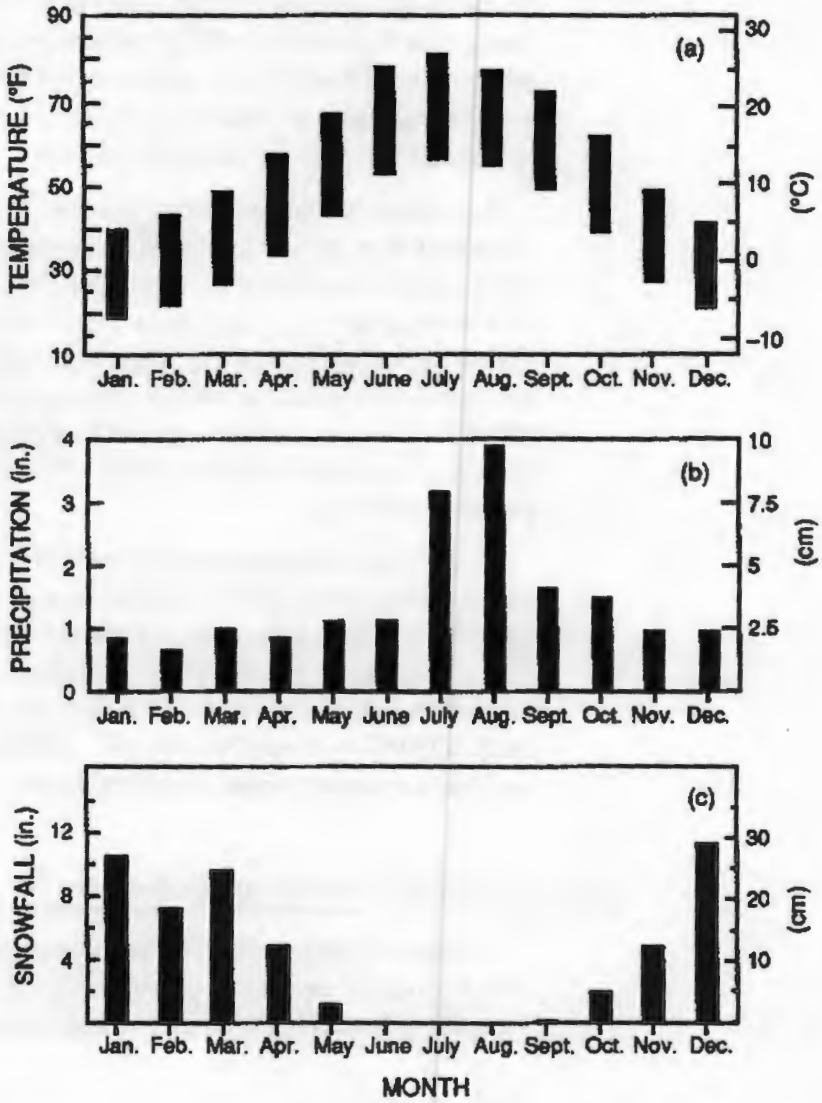

Fig. 1.3(a)–(c). Los Alamos (elevation 7380 ft [2249 m]) normal weather (1950–1980). The figure shows normal (a) temperature, (b) precipitation, and (c) snowfall for each month.

can make one feel quite comfortable, even when the temperature is low. Extremely low wind chills are rare in Los Alamos because strong winds usually do not occur at the same time as very cold temperatures.

Summers have moderately warm days and cool nights. Afternoon temperatures are in the 70s and 80s (°F) (21°C–32°C) and infrequently reach 90°F (32°C). The relatively thin air, light winds, clear skies, and dry atmosphere cause nighttime temperatures to drop to the 50s (°F) (10°C–15°C) even after the warmest day.

Daily temperature ranges are relatively large at Los Alamos, especially during the summer. Differences between lowest and highest daytime temperatures (that is, the daily temperature range) normally vary between 25°F (14°C) in June and 21°F (12°C) in December and January. The thin and dry air and frequent clear skies allow both strong daytime heating and nighttime cooling.

Wind direction can influence surface temperatures because of the relatively large slope of the Pajarito Plateau. Adiabatic cooling (or warming) accompanies rising (or sinking) air movement. Specifically, southerly or easterly winds cool the air as the air rises over the plateau, and westerly winds warm the air as the air descends. A wind switch can cause the temperature to rise or fall 5°F–10°F (3°C–6°C) from this effect alone.

The freeze-free growing season of 157 days in Los Alamos is short. The normal growing season in White Rock is even shorter at 145 days.

1.2.2 Precipitation

Normal annual precipitation, including rainfall and water-equivalent snowfall, totals nearly 18 in. (46 cm). Annual precipitation falls off rapidly toward the valley, with the normal White Rock precipitation at 13 in. (33 cm). Annual precipitation normally totals more than 20 in. (51 cm) in the adjacent Jemez Mountains.

Los Alamos precipitation is characteristic of a semiarid climate in that variations in precipitation from year to year are quite large. For instance, the annual precipitation extremes range from 6.80 to 30.34 in. (17.77 to 77.06 cm) over a 69-year period. The standard deviation over the same period was 4.81 in. (12.22 cm), or 25% of the mean.

Forty per cent of the annual precipitation falls in July and August during the height of the monsoon season. Thundershowers develop over the Jemez Mountains (and other mountains as well) during the afternoons and early evenings and drift out over the Pajarito Plateau, causing brief, but frequently intense, rains. The rainfall is often accompanied by small hailstones. A southeasterly wind pattern typically transports moisture from the Gulf of Mexico to New Mexico. This moisture, combined with strong surface heating, produces an unstable atmosphere that leads to clouds, thundershowers, and rain, especially over the mountains. Because upper-level winds most often have a westerly component, they transport the thunderstorms formed over the Jemez Mountains toward Los Alamos.

Winter precipitation falls primarily as snow, with accumulations of about 51 in. (130 cm) seasonally. Rainfall occurs occasionally during the winter, but freezing rain rarely occurs. Winter precipitation results from west-to-east–moving storms that originate over the Pacific Ocean. Most of the Pacific Ocean moisture precipitates or dries out before reaching New Mexico. However, Gulf of Mexico or tropical Pacific moisture is occasionally tapped by storms, resulting in heavy snow or rain.

Snowfall varies considerably from season to season. The seasonal snowfall extremes range from the minimum 9.3 in. (23.6 cm) to the record 153.2 in. (389.1 cm) that fell in 1986–1987. Snowfall is greatest in December, followed by that in January and March.

Snowstorms with accumulations exceeding 4 in. (10 cm) are common in Los Alamos. However, heavy snow cover seldom remains in exposed areas for lengthy periods because of strong sunshine and relatively mild temperatures. Some storms are associated with strong winds, frigid air, and dangerous wind chills, especially in the mountains. Many of the large snowstorms that have occurred in Los Alamos were caused by a

Table 1.1. Normals, means, and extremes (1911–1988).

Los Alamos, New Mexico Latitude = 35°32′ N, Longitude = 106°19′ W Elevation = 7380 ft

	Temperature (°F)										
	Normals			Extremes							
				High		Low		Record		Record	
	Maximum	Minimum	Average	Average	Year	Average	Year	Maximum	Date	Minimum	Date
January	39.7	18.5	29.1	37.6	1986	20.9	1930	64	1/12/81	−18	1/13/63
February	43.0	21.5	32.2	37.4	1934	23.0	1939	69	2/25/86	−14	2/01/51
March	48.7	26.5	37.6	45.8	1972	32.1	1948	72	3/09/89[a]	−3	3/11/48
April	57.6	33.7	45.6	54.3	1954	39.7	1973	79	4/23/38	5	4/09/28
May	67.0	42.8	54.9	60.5	1956	50.1	1957	89	5/29/35	24	5/01/76[a]
June	77.8	52.4	65.1	69.4	1980	60.4	1965	95	6/22/81	28	6/03/19
July	80.4	56.1	68.2	71.4	1980	63.3	1926	95	7/11/35	37	7/07/24
August	77.4	54.3	65.8	70.3	1936	60.9	1929	92	8/10/37	40	8/16/47
September	72.1	48.4	60.2	65.8	1956	56.2	1965	94	9/11/34	23	9/29/36
October	62.0	38.7	50.3	54.7	1963	42.8	1984	84	10/01/80	15	10/19/76
November	48.7	27.1	37.9	44.4	1949	30.5	1972	72	11/01/50	−14	11/28/76
December	41.4	20.3	30.8	38.4	1980	24.6	1931	64	12/27/80	−13	12/09/78
Annual	59.6	36.7	48.1	52.0	1954	46.2	1932	95	6/22/81[a]	−18	1/13/63

[a]Most recent occurrence.

	Relative Humidity (%)			Mean	Mean Wind			Percentage	Average Station
						Direction			
	Daily Maximum	Daily Minimum	Daily Average	Dew Point (°F)	Speed (mph)	Day	Night	of Possible Insolation	Pressure (in.)
January	71	39	55	15.0	5.0	SSE	WNW	80.4	22.86
February	75	37	56	18.0	5.5	SSE	WNW	80.6	22.83
March	70	34	52	20.5	7.1	S,W	WNW	74.3	22.77
April	60	26	41	22.5	8.0	S,W	WNW	77.5	22.84
May	62	24	44	31.0	7.8	S,W	WNW	75.7	22.86
June	58	22	39	38.0	7.3	S	WNW	78.6	22.96
July	69	30	48	46.0	6.0	S	WNW	72.3	23.03
August	77	35	57	48.0	5.7	S	WNW	71.4	23.04
September	72	32	55	41.5	6.3	S	WNW	73.5	23.00
October	70	34	55	31.0	6.2	S	WNW	75.4	22.94
November	70	36	55	21.5	5.9	SSE	WNW	74.1	22.87
December	72	40	56	17.0	5.0	SSE	WNW	75.0	22.86
Annual	69	32	51	29.0	6.3	S	WNW	75.4	22.91

Table 1.1 (Continued)

	Precipitation (in.)											
	Water Equivalent						Snow					
	Mean	Median	Max	Year	Max Daily	Date	Mean	Median	Max	Year	Max Daily	Date
January	0.85	0.69	6.75	1916	2.45	1/12/76	10.7	9.8	64.8	1987	22.0	1/15/87
February	0.68	0.63	2.78	1987	1.05	2/20/15	7.3	5.5	48.5	1987	20.0	2/19/87
March	1.01	0.90	4.11	1973	2.25	3/30/16	9.7	8.5	36.0	1973	18.0	3/30/16
April	0.86	0.70	4.64	1915	2.00	4/12/75	5.1	2.0	33.6	1958	20.0	4/12/75
May	1.13	1.24	4.47	1929	1.80	5/21/29	0.8	0.0	17.0	1917	12.0	5/02/78
June	1.12	1.05	5.67	1986	2.51	6/10/13	0.0	0.0	—	—	—	—
July	3.18	3.21	7.98	1919	2.47	7/31/68	0.0	0.0	—	—	—	—
August	3.93	3.31	11.18	1952	2.26	8/01/51	0.0	0.0	—	—	—	—
September	1.63	1.70	5.79	1941	2.21	9/22/29	0.1	0.0	6.0	1913	6.0	9/25/13
October	1.52	1.16	6.77	1957	3.48	10/05/11	1.7	0.0	20.0	1984	9.0	10/31/72
November	0.96	0.57	6.60	1978	1.77	11/25/78	5.0	3.1	34.5	1957	14.0	11/22/31
December	0.96	0.71	3.21	1984	1.60	12/06/78	11.4	7.2	41.3	1967	22.0	12/06/78
Annual	17.83	17.85	30.34	1941	3.48	10/05/11	50.8	50.0	178.4	1987	22.0	1/15/87
Season									153.2	1986–87		12/06/78

	Mean (Number of Days Occurring)										
	Temperature (°F)										
	Maximum		Minimum		Water Equivalent (in.)			Snowfall (in.)			
	90 and Above	32 and Below	32 and Below	0 and Below	0.01 or More	0.10 or More	0.50 or More	1.0 or More	4.0 or More	Thunder-storms	Fog (Visibility 0.6 mile [1 km] or less)
January	0	6	30	1	5	2	0	3	1	0	1
February	0	4	26	0	6	2	0	2	1	0	1
March	0	2	24	0	7	3	0	3	1	0	1
April	0	0	13	—	6	2	1	1	0	2	0
May	0	0	2	—	7	3	1	0	0	6	0
June	0	—	0	—	6	3	1	—	—	8	0
July	1	—	0	—	14	8	2	—	0	16	0
August	0	—	0	—	15	9	3	—	0	15	0
September	0	—	0	—	8	4	1	0	0	6	0
October	0	0	7	—	6	3	1	0	0	2	1
November	0	2	22	0	4	2	0	2	0	0	1
December	0	5	30	0	5	3	0	3	1	0	2
Annual	2	19	154	2	89	44	10	14	4	57	7

persistent upslope (southerly or southeasterly) wind, frequently over the top of a shallow arctic air mass. The preceding conditions were responsible for the largest single snowfall on record, 48 in. (122 cm) during January 15–17, 1987, with up to 70 in. (178 cm) falling in the Los Alamos North Community.

1.2.3 Surface Winds

Surface winds are quite light at Los Alamos, averaging 7 mph (3 m/s). Winds are light because New Mexico lies at the southern edge of the band of W'ly winds common over central North America. Wind speeds are strongest from March through June and weakest in December and January. Intense storms and associated cold fronts, occurring especially during the spring months, cause the strongest winds. Sustained winds exceeding 25 mph (11 m/s) and peak wind gusts exceeding 50 mph (22 m/s) are common during the spring. Thunderstorms can also cause brief strong winds, especially during spring and summer. The strongest winds are generally SW'ly through NW'ly and occur in the afternoon or evening. The highest recorded wind gust in recent history was 77 mph (34 m/s) from the SSW at East Gate on November 15, 1988, resulting from a storm system moving through the Rockies. Thunderstorms produced 76-mph (34-m/s) peak gusts from the SE at both East Gate and Area G on May 9 and 27, 1989, respectively. Average night winds are WNW'ly at Laboratory Technical Area (TA)-59 (7380 ft [2249 m] ASL) because of persistent cold-air drainage down the plateau. Daytime winds are generally S-SSE'ly, caused by upslope and up-valley winds, but daytime winds are also frequently W'ly during the windy season, March through May.

Los Alamos surface winds often vary dramatically with time of day, location, and height above ground because of the complex terrain (Fig. 1.4). On days with sunshine and light, large-scale winds, a 600- to 1000-ft-deep (180- to 300-m-deep), thermally driven (convective) upslope wind develops over the Pajarito Plateau. Upslope winds are generally light, less than 6 mph (3 m/s). Winds usually become more SSW'ly and S'ly at locations toward the Rio Grande Valley, where channeling of large-scale winds becomes more important and the slope of the plateau is less important.

When the sky is clear and upper-level winds are light, these local winds reverse at night. A shallow drainage wind (WNW'ly) often forms and flows down the plateau. These winds can reach speeds of 6–8 mph (3–3.5 m/s). Toward the valley, the drainage wind is more evenly distributed from the WNW through the N. Wind directions at only 150 ft (46 m) or so above ground level (AGL) are often NNE'ly or SSW'ly, resulting from valley channeling, whereas surface winds are WNW'ly.

The Rio Grande Valley channels light-to-moderate large-scale winds. Up-valley winds result from ESE through (clockwise) WNW large-scale winds, and down-valley winds result from WNW through (clockwise) ESE large-scale winds. Frequently, valley locations have channeling while plateau locations simultaneously have thermally driven slope flows. Intermediate locations can be affected by both channeled and slope flows, resulting in a compromised wind direction.

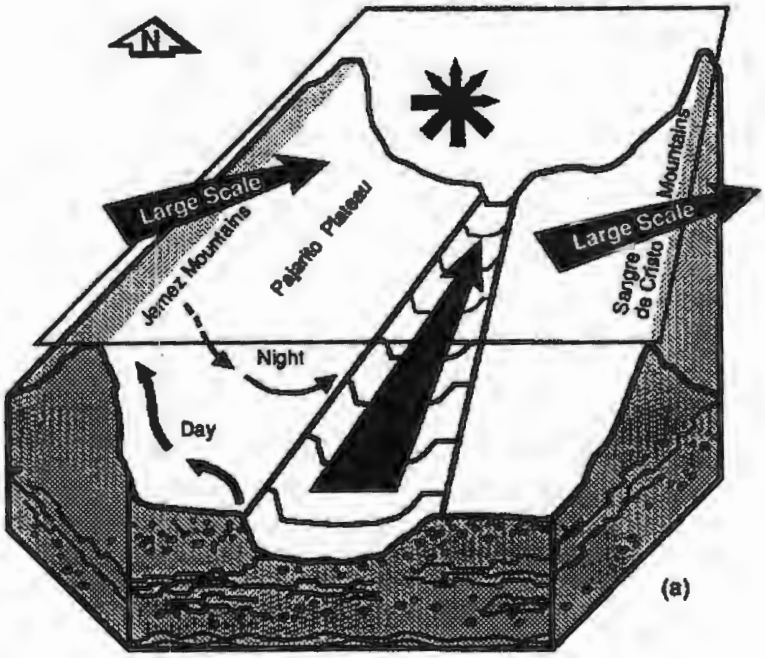

(a) Up-valley channeled winds result when light-to-moderate, large-scale winds blow from the ESE through (clockwise) the WNW (see four arrows at top). With fair skies, a thermally driven upslope (anabatic) wind forms over the Pajarito Plateau and East Jemez Mountain slopes. At night, a shallow, cold-air drainage (anabatic) wind flows down the plateau. Both day and night slope winds become more SSW'ly (up-valley) eastward on the plateau (toward the Rio Grande Valley).

(b) Down-valley channeled winds result when light-to-moderate, large-scale winds blow from the WNW through (clockwise) the ESE (see four arrows at top). The day and night slope winds become more NNE'ly (down-valley) eastward on the plateau (toward the Rio Grande Valley).

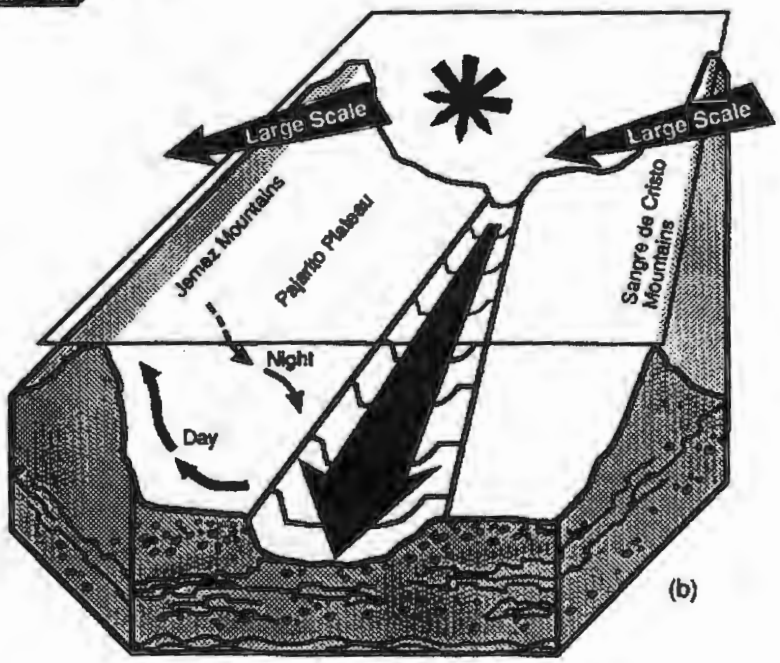

Fig. 1.4(a) and (b). Regional up-valley and down-valley winds.

1.2.4 Humidity

Atmospheric moisture content is relatively small in Los Alamos. Dew point, a good indicator of atmospheric water-vapor content, reaches a peak during July and August, averaging 46°F and 48°F (8°C and 9°C), respectively. During an active monsoon phase, the dew point reaches the 50s (°F) (10°C–15°C) and occasionally even exceeds 60°F (15.5°C). In contrast, much of the eastern United States can see dew points in the 60s and 70s (°F) (16°C–26°C) and occasionally in the low 80s (°F) (27°C–29°C) during summer. The air is driest in the winter, with a mean dew-point temperature of 15°F (–9.5°C) in January. The average atmospheric moisture content in August is nearly 7 times that recorded in January.

Relative humidity, a variable strongly dependent on temperature, has a different annual distribution. The months from August through March have nearly the same relative humidity, ranging between 52% and 57%. The late spring and early summer months have the lowest relative humidity, with the minimum of 39% occurring during June. Early summer relative humidity occasionally dips to 5% or less during warm afternoons. Relative humidities approaching 100% (saturation) occur frequently on cold winter mornings and also in the summer during showers and during mornings following showers.

Evaporation of free-standing water in Los Alamos is much greater than the amount of annual precipitation. Annual, mean, Class A pan* evaporation ranges from approximately 65 in. (165 cm) in the Jemez Mountains to 75 in. (190 cm) at White Rock (NOAA 1979). Annual lake evaporation is estimated to be 68% of the Class A pan evaporation, ranging from approximately 44 in. (112 cm) in the Jemez Mountains to 51 in. (130 cm) at White Rock.

1.2.5 Insolation (Sunshine)

Sunshine is plentiful at Los Alamos because of its southerly location and frequent clear skies. Los Alamos receives more than 75% of possible insolation (*in*coming *sol*ar radi*ation*) annually. Possible insolation is defined as the amount received assuming a perfectly cloud-free sky. Sunshine is especially prevalent during January and February, when more than 80% of possible insolation is received. The fraction of possible insolation received is almost as high in April and June, with 79% occurring in June. Frequent thundershowers and clouds during the monsoon season force the percentage of possible insolation received to decrease, with a minimum of 71% occurring during August. Even though cloudiness is greater during July and August than during January and February, Los Alamos receives twice as much insolation during July and August because of the higher sun angle and longer days.

*Class A pan refers to the standard pan that meteorologists and hydrologists use to measure evaporation of shallow, free-standing water.

1.2.6 Severe Storms

No tornadoes have been reported to touch down in Los Alamos in recent history. However, funnel clouds have been spotted nearby in White Rock and Santa Fe. Only weak tornadoes are possible in Los Alamos, but strong dust devils can produce winds up to 75 mph (33.5 m/s) at isolated spots in the county, especially at lower elevations. Strong winds with gusts exceeding 60 mph (27 m/s) are common and widespread during the spring.

Lightning is very common over the Pajarito Plateau. There are 57 thunderstorm days during an average year, with most occurring during the summer. Lightning protection is an important design factor for most facilities at the Laboratory and county. Brief downpours can cause local flash flooding, especially in canyons, streams, and other low spots.

Hail falls frequently during the summer, occasionally causing damage. Hailstones with diameters up to 0.25 in. (0.6 cm) are common, but hailstones larger than that fall more infrequently. Remnants of hurricanes originating in the Pacific and the Gulf of Mexico occasionally reach New Mexico during the summer and autumn. These storms are weak by the time they reach northern New Mexico and therefore do not cause strong winds. However, the storms can produce widespread and strong thunderstorm activity and heavy rains.

Severe winter storms can cause heavy snows, strong winds, and dangerous wind chills, and heavy snow accumulations occasionally make roadways impassable. Heavy snowfall and strong winds also severely reduce visibility. Snowstorms can quickly develop over mountain areas, even when the weather is relatively clear over valley areas.

1.2.7 Atmospheric Pressure

The atmospheric pressure at 7380 ft (2249 m) ASL averages 22.91 in. (775.7 mbar) of mercury, or 76%–77% of the standard sea-level pressure. In other words, Los Alamos lies above more than 24% of the atmosphere. Similarly, the air density is about 75% of the standard sea-level air density.

Annual, seasonal, and diurnal pressure variations are modest at Los Alamos. Pressure reaches a minimum during March (averaging 22.77 in. [771.2 mbar]) when intense storms frequently travel west to east across the central and southern Rockies. Average pressure reaches a maximum during the monsoon season, July and August, averaging 23.04 in. (780.1 mbar). The strong belt of subtropical high pressure is usually the farthest north during this time of year.

When Los Alamos atmospheric pressure is adjusted to equal that at sea level, the annual tendency is reversed: a maximum occurs during January (30.12 in. [1020.1 mbar]) and a minimum occurs during June (29.69 in. [1005.4 mbar]). This reversal from the actual pressure pattern results from the large effect of lower density of the high-temperature air assumed to fill the layer between sea level and the altitude at Los Alamos during the summer. In winter, this layer, which comprises nearly one-fourth

of the atmosphere, is assumed to have a lower temperature and, therefore, higher density. Denser air, in turn, contributes to higher atmospheric pressure.

The pressure displays a noticeable diurnal cycle on most days: a maximum during the late morning and a minimum during the late afternoon. This cycle results from the ground's diurnal heating and cooling of the low-level air (up to ~3000 ft [900 m] AGL). The effects of the atmospheric heating and cooling lag behind the surface maximum and minimum temperatures by several hours. A secondary cycle with smaller amplitude is apparent, especially during summer when a secondary maximum occurs near midnight and a secondary minimum occurs 4 to 6 hours later.

1.2.8 Atmospheric Dispersion

The irregular terrain at Los Alamos favorably and unfavorably affects the consequences of an air-pollution release by affecting atmospheric turbulence and dispersion. Favorable effects occur because increased dispersion promotes greater dilution of contaminants released into the atmosphere. The complex terrain and forests create an aerodynamically rough surface, forcing increased horizontal and vertical turbulence and dispersion. Although the dispersion generally decreases at lower elevations where the terrain becomes smoother and less vegetated, the frequent clear skies and light winds cause good daytime vertical dispersion, especially during the warm season. The strong daytime heating during the summer can force strong vertical mixing up to 4000–8000 ft (1200–2400 m) AGL.

Unfavorable effects occur because the generally light winds are limited in diluting contaminants horizontally. The same clear skies and light winds have a negative effect on dispersion at night, causing strong, shallow surface inversions to form. These inversions severely restrict near-surface vertical and, to a lesser extent, horizontal dispersion. The inversions are especially strong during the winter. Smoke from wood-burning stoves is often noticeable on clear winter evenings, especially near populated areas such as Santa Fe and Albuquerque. Shallow drainage winds fill lower areas with cold air, thereby creating deeper inversions, which are common toward the Rio Grande Valley (White Rock) on clear nights with light winds. Canyons also limit dispersion by channeling air flow. Strong, large-scale inversions during the winter can limit vertical mixing to under 10 000 ft (3050 m) ASL.

Overall dispersion is generally the greatest in the spring when winds are strongest. However, deep vertical mixing is the greatest during summer afternoons when the atmosphere is unstable up to 5000 ft (1500 m) or more AGL. Low-level dispersion, when averaged over day and night, is generally the least during summer and autumn evenings when winds are light. However, even though low-level dispersion is generally greater in the winter, intense surface inversions can cause low-level dispersive conditions during nights and early mornings.

The frequencies of atmospheric stability categories (estimates of atmospheric dispersive capability) are 52% unstable (A–C), 21% neutral (D), and 27% stable (E–F) during the winter at TA-59. The frequencies are 44%, 22%, and 34%, respectively,

during the summer. The stability category frequencies are based on vertical wind variations. Stability generally increases (less-dispersive atmosphere) slightly toward the valley.

1.3 Observation Network

The Laboratory's Environmental Protection Group (HSE-8) Air Quality and Meteorology Section maintains a meteorological tower and monitoring network.

The meteorological tower and monitoring data used in this report are given in Table 1.2, and present locations of the towers and sites are shown in Fig. 1.5. Measured meteorological variables include wind speed and direction, vertical wind speed, temperature, insolation, relative humidity, and precipitation. Not all variables are measured at each site, and some variables are measured at multiple tower levels. Measurements are taken at the six towers at ground level (1.2 m) and at various heights ranging from 34 to 300 ft (11 to 92 m).

Los Alamos weather data (temperature, precipitation, and snowfall) have been taken at TA-59 since 1979. (Note that these data have also been provided to the National Weather Service Cooperative Observer Network.) Temperature, humidity, and precipitation records have been kept for White Rock since late 1964. At three other sites, precipitation only is measured.

Additional information on historical locations of weather stations in this network and a brief discussion of future plans are provided in Appendixes A and B. Appendix C addresses quality-assurance issues for data accuracy.

1.4 Meteorological Units of Measurement

Although the scientific community has adopted the worldwide standard International System of Units (SI), this report primarily contains the English units and terms because they are widely used and because climate data, generally, are still compiled, distributed, and understood in these familiar units. In addition, some weather variables are preferably measured in English units. For example, weather temperatures, especially, are more accurately represented in degrees Fahrenheit rather than degrees Celsius (centigrade). Where feasible, both English and metric units are given. However, only metric units are given for some variables, such as insolation and atmospheric density. Also, because metric units are standard in dispersion meteorology, metric units are primarily used in the sections on turbulence and wind persistence.

Appendix D presents a further discussion of meteorological units and contains tables giving conversion factors for these units.

Table 1.2. Sites and meteorological data.

Site Number (see Fig. 1.5)	Location	Elevation (ft ASL)	Wind and Temperature Sensor Height (ft AGL)	Insolation	Surface Temperature (4 ft AGL)	Relative Humidity	Precipitation	Year Data-Taking Began
1	TA-16	7640	Ground	No	No	No	Yes	1974
2	North Community	7420	Ground	No	No	No	Yes	1986
3	TA-59[a]	7380	4,[b] 72	Yes	—	Yes	—	1979
4	Bandelier[a]	7040	4,[b] 38, 75, 150	Yes	Yes	Yes	Yes	1987
5	East Gate[a]	7020	4,[b] 39	Yes	Yes	Yes	Yes	1981
6	TA-54[a]	6690	4,[b] 34	Yes	Yes	Yes	Yes	1980
7	White Rock Y	6380	Ground	No	No	No	Yes	1986
8	White Rock	6380	4[b]	No	Yes	Yes	Yes	1964
9	TA-50[a]	7270	38, 75, 150, 300	No	No	No	No	1985
10	TA-53[a]	6990	79	No	No	No	No	1984
3	TA-59 cooperative weather data[c]	7380	Ground	—	—	—	Yes	1911
			4[b]	—	Yes	—	—	1919

[a]Meteorological tower location.

[b]Temperature sensor only.

[c]The Laboratory has provided data to the National Weather Service Cooperative Observer Network since the 1940s. Data have been taken at TA-59 since 1979. See Appendix A for historical locations of weather stations.

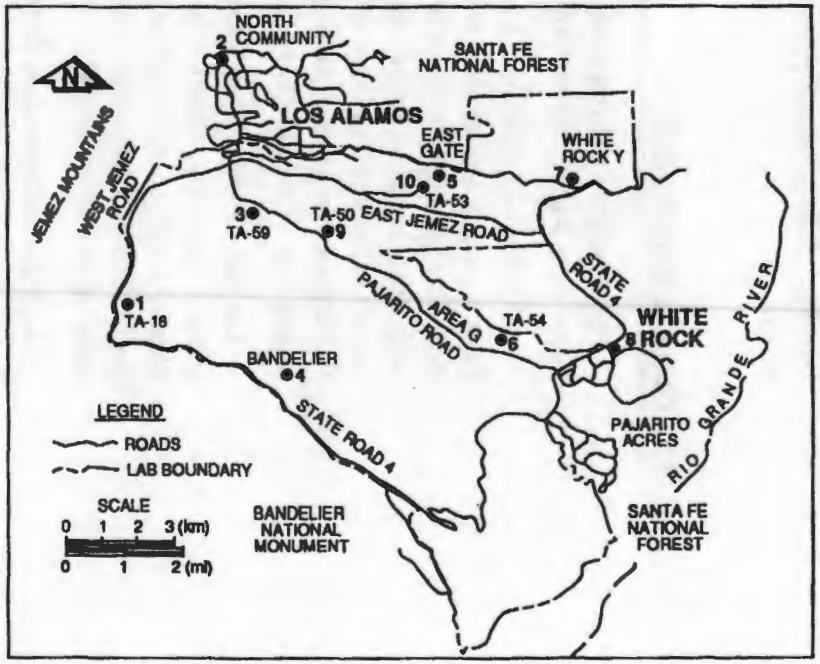

Fig. 1.5. Map showing meteorological tower locations and site numbers (see Table 1.2).

2 Surface Air Temperatures and Moisture Content

2.1 Monthly Mean Temperatures

Los Alamos and White Rock monthly mean temperatures are shown in Fig. 2.1 and Table 2.1. The temperature means are for the latest 30-year mean period (1951–1980) at Los Alamos and for 1965–1987 at White Rock. Note that mean maximum temperatures are substantially higher in White Rock than in Los Alamos for all months and that the mean minimum temperatures are generally lower in White Rock.

Temperatures usually are higher during the daytime in White Rock because its elevation is about 800 ft (240 m) lower than that of Los Alamos. The largest difference in high temperatures (about 5°F) occurs during the spring and summer months. Insolation is strongest during the summer, causing variations in daytime temperatures between the sites. Also, thunderstorms are most common during July and August. Often, thundershowers or clouds occur at Los Alamos but not at White Rock, thereby producing cooler temperatures in Los Alamos. The difference between maximum temperatures is minimal during December and January. It is during these months that cold air can drain toward lower elevations at night and cause a strong, ground-level inversion. In fact, the high temperature can actually be lower in White Rock than in Los Alamos on days when a strong inversion is present from overnight cooling.

Minimum temperatures are generally lower in White Rock, especially during the cold season when the atmosphere contains the least amount of moisture. Generally, during clear nights with light winds, strong radiational cooling of the ground promotes cold-air

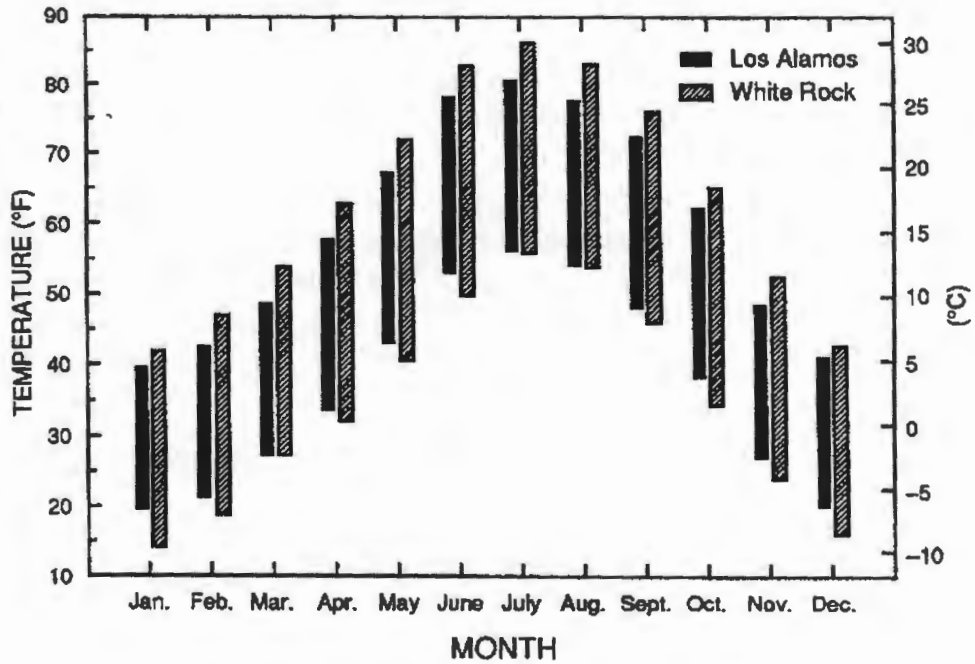

Fig. 2.1. Monthly mean maximum and minimum temperatures at Los Alamos (TA-59) and White Rock.

Table 2.1. Monthly mean temperatures (°F) at Los Alamos and White Rock.[a]

Month	Maximum	Minimum	Daily Range	Average
January	39.7 (41.8)	18.5 (14.7)	21.2 (27.1)	29.1 (28.3)
February	43.0 (47.0)	21.5 (19.2)	21.5 (27.8)	32.2 (33.1)
March	48.7 (54.5)	26.5 (26.1)	22.2 (28.4)	37.6 (40.3)
April	57.6 (62.6)	33.7 (32.5)	23.9 (30.1)	45.6 (47.5)
May	67.0 (71.7)	42.8 (40.9)	24.2 (30.8)	54.9 (56.3)
June	77.8 (82.4)	52.4 (50.2)	25.4 (32.2)	65.1 (66.3)
July	80.4 (85.9)	56.1 (55.9)	24.3 (30.0)	68.2 (70.9)
August	77.4 (82.6)	54.3 (53.9)	23.1 (28.7)	65.8 (68.3)
September	72.1 (75.7)	48.4 (46.3)	23.7 (29.4)	60.2 (61.0)
October	62.0 (65.1)	38.7 (34.9)	23.3 (30.2)	50.3 (50.0)
November	48.7 (52.4)	27.1 (24.4)	21.6 (28.0)	37.9 (38.4)
December	41.4 (42.9)	20.3 (16.1)	21.1 (26.8)	30.8 (29.5)
Annual	59.6 (63.7)	36.7 (34.6)	22.9 (29.1)	48.1 (49.2)

[a]White Rock temperatures are in parentheses.

drainage. The cold air settles into canyons, low spots, and the Rio Grande Valley. The minimum temperature averages are about 5°F cooler in White Rock than in Los Alamos during December and January. March and April are the exception, in that the minimum temperatures are very close at both sites. Strong winds during these months inhibit the formation of cold-air drainage. Minimum temperatures are also similar at both sites during July and August, the rainy months. Increased atmospheric moisture during these months reduces ground cooling and cold-air drainage. In addition, the increased water vapor absorbs the outgoing radiation given off by the ground and reradiates it back to the ground.

The warmest month of the year is normally July, with August and June, respectively, the second and third warmest at both sites. The coldest month is January, with December and February the second and third coldest months at both sites. Note that the largest differences between maximum and minimum daily temperatures occur during the spring months when humidity is relatively low and sunshine is relatively strong.

2.2 New Mexico Monthly Mean Temperatures

New Mexico temperature maps are shown in Figs. 2.2–2.15. A locator map (Fig. 2.2) and a list of sites (Table 2.2) assist in using the maps. Monthly mean temperatures in New Mexico are shown in Figs. 2.3–2.14, and annual temperatures are shown in Fig. 2.15. The maps are taken from the *New Mexico Climate Manual: Solar and*

Weather Data (Morris and Haggard 1985) and have been reproduced with permission from the New Mexico Research and Development Institute.

Temperatures vary by latitude and elevation, generally increasing toward the south, or with increasing sunshine. The temperature difference with latitude is smaller during the warm season when solar insolation is more uniform north and south in the state because of the high sun angle during the summer. During winter, the north-south change in temperatures is greater because the polar cold front often lies over, or just north of, New Mexico. The temperatures are also cooler in the state's northern parts because of cold-air masses plunging southward through the United States plains. These air masses do not reach the southern areas as often. Besides, the cold-air masses are modified by the time they reach southern New Mexico. Finally, snow cover, which is more common in the north, reflects insolation away from the surface, thereby reducing temperatures.

Temperatures are strongly dependent on elevation. The average temperature change with height (lapse rate) in New Mexico varies from 2.5°F/1000 ft in January to 4.0°F/1000 ft in July. The strong insolation in summer causes increased ground heating and greater vertical temperature differences. The more unstable atmosphere (greater lapse rate) in the summer forces increased thundershower activity, especially over the mountains. The more stable atmosphere (lower lapse rate) in the winter is partly caused by the long nights, the formation of inversions during the night in the valleys, and weaker surface heating. The dry atmosphere during winter promotes cold-air drainage and strong inversions.

2.3 Hourly Temperatures and Humidity

Hourly temperatures and atmospheric moisture variables were calculated using historical tower data (1980–1987) from TA-59 and Area G. Only temperature and relative humidity were measured directly; wet-bulb temperature, dew point, mixing ratio, and absolute humidity were calculated from the temperature and relative humidity using moisture and thermodynamic charts.

Following are brief definitions of atmospheric moisture variables presented in this section:

1. *Relative humidity* — ratio of moisture that a given volume of air contains at a specified temperature and atmospheric pressure to the moisture that the same volume can hold at saturation at the same temperature and pressure. Note that relative humidity is proportional to the inverse of temperature (warmer air can hold more moisture at saturation) and is insensitive to atmospheric pressure.

2. *Wet-bulb temperature* — the temperature to which air can be cooled by evaporating water into air until saturation occurs. Wet-bulb temperatures are useful for design and operation of evaporative-cooling systems and cooling towers used in industry, as well as being a forecasting tool in determining cooling of air because of precipitation.

Table 2.2. Site listing for New Mexico locator map (Fig. 2.2).

Site No. and Name	Latitude	Longitude	Elevation (ft)	Site No. and Name	Latitude	Longitude	Elevation (ft)
New Mexico				*New Mexico (Continued)*			
1 Abiquiu Dam	36°14′	106°26′	6 380	34 Las Vegas	35°36′	105°12′	6 470
2 Alamogordo	32°53′	105°57′	4 350	35 Lordsburg	32°18′	108°39′	4 250
3 Albuquerque	35° 3′	106°37′	5 326	36 Los Alamos	35°52′	106°19′	7 380
4 Artesia	32°46′	104°23′	3 320	37 Los Lunas	34°46′	106°45′	4 840
5 Aztec Ruins	36°50′	108° 0′	5 644	38 Magdalena	34° 7′	107°14′	6 540
6 Belen	34°40′	106°46′	4 800	39 Mescalero	33° 9′	105°47′	6 785
7 Bernalillo	35°19′	106°33′	5 070	40 Mosquero	35°48′	103°56′	5 485
8 Bloomfield	36°30′	107°58′	5 806	41 Mountainair	34°32′	106°15′	6 520
9 Bosque del Apache	33°46′	106°54′	4 520	42 Portales	34°11′	103°21′	4 010
10 Carlsbad	32°25′	104°14′	3 120	43 Raton	36°55′	104°26′	6 920
11 Carrizozo	33°39′	105°53	5 438	44 Reserve	33°43′	108°47′	5 847
12 Chaco Canyon	36° 2′	107°54′	6 179	45 Roswell	33°18′	104°32′	3 612
13 Chama	36°55′	106°35′	7 850	46 Ruidoso	33°22′	105°40′	6 838
14 Clayton	36°27′	103° 9′	4 970	47 Sandia Crest	35°13′	106°27′	10 680
15 Cloudcroft	32°58′	105°45′	8 801	48 Santa Fe	35°41′	105°54′	7 200
16 Clovis	34°24°	103°12′	4 280	49 Santa Rosa	34°57′	104°41′	4 620
17 Corona	34°15′	105°35′	6 664	50 Shiprock	36°47′	108°42′	4 870
18 Cuba	36° 2′	106°58	7 045	51 Silver City	32°47′	108°16′	5 940
19 Deming	32°15′	107°42′	4 301	52 Socorro	34° 5′	106°53′	4 585
20 Dulce	36°57′	107° 0′	6 793	53 Springer	36°21′	104°35′	5 878
21 Eagle Nest	36°33′	105°16′	8 262	54 Taos	36°23′	105°36′	6 965
22 Española	36° 0′	106° 5′	5 643	55 Tatum	33°16′	103°19′	4 100
23 Farmington	36°45′	108°10′	5 395	56 Thoreau	35°26′	108° 9′	7 100
24 Fence Lake	34°39′	108°40′	7 055	57 Tierra Amarilla	36°45′	106°34′	7 425
25 Fort Sumner	34°28′	104°15′	4 025	58 Tohatchi	35°51′	108°44′	6 420
26 Gallup	35°31′	108°47′	6 465	59 Truth or Consequences	33°14′	107°16′	4 820
27 Glenwood	33°20′	108°53′	4 725	60 Tucumcari	35°12′	103°41′	4 096
28 Grants	35°10′	107°54′	6 520	61 Tularosa	33° 5′	106° 3′	4 430
29 Hatch	32°40′	107°11′	4 052	62 Zuni	35° 6′	108°47′	6 440
30 Hobbs	32°42′	103° 8′	3 615				
31 Jal	32° 6′	103°12′	3 060				
32 Jemez Springs	35°46′	106°41′	6 230	*Texas*			
33 Las Cruces	32°17′	106°45′	3 881	63 El Paso	31°48′	106°24′	3 918

3. *Dew point* — the temperature to which a volume of air must be cooled for saturation (precipitation) to occur. The cooling is assumed to take place during constant pressure and constant moisture content of the volume of air. Dew point is a good indicator of actual moisture content because it is not temperature dependent (except at saturation) and is only slightly pressure dependent.

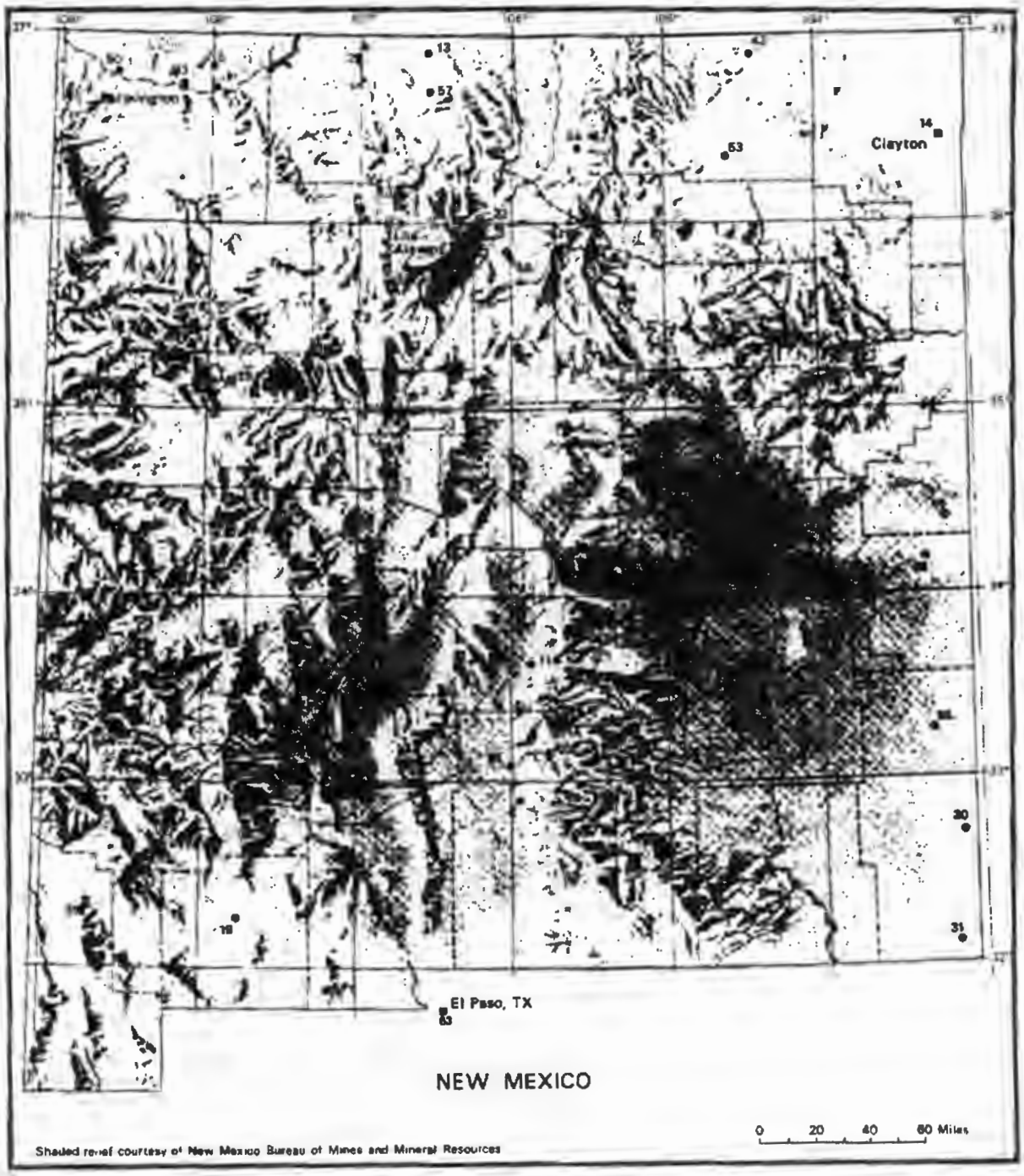

Fig. 2.2. New Mexico locator map. The temperature maps in this section are from Morris and Haggard (1985) and have been reproduced with permission from the New Mexico Research and Development Institute.

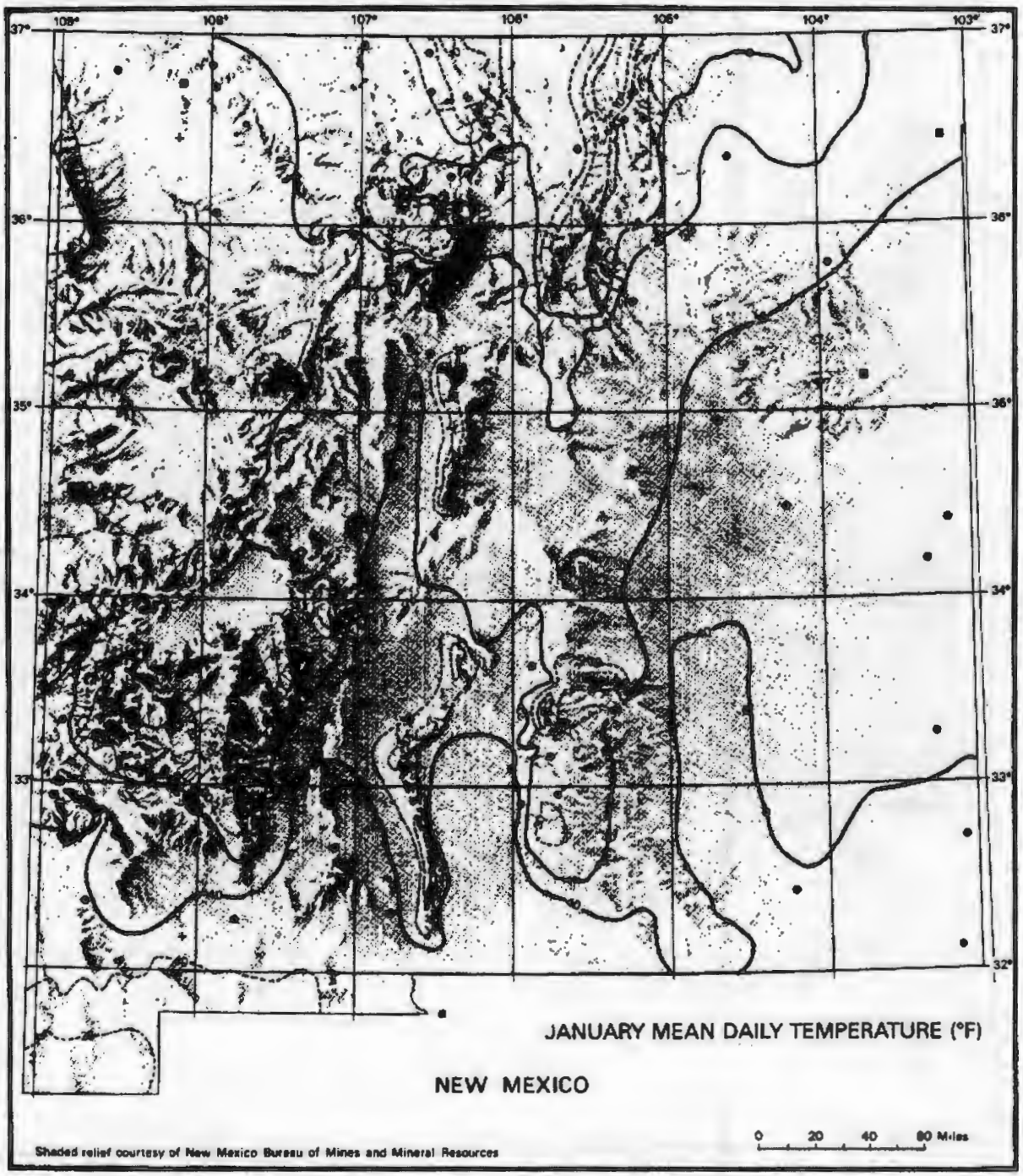

Fig. 2.3. January mean temperatures in New Mexico.

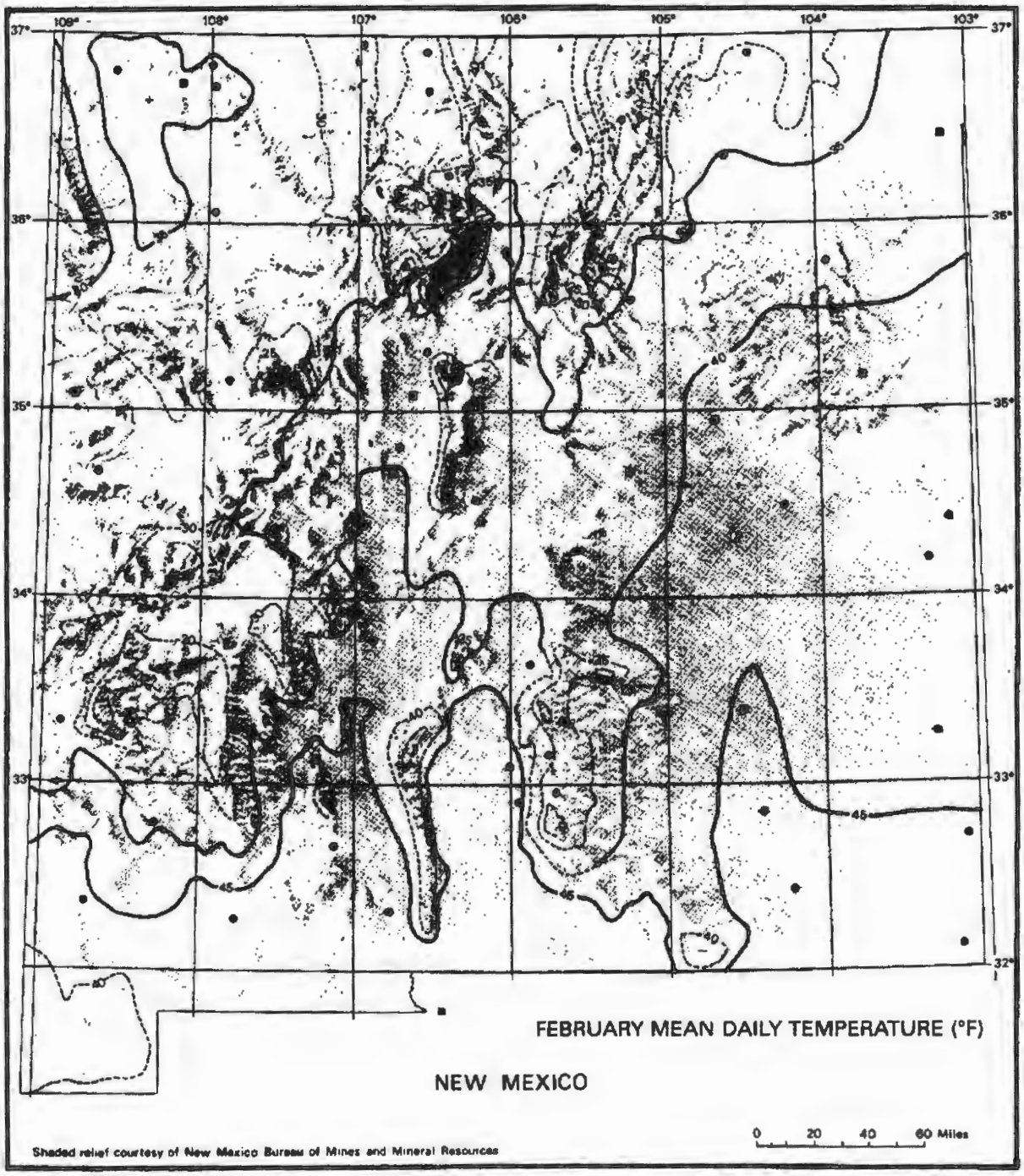

Fig. 2.4. February mean temperatures in New Mexico.

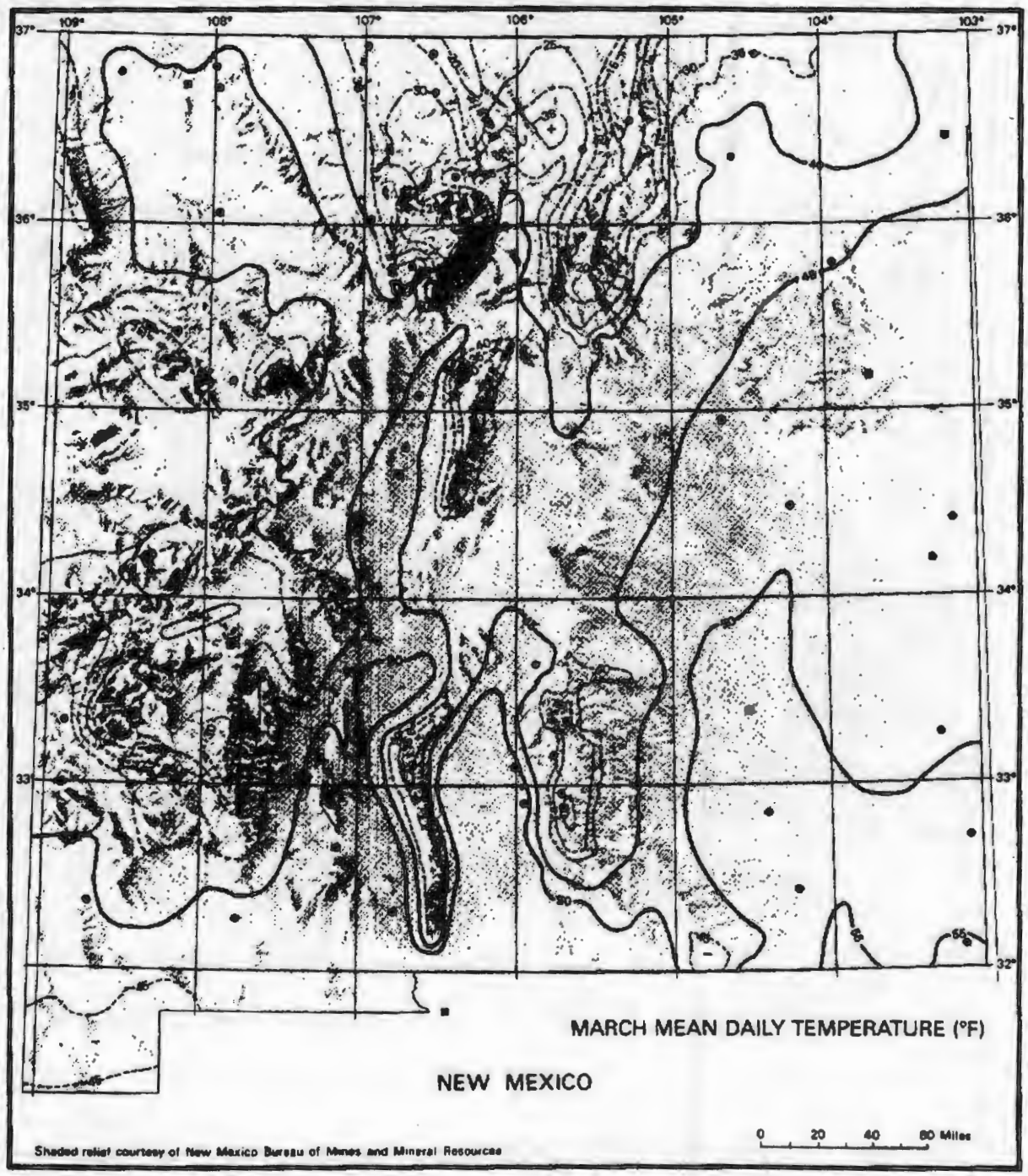

Fig. 2.5. March mean temperatures in New Mexico.

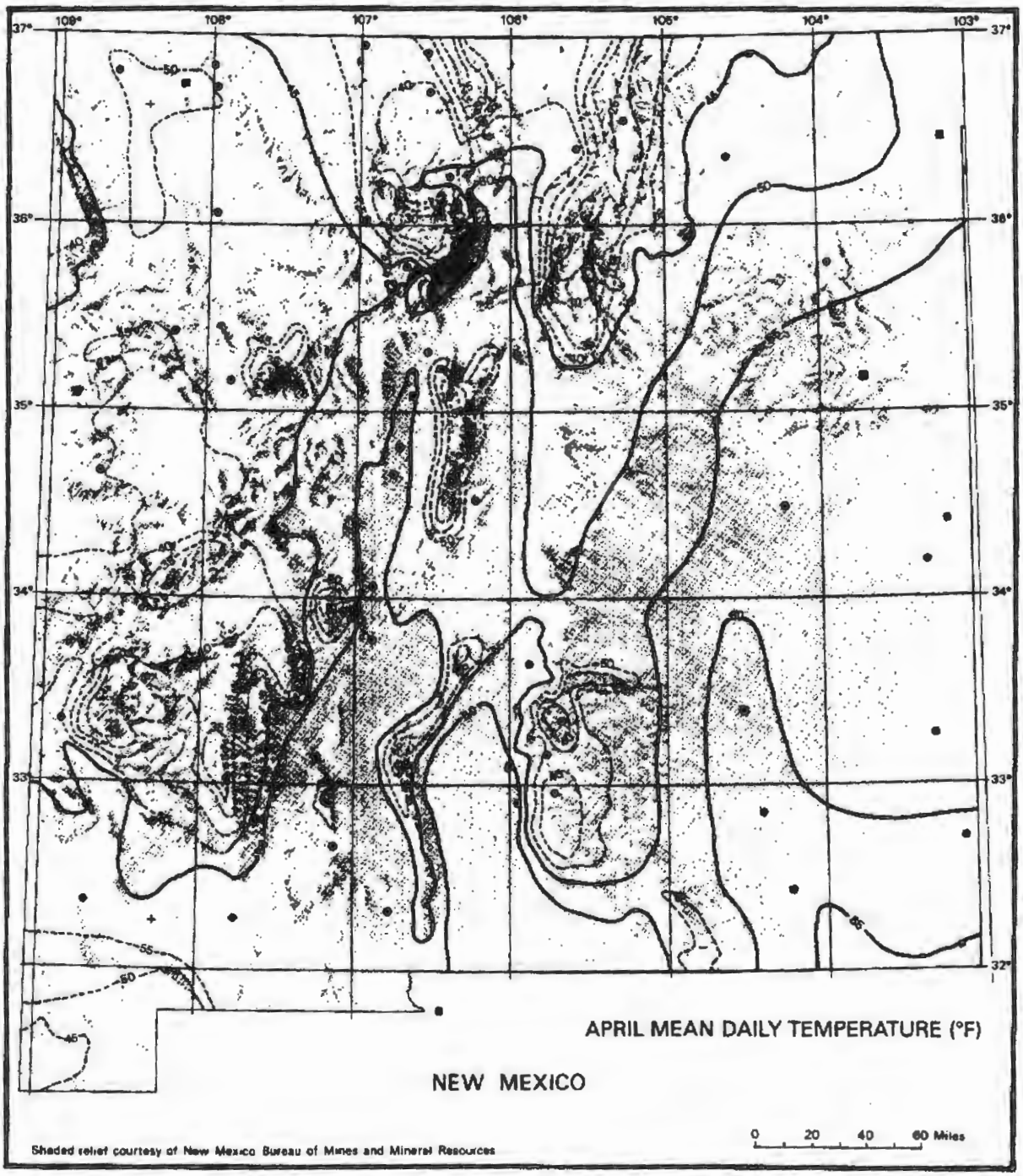

Fig. 2.6. April mean temperatures in New Mexico.

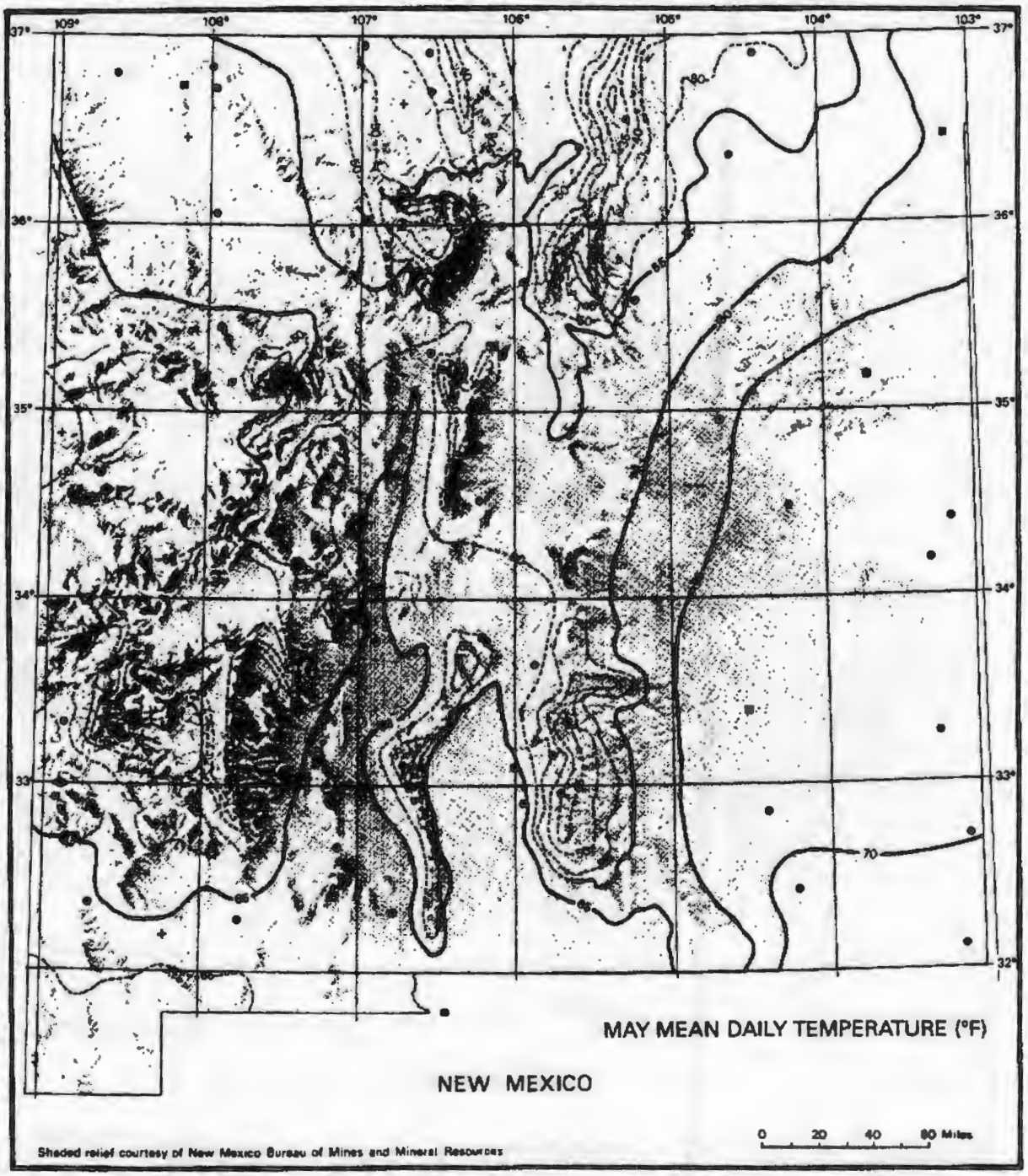

Fig. 2.7. May mean temperatures in New Mexico.

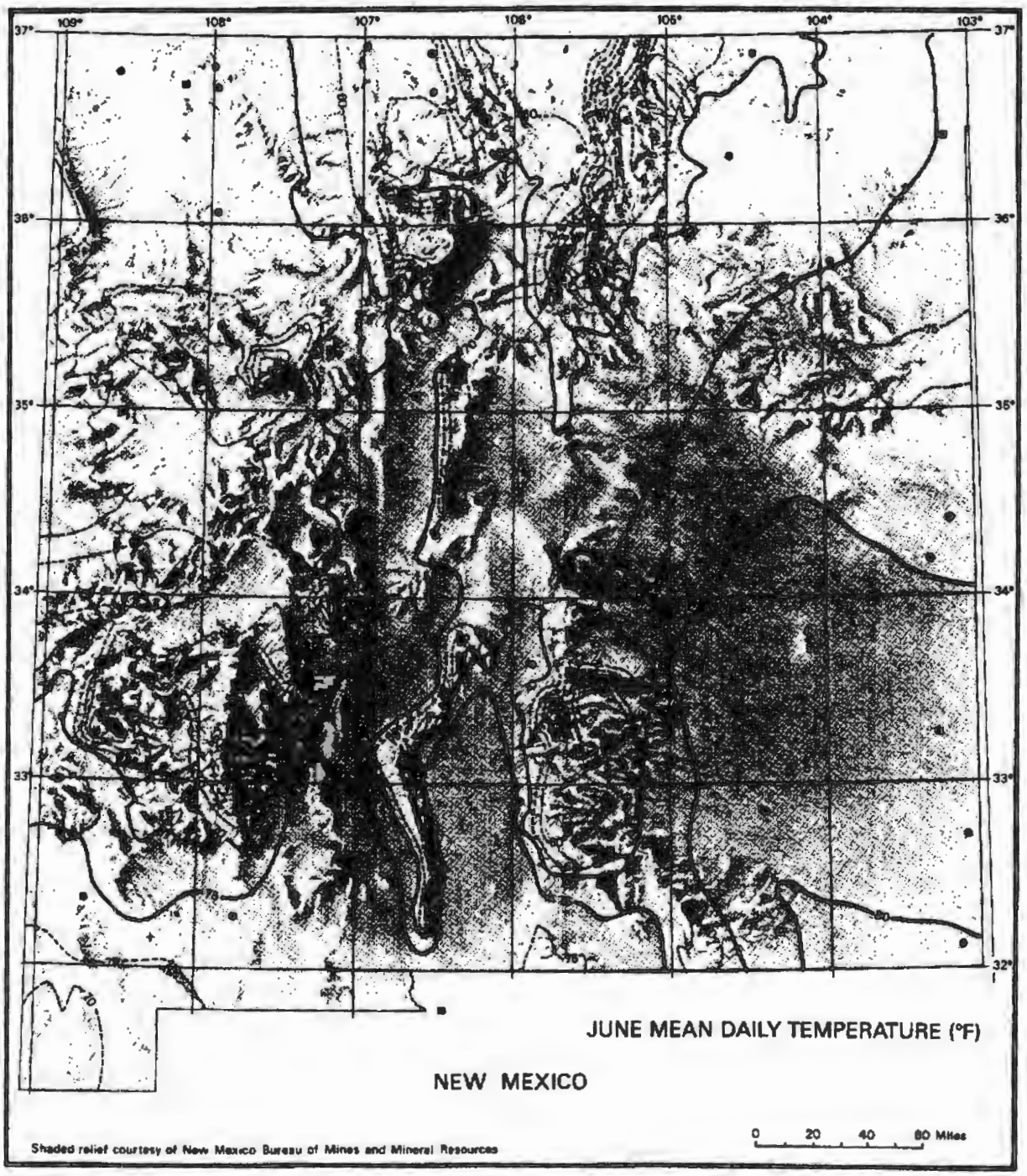

Fig. 2.8. June mean temperatures in New Mexico.

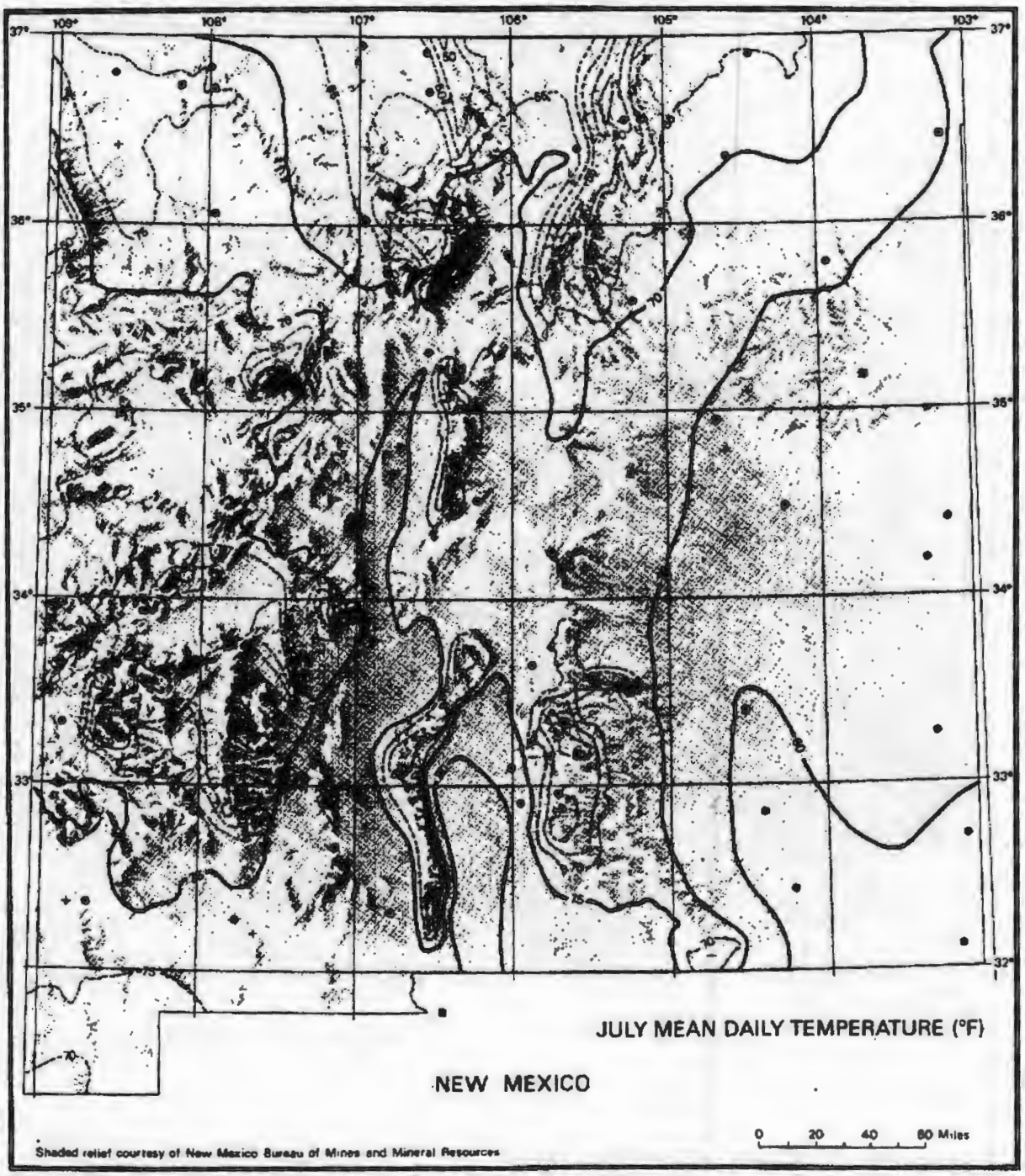

Fig. 2.9. July mean temperatures in New Mexico.

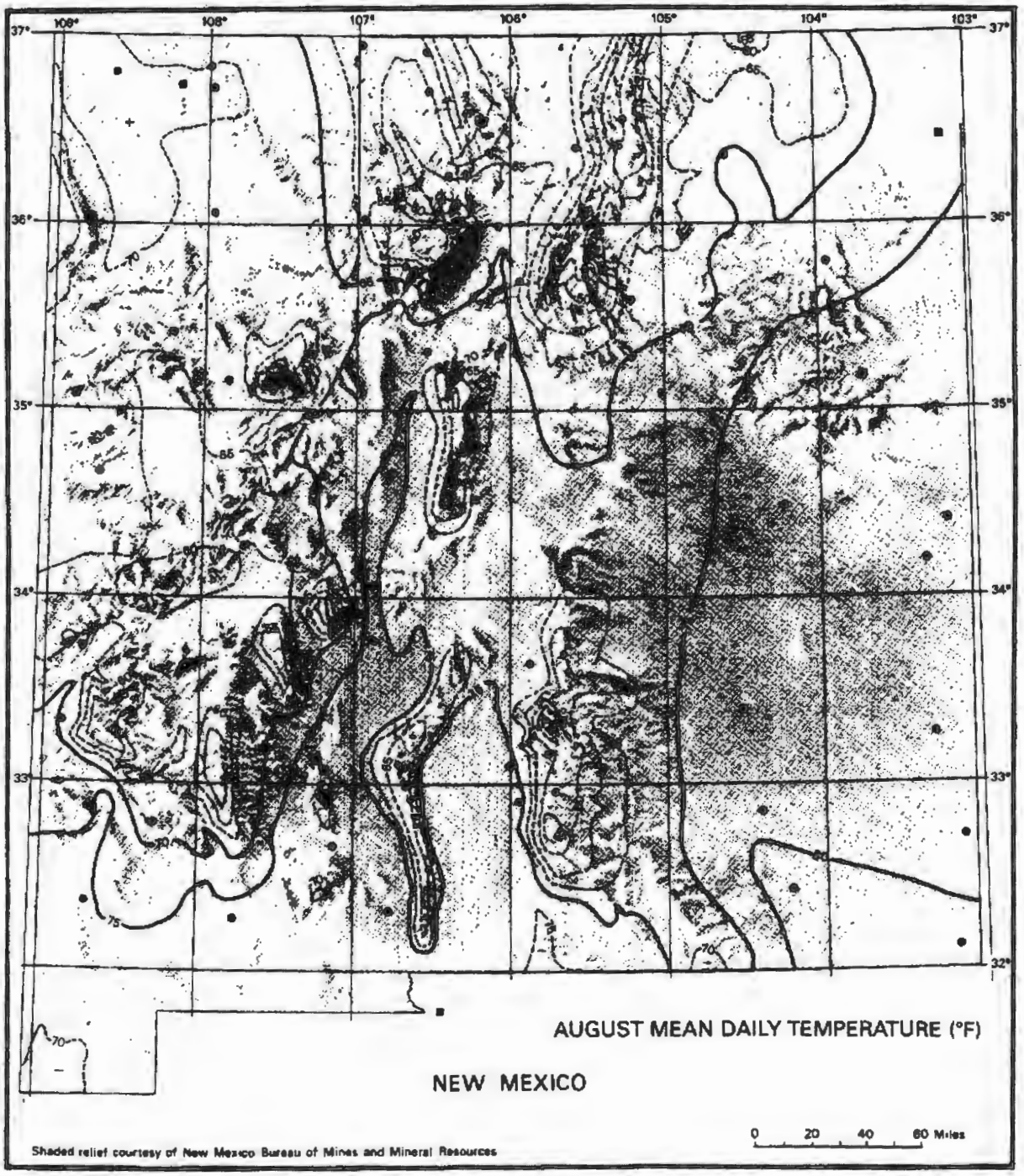

Fig. 2.10. August mean temperatures in New Mexico.

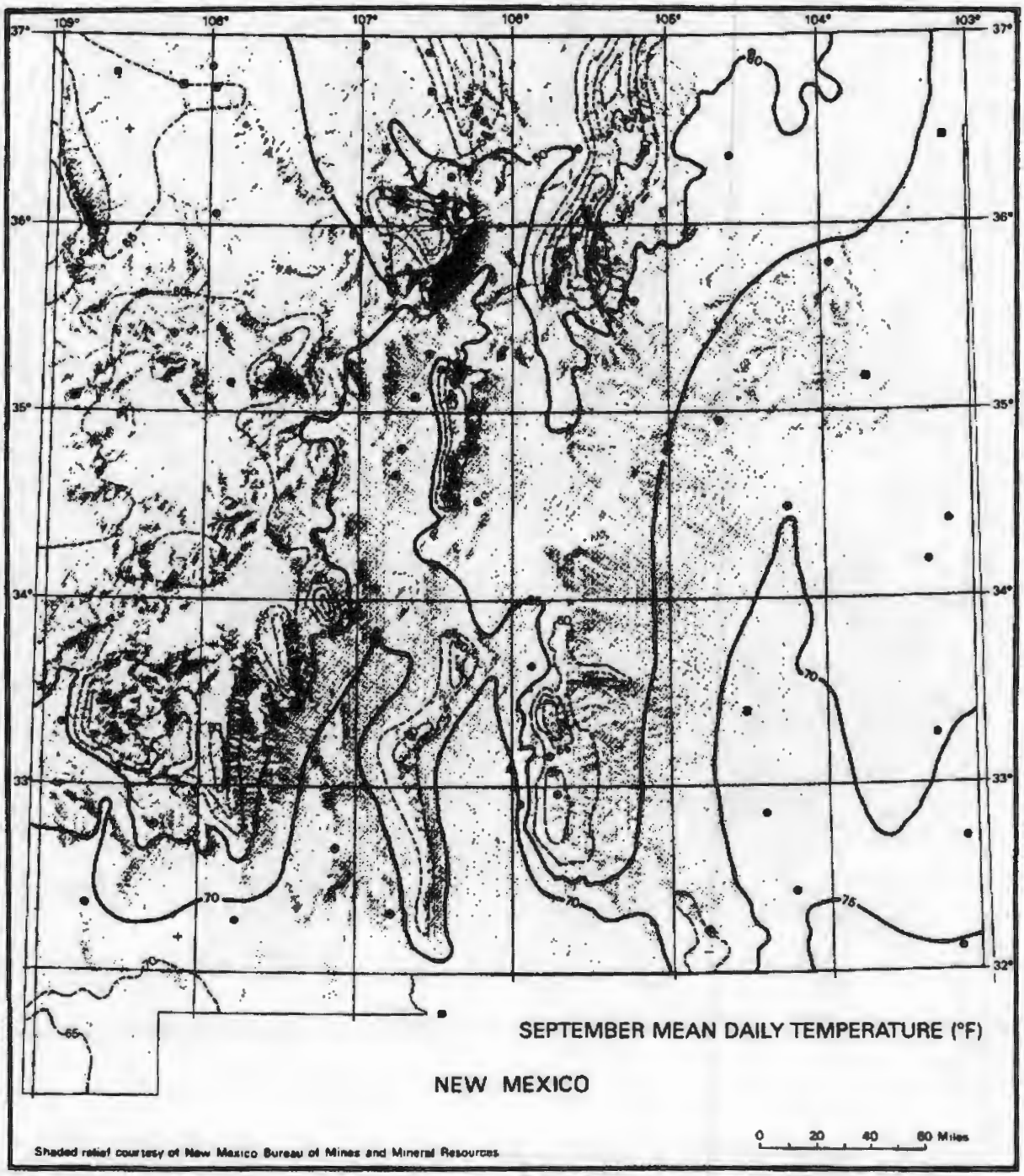

Fig. 2.11. September mean temperatures in New Mexico.

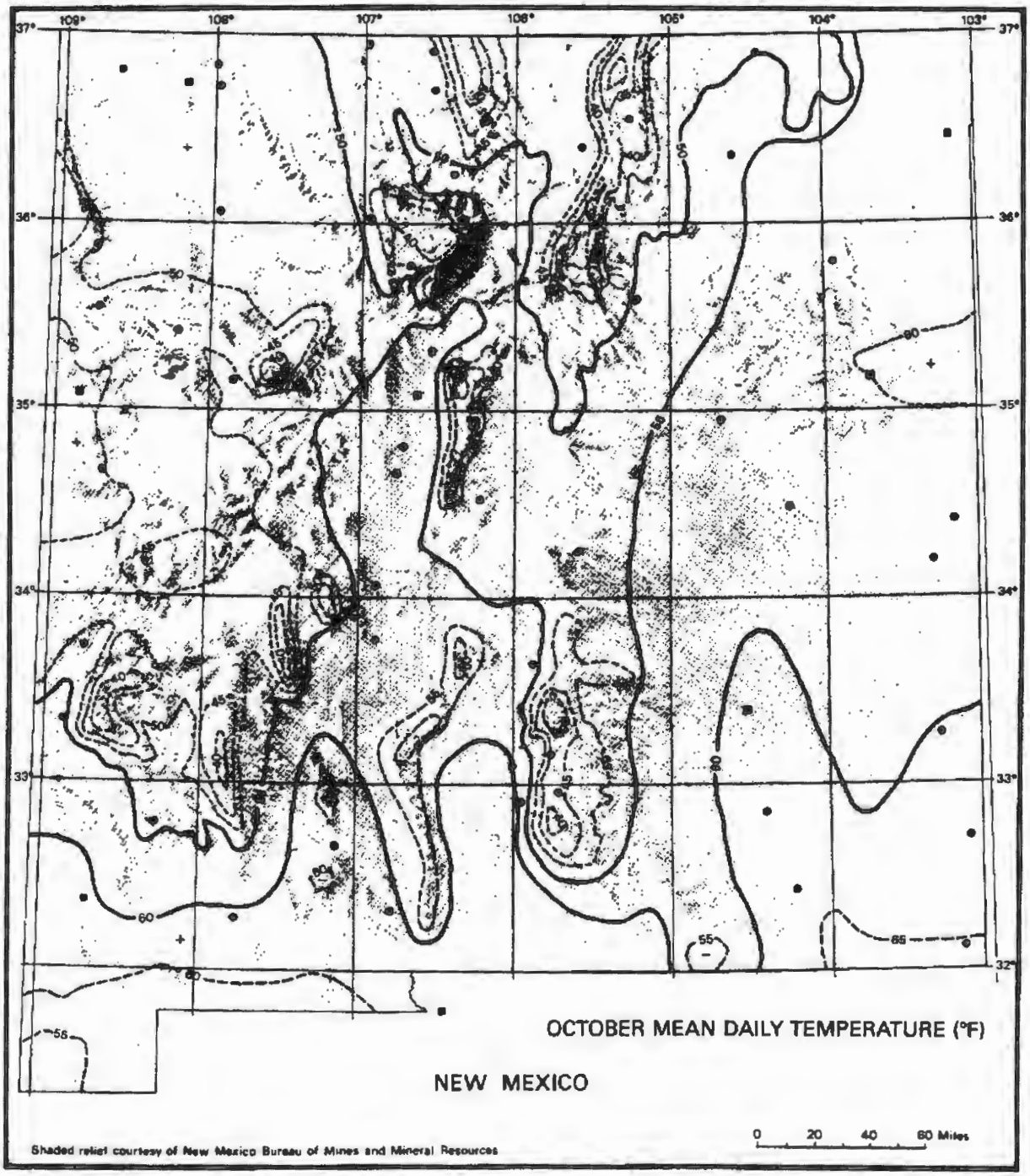

Fig. 2.12. October mean temperatures in New Mexico.

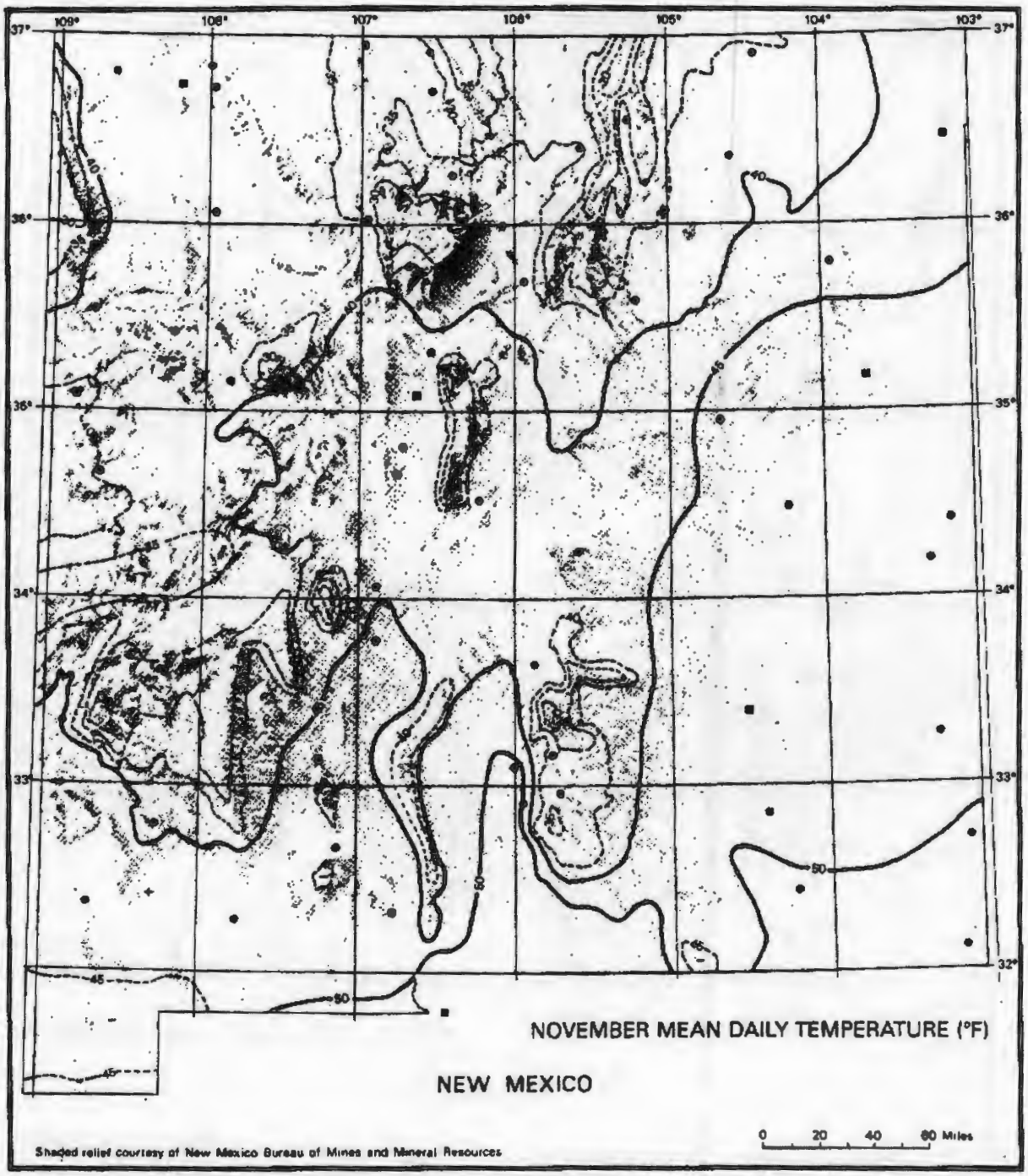

Fig. 2.13. November mean temperatures in New Mexico.

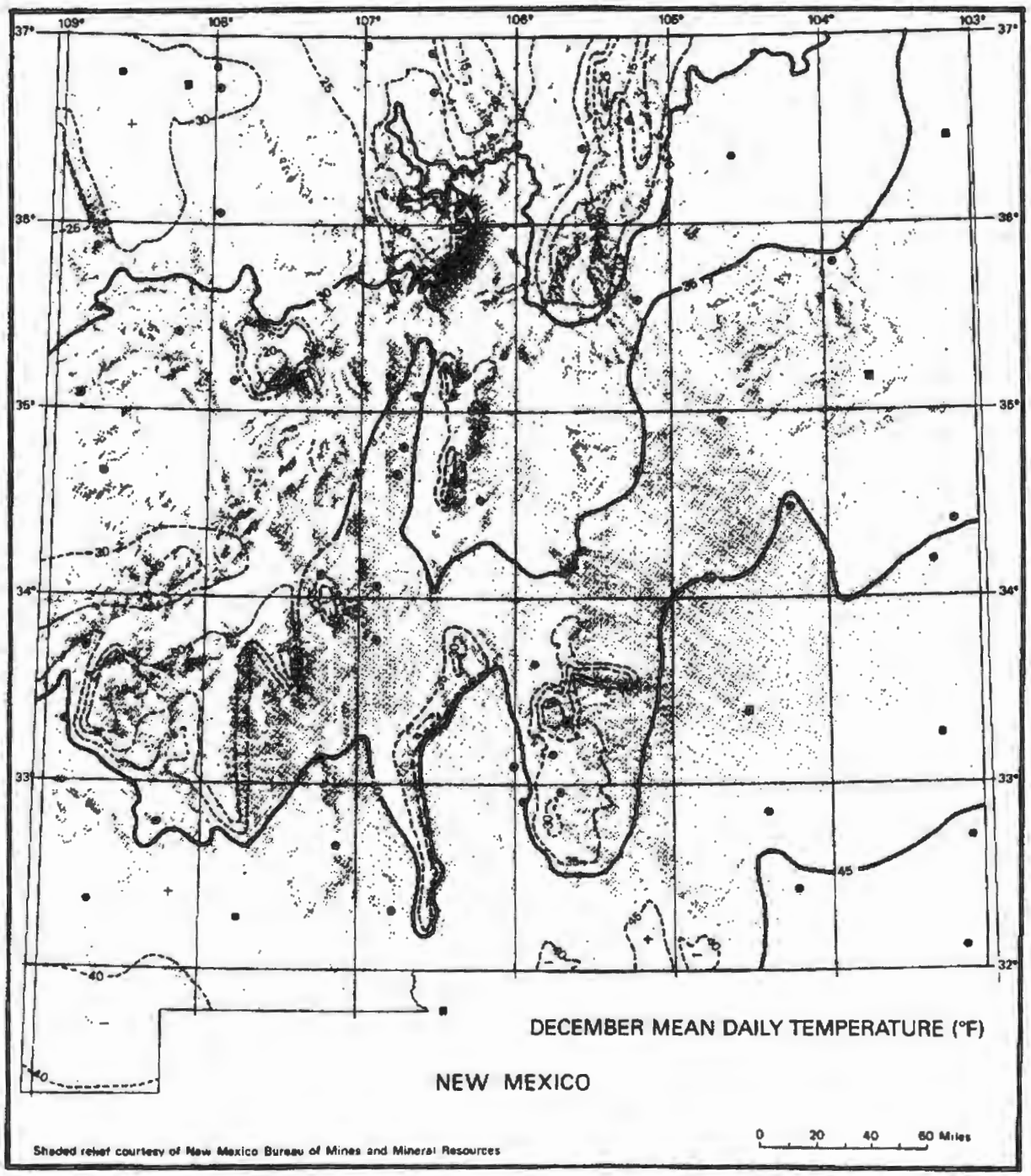

Fig. 2.14. December mean temperatures in New Mexico.

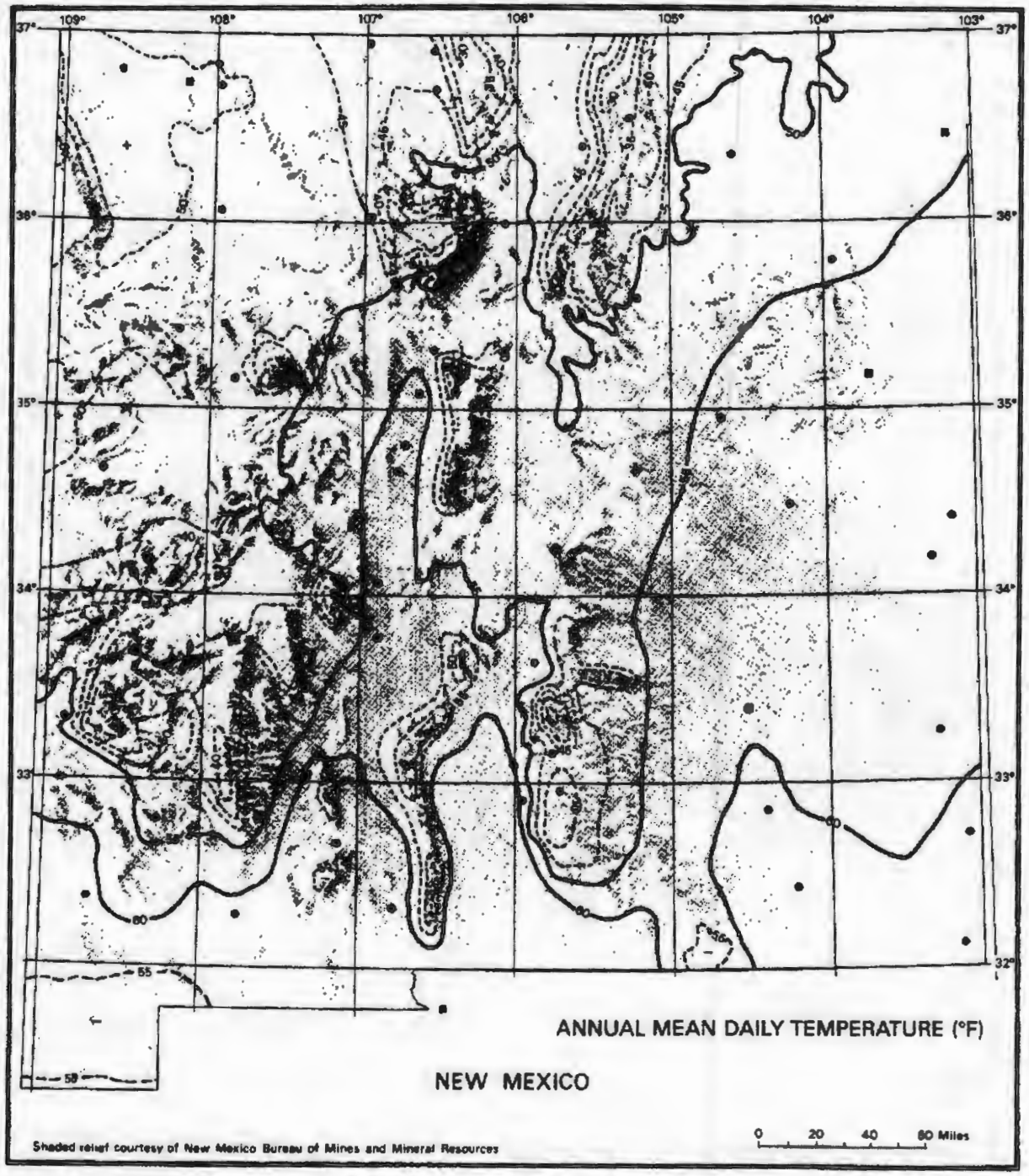

Fig. 2.15. Annual mean temperatures in New Mexico.

4. *Mixing ratio* — the ratio of the mass of water vapor to the mass of dry air in a given volume. Mixing ratio is usually expressed in grams of water vapor per kilogram of dry air. Mixing ratio is nearly identical to specific humidity,which is the ratio of the mass of water vapor to the mass of moist air. The two variables are usually identical because the mass of water vapor is usually <2% of dry air.

5. *Absolute humidity* — the mass of water vapor (grams) per cubic meter of air (g/m^3).

Mean temperature statistics and atmospheric moisture variables are plotted for January, April, July, and October in Fig. 2.16(a)–(d) and are listed in Tables 2.3–2.14 for all months. (Psychometric charts for Los Alamos are given in Appendix E.) The January hourly means are plotted in Fig. 2.16(a). Notice that the nighttime temperatures are slightly cooler at Area G than at TA-59, with the low temperature (0700–0800) averaging about 2°F lower at Area G. The cooler nighttime temperatures at Area G and toward the Rio Grande Valley result from cold-air drainage. Typical January weather conditions of frequent clear skies, light winds, and very low atmospheric moisture content encourage cold-air drainage toward lower elevations. The afternoon temperatures become only slightly warmer at Area G than at TA-59. The slight difference in the afternoon high temperatures between the two sites during January is from the weak winter sunshine and the strong inversions formed by cold-air drainage. Because of the deep pool of cold air centered over the valley in the morning, a relatively large amount of solar energy is required to break the inversion as well as heat the ground-level air.

The relative humidity values mirror the temperatures at both sites. The relative humidity is greater at Area G than at TA-59, especially at night and in the morning when temperatures are lower. The temperatures and wet-bulb temperatures are similar in that the maximums are higher and the minimums are lower at Area G. Dew-point temperatures, good indicators of atmospheric moisture content, show that air at Area G contains slightly more moisture than air at TA-59. The dew-point temperature difference between the two sites reaches a minimum at 0600–0800, the time of the lowest temperature, probably because some of the atmospheric moisture is sublimated into frost as the temperatures approach the dew point. Values of the mixing ratio and absolute humidity (see Table 2.3) confirm that air at Area G has slightly more moisture than air at TA-59.

The temperatures show a quite different pattern at the two sites during April [Fig. 2.16(b)]. First, temperatures remain higher at Area G than at TA-59 for the entire day. However, the temperatures at Area G approach those at TA-59, but only around 0600, the time of the lowest temperature. Strong winds, common during April, help to repress cold-air drainage. Also, the high temperatures are up to 3°F higher at Area G. Because of the warmer temperatures at Area G, the relative humidities are quite similar at both sites. The relative humidity actually becomes greater at TA-59 than at Area G during the afternoon and evening hours. Dew points indicate that more moisture is present at Area G than at TA-59, especially during the daytime. The dew points (and mixing ratio and absolute humidity [see Table 2.6]) are highest during the daytime at both sites. Atmospheric moisture content near the ground decreases during the evening

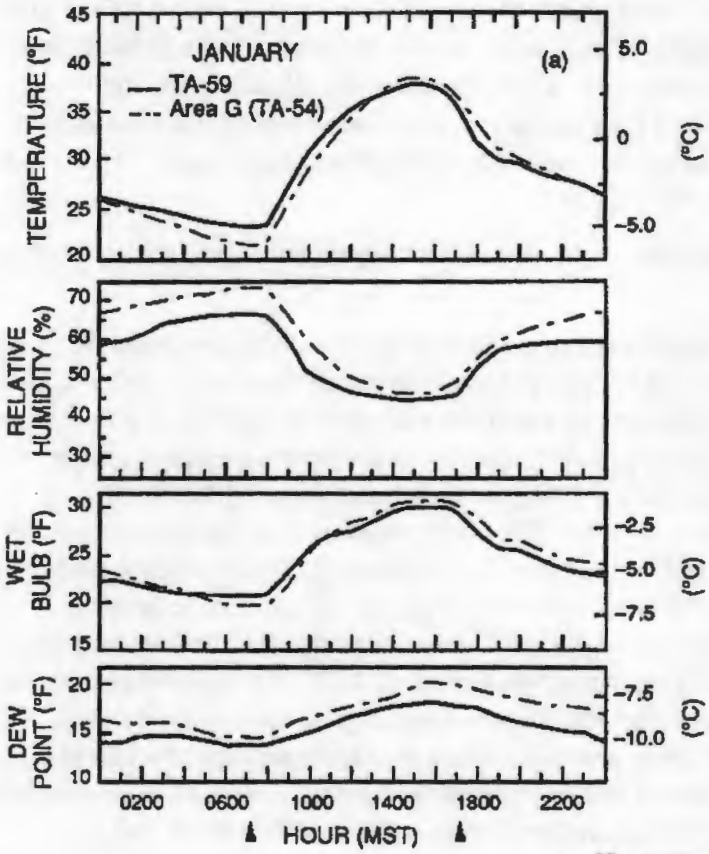

Fig. 2.16(a)–(d). Mean temperatures, relative humidity, and wet-bulb and dew-point temperatures, plotted by hour (Mountain Standard Time), for (a) January, (b) April, (c) July, and (d) October. (Triangles denote mean sunrise and sunset times.)

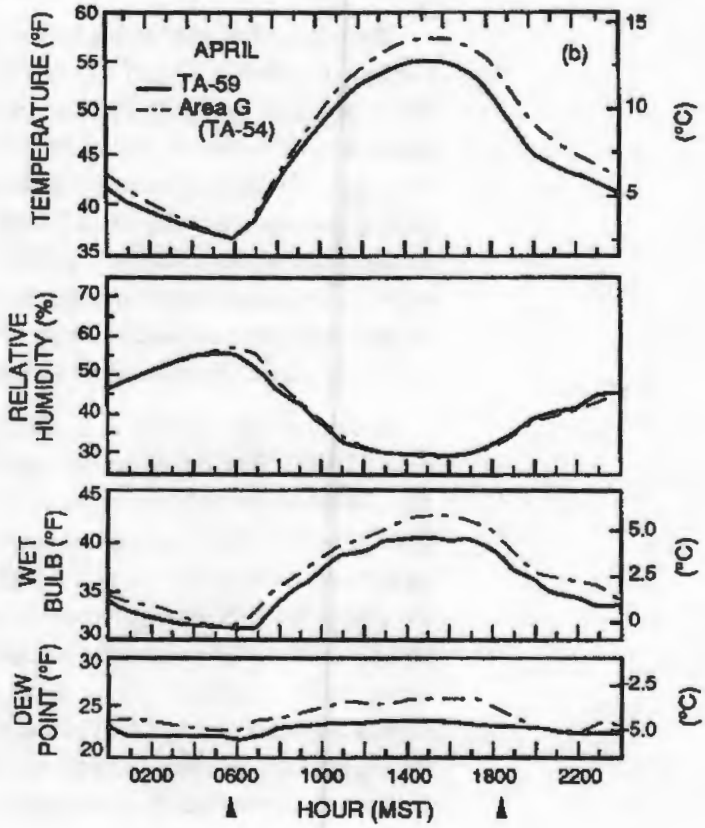

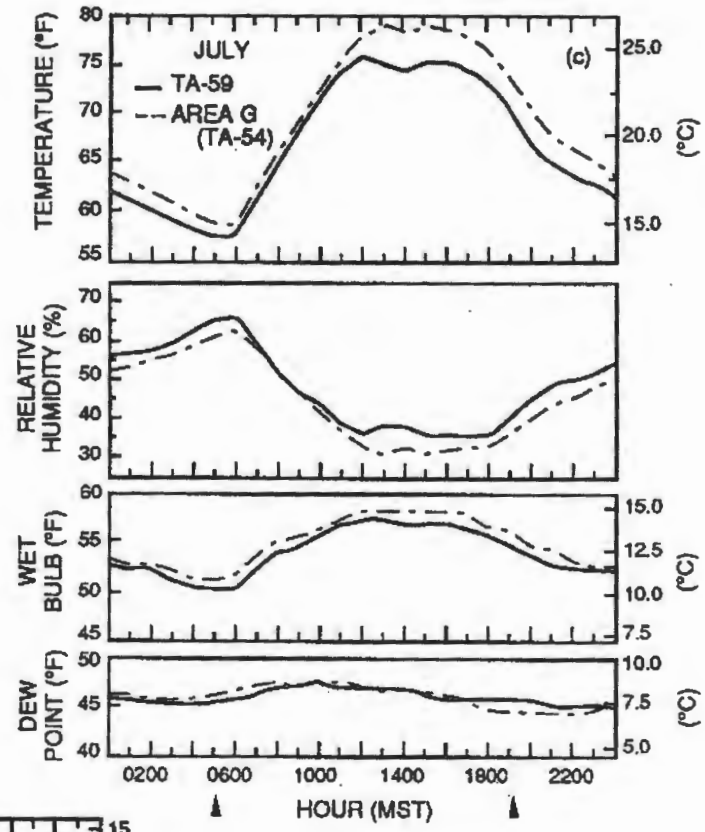

Fig. 2.16 (Continued)

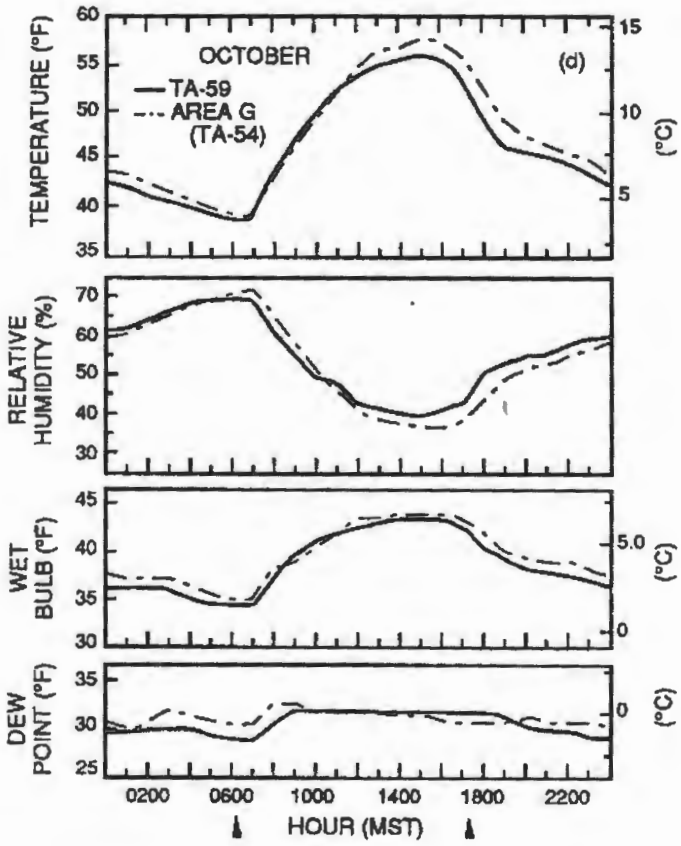

Table 2.3. January hourly temperature, wet-bulb temperature, and relative humidity, with calculations of dew-point temperature, mixing ratio, and absolute humidity given for every 3 hours.

	TA-59					Area G (TA-54)				
	Temperature (°F)			Wet-Bulb	Relative	Temperature (°F)			Wet-Bulb	Relative
Hour	Avg.	Upper 10%	Lower 10%	Temp. (°F)	Humidity (%)	Avg.	Upper 10%	Lower 10%	Temp. (°F)	Humidity (%)
1	26.0	34.5	16.0	22.5	60	25.6	34.0	14.0	23.0	68
2	25.5	33.8	15.1	22.0	61	24.8	33.8	13.8	22.5	69
3	25.0	33.3	14.7	21.5	61	24.1	33.3	13.3	21.5	70
4	24.7	33.6	13.8	21.5	63	23.4	32.9	12.6	21.0	71
5	24.1	32.9	13.1	21.0	64	22.6	32.0	11.8	20.5	72
6	23.8	32.2	13.3	21.0	65	22.0	31.6	11.3	20.0	73
7	23.4	31.8	12.7	20.5	65	21.5	31.5	10.4	19.5	74
8	23.6	32.2	13.3	21.0	64	21.9	31.3	10.2	20.0	73
9	27.6	36.5	17.1	23.5	58	25.4	34.0	14.4	22.0	67
10	31.0	41.0	20.1	25.5	51	29.3	37.4	18.1	25.0	59
11	33.5	44.2	21.7	27.0	48	32.0	40.5	21.4	27.0	54
12	35.4	46.2	23.5	28.0	46	34.4	43.3	23.9	28.5	50
13	36.5	47.5	24.6	29.0	45	36.4	45.9	24.8	29.5	48
14	37.2	48.4	25.5	29.5	44	37.6	47.5	25.9	30.0	47
15	37.8	49.8	25.7	30.0	43	38.2	48.6	26.6	30.5	46
16	37.5	49.5	25.3	29.5	44	38.2	48.6	26.4	30.5	47
17	35.7	46.9	23.9	29.0	45	36.7	47.1	24.8	30.0	49
18	32.2	41.4	21.7	26.5	53	33.5	43.2	22.1	28.0	55
19	30.1	39.0	19.9	25.5	56	31.2	39.7	19.9	26.5	59
20	29.4	38.1	18.9	24.5	57	30.6	38.5	18.7	26.0	62
21	28.7	37.0	18.0	24.0	57	29.1	37.6	17.6	25.0	63
22	27.9	36.5	17.4	24.0	58	28.1	36.5	16.9	24.5	64
23	27.1	35.8	17.2	23.0	58	27.2	35.4	16.0	24.0	66
24	26.6	34.9	16.9	22.5	59	26.4	34.9	14.9	23.0	67
Avg.	29.6			24.5	55	29.2			25.0	61

Hour	Dew-Point Temp. (°F)	Mixing Ratio (g/kg)	Absolute Humidity (g/m^3)	Dew-Point Temp. (°F)	Mixing Ratio (g/kg)	Absolute Humidity (g/m^3)
3	14.0	2.3	2.3	15.5	2.4	2.5
6	13.0	2.2	2.2	14.5	2.3	2.4
9	15.0	2.4	2.4	16.0	2.5	2.6
12	16.0	2.5	2.4	17.5	2.6	2.6
15	17.0	2.6	2.5	19.0	2.8	2.7
18	16.5	2.6	2.5	18.5	2.8	2.9
21	15.0	2.4	2.4	17.5	2.6	2.7
24	13.5	2.2	2.2	16.0	2.5	2.6
Avg.	15.0	2.4	2.4	17.0	2.6	2.6

Table 2.4. February hourly temperature, wet-bulb temperature, and relative humidity, with calculations of dew-point temperature, mixing ratio, and absolute humidity given for every 3 hours.

	TA-59					Area G (TA-54)				
	Temperature (°F)			Wet-Bulb Temp. (°F)	Relative Humidity (%)	Temperature (°F)			Wet-Bulb Temp. (°F)	Relative Humidity (%)
Hour	Avg.	Upper 10%	Lower 10%			Avg.	Upper 10%	Lower 10%		
1	28.0	37.0	16.5	25.0	62	28.8	39.0	18.3	25.5	67
2	27.5	36.5	16.0	24.0	64	27.9	37.6	16.9	24.5	69
3	26.9	36.5	15.1	23.5	65	27.1	36.9	15.8	24.0	70
4	26.3	36.1	14.8	23.0	66	26.4	36.0	14.5	23.5	71
5	25.8	35.8	14.4	23.0	67	25.7	35.8	14.4	23.5	73
6	25.5	34.9	13.5	22.5	68	25.1	35.1	14.2	23.0	74
7	25.1	34.7	13.6	22.5	69	24.5	34.7	14.0	22.5	75
8	26.6	36.3	14.7	23.5	66	25.6	35.4	15.1	24.0	74
9	30.8	41.5	17.8	26.0	57	29.8	39.2	19.2	26.5	66
10	33.6	44.6	20.3	28.5	51	33.1	42.6	21.2	29.0	60
11	35.9	47.3	22.5	29.0	48	35.8	46.0	22.8	30.0	55
12	37.8	49.1	23.2	30.5	45	38.3	49.1	24.1	31.5	52
13	39.2	51.1	23.9	31.0	44	40.3	51.8	25.3	32.5	49
14	40.2	52.5	25.2	31.5	42	41.7	53.8	26.6	34.0	47
15	40.8	53.1	26.1	32.0	41	42.6	54.7	27.8	35.0	47
16	40.5	52.5	25.5	31.5	42	42.9	55.2	28.6	34.5	46
17	39.5	51.4	25.3	31.0	44	42.1	54.0	27.9	34.0	48
18	36.7	48.4	24.1	30.0	48	39.5	51.4	26.6	32.5	52
19	33.4	43.5	21.7	28.5	54	36.1	47.1	24.8	30.5	57
20	32.3	41.4	21.0	27.5	58	34.2	43.7	23.4	29.0	60
21	31.7	41.4	20.1	27.0	58	33.1	42.4	22.3	28.5	62
22	31.0	41.0	19.2	26.5	59	32.0	41.9	21.2	28.0	63
23	30.1	40.3	18.5	25.5	60	31.1	40.8	19.9	27.0	64
24	29.3	39.2	18.0	25.0	61	30.0	39.9	19.0	26.5	65
Avg.	32.3		27.0	56	33.1				28.5	61

Hour	Dew-Point Temp. (°F)	Mixing Ratio (g/kg)	Absolute Humidity (g/m^3)	Dew-Point Temp. (°F)	Mixing Ratio (g/kg)	Absolute Humidity (g/m^3)
3	16.5	2.6	2.6	19.0	2.8	2.9
6	16.0	2.5	2.5	18.0	2.7	2.8
9	18.0	2.7	2.7	20.0	2.9	3.0
12	18.5	2.8	2.7	22.0	3.2	3.2
15	19.0	2.8	2.7	24.0	3.5	3.5
18	19.0	2.8	2.7	23.5	3.4	3.4
21	18.0	2.7	2.7	21.5	3.2	3.3
24	17.0	2.6	2.6	20.0	2.9	3.0
Avg.	18.0	2.7	2.7	21.5	3.2	3.1

Table 2.5. March hourly temperature, wet-bulb temperature, and relative humidity, with calculations of dew-point temperature, mixing ratio, and absolute humidity given for every 3 hours.

	TA-59					Area G (TA-54)				
	Temperature (°F)			Wet-Bulb Temp. (°F)	Relative Humidity (%)	Temperature (°F)			Wet-Bulb Temp. (°F)	Relative Humidity (%)
Hour	Avg.	Upper 10%	Lower 10%			Avg.	Upper 10%	Lower 10%		
1	33.4	42.8	25.2	28.5	54	34.5	44.1	25.3	29.5	60
2	32.6	41.4	24.6	28.0	58	33.5	42.8	24.8	29.0	62
3	31.9	40.8	23.7	27.5	61	32.8	41.7	24.0	28.5	63
4	31.2	40.1	23.2	27.0	63	32.0	40.8	23.5	28.0	65
5	30.5	39.2	22.8	26.5	64	31.2	40.3	22.3	27.5	67
6	30.1	38.8	22.1	26.0	65	30.6	39.0	21.9	27.5	68
7	30.1	38.5	21.9	26.0	65	30.4	39.6	21.7	27.0	70
8	33.2	42.4	25.2	28.0	56	33.6	42.3	25.0	29.5	65
9	36.3	45.9	28.2	30.0	53	37.2	46.9	28.6	31.5	58
10	38.9	49.1	29.8	31.5	47	40.0	50.5	30.7	33.0	52
11	40.9	51.8	30.7	32.5	45	42.4	53.8	31.5	34.0	48
12	42.6	54.1	31.6	34.5	42	44.6	56.7	32.4	35.5	44
13	44.0	55.9	32.2	34.0	40	46.4	58.5	33.1	36.5	41
14	44.9	56.7	32.5	34.5	39	47.5	59.9	33.6	37.0	39
15	45.4	57.6	33.3	35.0	38	48.3	60.8	34.2	37.0	38
16	45.2	57.2	34.0	34.5	39	48.4	61.2	35.1	37.0	37
17	44.3	56.5	33.1	34.0	41	47.7	60.3	34.5	37.0	38
18	42.0	53.6	32.0	33.0	44	45.7	57.9	33.4	36.0	40
19	38.9	48.9	30.2	32.0	49	42.3	53.6	31.5	33.5	45
20	37.4	47.1	29.3	31.0	52	40.0	50.7	30.6	32.5	49
21	36.7	46.4	27.9	30.5	54	38.8	48.9	30.0	32.0	51
22	36.0	45.9	27.3	30.0	55	37.8	48.0	28.8	31.5	53
23	35.2	44.8	26.8	29.5	56	36.6	46.2	27.7	31.0	55
24	34.4	44.4	26.4	29.0	57	35.7	45.1	26.8	30.5	57
Avg.	37.3			30.5	52	39.1			32.0	53

Hour	Dew-Point Temp. (°F)	Mixing Ratio (g/kg)	Absolute Humidity (g/m^3)	Dew-Point Temp. (°F)	Mixing Ratio (g/kg)	Absolute Humidity (g/m^3)
3	20.0	3.0	3.0	22.0	3.2	3.3
6	19.5	2.9	2.9	21.5	3.2	3.3
9	20.5	3.1	3.0	23.0	3.4	3.4
12	21.0	3.2	3.1	24.5	3.5	3.5
15	21.0	3.2	3.1	23.0	3.4	3.4
18	21.0	3.2	3.1	22.5	3.3	3.3
21	21.5	3.2	3.1	22.0	3.2	3.2
24	20.5	3.1	3.1	22.0	3.2	3.2
Avg.	20.5	3.1	3.1	22.5	3.3	3.3

Table 2.6. April hourly temperature, wet-bulb temperature, and relative humidity, with calculations of dew-point temperature, mixing ratio, and absolute humidity given for every 3 hours.

	TA-59					Area G (TA-54)				
	Temperature (°F)			Wet-Bulb Temp. (°F)	Relative Humidity (%)	Temperature (°F)			Wet-Bulb Temp. (°F)	Relative Humidity (%)
Hour	Avg.	Upper 10%	Lower 10%			Avg.	Upper 10%	Lower 10%		
1	40.4	51.1	28.4	32.5	48	41.5	50.9	29.8	33.5	48
2	39.3	49.5	27.5	32.0	51	40.2	49.8	29.1	33.0	51
3	38.3	48.0	27.1	31.5	53	39.2	48.6	28.0	32.5	53
4	37.5	47.5	26.8	31.0	54	38.2	47.5	27.7	31.5	54
5	36.8	46.8	26.1	30.5	55	37.3	46.8	27.0	31.0	56
6	36.2	46.0	25.3	30.0	55	36.5	45.9	26.4	31.0	57
7	38.3	48.4	26.4	31.5	52	38.9	48.7	28.2	32.5	55
8	42.3	52.9	29.3	34.0	47	43.1	53.1	32.0	35.0	49
9	45.4	56.3	31.6	35.5	42	46.3	57.2	34.3	36.5	43
10	48.2	59.7	33.3	37.0	38	49.4	60.8	35.8	38.0	39
11	50.6	62.8	34.5	38.5	34	52.1	63.7	37.9	39.5	35
12	52.5	64.6	37.2	39.0	32	54.4	66.0	39.9	40.0	32
13	53.8	65.3	37.9	40.0	31	55.9	67.6	40.8	41.0	30
14	54.7	66.2	39.0	40.5	30	56.9	68.3	42.4	42.0	30
15	55.1	67.1	39.4	40.5	30	57.6	69.4	42.8	42.5	29
16	55.0	66.6	39.6	40.5	29	57.5	69.3	42.8	42.5	29
17	53.9	65.5	38.3	40.0	30	56.6	68.2	42.3	42.0	30
18	52.0	63.3	36.7	39.0	32	54.9	66.2	40.1	41.0	31
19	48.3	58.8	34.7	36.5	35	51.5	62.6	37.6	39.0	34
20	45.5	55.0	33.1	35.0	39	48.4	58.8	36.1	37.0	38
21	44.4	54.0	31.8	34.5	41	46.7	56.5	34.9	36.5	40
22	43.6	53.6	31.3	34.5	43	45.5	55.2	33.4	36.0	42
23	42.6	52.3	30.6	34.0	46	44.5	54.1	32.5	35.5	44
24	41.7	52.0	29.7	34.0	47	43.1	52.7	31.6	34.5	47
Avg.	45.7			35.5	41	47.3			37.0	42

Hour	Dew-Point Temp. (°F)	Mixing Ratio (g/kg)	Absolute Humidity (g/m^3)	Dew-Point Temp. (°F)	Mixing Ratio (g/kg)	Absolute Humidity (g/m^3)
3	22.5	3.3	3.2	23.0	3.4	3.4
6	21.5	3.2	3.1	22.5	3.3	3.3
9	23.0	3.4	3.3	24.5	3.5	3.4
12	23.0	3.4	3.2	25.0	3.6	3.5
15	24.0	3.5	3.3	26.0	3.8	3.8
18	23.0	3.4	3.2	25.0	3.6	3.5
21	22.0	3.3	3.2	23.5	3.5	3.5
24	23.0	3.4	3.3	23.5	3.5	3.5
Avg.	22.5	3.3	3.2	24.0	3.5	3.5

Table 2.7. May hourly temperature, wet-bulb temperature, and relative humidity, with calculations of dew-point temperature, mixing ratio, and absolute humidity given for every 3 hours.

	TA-59					Area G (TA-54)				
	Temperature (°F)			Wet-Bulb Temp. (°F)	Relative Humidity (%)	Temperature (°F)			Wet-Bulb Temp. (°F)	Relative Humidity (%)
Hour	Avg.	Upper 10%	Lower 10%			Avg.	Upper 10%	Lower 10%		
1	47.1	55.9	37.8	38.5	51	49.1	57.6	39.9	39.5	47
2	46.4	55.2	37.2	38.0	53	47.8	56.5	39.0	39.0	49
3	45.5	53.6	37.0	37.5	54	46.9	55.0	37.9	38.5	51
4	44.7	52.7	36.0	37.5	56	45.8	53.4	36.3	38.0	53
5	43.9	51.8	34.7	37.0	58	44.8	52.7	35.2	37.5	55
6	44.0	52.0	34.7	37.5	60	44.8	52.7	36.0	38.0	56
7	47.6	55.8	38.5	40.0	56	48.9	56.3	39.9	40.5	52
8	51.1	58.8	41.5	41.5	50	52.7	60.6	43.0	42.0	46
9	54.0	62.1	44.2	43.0	43	55.8	64.0	45.9	44.0	41
10	56.7	65.3	46.6	44.0	39	58.9	67.8	48.6	45.0	36
11	58.6	67.6	48.4	45.0	36	61.5	71.4	50.7	45.5	33
12	59.7	68.9	48.7	45.5	34	63.1	73.0	52.0	46.0	30
13	60.6	70.3	49.1	46.0	32	64.1	76.1	53.2	47.0	29
14	61.6	71.6	50.0	46.0	31	65.2	76.8	53.6	47.5	28
15	62.3	72.0	50.7	46.0	31	66.0	77.5	54.7	47.0	26
16	62.0	71.8	50.7	45.5	30	65.8	76.6	54.0	47.0	26
17	61.1	71.2	48.7	45.0	31	64.9	76.3	51.3	47.0	26
18	59.2	69.6	46.4	44.5	35	63.3	73.9	49.5	46.0	28
19	56.3	66.0	45.1	43.5	39	60.4	71.2	47.5	45.0	32
20	52.9	62.2	43.5	42.0	43	56.7	66.9	46.0	43.4	36
21	51.2	60.1	42.6	41.0	47	54.2	63.7	45.1	42.0	39
22	50.3	59.5	41.9	40.5	49	52.7	62.1	44.1	41.5	42
23	49.4	58.5	40.5	40.0	50	51.5	60.4	42.6	41.0	44
24	48.3	57.2	38.8	39.5	51	50.4	58.6	41.5	40.5	45
Avg.	53.1			42.0	44	55.6			43.0	40

Hour	Dew-Point Temp. (°F)	Mixing Ratio (g/kg)	Absolute Humidity (g/m^3)	Dew-Point Temp. (°F)	Mixing Ratio (g/kg)	Absolute Humidity (g/m^3)
3	30.0	4.5	4.3	30.0	4.5	4.5
6	31.0	4.7	4.5	30.5	4.6	4.6
9	32.5	5.0	4.7	33.0	5.0	4.9
12	31.5	4.8	4.5	31.0	4.7	4.5
15	31.0	4.7	4.4	30.0	4.5	4.3
18	31.0	4.7	4.4	29.0	4.3	4.1
21	31.5	4.8	4.6	30.0	4.5	4.4
24	31.0	4.7	4.7	30.0	4.5	4.4
Avg.	31.0	4.7	4.5	30.5	4.6	4.5

Table 2.8. June hourly temperature, wet-bulb temperature, and relative humidity, with calculations of dew-point temperature, mixing ratio, and absolute humidity given for every 3 hours.

	TA-59					Area G (TA-54)				
	Temperature (°F)			Wet-Bulb	Relative	Temperature (°F)			Wet-Bulb	Relative
Hour	Avg.	Upper 10%	Lower 10%	Temp. (°F)	Humidity (%)	Avg.	Upper 10%	Lower 10%	Temp. (°F)	Humidity (%)
1	57.8	66.9	47.8	46.5	46	59.7	68.2	50.4	47.0	45
2	56.8	65.7	47.7	46.0	47	58.1	66.2	49.8	47.0	48
3	55.8	64.2	46.9	45.5	49	57.0	65.1	49.1	46.5	49
4	55.1	63.5	46.4	45.5	52	55.8	64.0	48.0	46.0	51
5	54.3	62.4	45.5	45.0	54	54.4	62.2	46.6	45.0	54
6	54.6	62.4	46.4	45.5	53	54.9	62.6	47.8	46.0	55
7	58.3	66.6	50.2	47.5	48	59.1	67.1	51.6	48.5	50
8	61.8	70.2	53.1	49.0	44	62.6	70.7	55.2	50.0	44
9	65.1	74.3	55.4	50.0	39	66.0	74.3	57.9	51.0	39
10	68.2	77.4	58.6	51.5	35	69.4	78.3	60.6	52.0	34
11	70.7	80.8	60.1	52.5	32	72.4	81.9	63.1	53.0	31
12	72.2	82.9	61.0	53.0	31	74.5	84.2	64.8	54.0	29
13	72.7	84.0	60.3	53.5	30	75.5	86.7	64.9	54.5	28
14	73.3	84.6	60.3	52.5	28	76.1	87.4	65.1	54.5	27
15	73.9	85.1	61.9	52.5	26	76.8	88.2	66.7	55.0	26
16	73.7	84.4	59.7	52.5	26	76.8	87.6	66.4	54.5	25
17	72.6	83.7	58.3	52.0	28	75.9	86.9	63.5	54.5	27
18	71.2	81.9	57.7	51.5	29	74.7	85.8	63.0	54.0	28
19	68.5	78.8	55.9	50.5	32	72.4	82.4	60.6	52.5	29
20	64.4	73.6	54.1	49.5	37	68.3	78.1	57.7	51.0	33
21	62.4	71.1	53.1	49.0	40	64.9	74.1	55.1	49.5	37
22	61.5	70.0	52.3	48.5	41	63.5	72.1	54.0	49.0	39
23	60.6	69.1	51.6	48.0	43	62.2	70.9	52.9	48.5	41
24	59.3	68.0	49.8	47.5	45	60.6	69.1	51.4	48.0	43
Avg.	64.4			49.5	39	66.3			50.5	38

Hour	Dew-Point Temp. (°F)	Mixing Ratio (g/kg)	Absolute Humidity (g/m^3)	Dew-Point Temp. (°F)	Mixing Ratio (g/kg)	Absolute Humidity (g/m^3)
3	37.0	6.0	5.8	38.0	6.2	6.0
6	38.0	6.3	6.0	39.0	6.4	6.2
9	39.5	6.7	6.2	40.0	6.7	6.4
12	39.0	6.6	6.0	40.5	6.8	6.4
15	37.0	5.8	5.2	40.0	6.7	6.3
18	37.0	6.0	5.4	39.0	6.4	6.0
21	38.0	6.3	5.9	38.0	6.2	5.9
24	38.0	6.3	5.9	38.0	6.2	6.0
Avg.	38.0	6.3	5.8	39.0	6.4	6.2

Table 2.9. July hourly temperature, wet-bulb temperature, and relative humidity, with calculations of dew-point temperature, mixing ratio, and absolute humidity given for every 3 hours.

	TA-59					Area G (TA-54)				
	Temperature (°F)			Wet-Bulb	Relative	Temperature (°F)			Wet-Bulb	Relative
Hour	Avg.	Upper 10%	Lower 10%	Temp. (°F)	Humidity (%)	Avg.	Upper 10%	Lower 10%	Temp. (°F)	Humidity (%)
1	61.0	66.0	55.4	51.5	55	62.8	68.0	57.0	52.5	53
2	60.1	64.9	55.0	51.0	57	61.8	68.1	56.1	52.5	55
3	59.1	64.2	53.8	50.5	59	60.7	65.7	55.8	52.0	57
4	58.2	62.9	53.2	50.5	63	59.5	64.2	54.7	51.0	59
5	57.4	62.1	52.9	50.0	65	58.6	63.1	54.0	51.0	62
6	57.5	61.9	53.2	50.5	65	58.6	63.0	54.1	51.5	63
7	61.3	66.2	56.5	52.0	59	62.5	67.5	57.0	63.5	58
8	65.1	70.2	59.0	54.0	52	66.1	71.1	60.4	55.0	52
9	68.5	74.1	62.6	55.0	47	69.3	74.7	63.3	55.5	46
10	71.8	77.7	65.5	56.5	42	72.6	78.3	66.0	56.5	41
11	74.5	81.0	67.8	57.0	38	75.6	81.3	68.7	57.5	37
12	75.9	82.9	68.2	57.5	36	78.0	83.8	70.7	58.5	34
13	75.2	83.7	64.4	57.5	38	79.0	85.8	70.9	58.5	32
14	74.6	84.2	61.9	58.0	38	78.6	86.2	68.5	58.5	32
15	75.2	84.0	63.5	57.5	37	78.9	86.5	69.0	58.5	32
16	75.4	83.5	65.3	57.5	36	78.7	86.2	68.0	59.0	33
17	74.6	82.2	64.0	57.0	36	77.9	85.3	67.3	58.0	33
18	72.8	80.8	63.0	56.0	38	76.2	83.8	66.0	57.0	34
19	70.0	77.7	61.5	55.5	43	73.6	81.7	63.7	56.5	37
20	66.7	73.6	59.2	54.0	47	70.4	77.4	62.6	55.0	41
21	64.9	71.4	57.6	53.5	50	67.8	74.5	59.9	54.5	45
22	63.8	70.0	57.0	52.5	51	66.4	72.7	59.2	53.5	47
23	63.0	68.7	56.3	52.0	52	65.1	71.1	58.6	53.0	49
24	61.9	68.7	56.3	52.0	52	65.1	71.1	58.6	53.0	49
Avg.	67.0			54.0	48	69.3			55.0	45

Hour	Dew-Point Temp. (°F)	Mixing Ratio (g/kg)	Absolute Humidity (g/m^3)	Dew-Point Temp. (°F)	Mixing Ratio (g/kg)	Absolute Humidity (g/m^3)
3	45.0	8.3	7.8	45.5	8.2	8.5
6	45.5	8.5	8.0	46.5	8.6	8.9
9	47.0	9.0	8.2	47.0	8.8	8.2
12	47.0	9.0	8.1	47.0	8.8	8.1
15	46.5	8.9	8.1	46.5	8.6	8.0
18	46.5	8.9	8.1	45.0	8.1	7.5
21	45.5	8.5	7.9	45.5	8.2	7.6
24	46.0	8.7	8.2	46.0	8.4	8.1
Avg.	46.0	8.7	8.1	46.0	8.4	8.1

Table 2.10. August hourly temperature, wet-bulb temperature, and relative humidity, with calculations of dew-point temperature, mixing ratio, and absolute humidity given for every 3 hours.

	TA-59					Area G (TA-54)				
	Temperature (°F)			Wet-Bulb	Relative	Temperature (°F)			Wet-Bulb	Relative
Hour	Avg.	Upper 10%	Lower 10%	Temp. (°F)	Humidity (%)	Avg.	Upper 10%	Lower 10%	Temp. (°F)	Humidity (%)
1	59.1	63.3	54.9	52.0	65	61.0	65.3	56.8	52.5	59
2	58.3	62.6	54.0	52.0	69	60.2	64.4	55.9	52.0	61
3	57.5	61.7	53.6	51.5	70	59.4	63.3	55.2	52.0	64
4	56.7	60.8	52.9	51.5	72	58.5	61.9	54.0	51.5	66
5	56.1	60.1	52.0	51.0	74	57.7	61.5	53.6	51.5	68
6	55.8	59.4	51.6	51.0	73	57.3	61.5	53.1	51.0	69
7	58.4	62.6	54.0	52.0	70	59.8	64.0	55.2	53.0	66
8	62.4	66.6	57.6	54.0	63	63.4	68.0	58.8	54.0	57
9	65.7	70.2	60.4	55.5	56	66.3	70.9	61.5	54.5	49
10	68.6	73.4	63.0	56.6	50	69.2	74.5	61.3	55.0	44
11	71.2	76.5	65.3	57.0	46	72.0	77.7	61.8	55.5	39
12	72.7	78.8	65.0	57.0	41	74.3	80.6	63.3	56.5	36
13	72.6	79.7	62.4	57.5	42	75.3	82.2	64.2	57.0	35
14	72.2	80.1	61.9	57.5	44	75.9	82.8	65.8	57.5	36
15	72.7	80.4	63.0	57.5	42	76.5	82.8	67.3	57.5	35
16	72.9	80.1	64.6	57.0	41	76.9	82.9	69.4	57.5	33
17	72.0	79.3	63.9	57.0	42	75.9	82.2	68.2	57.0	34
18	69.7	77.0	62.1	56.0	46	74.0	81.3	65.8	56.5	36
19	66.3	72.1	59.7	55.5	53	70.8	77.5	63.3	55.5	41
20	63.7	68.5	58.3	54.0	56	67.3	73.2	61.5	54.0	47
21	62.6	67.3	57.4	53.5	58	65.3	70.9	59.4	53.5	50
22	61.8	66.7	56.8	53.0	60	64.1	70.2	59.0	53.0	52
23	60.9	65.8	56.1	53.0	62	63.3	68.7	58.1	53.0	54
24	60.0	64.6	55.6	52.5	63	61.5	66.9	56.8	52.5	57
Avg.	64.6			54.5	57	66.9			54.5	50

Hour	Dew-Point Temp. (°F)	Mixing Ratio (g/kg)	Absolute Humidity (g/m^3)	Dew-Point Temp. (°F)	Mixing Ratio (g/kg)	Absolute Humidity (g/m^3)
3	48.0	9.3	8.8	47.5	9.1	8.8
6	47.5	9.1	8.6	47.0	8.8	8.5
9	49.5	9.9	9.2	46.0	8.4	8.0
12	48.5	9.5	8.7	45.5	8.2	7.7
15	48.5	9.5	8.7	46.5	8.6	8.1
18	48.5	9.5	8.8	45.5	8.2	7.7
21	47.5	9.1	8.5	45.5	8.2	7.8
24	47.5	9.1	8.5	46.0	8.4	8.1
Avg.	48.0	9.3	8.7	46.0	8.4	8.1

Table 2.11. September hourly temperature, wet-bulb temperature, and relative humidity, with calculations of dew-point temperature, mixing ratio, and absolute humidity given for every 3 hours.

	TA-59					Area G (TA-54)				
	Temperature (°F)			Wet-Bulb	Relative	Temperature (°F)			Wet-Bulb	Relative
Hour	Avg.	Upper 10%	Lower 10%	Temp. (°F)	Humidity (%)	Avg.	Upper 10%	Lower 10%	Temp. (°F)	Humidity (%)
1	53.5	60.8	46.0	46.5	61	53.9	60.3	45.9	46.5	61
2	52.7	60.6	46.0	46.5	65	53.1	59.4	45.5	46.0	63
3	52.0	59.4	45.3	46.0	67	52.2	58.5	45.0	45.5	64
4	51.3	58.8	44.1	45.5	69	51.3	57.7	43.9	45.0	66
5	50.6	57.7	43.5	45.0	70	50.4	57.2	42.8	44.5	67
6	50.0	56.8	42.6	44.5	70	49.8	56.1	41.5	44.5	69
7	51.4	58.5	43.7	45.5	69	50.9	57.2	43.0	45.5	69
8	55.5	63.5	47.7	47.5	61	54.9	61.7	47.5	48.0	63
9	58.7	67.3	49.6	49.0	54	58.0	65.3	50.5	49.0	56
10	61.7	70.9	50.7	51.0	50	61.1	68.9	51.8	50.0	50
11	64.3	74.1	52.9	52.0	47	63.8	72.3	53.8	51.0	45
12	66.0	76.1	54.5	52.5	45	66.3	75.2	55.6	52.0	42
13	66.3	76.6	55.4	53.0	43	67.6	77.0	57.0	52.5	40
14	66.9	77.5	55.9	52.5	40	68.4	77.9	58.1	52.5	38
15	67.1	78.1	56.5	52.0	40	68.8	78.1	58.5	52.5	36
16	66.9	77.9	55.9	52.0	39	68.4	77.5	57.7	52.0	35
17	65.7	76.1	55.2	51.5	41	67.4	76.6	57.0	51.5	37
18	62.7	72.7	52.7	50.0	44	65.3	74.3	55.4	50.5	39
19	59.0	67.5	50.5	49.0	51	61.6	70.0	53.1	49.0	45
20	57.5	65.7	49.1	48.5	55	59.1	66.7	50.9	48.5	50
21	56.7	64.9	48.4	48.0	57	57.8	65.3	49.8	48.0	52
22	55.9	64.4	47.3	47.5	58	56.6	63.5	48.2	47.5	55
23	54.9	63.1	46.0	47.0	59	55.6	62.4	47.5	47.0	57
24	53.4	61.5	43.5	46.5	60	53.8	61.0	44.4	46.5	59
Avg.	58.4			48.5	55	59.0			48.5	52

Hour	Dew-Point Temp. (°F)	Mixing Ratio (g/kg)	Absolute Humidity (g/m^3)	Dew-Point Temp. (°F)	Mixing Ratio (g/kg)	Absolute Humidity (g/m^3)
3	41.0	7.1	6.8	40.0	6.6	6.5
6	40.5	7.0	6.7	40.0	6.6	6.5
9	42.5	7.5	7.0	42.0	7.3	7.2
12	43.5	7.9	7.3	42.0	7.3	7.0
15	41.5	7.3	6.7	41.0	7.0	6.6
18	41.0	7.1	6.6	39.5	6.5	6.2
21	41.0	7.1	6.7	40.0	6.6	6.4
24	40.5	7.0	6.6	40.0	6.6	6.4
Avg.	41.5	7.3	6.8	40.5	6.9	6.6

Table 2.12. October hourly temperature, wet-bulb temperature, and relative humidity, with calculations of dew-point temperature, mixing ratio, and absolute humidity given for every 3 hours.

	TA-59					Area G (TA-54)				
	Temperature (°F)			Wet-Bulb Temp. (°F)	Relative Humidity (%)	Temperature (°F)			Wet-Bulb Temp. (°F)	Relative Humidity (%)
Hour	Avg.	Upper 10%	Lower 10%			Avg.	Upper 10%	Lower 10%		
1	42.0	50.4	31.5	36.5	62	43.3	52.3	32.4	37.0	61
2	41.3	49.5	31.3	36.5	64	42.5	51.4	31.5	37.0	63
3	40.7	49.1	30.9	36.0	66	41.6	50.5	31.1	37.0	66
4	40.1	48.4	30.6	35.5	68	40.8	49.6	31.1	36.5	68
5	39.4	47.3	30.0	35.0	69	40.0	48.7	30.6	35.5	70
6	38.8	46.4	30.0	34.5	70	39.3	47.8	30.4	35.0	72
7	39.0	46.6	30.2	34.5	69	39.2	47.7	30.2	35.0	72
8	43.3	51.3	32.0	37.0	62	42.7	51.3	32.0	38.0	66
9	46.9	55.4	34.7	39.5	55	46.3	55.0	34.9	39.0	58
10	49.7	58.5	37.4	41.0	51	49.2	58.1	37.9	40.5	51
11	52.1	61.0	40.1	42.0	48	52.0	61.0	40.8	42.0	46
12	53.8	63.3	41.9	43.0	44	54.6	63.5	42.6	43.5	41
13	54.9	64.4	42.4	43.0	42	56.3	65.1	45.0	43.5	39
14	55.4	65.8	42.3	43.5	41	56.9	66.2	44.6	44.0	38
15	55.7	66.0	43.0	43.5	40	57.5	66.7	45.1	44.0	37
16	55.1	65.5	42.4	43.5	41	57.2	66.9	44.4	44.0	37
17	53.1	63.3	41.4	42.5	43	55.6	66.2	43.7	43.5	39
18	48.8	58.5	37.8	40.5	50	52.5	62.4	40.1	42.0	44
19	46.4	55.0	34.7	39.0	54	49.4	58.8	37.2	41.0	50
20	45.8	55.2	33.6	38.0	56	47.8	57.0	35.1	40.0	52
21	45.2	54.5	33.3	37.5	58	46.7	56.3	34.3	39.5	54
22	44.4	54.0	32.2	37.5	59	45.8	54.9	33.8	39.0	56
23	43.5	52.7	31.8	37.0	60	44.8	53.8	32.9	38.0	57
24	42.5	51.4	31.6	37.0	61	43.5	53.1	32.0	37.5	59
Avg.	46.6			39.0	56	47.7			39.5	54

Hour	Dew-Point Temp. (°F)	Mixing Ratio (g/kg)	Absolute Humidity (g/m^3)	Dew-Point Temp. (°F)	Mixing Ratio (g/kg)	Absolute Humidity (g/m^3)
3	30.0	4.5	4.4	32.0	4.9	4.9
6	29.5	4.4	4.3	30.5	4.6	4.6
9	32.0	5.0	4.8	32.5	5.0	4.9
12	32.0	5.0	4.7	32.0	4.9	4.8
15	32.0	5.0	4.7	31.5	4.8	4.6
18	32.0	5.0	4.8	31.0	4.7	4.6
21	30.5	4.6	4.4	31.0	4.7	4.7
24	29.5	4.4	4.3	30.5	4.6	4.6
Avg.	31.0	4.7	4.6	31.5	4.8	4.7

Table 2.13. November hourly temperature, wet-bulb temperature, and relative humidity, with calculations of dew-point temperature, mixing ratio, and absolute humidity given for every 3 hours.

	TA-59					Area G (TA-54)				
	Temperature (°F)			Wet-Bulb	Relative	Temperature (°F)			Wet-Bulb	Relative
Hour	Avg.	Upper 10%	Lower 10%	Temp. (°F)	Humidity (%)	Avg.	Upper 10%	Lower 10%	Temp. (°F)	Humidity (%)
1	32.8	43.5	20.5	29.0	63	33.6	43.9	22.3	29.0	64
2	32.2	43.0	19.6	28.0	64	32.7	42.6	22.3	28.5	65
3	32.5	42.3	19.9	27.5	65	31.9	41.9	20.8	28.0	67
4	30.9	41.5	19.8	27.0	65	31.2	41.0	20.3	27.5	68
5	30.6	41.2	19.4	26.5	65	30.7	40.5	19.8	27.0	70
6	30.3	41.2	18.3	26.5	65	30.1	39.6	18.9	27.0	71
7	29.9	40.1	18.1	26.5	65	29.5	38.7	18.1	26.5	72
8	32.3	43.2	20.5	27.5	61	31.2	41.0	19.8	27.5	68
9	36.4	48.9	24.1	30.0	54	35.1	45.3	24.4	30.0	60
10	39.4	52.5	26.4	31.5	49	38.3	49.3	26.4	31.5	53
11	41.7	54.9	27.9	33.0	46	41.0	52.7	28.4	33.0	47
12	43.2	56.3	29.3	34.0	44	43.4	55.4	30.4	34.5	44
13	44.0	57.0	29.8	34.5	43	45.3	57.7	31.5	35.5	42
14	44.9	58.6	30.9	35.5	43	46.4	59.7	32.0	36.5	41
15	45.0	59.0	31.5	35.5	42	46.9	60.6	32.5	37.0	41
16	44.2	58.1	30.7	35.0	44	46.4	60.3	32.4	36.5	42
17	41.5	54.7	28.6	33.5	49	44.3	57.7	30.9	35.0	45
18	37.7	49.5	25.9	31.5	53	41.2	53.6	28.6	33.5	50
19	36.5	48.2	24.8	31.0	54	38.9	50.5	27.0	32.5	54
20	36.1	47.8	23.9	30.5	55	37.8	48.9	25.7	32.0	56
21	35.4	47.3	23.0	30.0	56	36.8	48.2	24.6	31.5	57
22	34.7	46.6	22.1	20.5	57	35.9	47.1	23.9	30.5	59
23	33.8	45.5	21.4	29.0	58	35.1	46.0	23.0	30.0	61
24	33.1	43.9	20.8	28.5	60	34.2	45.1	22.5	29.5	62
Avg.	36.6			30.5	55	37.4			31.0	57

Hour	Dew-Point Temp. (°F)	Mixing Ratio (g/kg)	Absolute Humidity (g/m^3)	Dew-Point Temp. (°F)	Mixing Ratio (g/kg)	Absolute Humidity (g/m^3)
3	20.5	3.1	3.1	22.0	3.2	3.3
6	20.0	3.0	3.0	22.0	3.2	3.3
9	21.0	3.2	3.1	23.0	3.4	3.4
12	22.0	3.3	3.2	23.5	3.5	3.5
15	23.5	3.5	3.4	24.5	3.5	3.5
18	22.5	3.3	3.3	23.5	3.5	3.6
21	21.5	3.2	3.2	23.0	3.4	3.5
24	21.0	3.2	3.2	22.0	3.2	3.3
Avg.	21.5	3.2	3.2	23.0	3.4	3.4

Table 2.14. December hourly temperature, wet-bulb temperature, and relative humidity, with calculations of dew-point temperature, mixing ratio, and absolute humidity given for every 3 hours.

	TA-59					Area G (TA-54)				
	Temperature (°F)			Wet-Bulb Temp. (°F)	Relative Humidity (%)	Temperature (°F)			Wet-Bulb Temp. (°F)	Relative Humidity (%)
Hour	Avg.	Upper 10%	Lower 10%			Avg.	Upper 10%	Lower 10%		
1	27.6	37.4	17.6	23.5	60	27.6	36.3	18.0	25.0	70
2	27.2	37.0	17.4	23.0	61	26.9	35.2	17.2	24.5	71
3	26.9	36.3	16.7	23.0	62	26.3	34.7	16.0	24.0	72
4	26.5	35.4	16.2	22.5	64	25.7	34.3	15.4	23.5	73
5	25.8	34.5	15.4	22.5	66	25.0	33.6	14.7	23.0	75
6	25.3	34.0	15.3	22.0	67	24.5	33.3	14.2	22.5	76
7	25.0	33.6	15.3	22.0	67	24.1	32.9	13.6	22.0	76
8	25.7	34.3	15.6	22.5	65	24.4	33.3	14.5	22.5	76
9	29.8	39.4	19.0	25.5	58	27.7	36.1	17.8	25.0	70
10	33.1	43.0	22.1	27.0	51	31.2	39.9	21.6	27.0	63
11	35.4	45.9	24.4	29.0	49	34.0	43.7	24.6	29.0	58
12	37.0	47.5	26.1	30.0	47	36.3	46.0	26.4	30.0	54
13	37.8	48.0	26.8	31.0	45	38.2	48.6	27.3	31.5	51
14	38.4	48.9	26.6	31.5	44	39.4	50.0	28.2	32.5	50
15	38.6	48.9	27.1	31.0	44	39.9	50.5	28.8	32.5	50
16	37.8	48.0	26.6	30.5	45	39.5	50.2	28.0	32.5	51
17	35.2	44.6	25.2	29.0	49	37.3	47.8	26.6	31.0	54
18	31.9	39.9	23.0	27.0	55	34.2	43.9	24.3	29.0	60
19	30.9	39.2	21.7	26.5	58	32.5	41.5	22.8	28.5	63
20	30.4	38.7	21.0	25.5	59	31.5	39.9	22.1	27.5	64
21	29.6	37.9	19.9	25.0	59	30.7	39.4	21.4	27.0	65
22	29.1	37.8	19.6	24.5	59	29.9	38.3	20.3	26.5	66
23	28.7	37.6	18.7	24.5	60	29.1	38.1	18.9	25.5	67
24	28.3	37.6	18.3	24.0	60	28.3	37.4	18.1	25.0	69
Avg.	30.9			26.0	56	29.4			27.0	64

Hour	Dew-Point Temp. (°F)	Mixing Ratio (g/kg)	Absolute Humidity (g/m^3)	Dew-Point Temp. (°F)	Mixing Ratio (g/kg)	Absolute Humidity (g/m^3)
3	16.0	2.5	2.5	17.5	2.6	2.7
6	15.5	2.4	2.4	17.5	2.6	2.7
9	17.0	2.6	2.6	19.0	2.8	2.9
12	19.0	2.8	2.7	21.0	3.1	3.1
15	19.0	2.8	2.7	23.0	3.3	3.3
18	18.0	2.7	2.7	21.0	3.1	3.1
21	17.0	2.6	2.7	20.5	3.0	3.1
24	16.5	2.6	2.7	19.0	2.8	2.9
Avg.	17.0	2.6	2.6	20.0	2.9	3.0

and early morning hours as cooling causes condensation (dew or frost) of the water vapor.

The analyses for the warmest month, July, are shown in Fig. 2.16(c). Temperatures are higher at Area G than at TA-59 for all hours, especially during the afternoon when the Area G temperatures are up to 4°F higher.

Notice the curious small dip in temperatures at the sites at 1400. Frequent thundershower activity at this time is responsible for the slight temperature decreases. Mean temperatures again rise for the next few hours when thundershowers and associated clouds are less frequent. The figure also shows that the average maximum temperature occurs around 1200 at TA-59 and 1300 at Area G. Thundershowers, on average, cool TA-59 temperatures between 1200 and 1300, whereas sunshine still warms Area G during this time.

Relative humidity is greater at TA-59 than at Area G for most of the day, reflecting the higher Area G temperatures. Note the small increase in average relative humidity at both sites during the early afternoon because of increased thundershower activity. Contrary to January and April statistics, dew-point values at TA-59 are similar to those at Area G during July. In fact, the mixing ratio and absolute humidity values at TA-59 are actually higher than those at Area G during July (see Table 2.9). The greater rainfall amounts and frequencies at TA-59 (and areas near the Jemez Mountains) are responsible for the relatively high atmospheric moisture content. The average mixing ratio and atmospheric moisture content at TA-59 is more than 3.5 times higher during July than during January.

Temperature differences are narrower during October, as shown in Fig. 2.16(d). Temperatures at Area G are generally 1°F–2°F greater than those at TA-59, except during the late morning hours when temperatures are equal to, or slightly greater than, those at TA-59. The relative humidity at TA-59 is generally greater, except for late-morning hours. Dew-point temperatures are slightly higher at Area G, and mixing ratios and absolute humidity are greater at Area G (see Table 2.12).

2.4 Temperature Probabilities

Maximum and minimum temperatures were analyzed for frequency of occurrence by month at both Los Alamos (TA-59) and White Rock. Results are shown for Los Alamos and White Rock in Tables 2.15 and 2.16, respectively. The maximum White Rock temperatures are somewhat higher than those at Los Alamos for all probabilities. The White Rock maximum temperatures are especially higher during summer months. White Rock minimum temperatures are generally lower during winter months and higher during summer months, especially at probabilities less than 50% (colder-than-normal temperatures).

The variation in both the maximum and minimum temperatures, as indicated by the standard deviation, is greater during winter months at both sites. Stronger storms and pressure patterns, common during the winter, cause the larger temperature variations. At

both sites, the extreme low values are further from the median value (50%) than are the extreme high values. The median values are very close to the mean values at both sites.

Users of these data should be cautioned about comparing extreme values between the two sites because of the disparity in data: the records from Los Alamos cover a much longer time period than those from White Rock.

2.5 Design Temperatures

Design temperatures represent expected extreme hot and cold conditions based on compiled data. Winter and summer design data are used in specifications for heating, ventilating, and air-conditioning equipment.

Design temperatures are temperatures that are equaled or exceeded for a specified number of hours in a year. The number of hours is given as a percentage of the 8760 hours contained in a 365-day year. For example, a 0.1% design temperature indicates a temperature that is equaled or exceeded for 8.75 hours during the year. Summer and winter design temperatures were calculated at TA-59 and Area G using historical, 15-minute-averaged temperatures. Winter and summer design temperatures represent extreme cold and warm temperatures, respectively, for the entire year, not just for the respective season.

The winter and summer extreme design temperatures for 0.1%, 0.2%, 0.5%, 1.0%, 2.0%, and 5.0% are shown in Table 2.17. The winter design temperatures for Area G are lower than those for TA-59 because of cold-air drainage. In fact, the lowest recorded 15-minute-averaged temperature at Area G is almost 8°F colder than at TA-59. The 0.1% and 0.2% winter design temperatures are also lower at Area G. The design temperatures become similar at the two sites for the higher frequencies, with identical design temperatures at the 5% frequency.

Summer design temperatures are also more extreme at Area G. The highest recorded 15-minute-averaged temperature at Area G is 93.9°F, which is 2.3°F higher than at TA-59. The design temperatures are 2.1°F–2.7°F higher at Area G than at TA-59 for the 0.1%–5.0% frequencies.

2.6 Vertical Temperature Profiles

Vertical temperature profiles (measurements of temperature at different heights) are useful in determining low-level, atmospheric thermal stability. Vertical mean temperature profiles were calculated from the 15-minute-averaged data taken at four heights on the meteorological tower at TA-50 during the years 1985–1987. The January, April, July, and October profiles are presented in Fig. 2.17(a)–(d), respectively. The four levels at TA-50 (12, 23, 46, and 92 m) are indicated by black dots. In addition, a 1.2-m-level temperature was estimated using the 1.2-m level at TA-59 (also indicated by black dots on the figure).

Table 2.15. Los Alamos temperature probabilities, 1918–1988. Column headings represent the percentage of time that the maximum (minimum) temperature will equal or exceed (fall below) the indicated temperature.

	Low	1%	5%	10%	25%	50%	75%	90%	95%	99%	High	Std Dev
Maximum Temperature (°F)												
January	4	17	25	29	34	40	45	50	53	57	64	9
February	10	21	28	31	37	44	50	54	57	62	69	9
March	17	26	33	37	43	50	56	61	64	68	73	9
April	24	34	42	45	53	60	65	69	71	74	80	9
May	33	44	52	56	63	69	73	77	78	83	89	8
June	52	60	65	69	74	79	83	86	88	90	95	7
July	57	65	70	73	77	81	84	87	89	92	95	6
August	52	65	68	71	75	78	82	84	86	89	92	5
September	37	52	59	63	68	73	77	80	82	86	94	7
October	28	38	45	50	57	63	68	72	74	78	84	8
November	11	26	32	35	42	50	56	60	63	66	72	9
December	11	22	27	30	35	41	48	52	54	59	64	8
Minimum Temperature (°F)												
January	−18	−4	2	6	12	19	24	28	31	35	41	9
February	−14	−1	6	10	16	22	27	31	33	36	43	8
March	−3	6	12	15	21	27	32	35	38	42	53	8
April	5	15	21	24	29	34	39	42	45	49	58	7
May	24	26	31	33	38	42	47	51	53	58	66	7
June	28	37	41	43	47	52	56	59	61	65	69	6
July	37	45	49	50	52	55	58	60	62	65	71	4
August	40	45	48	49	51	54	56	59	60	64	72	4
September	23	32	37	40	45	48	52	54	56	60	68	6
October	15	20	25	28	33	38	42	46	49	52	58	7
November	−14	6	12	16	22	28	32	36	38	42	47	8
December	−13	0	6	10	15	21	26	30	32	36	40	8

The January temperature profiles show the strongest and most persistent inversions; the long nights and dry atmosphere encourage strong radiational cooling from the ground. At 0600, the temperature at 12 m averages almost 4°F higher than at 1.2 m. The mean surface temperature is still slightly below the 12-m temperature at 0900, 2 hours after sunrise. Solar heating produces profiles that indicate cooler temperatures with height at 1200 and 1500. However, by 1800, strong radiational cooling causes an inversion to form from the ground to 23 m above the ground.

In April, stronger winds and less radiational cooling at night (because of shorter nights than in winter) give weaker and shallower inversions [Fig. 2.17(b)]. The stronger winds mix the lower atmosphere, thereby limiting the depth and intensity of surface-based inversions. Even at the coldest time (0600) of the day, radiational cooling is insufficient to cause a mean inversion extending to the 92-m level. The inversion is also

Table 2.16. White Rock temperature probabilities, 1965–1988. Column headings represent the percentage of time that the maximum (minimum) temperature will equal or exceed (fall below) the indicated temperature.

	Low	1%	5%	10%	25%	50%	75%	90%	95%	99%	High	Std Dev
Maximum Temperature (°F)												
January	8	17	26	30	36	42	48	53	57	61	65	9
February	18	24	30	34	40	47	54	59	61	65	73	10
March	20	30	38	41	48	55	62	68	70	73	78	10
April	30	37	44	48	57	64	69	73	75	79	83	9
May	36	46	56	61	68	72	78	82	84	87	90	9
June	57	62	68	72	77	83	88	92	94	96	100	8
July	60	71	76	79	83	86	90	92	94	96	100	5
August	58	67	73	76	80	83	86	89	90	94	98	5
September	40	54	60	65	72	76	81	85	87	90	98	8
October	33	38	48	53	60	66	72	76	78	82	90	9
November	17	30	36	40	45	53	60	65	67	70	73	10
December	15	23	28	32	37	43	49	54	56	60	65	8
Minimum Temperature (°F)												
January	−29	−10	−4	0	9	16	21	26	29	33	38	9
February	−12	−4	4	8	15	19	24	29	32	38	42	8
March	−5	7	13	17	22	27	31	35	37	43	49	7
April	12	18	21	24	28	32	37	42	45	49	52	7
May	18	25	29	32	36	41	46	50	52	56	60	7
June	34	37	40	42	46	50	54	58	60	63	67	6
July	45	47	49	51	54	56	58	60	62	64	66	4
August	36	42	46	48	51	54	57	59	60	64	67	4
September	28	30	35	38	42	47	51	54	56	59	61	6
October	14	18	24	26	30	35	40	44	46	52	56	7
November	−14	6	12	16	20	24	29	34	36	39	46	7
December	−17	−7	0	5	11	16	22	27	29	34	44	9

weaker in April, with only a 2°F decrease from the 1.2- to 12-m levels. The increased sunshine gives strong warming at the surface by 0900. The surface-based inversion does not form until after 1800.

Short nights and relatively high humidity also help keep inversions weak in July [Fig. 2.17(c)]. As in April, mean inversions do not extend to the 92-m level. Strong sunshine forces an unstable temperature structure as early as 0900. Low-level temperatures peak at 1200, whereas upper temperatures peak at 1500. This mean temperature difference is caused by frequent afternoon thundershowers that cool temperatures at the lower levels through evaporation.

Weaker sunshine, longer nights, and a drier atmosphere promote stronger inversions in October [Fig. 2.17(d)]. A ground-based inversion extending to the 92-m level

Table 2.17. Winter and summer design temperatures at TA-59 and Area G. Column headings represent the percentage of time[a] the temperature is equaled or exceeded.

	Winter						
	Low	0.1%	0.2%	0.5%	1.0%	2.0%	5.0%
Temperature (°F)							
TA-59	−8.5	3.2	6.3	10.2	13.5	17.6	23.2
Area G	−16.4	1.2	5.0	9.9	13.3	17.1	23.2

	Summer						
	5.0%	2.0%	1.0%	0.5%	0.2%	0.1%	High
Temperature (°F)							
TA-59	73.4	79.0	81.5	83.7	85.8	87.1	91.6
Area G	76.1	81.5	83.8	85.8	88.0	89.2	93.9

[a]Percentage of 8760 hours in a 365-day year.

typically forms by 1800 and continues through 0600. The weaker October sunshine produces a modest lapse rate at 1200 and 1500.

2.7 Degree Days

2.7.1 Heating-Degree Days

A heating-degree day is defined as the number of degrees (Fahrenheit) the daily mean temperature is *below* a certain temperature; 65°F is a commonly used base. For example, if a certain day has a high temperature of 60°F and a low temperature of 40°F, the daily mean would be 50°F, which would give 15 heating-degree days (from the 65°F base) for this day. Heating-degree days (65° base) are good for estimating fuel requirements for heating and are also used for structural design considerations.

Los Alamos heating-degree days for different temperature bases (40°F–75°F) are listed in Table 2.18. Monthly heating-degree days are inversely proportional to mean temperatures: on average, January has the most and July has the least heating-degree days. For the most commonly used 65°F base, heating-degree days average from more than 1100 in January and December down to 14 during July. The cold-season monthly minimum and maximum heating-degree days (65°F base) show that maximums exceed minimums by 60%–100%. Heating-fuel needs are also expected to vary this much.

White Rock heating-degree days are shown in Table 2.19. Monthly heating-degree days are similar for Los Alamos and White Rock. Heating-degree days at White Rock are generally fewer than at Los Alamos, except for January, October, and December.

Again, caution should be used in comparing heating-degree-day extremes between the sites because of the smaller data record for White Rock.

Monthly heating-degree days, using the 65°F base, are listed in Tables 2.20 and 2.21 for Los Alamos and White Rock, respectively. The data record begins in 1951 for Los Alamos and in 1965 for White Rock.

New Mexico annual heating-degree days (65°F base) are plotted in Fig. 2.18 (Morris and Haggard 1985, reproduced with permission). The heating-degree days follow the temperature pattern, increasing toward the north and somewhat toward the northeast.

2.7.2 Cooling-Degree Days

A cooling-degree day differs from a heating-degree day in that it represents the number of degrees (Fahrenheit) that the daily mean temperature is *above* a certain temperature. Cooling-degree days are used for estimating fuel costs for cooling buildings and are also used for structural design considerations. The base of 65°F is commonly used. However, a slightly higher base, such as 70°F, may correlate better with cooling costs, depending on building characteristics. The effect of sunshine must also be considered in calculating cooling needs during the summer. For example, a building would require more cooling on a sunny day than on a cloudy one, assuming an equal number of cooling-degree days for both days.

Cooling-degree days are also known as growing-degree days, especially for some of the lower temperature bases. The growth of many types of plants correlates to the number of growing-degree days of a specified temperature base.

Los Alamos and White Rock cooling- (growing-) degree days, calculated for various temperature bases (40°F–75°F), are shown in Tables 2.22 and 2.23, respectively. The most cooling- (growing-) degree days occur in July, followed closely by those in August and June. These three months contain the majority of annual cooling-degree days for the bases of 65°F and 70°F used in computing cooling needs. White Rock has more cooling-degree days for the 65°F and 70°F bases than does Los Alamos. In general, White Rock buildings require some cooling during the summer, whereas Los Alamos buildings generally require very little. From an agricultural standpoint, the greater number of lower-base growing-degree days at White Rock indicates that more types of plants can potentially mature there. However, the shorter White Rock growing season can offset the benefit of more growing-degree days, especially for sensitive plants. As with heating-degree days, one should use caution in comparing the cooling- (growing-) degree days between the two sites because the data record is considerably smaller for White Rock.

Monthly cooling-degree days using the 65°F base are listed in Tables 2.24 and 2.25 for Los Alamos and White Rock, respectively. The data record begins in 1951 for Los Alamos and in 1965 for White Rock.

New Mexico annual cooling-degree days (70°F base) are plotted in Fig. 2.19 (Morris and Haggard 1985, reproduced with permission). As summer temperatures increase, the number of cooling-degree days increases dramatically in the southern part of the state and in the valleys. Cooling is a significant problem in these areas of the state.

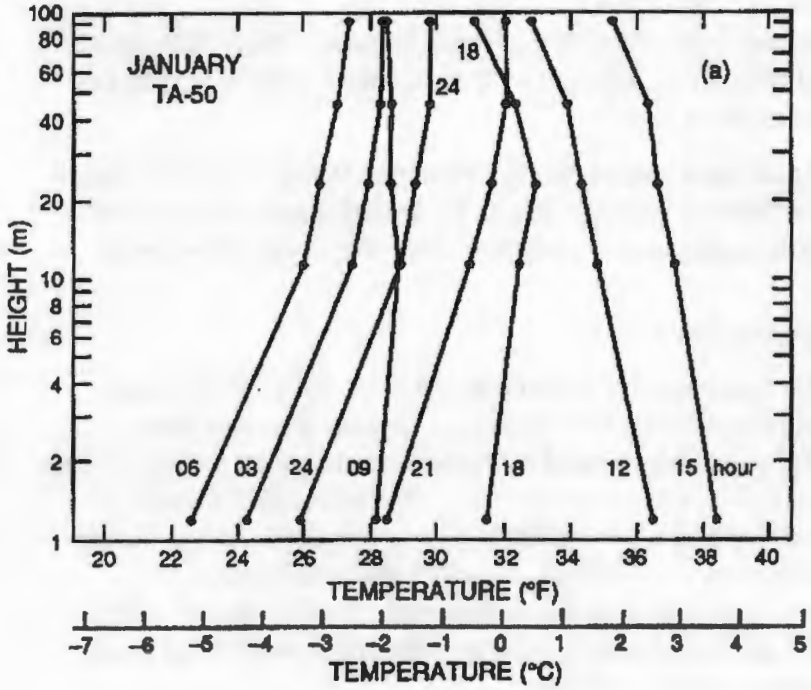

Fig. 2.17(a)–(d). Vertical mean temperature profiles calculated from TA-50 data (1985–1987) for (a) January, (b) April, (c) July, and (d) October. The solid vertical lines indicate the hours (numbers next to lines) data were taken. The black dots indicate the tower levels where data were collected (12-, 23-, 46-, and 92-m levels at TA-50 and the 1.2-m level [estimated data] at TA-59).

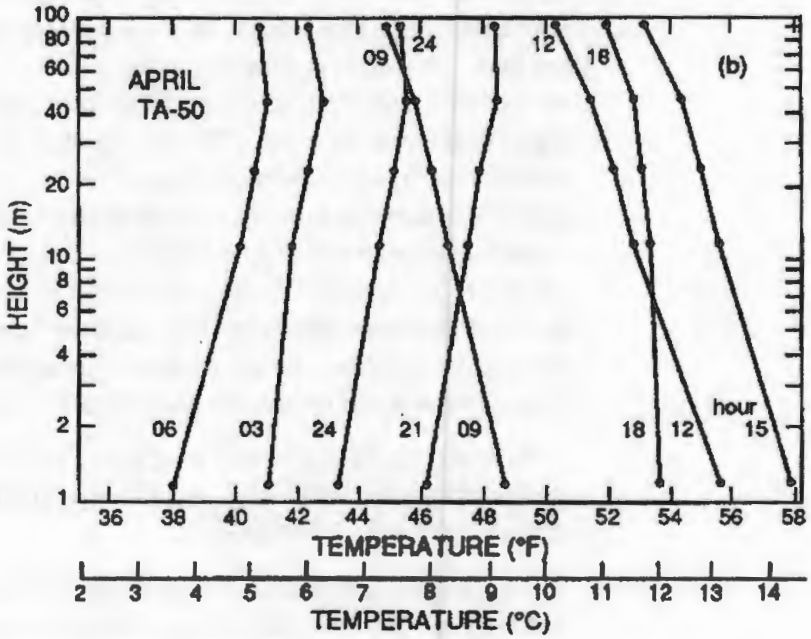

Fig. 2.17 (Continued)

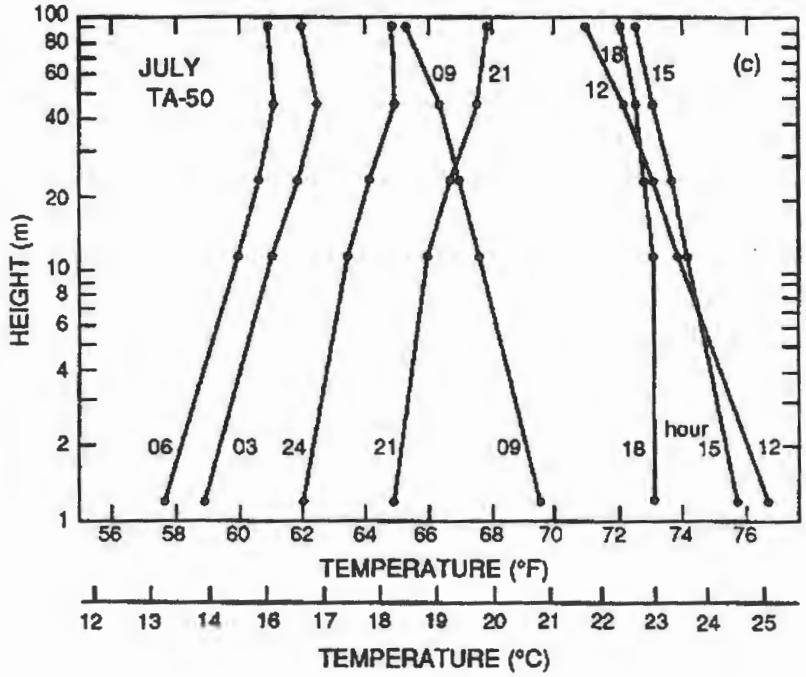

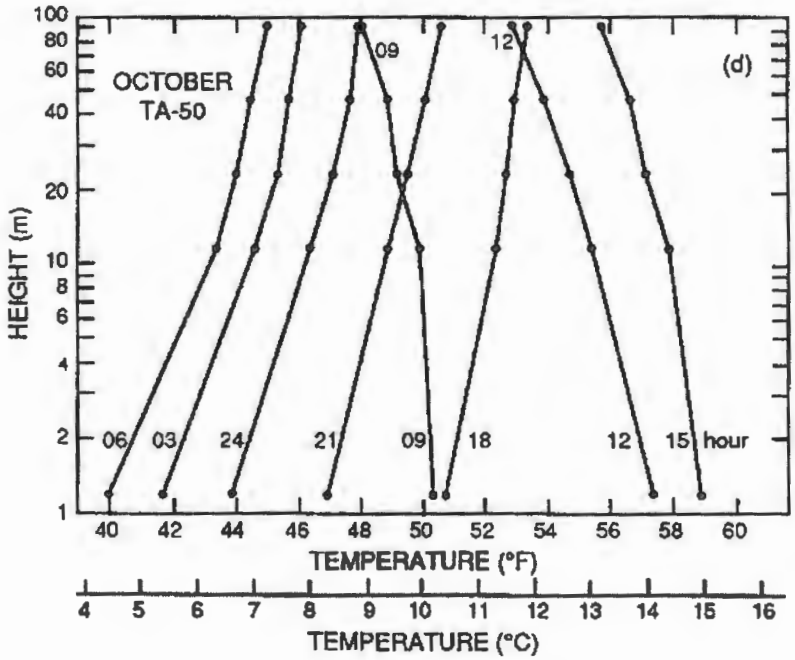

Table 2.18. Los Alamos heating-degree days, 1918–1988 (mean based on 1951–1980 period).

Base (°F)	Statistic	July	Aug.	Sept.	Oct.	Nov.	Dec.	Jan.	Feb.	Mar.	Apr.	May	June	Seasonal
40	Mean	0	0	0	12	130	292	344	236	147	35	3	0	1 200
	Std dev	0	0	2	12	70	93	103	99	64	27	6	0	203
	Min	0	0	0	0	15	91	101	45	26	0	0	0	631
	Max	0	0	9	79	291	467	546	469	277	128	30	0	1 655
45	Mean	0	0	1	39	232	439	493	362	254	84	13	0	1 916
	Std dev	0	0	4	31	89	100	109	111	89	45	14	0	239
	Min	0	0	0	0	66	212	229	113	82	1	0	0	1 186
	Max	0	0	20	149	437	622	701	614	418	201	62	0	2 437
50	Mean	0	0	6	90	365	593	647	501	389	166	39	1	2 796
	Std dev	0	0	10	56	97	101	110	114	105	65	28	1	269
	Min	0	0	0	15	175	359	384	237	157	116	0	0	1 949
	Max	0	0	48	246	587	777	856	759	573	318	114	14	3 350
55	Mean	0	0	21	176	513	748	802	642	539	287	92	6	3 826
	Std dev	0	1	23	77	98	101	110	114	110	79	46	7	306
	Min	0	0	0	63	311	514	539	377	284	78	3	0	2 844
	Max	3	4	93	377	737	932	1 011	904	728	461	195	34	4 414
60	Mean	1	4	65	303	663	903	957	784	694	430	185	25	5 012
	Std dev	0	1	23	77	98	101	110	114	110	79	46	7	269
	Min	0	0	0	174	468	647	694	517	439	180	43	0	3 883
	Max	21	16	168	531	887	1 087	1 166	1 049	883	611	309	74	5 617
65	Mean	14	36	159	454	813	1 058	1 112	925	849	579	318	73	6 390
	Std dev	11	24	65	94	98	101	110	115	111	87	76	39	395
	Min	0	0	34	320	618	772	839	657	576	321	154	3	5 141
	Max	73	107	263	686	1 037	1 242	1 321	1 194	1 038	761	463	154	6 993
70	Mean	81	136	293	609	963	1 213	1 267	1 066	1 004	729	469	166	7 997
	Std dev	34	49	76	94	98	101	110	115	111	87	78	60	435
	Min	15	45	133	475	751	897	964	797	711	471	294	50	6 686
	Max	195	244	413	841	1 187	1 397	1 476	1 339	1 193	911	618	288	8 600
75	Mean	210	283	443	764	1 113	1 368	1 422	1 208	1 159	879	623	299	9 771
	Std dev	48	54	77	94	98	101	110	116	111	87	78	70	456
	Min	114	142	277	612	881	1 022	1 089	937	846	621	449	172	8 411
	Max	339	399	563	996	1 337	1 552	1 631	1 484	1 348	106	7731	438	10 401

Table 2.19. White Rock heating-degree days, 1965–1988.

Base (°F)	Statistic	July	Aug.	Sept.	Oct.	Nov.	Dec.	Jan.	Feb.	Mar.	Apr.	May	June	Seasonal
40	Mean	0	0	0	10	111	327	377	199	83	20	1	0	1 146
	Std dev	0	0	0	13	52	112	112	74	44	23	4	0	255
	Min	0	0	3	0	38	115	73	86	24	0	0	0	492
	Max	0	0	0	56	228	515	542	352	208	83	21	0	1 641
45	Mean	0	0	0	31	213	478	528	325	173	56	6	0	1 830
	Std dev	0	0	2	29	67	116	118	82	67	42	11	0	314
	Min	0	0	0	0	103	256	196	193	62	9	0	0	976
	Max	0	0	11	119	375	670	697	492	329	145	49	0	2 431
50	Mean	0	0	4	83	348	632	683	464	302	125	22	0	2 676
	Std dev	0	0	9	54	73	116	119	90	86	64	22	0	353
	Min	0	0	0	9	229	411	349	298	122	50	0	0	1 666
	Max	0	0	34	210	525	825	852	632	467	244	94	2	3 351
55	Mean	0	0	17	180	497	787	838	604	450	237	63	2	3 690
	Std dev	0	0	19	71	75	116	119	86	94	81	39	4	383
	Min	0	0	0	82	376	566	504	426	242	134	12	0	2 593
	Max	0	0	76	342	675	980	1 007	772	620	385	156	18	4 438
60	Mean	0	1	54	316	647	942	993	745	604	378	148	13	4 873
	Std dev	0	2	35	78	75	116	119	86	94	85	56	14	401
	Min	0	0	6	185	526	721	659	565	397	261	53	0	3 765
	Max	3	11	139	492	825	1 135	1 162	912	775	533	255	56	5 662
65	Mean	2	14	142	468	797	1 097	1 148	886	759	526	272	52	6 197
	Std dev	3	15	46	79	75	116	119	85	94	89	72	32	413
	Min	0	0	45	337	676	876	814	705	552	408	131	2	5 091
	Max	12	45	218	647	975	1 290	1 317	1 052	930	683	399	120	7 026
70	Mean	30	78	272	623	947	1 252	1 303	1 027	914	677	420	134	7 715
	Std dev	20	45	53	80	75	116	119	84	94	86	80	48	440
	Min	2	15	131	492	826	1 031	969	845	707	558	247	43	6 609
	Max	69	161	361	802	1 125	1 445	1 472	1 192	1 085	833	554	227	8 612
75	Mean	131	209	421	773	1 097	1 406	1 458	1 168	1 069	827	575	260	9 442
	Std dev	37	60	56	80	75	116	119	83	94	86	80	60	457
	Min	59	110	263	647	976	1 186	1 124	985	862	708	393	157	8 359
	Max	202	316	511	957	1 275	1 600	1 627	1 332	1 240	983	709	375	10 379

Table 2.20. Los Alamos heating-degree days (65°F base), 1951–1989.

Years	July	Aug.	Sept.	Oct.	Nov.	Dec.	Jan.	Feb.	Mar.	Apr.	May	June	Total
1951–52	1	32	102	396	818	1 054	1 034	969	1 001	568	301	40	6 316
1952–53	18	13	116	324	939	1 154	850	905	706	533	410	13	5 981
1953–54	10	27	34	395	706	1 113	972	657	842	321	252	44	5 373
1954–55	3	22	77	326	642	983	1 144	1 050	805	584	351	90	6 077
1955–56	12	7	68	322	756	937	901	1 041	733	561	154	3	5 495
1956–57	4	38	36	391	895	1 021	1 046	717	822	644	463	91	6 168
1957–58	21	51	159	575	1 022	1 023	1 149	855	1 038	704	263	31	6 891
1958–59	12	29	158	472	757	881	1 066	949	872	578	313	43	6 130
1959–60	13	32	138	510	833	977	1 249	1 125	783	503	330	66	6 559
1960–61	24	17	128	510	760	1 143	1 125	886	847	638	284	47	6 409
1961–62	8	41	231	446	891	1 165	1 181	813	960	452	265	78	6 531
1962–63	20	3	153	407	721	998	1 248	907	862	540	168	96	6 123
1963–64	0	32	90	320	728	1 057	1 215	1 194	952	672	314	72	6 646
1964–65	13	21	186	402	836	1 116	1 065	994	971	578	396	150	6 728
1965–66	7	59	263	408	699	1 028	1 245	1 098	768	539	224	72	6 410
1966–67	0	36	142	461	694	1 060	1 089	862	646	537	360	111	5 998
1967–68	10	69	201	416	724	1 242	1 088	870	821	692	361	69	6 563
1968–69	35	92	182	420	860	1 154	963	919	1 008	529	267	135	6 564
1969–70	3	12	159	609	841	979	1 130	805	955	664	256	149	6 562
1970–71	7	8	212	631	788	1 016	1 112	953	803	604	358	55	6 547
1971–72	41	42	253	586	837	1 172	1 094	841	594	468	298	50	6 276
1972–73	22	71	203	527	1 037	1 136	1 205	976	976	761	361	120	7 395
1973–74	27	14	168	434	702	1 042	1 200	1 004	670	570	184	58	6 073
1974–75	20	75	263	527	834	1 184	1 183	1 004	862	702	380	86	7 120
1975–76	21	24	249	490	847	1 057	1 127	808	854	589	344	93	6 493
1976–77	30	79	258	639	893	1 148	1 261	909	925	543	307	21	7 013
1977–78	16	32	123	403	737	929	1 099	959	769	526	405	79	6 077
1978–79	6	41	175	399	806	1 201	1 314	957	843	559	409	133	6 843
1979–80	24	61	124	341	962	945	978	835	916	643	416	23	6 268
1980–81	0	11	116	538	813	824	958	800	878	430	362	73	5 803
1981–82	6	40	132	507	698	946	1 120	962	832	563	388	60	6 254
1982–83	7	18	202	561	859	1 143	1 046	894	842	739	437	125	6 873
1983–84	12	9	110	451	811	1 115	1 185	948	879	666	177	74	6 437
1984–85	1	21	171	686	812	1 054	1 183	996	828	498	304	69	6 623
1985–86	24	24	258	497	803	1 025	849	813	658	521	324	114	5 910
1986–87	31	23	241	578	845	1 048	1 173	940	908	532	373	59	6 751
1987–88	7	90	189	383	822	1 170	1 244	883	850	530	366	74	6 608
1988–89	20	51	211	357	818	1 129	1 155	907	626	369	184	78	5 905
1989–90	24	39	142										
Mean	14	35	165	466	811	1 060	1 110	921	845	570	319	75	6 389
Std dev	10	24	63	97	90	96	114	108	105	95	79	37	426

Table 2.21. White Rock heating-degree days (65°F base), 1965–1989.

Years	July	Aug.	Sept.	Oct.	Nov.	Dec.	Jan.	Feb.	Mar.	Apr.	May	June	Total
1965–66	1	17	213	445	692	1 071	1 277	1 052	733	467	143	33	6 144
1966–67	0	37	171	466	731	1 159	1 161	826	594	544	342	102	6 133
1967–68	5	25	133	410	707	1 269	1 151	837	781	670	342	65	6 395
1968–69	12	42	167	454	837	1 227	930	878	930	445	228	72	6 222
1969–70	0	0	90	515	802	968	1 119	768	867	618	189	113	6 049
1970–71	0	0	172	588	769	1 033	1 148	903	744	532	301	40	6 230
1971–72	9	7	218	510	804	1 191	1 110	822	552	428	251	21	5 923
1972–73	5	15	124	436	975	1 143	1 196	938	859	683	296	78	6 748
1973–74	1	8	120	401	710	1 039	1 220	988	625	549	174	43	5 878
1974–75	0	34	198	449	839	1 290	1 317	997	840	666	343	53	7 026
1975–76	0	1	182	449	871	1 077	1 152	796	792	496	230	37	6 083
1976–77	5	18	186	634	912	1 266	1 312	878	864	480	261	2	6 818
1977–78	0	3	86	373	818	996	1 117	938	737	488	399	46	6 001
1978–79	0	23	146	433	793	1 234	1 300	925	748	486	348	120	6 556
1979–80	6	41	118	—	—	—	—	—	—	—	363	12	—
1980–81	0	9	84	472	809	876	1 025	—	—	—	254	47	—
1981–82	0	0	83	443	676	936	1 129	975	747	486	305	22	5 802
1982–83	0	0	123	513	843	1 134	1 075	850	741	656	344	78	6 357
1983–84	0	0	45	416	806	1 090	1 210	923	797	572	131	42	6 032
1984–85	0	2	122	647	809	1 077	1 145	946	740	462	247	38	6 235
1985–86	6	3	181	392	683	956	814	705	652	408	228	63	5 091
1986–87	2	2	184	531	829	1 042	1 131	857	824	486	311	14	6 213
1987–88	0	45	114	337	811	1 056	1 219	806	769	447	233	13	5 850
1988–89	0	25	166	313	735	1 062	1 191	860	597	325	144	39	5 457
1989–90	9	1											
Mean	2	14	142	468	797	1 097	1 148	886	759	518	267	50	6 147
Std dev	3	15	46	79	75	116	119	85	94	94	76	32	428

2.8 Growing-Season Data

Means and extremes of early- and late-season cold temperature occurrences were calculated from the historical Los Alamos and White Rock temperature data bases. The calculations were based on temperatures of 36°F, 32°F, 28°F, 24°F, 20°F, and 16°F. Because the temperatures are measured at a 4- to 5-ft (1.2- to 1.5-m) height, ground temperatures may actually be lower under some weather conditions. For example, a 36°F low temperature indicates a light frost, because actual ground temperatures may approach 32°F under clear skies and light winds. A 32°F low temperature is defined as a freeze; a 28°F low temperature represents a hard freeze. The difference between 28°F and 32°F is enough to affect plants differently. A low temperature of 32°F may have little effect on fruit trees (elevated above ground), whereas plants near the ground may be heavily damaged because ground-level temperatures or temperatures in local low spots may be several degrees colder than the indicated temperatures. A 28°F low temperature,

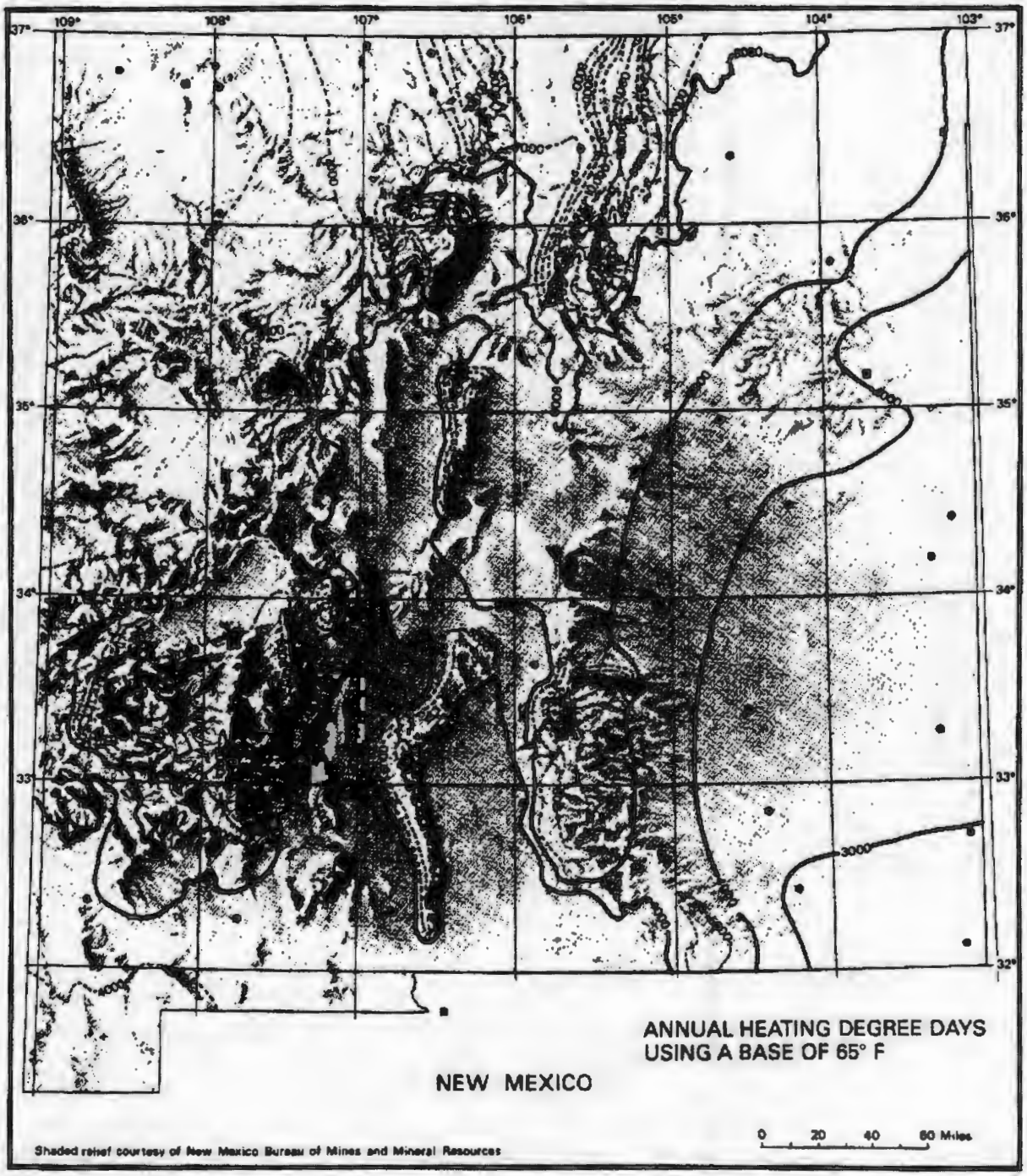

Fig. 2.18. Annual mean heating-degree days (65°F base) in New Mexico.

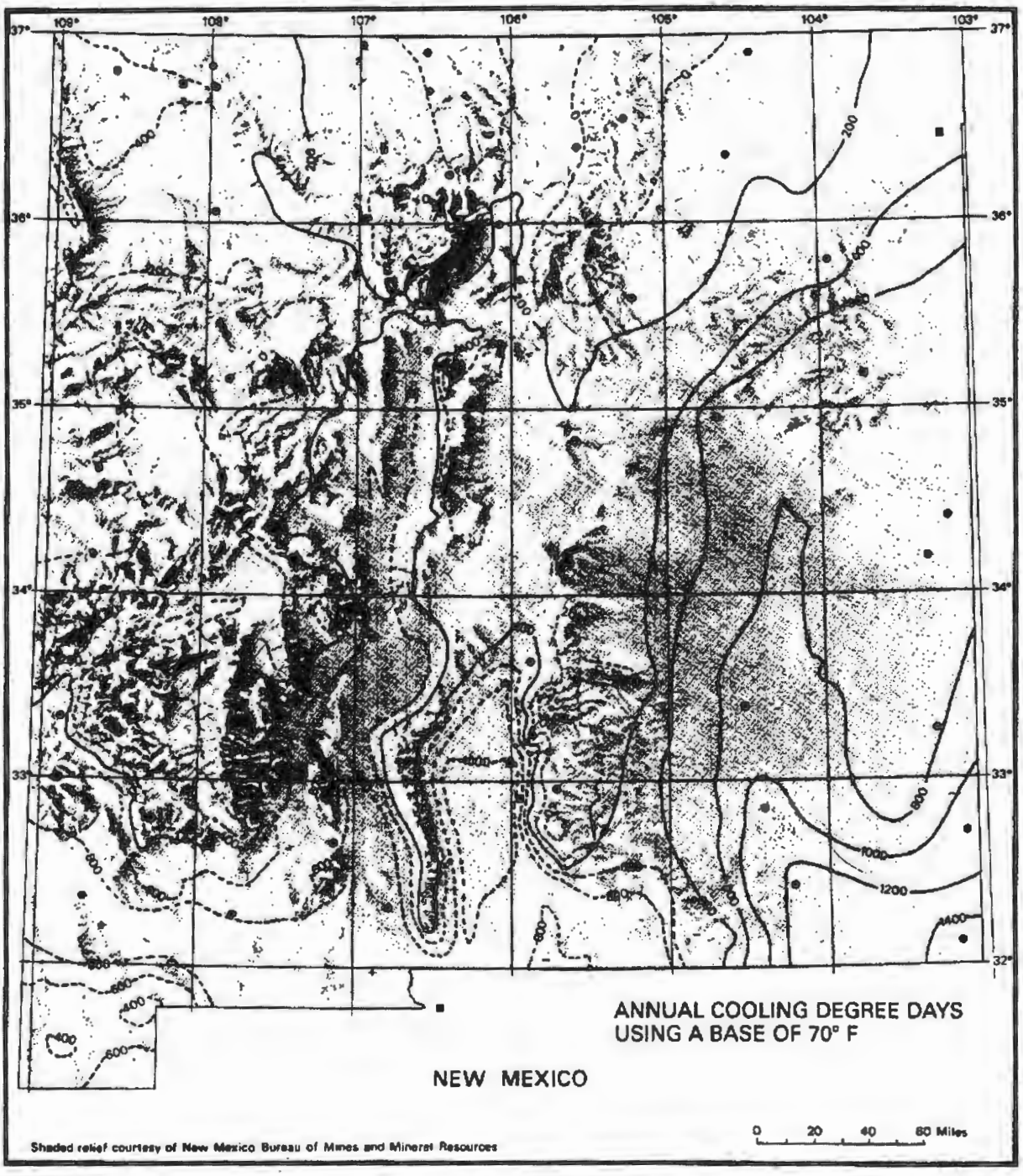

Fig. 2.19. Annual mean cooling-degree days (70°F base) in New Mexico.

Table 2.22. Los Alamos cooling-degree days, 1918–1988 (mean based on 1951–1980 period).

Base (°F)	Statistic	Jan.	Feb.	Mar.	Apr.	May	June	July	Aug.	Sept.	Oct.	Nov.	Dec.	Annual
40	Mean	7	17	73	206	464	752	876	800	607	333	67	9	4 211
	Std dev	12	20	55	66	77	71	49	54	77	84	40	112	327
	Min	0	0	2	76	291	502	633	543	422	165	0	0	3 662
	Max	61	87	226	429	635	882	977	914	772	456	148	49	4 998
45	Mean	1	3	25	104	320	602	721	645	458	204	19	1	3 102
	Std dev	3	4	27	49	72	71	49	54	76	68	19	2	283
	Min	0	0	0	21	171	372	508	413	297	71	0	0	2 592
	Max	14	23	111	285	483	732	822	759	622	319	68	10	3 727
50	Mean	0	0	5	37	190	453	566	491	313	100	2	0	2 156
	Std dev	0	0	8	30	60	71	49	54	72	47	4	0	246
	Min	0	0	0	1	67	246	378	283	176	11	0	0	1 711
	Max	0	6	28	157	333	582	667	604	472	198	16	0	2 683
55	Mean	0	0	0	8	88	308	411	336	178	31	0	0	1 360
	Std dev	0	0	1	11	41	67	49	54	63	25	0	0	206
	Min	0	0	0	0	14	130	244	153	75	0	0	0	985
	Max	0	0	4	56	202	432	512	449	322	92	2	0	1 803
60	Mean	0	0	0	1	26	177	257	185	72	4	0	0	721
	Std dev	0	0	0	2	20	59	48	51	44	6	0	0	157
	Min	0	0	0	0	1	50	116	39	7	0	0	0	437
	Max	0	0	0	9	103	289	357	294	172	26	0	0	1 039
65	Mean	0	0	0	0	4	75	116	63	16	0	0	0	274
	Std dev	0	0	0	0	8	40	42	33	6	1	0	0	95
	Min	0	0	0	0	0	6	18	1	0	0	0	0	109
	Max	0	0	0	0	39	155	204	147	58	2	0	0	467
70	Mean	0	0	0	0	0	19	27	8	0	0	0	0	54
	Std dev	0	0	0	0	2	16	20	8	1	0	0	0	35
	Min	0	0	0	0	0	0	0	0	0	0	0	0	6
	Max	0	0	0	0	12	55	80	57	14	0	0	0	130
75	Mean	0	0	0	0	0	1	1	0	0	0	0	0	3
	Std dev	0	0	0	0	0	2	2	0	0	0	0	0	4
	Min	0	0	0	0	0	0	0	0	0	0	0	0	0
	Max	0	0	0	0	0	8	8	16	0	0	0	0	11

Table 2.23. White Rock cooling-degree days, 1965–1988.

Base (°F)	Statistic	Jan.	Feb.	Mar.	Apr.	May	June	July	Aug.	Sept.	Oct.	Nov.	Dec.	Annual
40	Mean	5	18	97	249	507	788	958	876	629	321	64	4	4 512
	Std dev	9	25	63	71	79	65	39	62	56	72	38	5	223
	Min	0	0	14	106	397	675	882	768	538	171	2	0	4 020
	Max	34	111	254	373	691	914	1 045	977	787	448	135	15	4 989
45	Mean	0	3	33	134	357	638	803	721	479	187	16	0	3 370
	Std dev	0	9	36	53	76	65	39	62	55	58	18	0	193
	Min	0	0	0	26	243	525	727	613	393	73	0	0	2 924
	Max	3	47	129	241	536	764	890	822	637	304	65	3	3 752
50	Mean	0	1	7	52	218	488	648	566	333	82	1	0	2 395
	Std dev	0	2	12	31	67	65	39	62	53	39	2	0	168
	Min	0	0	0	0	125	375	572	458	265	17	0	0	2 029
	Max	0	12	41	130	384	614	794	667	487	165	11	0	2 719
55	Mean	0	0	1	12	106	341	493	411	196	22	0	0	1 581
	Std dev	0	0	2	11	49	64	39	62	47	19	0	0	146
	Min	0	0	0	0	47	225	417	303	142	0	0	0	1 302
	Max	0	0	14	50	241	466	580	512	337	69	0	0	1 836
60	Mean	0	0	0	1	36	203	338	257	83	2	0	0	921
	Std dev	0	0	0	2	29	57	38	61	37	4	0	0	128
	Min	0	0	0	0	1	97	265	150	39	0	0	0	705
	Max	0	0	1	13	124	331	425	357	194	15	0	0	1 145
65	Mean	0	0	0	0	6	93	185	116	20	0	0	0	427
	Std dev	0	0	0	0	11	44	37	50	20	0	0	0	94
	Min	0	0	0	0	0	27	120	31	1	0	0	0	263
	Max	0	0	0	0	47	211	270	202	82	1	0	0	586
70	Mean	0	0	0	0	0	26	58	24	1	0	0	0	111
	Std dev	0	0	0	0	1	24	23	20	3	0	0	0	45
	Min	0	0	0	0	0	2	20	0	0	0	0	0	44
	Max	0	0	0	0	8	105	117	71	18	0	0	0	221
75	Mean	0	0	0	0	0	2	5	1	0	0	0	0	9
	Std dev	0	0	0	0	0	5	6	2	0	0	0	0	9
	Min	0	0	0	0	0	0	0	0	0	0	0	0	0
	Max	0	26	22	11	0	26	22	11	0	0	0	0	36

Table 2.24. Los Alamos cooling-degree days (65°F base), 1951–1989.

Year	Jan.	Feb.	Mar.	Apr.	May	June	July	Aug.	Sept.	Oct.	Nov.	Dec.	Total
1951	0	0	0	0	39	84	204	78	39	0	0	0	444
1952	0	0	0	0	4	143	109	93	22	0	0	0	371
1953	0	0	0	0	11	138	182	93	40	0	0	0	464
1954	0	0	0	0	2	128	149	82	37	2	0	0	400
1955	0	0	0	0	0	70	95	71	40	0	0	0	276
1956	0	0	0	0	15	130	124	90	58	0	0	0	417
1957	0	0	0	0	0	68	107	20	4	0	0	0	199
1958	0	0	0	0	4	72	117	72	11	0	0	0	276
1959	0	0	0	0	0	77	94	58	34	0	0	0	263
1960	0	0	0	0	3	117	111	89	18	0	0	0	338
1961	0	0	0	0	2	50	100	43	2	0	0	0	197
1962	0	0	0	0	4	46	51	120	7	0	0	0	228
1963	0	0	0	0	2	50	171	41	3	0	0	0	267
1964	0	0	0	0	5	31	137	67	14	0	0	0	254
1965	0	0	0	0	0	12	88	47	0	0	0	0	147
1966	0	0	0	0	0	28	176	33	1	0	0	0	238
1967	0	0	0	0	2	23	105	24	1	0	0	0	155
1968	0	0	0	0	3	96	74	3	2	0	0	0	178
1969	0	0	0	0	5	34	138	120	1	0	0	0	298
1970	0	0	0	0	4	62	95	88	6	0	0	0	255
1971	0	0	0	0	0	67	121	17	18	0	0	0	223
1972	0	0	0	0	0	40	95	30	0	0	0	0	165
1973	0	0	0	0	0	83	98	107	2	0	0	0	290
1974	0	0	0	0	11	127	84	26	22	0	0	0	270
1975	0	0	0	0	0	37	48	69	8	0	0	0	162
1976	0	0	0	0	0	48	49	11	1	0	0	0	109
1977	0	0	0	0	8	96	72	94	15	0	0	0	285
1978	0	0	0	0	2	114	151	54	3	0	0	0	324
1979	0	0	0	0	0	47	128	53	42	0	0	0	270
1980	0	0	0	0	0	155	197	89	24	2	0	0	467
1981	0	0	0	0	0	137	113	46	2	0	0	0	298
1982	0	0	0	0	0	37	118	66	14	0	0	0	235
1983	0	0	0	0	0	50	110	77	53	0	0	0	290
1984	0	0	0	0	35	51	127	52	24	0	0	0	289
1985	0	0	0	0	0	62	118	64	5	0	0	0	249
1986	0	0	0	0	0	24	80	84	1	0	0	0	189
1987	0	0	0	0	0	51	126	59	0	0	0	0	236
1988	0	0	0	0	6	50	83	41	7	0	0	0	187
1989	0	0	0	0	21	77	128	21	4				
Mean	0	0	0	0	5	72	115	61	15	0	0	0	270
Std dev	0	0	0	0	9	39	37	29	16	0	0	0	87

Table 2.25. White Rock cooling-degree days (65°F base), 1965–1989.

Year	Jan.	Feb.	Mar.	Apr.	May	June	July	Aug.	Sept.	Oct.	Nov.	Dec.	Total
1965	0	0	0	0	0	54	191	71	1	0	0	0	317
1966	0	0	0	0	18	45	218	62	2	0	0	0	345
1967	0	0	0	0	0	27	208	74	12	0	0	0	321
1968	0	0	0	0	3	107	120	35	8	0	0	0	273
1969	0	0	0	0	25	45	222	202	7	0	0	0	501
1970	0	0	0	0	5	88	186	160	27	0	0	0	466
1971	0	0	0	0	0	113	198	87	47	0	0	0	445
1972	0	0	0	0	3	66	152	94	4	0	0	0	319
1973	0	0	0	0	0	93	154	142	7	0	0	0	396
1974	0	0	0	0	19	168	139	58	29	0	0	0	413
1975	0	0	0	0	1	71	155	150	19	0	0	0	396
1976	0	0	0	0	3	99	125	31	5	0	0	0	263
1977	0	0	0	0	9	138	213	188	35	0	0	0	583
1978	0	0	0	0	0	130	200	69	4	0	0	0	403
1979	0	0	0	0	0	69	179	110	43	0	0	0	401
1980	0	0	0	0	1	163	270	124	16	1	0	0	575
1981	0	0	0	0	1	211	231	137	6	0	0	0	586
1982	0	0	0	0	1	85	216	165	40	0	0	0	507
1983	0	0	0	0	0	66	213	188	82	0	0	0	549
1984	0	0	0	0	47	64	171	107	51	0	0	0	440
1985	0	0	0	0	7	85	171	126	17	0	0	0	406
1986	0	0	0	0	2	69	140	172	14	0	0	0	397
1987	0	0	0	0	0	85	197	111	1	0	0	0	394
1988	0	0	0	0	15	120	153	123	9	0	0	0	420
1989	0	0	0	0	22	122	215	111					
Mean	0	0	0	0	7	95	185	116	20	0	0	0	421
Std dev	0	0	0	0	11	43	37	50	20	0	0	0	94

however, may be cold enough to damage plants, such as fruit trees, well above the ground.

The duration of low temperatures and atmospheric humidity also affect the amount of plant damage. For example, a brief occurrence of 28°F may not heavily damage sensitive plants, but several hours at that temperature could cause significant damage. Also, a moist atmosphere at 28°F may cause ice and frost to form, thereby reducing damage because heat is liberated as water vapor condenses into ice. Spraying water onto plants is an effective strategy to reduce damage on nights when temperatures are at, or slightly below, freezing. Conversely, frost and ice may not form in a dry atmosphere at 28°F.

The early and late occurrences of specified temperatures in the spring and autumn are given for Los Alamos and White Rock in Tables 2.26 and 2.27, respectively. The specified cold temperatures are generally reached later in the spring and earlier in the autumn at White Rock, resulting in a shorter growing season than in Los Alamos.

Table 2.26. Los Alamos growing-season data, 1919–1988 (means are based on 1951–1980 period).

Temperature (°F)	Means: Latest Spring Date	Means: Earliest Fall Date	Means: No. of Days Between Dates
36	5/22	10/03	132
32	5/07	10/14	157
28	4/26	10/24	181
24	4/14	11/05	204
20	3/29	11/08	223
16	3/19	11/20	245

Temperature (°F)	Extremes: Spring Date Earliest	Spring Date Latest	Fall Date Earliest	Fall Date Latest	No. of Days Between Dates Least	Most
36	4/26/37	6/15/76	9/03/61	10/31/63	91 (1941)	184 (1963)
32	4/19/56	6/11/75	9/09/41	11/02/51	110 (1941)	185 (1963)
28	3/27/54	6/03/19	9/21/83	11/09/44	125 (1983)	220 (1967)
24	3/26/69	5/11/46	9/28/36	12/09/54	158 (1976)	256 (1954)
20	3/06/53	4/27/20	10/08/76	12/11/49	173 (1976)	265 (1954)
16	2/12/86	4/20/20	10/19/76	12/23/39	184 (1976)	291 (1939)

Specifically, the White Rock growing season averages 12 and 14 days fewer for the 32°F and 28°F temperatures, respectively.

Ordinarily, White Rock has a shorter growing season than does Los Alamos. However, the records show a mixed picture for different temperature bases because of early and late freezes. For example, White Rock has the record short growing season at a temperature base of 36°F; Los Alamos has the record at a temperature base of 32°F. The record long growing seasons similarly alternate between the two sites for different bases.

The White Rock growing-season temperature extremes are understated when White Rock data are compared with Los Alamos data because temperature records have been kept for a much shorter time at White Rock.

2.9 Freeze-Thaw Data

Freeze-thaw days are defined as days in which the maximum temperature is greater than 32°F and the minimum temperature is 32°F or lower. The change in temperatures from above freezing to below freezing is stressful to materials such as concrete and asphalt. In fact, damage to roads and highways increases with frequent freezing and thawing.

Table 2.27. White Rock growing-season data, 1965–1988 (means are based on entire period).

Temperature (°F)	Means: Latest Spring Date	Means: Earliest Fall Date	Means: No. of Days Between Dates
36	5/23	9/26	124
32	5/12	10/06	145
28	5/01	10/16	167
24	4/15	10/27	193
20	4/05	11/07	215
16	3/18	11/15	241

Temperature (°F)	Extremes: Spring Date Earliest	Spring Date Latest	Fall Date Earliest	Fall Date Latest	No. of Days Between Dates Least	Most
36	5/09/70	6/11/75	8/24/68	10/14/80	74 (1968)	148 (1981)
32	4/09/81	5/30/78	9/17/68	10/21/72	121 (1968)	190 (1981)
28	4/06/81	5/21/74	9/20/71	11/07/85	123 (1971)	195 (1981)
24	3/21/86	5/09/65	10/08/76	11/17/78	161 (1970)	240 (1978)
20	3/16/78	5/03/67	10/08/76	11/27/65	173 (1976)	250 (1965)
16	2/09/79	4/09/73	10/18/76	12/10/86	204 (1975)	301 (1986)

The number of days with maximums exceeding 32°F and minimums at or below 32°F and the mean number and standard deviations of monthly freeze-thaw days are listed for Los Alamos and White Rock in Tables 2.28 and 2.29, respectively. Most of the freeze-thaw days occur from November to March at both sites. More freeze-thaw days occur at White Rock than at Los Alamos because of its larger diurnal temperature range. The Los Alamos temperature occasionally remains at 32°F or below for the entire day, whereas the White Rock temperature exceeds 32°F even during some colder winter days. Also, during the autumn and spring months, temperatures can remain above freezing all day at Los Alamos while the low temperatures at White Rock dip to freezing or below on that same day. During October, the White Rock mean of 12.3 freeze-thaw days is almost twice the Los Alamos mean. Note that the record minimum number of monthly freeze-thaw days at White Rock is greater than at Los Alamos.

As with other data in this report, caution must be used in comparing the extremes between the two sites because the Los Alamos temperature record is much larger. Also, temperatures in the freeze-thaw data are measured at a 4- to 5-ft (1.2- to 1.5-m) height above ground. Thus, the number of freeze-thaw days at ground level may actually be more than indicated because the diurnal temperature range is greatest at the ground. In addition, this analysis does not account for multiple freeze-thaw cycles during individual days. However, the calculated monthly freeze-thaw days should give a good idea of the trends.

Table 2.28. Los Alamos freeze-thaw days, 1919–1988 (means are based on 1951–1980 period).

	Number of Freeze-Thaw Days			
	Maximum on Record	Minimum on Record	Mean	Standard Deviation
January	31	7	23.6	3
February	28	14	22.3	4
March	31	11	21.5	5
April	24	2	13.0	5
May	11	0	2.4	2
June	3	0	0.1	0
July	0	0	0.0	0
August	0	0	0.0	0
September	3	0	0.2	1
October	20	0	6.6	5
November	27	11	20.4	4
December	31	14	24.5	4

Table 2.29. White Rock freeze-thaw days, 1965–1988.

	Number of Freeze-Thaw Days			
	Maximum on Record	Minimum on Record	Mean	Standard Deviation
January	30	21	26.5	2
February	29	12	24.0	4
March	30	18	24.9	4
April	24	7	15.7	6
May	11	0	3.7	3
June	0	0	0.0	0
July	0	0	0.0	0
August	0	0	0.0	0
September	3	0	0.7	1
October	23	1	12.3	6
November	30	17	25.9	3
December	30	22	26.6	3

2.10 Apparent and Wind-Chill-Equivalent Temperatures

Apparent temperature incorporates primarily temperature, together with wind speed and atmospheric humidity, to gauge the relative weather effects on the human body. Greater wind speeds increase the amount of heat removed from an exposed body, thereby lowering apparent temperature; greater atmospheric moisture lowers evaporation, thereby

increasing apparent temperature. Apparent temperature can also be affected by sunshine intensity.

Apparent temperature is a convenient comfort indicator because it can be compared between winter and summer. The National Weather Service routinely reports apparent temperatures during the summer; the wind-chill factor is commonly used in the winter. As stated, the apparent temperature includes the effects of both wind and moisture. In practice, calculated mean apparent temperatures are usually similar to calculated mean wind-chill values.

Apparent temperatures were calculated from 15-minute-averaged temperatures measured at TA-59 during January and July, the 2 months with the most extreme temperatures. A simplified equation, suggested by Steadman (1984), was used to estimate apparent temperature in the shade:

$$AT_{ue} = -2.7 + 1.04T + 0.2e - 0.65u \ , \tag{2.1}$$

where

AT_{ue} = apparent temperature (°C),

T = temperature (°C),

e = vapor pressure (mbar), and

u = near-surface wind speed (m/s).

The 15-minute-averaged vapor pressure was calculated from the relationship between relative humidity and the saturation vapor pressure:

$$e = e_s\,(\mathrm{RH}) \ , \tag{2.2}$$

where

e = vapor pressure (mbar),

e_s = saturation vapor pressure (mbar), and

RH = relative humidity (%).

The e_s is simply dependent on temperature. The following expression from the *Handbook of Meteorology* (Berry, Bollay, and Beers 1945) was used to calculate e_s:

$$\ln e_s = \frac{25\,(T - 273)}{T} - 5.2 \ln \left(\frac{T}{273}\right) + \ln 6.105 \ ,$$

where

T = absolute temperature (K).

In addition, apparent temperature can be calculated for exposure in the sun. A slightly different equation, including solar radiation, was used to determine apparent temperature in the sunlight:

$$AT_{uei} = 4.5 + 1.02T - 0.28e - 1.00u - 5.8\phi + 0.0054i \ ,$$

where

ϕ = fraction of direct solar radiation on a horizontal surface, and

i = incoming solar radiation (W/m^2).

Apparent temperatures are relatively low during July because humidity is quite moderate at Los Alamos. Only 2% of the time does the apparent temperature equal 81°F or higher during July. The mean high and low apparent temperatures are only slightly lower than the ambient temperatures because 2°F–3°F cooling by the wind only slightly exceeds the warming effect of increased humidity. The strong summer sunshine does cause relatively high apparent temperatures in the sun. Apparent temperature in sunshine equals or exceeds 92°F for 5% of the time and 100°F for 0.5% of the time. On warm, sunny days, caution should be taken when skin is exposed to sunlight, as apparent temperatures can become quite high. Because afternoon temperatures average 5.5°F higher and the atmospheric moisture content is slightly higher in White Rock, extreme and average apparent temperatures in sunlight are 6°F or so higher, reaching potentially dangerous levels.

Los Alamos extreme and mean apparent temperatures for July and January are shown in Tables 2.30 and 2.31, respectively. The apparent temperatures are rather modest in

Table 2.30. July extreme and mean apparent temperatures at Los Alamos (TA-59). Column headings represent the percentage of time temperature reaches specified amount.

	5%	2%	1%	0.5%	0.2%	0.1%	High
Shade (°F)	79	81	82	84	86	87	91
Mean maximum = 79							
Mean minimum = 54							
Average = 67							
Sun (°F)	92	95	97	100	102	103	107
Mean maximum = 88							

Table 2.31. January extreme and mean apparent temperatures at Los Alamos (TA-59). Column headings represent the percentage of time temperature reaches specified amount.

	Low	0.1%	0.2%	0.5%	1%	2%	5%
Shade (°F)	−18	−10	−7	−4	−2	1	5
Mean maximum = 33							
Mean minimum = 11							
Average = 22							
Sun (°F)							
Mean maximum = 46							

January, especially when compared with those in other parts of the United States. Only 2% of the time in January does the apparent temperature reach 1°F or lower. The reason that apparent temperatures are relatively high is that winds are light in Los Alamos. Even more important, winds are usually very light during times of coldest temperatures, usually in the early morning. Conversely, temperatures are typically mild when stronger winds blow in January. Surprisingly, extreme apparent winter temperatures are as low, or lower, in the valley (Albuquerque or White Rock) because strong, easterly canyon winds accompany cold-air masses there. Besides temperature, cooling by wind is the predominant factor affecting apparent temperature in the winter. During January, the average wind provides enough cooling to make the air feel like it is about 7°F cooler.

Strong sunshine, prevalent in Los Alamos, can make the winter air feel much warmer. Sunlight is generally strong at Los Alamos' high elevation because only three-fourths of the atmosphere is above 7400 ft. The thinner atmosphere blocks out less sunshine than the full atmosphere does at locations near sea level. Also, water vapor, a scatterer of sunlight, is greatly reduced during winter and at higher elevations. The mean maximum apparent temperature in January is 46°F, a full 13°F higher than apparent temperature in the shade and 6°F higher than the ambient temperature.

Extreme and mean wind-chill-equivalent temperatures for January are given in Table 2.32. It is obvious that extreme wind-chill-equivalent temperatures are 10°F–20°F lower when compared with apparent temperatures (Table 2.31). Wind-chill-equivalent temperatures are generally lower than apparent temperatures at light wind speeds. The Los Alamos mean wind-chill temperatures are similar to mean apparent temperatures, however.

Wind-chill-equivalent temperature tables appear in Appendix F to allow calculations from temperature and wind speed.

2.11 Daily Mean High and Low Temperatures

Los Alamos and White Rock daily mean high and low temperatures were calculated and are listed in Tables 2.33 and 2.34, respectively. The Los Alamos means are based on the most recent 30-year period, ending in 1980, whereas the White Rock means are based on the 1965–1987 period. The daily means listed are actually centrally averaged, 5-day moving averages. The 5-day averages were chosen to filter out large day-to-day changes.

Table 2.32. January extreme and mean wind-chill-equivalent temperatures at Los Alamos (TA-59). Column headings represent the percentage of time temperature reaches specified amount.

	Low	0.1%	0.2%	0.5%	1%	2%	5%
Temperature (°F)	−38	−22	−19	−15	−13	−9	−5
Mean maximum = 34 Mean minimum = 12 Average = 23							

Table 2.33. Los Alamos (TA-59) daily mean high and low temperatures (°F) for 1951–1980.

Day	Jan.	Feb.	Mar.	Apr.	May	June	July	Aug.	Sept.	Oct.	Nov.	Dec.
1	35/15	42/20	44/23	52/29	61/38	71/47	81/56	79/55	76/52	67/43	53/30	43/22
2	34/14	42/21	44/22	53/29	62/38	72/47	81/56	79/55	75/51	67/43	52/30	43/22
3	35/14	42/21	44/23	54/30	63/39	72/47	81/56	79/55	75/51	66/42	53/30	43/22
4	35/14	41/21	44/22	54/30	62/38	72/48	81/56	79/55	75/51	66/43	52/30	43/23
5	36/15	41/21	44/23	54/30	63/39	73/48	81/56	79/55	75/51	66/42	52/30	43/22
6	37/15	42/21	45/23	55/31	63/39	73/48	81/56	79/55	75/51	66/42	52/30	42/21
7	37/16	42/21	46/24	55/31	64/40	74/49	80/56	79/55	75/50	66/42	52/30	41/20
8	38/16	42/21	46/25	56/32	64/40	74/49	81/56	79/55	74/50	66/42	53/30	41/20
9	38/17	42/21	47/25	55/32	64/40	74/49	81/56	78/55	74/50	66/41	52/30	40/19
10	39/17	43/21	47/25	55/32	65/40	75/50	81/56	78/55	73/50	65/41	52/30	40/19
11	39/17	43/21	47/25	55/32	65/40	75/50	81/56	78/55	73/50	65/41	52/30	40/19
12	40/18	43/21	47/25	56/32	65/41	76/51	81/56	77/54	72/50	65/40	51/30	40/19
13	40/18	43/21	47/25	57/33	66/42	76/51	81/56	77/54	72/49	64/40	51/29	41/19
14	40/19	42/21	47/25	57/33	66/42	77/52	80/56	77/54	72/49	63/39	50/28	41/19
15	41/19	43/22	48/25	58/33	66/42	78/52	80/56	77/54	71/48	62/39	48/27	41/19
16	40/20	43/22	49/25	58/34	67/42	78/53	80/55	77/54	71/48	61/38	47/27	41/20
17	41/20	42/21	49/26	59/34	67/43	78/53	79/55	76/54	71/48	61/38	47/25	42/20
18	40/20	42/21	50/26	59/34	68/43	79/53	79/55	76/53	71/47	61/32	46/25	42/20
19	40/20	42/21	50/27	59/35	68/43	79/53	79/55	76/53	70/47	60/37	45/24	41/20
20	39/19	42/21	50/27	59/35	68/43	79/54	79/55	76/53	70/46	60/32	45/24	41/20
21	39/19	42/21	50/27	59/35	68/44	80/54	79/55	75/53	69/46	59/36	45/24	41/20
22	39/19	42/21	50/28	60/35	68/44	80/54	79/55	75/53	69/46	59/36	45/24	41/20
23	40/19	42/21	51/28	60/36	69/44	81/55	79/55	75/52	68/45	59/36	45/24	40/20
24	40/19	43/21	51/28	60/36	69/45	81/55	79/55	75/52	68/45	58/35	45/24	40/20
25	40/19	44/21	51/29	60/36	69/45	82/55	79/56	76/53	68/44	57/35	44/23	40/20
26	41/20	45/22	51/29	60/36	69/45	82/56	79/56	76/53	68/45	57/34	44/23	39/19
27	42/20	45/23	51/29	60/36	70/46	82/56	79/56	76/53	68/44	56/34	44/22	39/19
28	42/21	45/23	52/29	59/36	70/46	82/56	79/56	76/53	68/44	55/33	43/22	38/18
29	43/21	45/23	52/29	60/36	70/46	82/56	79/56	76/52	68/44	53/33	43/22	37/18
30	42/21		52/29	60/37	71/46	82/56	79/56	76/52	68/44	54/32	43/22	37/17
31	42/20		52/29		71/47		79/55	76/52		53/51		36/16

Table 2.34. White Rock daily mean high and low temperatures (°F) for 1965–1987.

Day	Jan.	Feb.	Mar.	Apr.	May	June	July	Aug.	Sept.	Oct.	Nov.	Dec.
1	37/11	44/16	52/24	57/28	67/36	76/46	86/55	84/56	81/51	72/40	58/29	46/19
2	36/ 9	43/16	52/24	57/28	67/37	76/46	87/55	84/56	81/51	71/40	58/29	46/19
3	36/ 9	44/16	50/23	57/28	67/37	77/46	87/55	84/56	80/51	71/40	58/28	47/19
4	37/ 9	44/16	50/23	58/29	67/37	77/47	87/55	84/56	80/51	71/40	59/28	47/19
5	38/10	44/16	50/23	59/29	68/37	78/47	87/55	84/56	80/50	70/40	59/28	47/19
6	38/11	44/17	52/23	60/29	68/37	78/48	87/55	88/55	80/50	70/39	58/28	46/19
7	39/12	44/17	53/24	61/30	68/37	78/48	87/56	85/55	79/50	70/38	58/28	45/18
8	40/12	44/17	54/26	62/31	69/37	79/48	87/56	84/55	79/50	70/38	58/28	44/17
9	40/12	45/17	54/27	62/32	70/37	79/48	87/56	83/55	79/50	69/37	52/27	44/17
10	41/13	46/17	54/27	62/32	70/38	79/48	87/57	83/54	78/49	69/37	56/26	44/16
11	42/14	47/18	54/29	62/33	70/39	80/48	87/57	82/54	77/48	68/37	56/26	43/16
12	43/14	47/19	54/27	62/33	70/39	81/48	87/57	83/54	76/48	67/37	53/26	43/16
13	43/14	47/20	54/26	62/33	71/40	82/49	87/56	82/54	76/48	66/36	54/26	42/16
14	43/15	47/20	54/26	62/32	71/40	83/50	87/56	83/54	76/47	65/36	54/26	42/15
15	44/16	47/21	55/26	63/32	71/40	84/50	86/56	83/54	75/46	65/35	53/26	42/15
16	43/16	47/22	55/26	64/33	72/41	84/51	86/56	83/54	75/46	64/34	52/25	42/15
17	43/17	48/22	55/26	64/33	73/42	84/51	86/56	83/54	75/46	63/34	51/24	43/15
18	43/17	48/22	55/26	63/33	73/42	84/52	86/56	83/54	75/45	63/33	51/23	43/15
19	43/17	48/22	55/26	63/33	73/42	85/52	86/56	83/54	74/45	63/33	50/23	43/15
20	43/17	48/21	55/26	63/33	74/42	85/52	86/56	82/54	73/44	63/33	50/22	43/16
21	43/16	48/21	55/26	63/33	74/43	86/52	85/56	82/54	73/44	62/33	50/22	43/16
22	43/16	48/20	56/26	64/33	74/43	86/52	85/56	81/53	73/44	62/33	50/22	42/16
23	43/16	49/20	57/27	65/34	74/43	86/53	85/56	81/53	72/43	62/33	49/22	42/16
24	43/16	50/20	57/28	66/35	74/44	86/53	85/56	81/53	72/43	62/32	49/22	42/16
25	44/17	50/21	57/28	66/35	75/44	86/53	85/56	81/52	72/43	62/32	47/22	42/16
26	44/17	51/22	57/29	66/36	75/45	86/53	85/56	81/52	72/42	62/32	46/21	41/15
27	45/18	52/23	56/29	66/36	75/45	87/54	85/56	81/52	72/42	62/31	45/20	41/15
28	45/18	52/23	56/28	66/36	76/46	87/54	85/56	81/52	72/41	61/31	44/19	40/15
29	45/18	52/24	56/28	66/36	76/46	87/54	85/56	81/52	72/41	60/30	44/19	40/14
30	45/18		56/28	66/36	76/46	87/55	88/56	81/52	72/40	59/30	45/19	39/13
31	44/17		57/28		76/46		85/56	81/51		59/29		38/12

3 Precipitation, Including Snowfall

This section presents precipitation data. Precipitation includes rainfall and the water equivalent of frozen precipitation, such as snow.

3.1 Precipitation

3.1.1 Monthly Precipitation Means

Monthly precipitation means for the two stations with relatively long data records, Los Alamos and White Rock, are shown in Fig. 3.1 and Table 3.1. Precipitation reaches

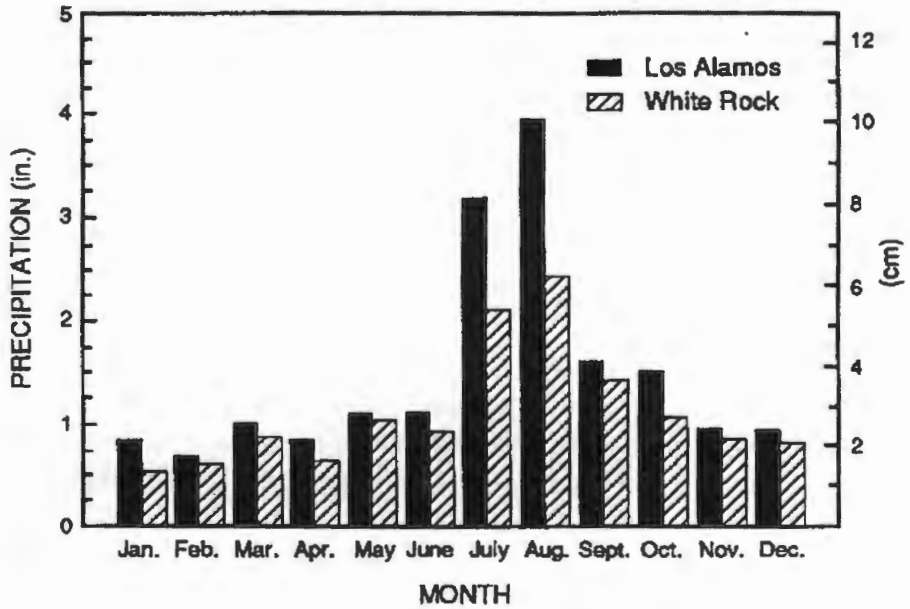

Fig. 3.1. Los Alamos (TA-59) and White Rock monthly mean precipitation.

Table 3.1. Los Alamos (TA-59) and White Rock monthly and annual precipitation means and medians.

	Jan.	Feb.	Mar.	Apr.	May	June	July	Aug.	Sept.	Oct.	Nov.	Dec.	Annual
Mean Precipitation (in.)													
Los Alamos	0.85	0.68	1.01	0.86	1.13	1.12	3.18	3.93	1.63	1.52	0.96	0.96	17.83
White Rock	0.53	0.61	0.88	0.63	1.04	0.92	2.10	2.43	1.39	1.10	0.86	0.79	13.28
Median Precipitation (in.)													
Los Alamos	0.69	0.63	0.90	0.70	1.24	1.05	3.21	3.31	1.70	1.16	0.57	0.71	17.85
White Rock	0.49	0.54	0.71	0.41	0.95	0.66	2.03	2.24	1.52	0.88	0.55	0.56	12.91

a peak at both sites during the monsoon season in July and August. The August means are 4 to 5 times those for the winter months. Precipitation records for Los Alamos and White Rock show 40% and 34%, respectively, of the annual amount falling during July and August and 58% and 53% falling from July through October.

Medians are also given in Table 3.1. The median is often a better indicator of typical precipitation, especially for drier months. Dry months typically have a skewed distribution, with frequent occurrences of below-mean precipitation and few occurrences of above-mean precipitation. Some of the above-normal occurrences are quite high, thereby raising the mean. For example, the medians are significantly lower than the means at both sites for October, November, and December. The monthly means are especially affected by a relatively few months with heavy precipitation.

3.1.2 Hourly Precipitation Means and Frequencies

Hourly precipitation means and frequencies for each month were calculated at three sites: TA-59, East Gate, and Area G (sites 3, 5, and 6, respectively [see Fig. 1.5 for locations]). Precipitation record keeping began in 1982 at East Gate and in 1980 for the other two sites. The average hourly precipitation amount was calculated, along with the frequency of hourly measurable precipitation (≥0.01 in. [0.025 cm]). The analyses for most of the drier months are similar; analyses for the summer months (June–August) show high amounts and frequencies of precipitation, along with large hourly variations. The hourly precipitation amounts and frequencies are plotted for January, June, July, and August in Fig. 3.2(a)–(d).

Precipitation is light in January, typical of cold-season months. The January analyses indicate increased convective activity during the day, even during the middle of winter. Note that precipitation amounts are greater in the late morning and from midafternoon to shortly after midnight, especially at TA-59 near the mountains. The sites nearest the mountains, where precipitation and showers are more common, generally have the greatest precipitation. Precipitation amounts are very low for most of the morning hours. The frequencies are also lowest from 0500 to 0900, but increase somewhat in the late morning and peak in the late afternoon. A secondary peak occurs at TA-59 and East Gate shortly after midnight.

The June precipitation pattern is very different from that in January. Note the peak in amounts during the early afternoon, especially at TA-59. The precipitation decreases markedly at 1500 from the early peaks. Frequencies indicate that rainfall reaches a peak at 1300 at TA-59; it peaks at East Gate and Area G an hour later. The lag results because of the time required for showers formed over the mountains to travel down the plateau. Rainfall frequency reaches a relative minimum at all sites by 2200 and then increases somewhat toward midnight. Comparison with January precipitation shows that measurable precipitation in June is somewhat more frequent at TA-59 and East Gate during afternoon hours and is less frequent at Area G. Precipitation is generally more frequent at all sites during June than during January.

Increased thundershower activity in July increases precipitation amounts and frequency. Note the dramatic peak in amount and frequency at TA-59 at 1400.

Maximum amounts and frequency at Area G occur later, at 1800. A small secondary frequency maximum occurs late in the day, and even later at East Gate. Both frequency and amounts are generally quite low at all sites during the morning hours because of greater atmospheric stability.

Rainfall is also heavy during August, with a maximum occurring between 1300 and 1500. The TA-59 hourly peak during August only reaches 0.4 in. (0.9 cm) versus 0.6 in. (1.5 cm) in July, even though—as at East Gate and Area G—total rainfall is generally greater in August than in July. Following the first peak at 1400, hourly precipitation amounts decrease through 1700, after which the TA-59 and East Gate rainfall amounts reach a second peak by 1900. Note how the Area G second peak for precipitation amount lags, occurring at 2100. This amount peak is accompanied by a frequency peak. The August analyses show that rainfall is heaviest in the early afternoon and early evening. Rains at TA-59 and East Gate occur most frequently during the early afternoon; at Area G, during the evening (2100).

3.1.3 Precipitation Probabilities

Los Alamos (TA-59) and White Rock precipitation probabilities were calculated by month, season, and year. These data can help planners determine probabilities that a certain precipitation amount will fall during a given period. The results are shown in Tables 3.2 and 3.3. Note that the Los Alamos amounts are higher than those at White Rock for most probabilities and periods. The Los Alamos precipitation increase over that at White Rock is larger during the spring and summer months. Precipitation is greatest at both sites during the warm season. It must be stressed that caution should be used when comparing the extremes between the two sites because the Los Alamos data record is much larger than White Rock's. Specifically, Los Alamos low-precipitation extremes are occasionally lower than those at White Rock simply because of larger data records.

3.1.4 Specified Daily Precipitation Amounts

The monthly mean and maximum numbers of days on which precipitation exceeded specified amounts were calculated for Los Alamos and White Rock. Results are shown in Tables 3.4 and 3.5, respectively. The Los Alamos means and maximums are greater than those at White Rock for all months and precipitation amounts. Occurrences of all precipitation amounts are generally twice or more as frequent during July and August as during other months at both sites. The smallest precipitation amount that can be measured is 0.01 in. (0.025 cm).

3.1.5 Precipitation Network Data

Precipitation was calculated from data obtained from a network of eight tipping buckets. Except for data from TA-59 and White Rock, data records have not been kept long enough at other sites to compile monthly means. However, summer and annual precipitation for each site was determined for comparisons.

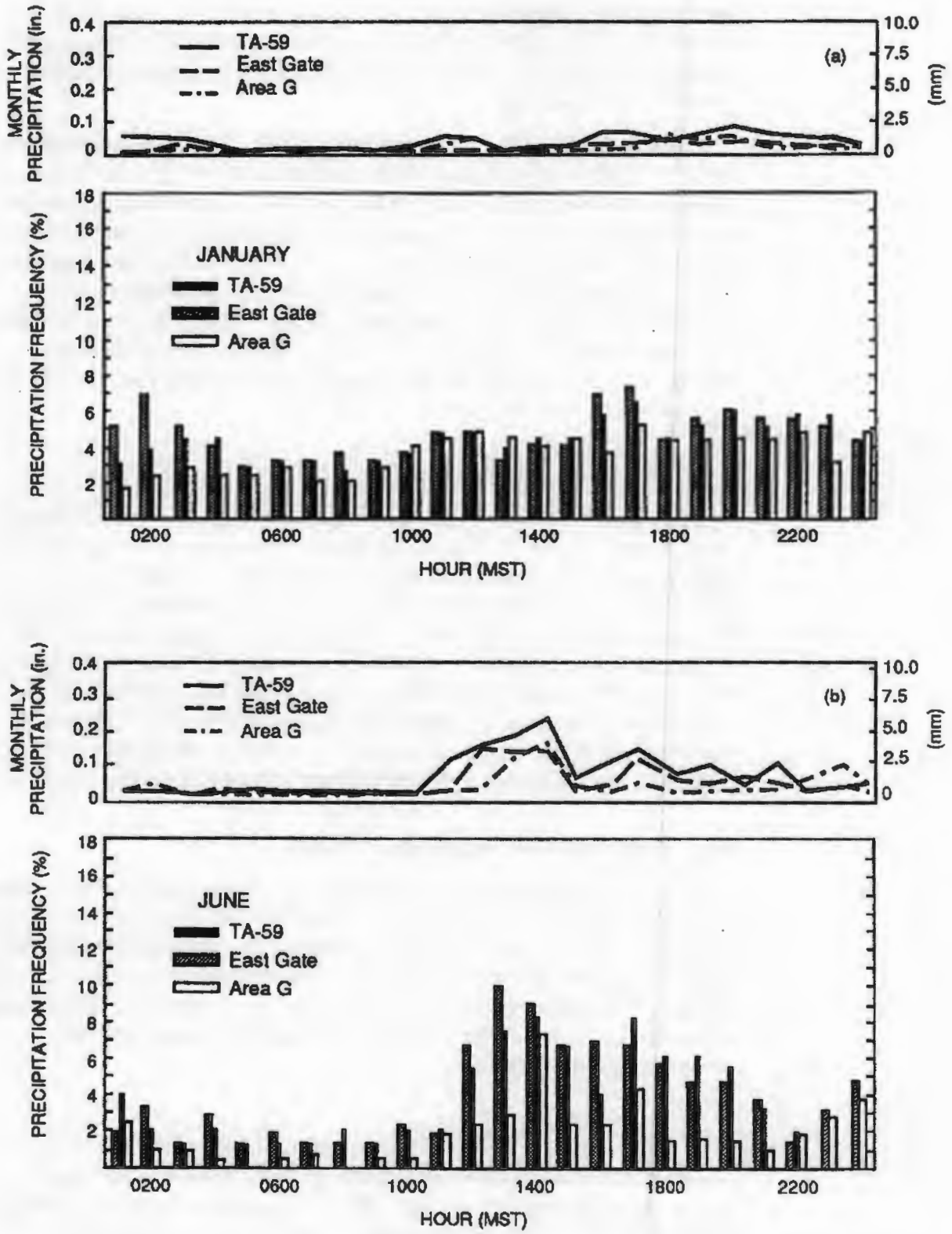

Fig. 3.2(a)–(d). Hourly (Mountain Standard Time) precipitation amounts and frequencies at three sites (TA-59, East Gate, and Area G) during (a) January, (b) June, (c) July, and (d) August.

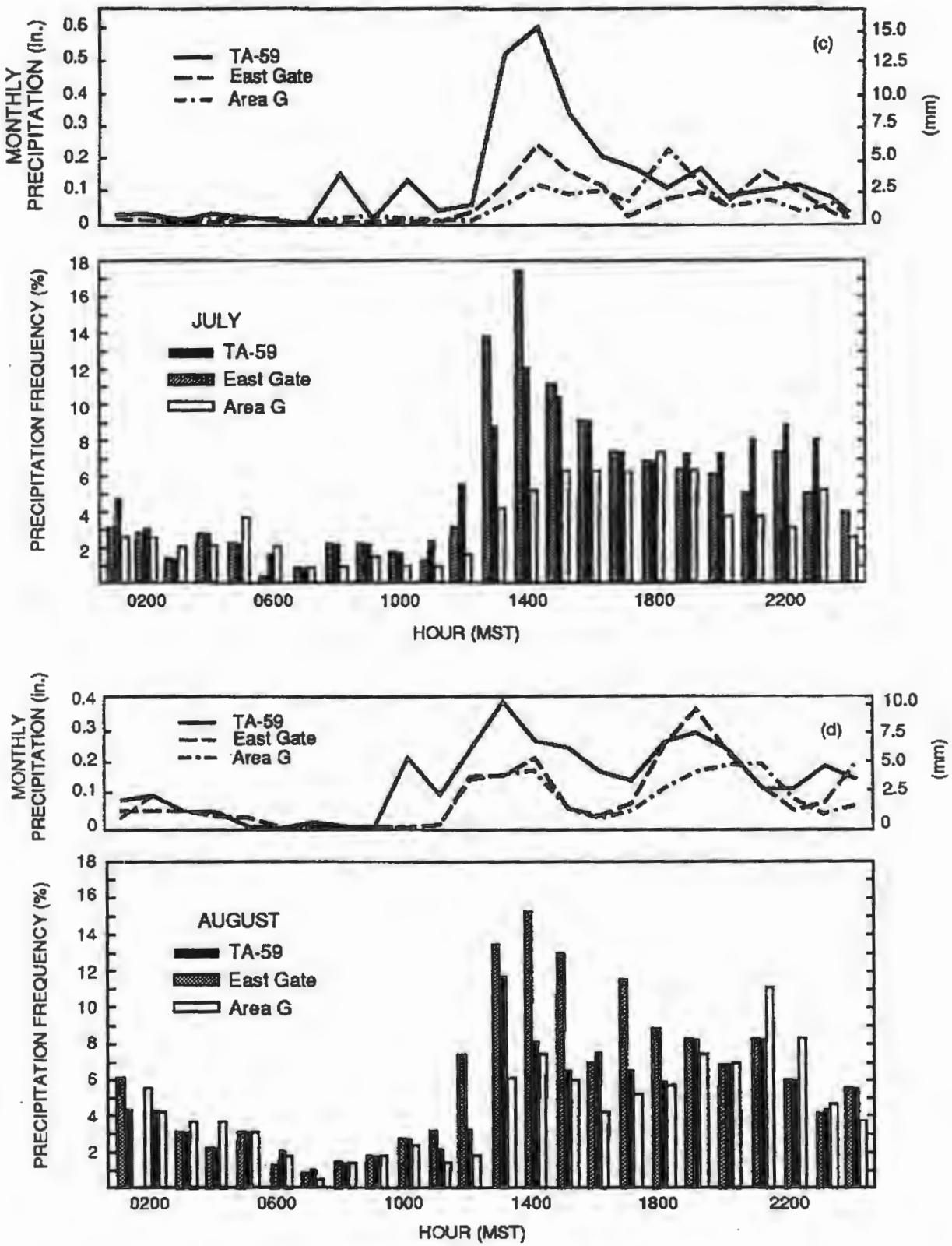

Fig. 3.2 (Continued)

Table 3.2. Los Alamos precipitation probabilities, 1911–1987. Column headings represent the percentage of time precipitation is less than, or equal to, the specified amount for a given month, year, or season.

	Low	5%	10%	25%	50%	75%	90%	95%	High
Precipitation (in.)									
January	0.00	0.03	0.10	0.25	0.69	1.16	1.60	2.43	6.75
February	0.00	0.04	0.11	0.33	0.63	1.00	1.65	1.87	2.44
March	0.00	0.09	0.23	0.50	0.90	1.34	2.33	2.96	4.11
April	0.00	0.00	0.03	0.28	0.70	1.38	2.43	3.21	4.64
May	0.00	0.08	0.17	0.49	1.24	1.97	2.64	3.35	4.47
June	0.00	0.01	0.13	0.42	1.05	1.86	3.21	3.72	5.67
July	0.35	0.95	1.35	1.98	3.21	4.10	5.00	6.37	7.98
August	0.51	1.09	1.39	2.37	3.31	4.67	5.60	6.51	11.18
September	0.00	0.16	0.45	1.23	1.70	2.76	3.77	4.09	5.79
October	0.00	0.09	0.25	0.46	1.16	2.10	3.69	4.55	6.77
November	0.00	0.00	0.00	0.23	0.57	1.06	1.81	2.23	6.60
December	0.00	0.06	0.09	0.33	0.71	1.55	2.16	2.69	3.21
Annual	6.80	11.35	13.13	15.35	17.85	20.67	25.38	29.26	30.34
Winter	0.00	1.07	1.15	1.56	2.15	3.21	4.02	4.65	9.06
Spring	0.00	0.09	1.15	2.19	3.19	4.56	5.92	7.26	9.97
Summer	2.32	3.99	4.64	6.74	8.20	9.52	11.32	12.88	16.50
Fall	0.23	1.40	1.78	2.81	3.80	5.35	7.49	9.00	11.23

The summer and annual mean precipitation amounts are plotted in Fig. 3.3. Generally, precipitation is greatest for areas with the highest elevations or proximity to the Jemez Mountains. The increased amount of precipitation (rain) toward the mountains is especially noticeable during the summer when thundershowers develop over the mountains. Showers tend to form, or be stronger, over the mountains for much of the year. Also, winter storms associated with upslope winds drop more precipitation higher on the plateau (note that the precipitation becomes relatively uniform toward the Rio Grande Valley). The White Rock Y location receives the least precipitation, slightly less than that at White Rock.

3.2 Snowfall

3.2.1 Monthly Snowfall Means

Los Alamos snowfall is quite heavy, averaging almost 52 in. (132 cm) annually for the period 1951–1980. Snowfall becomes heavier at higher elevations, averaging nearly 100 in. (254 cm) at the tops of the Jemez Mountains. Many large snowfalls at Los Alamos result from a low-level, up-plateau wind from the southeast and south. Westerly winds, while accompanying some heavy snows high in the mountains, generally inhibit

Table 3.3. White Rock precipitation probabilities, 1964–1987. Column headings represent the percentage of time precipitation is less than, or equal to, the specified amount for a given month, year, or season.

	Low	5%	10%	25%	50%	75%	90%	95%	High
Precipitation (in.)									
January	0.00	0.00	0.01	0.08	0.49	0.94	1.12	1.31	1.33
February	0.02	0.05	0.07	0.33	0.54	1.00	1.20	1.32	1.42
March	0.07	0.08	0.12	0.31	0.71	1.21	1.74	2.58	3.36
April	0.00	0.00	0.00	0.20	0.41	0.93	1.44	2.31	2.80
May	0.00	0.01	0.08	0.37	0.95	1.44	2.42	2.82	3.01
June	0.00	0.04	0.12	0.45	0.66	1.01	2.19	2.58	3.26
July	0.45	0.54	0.85	1.38	2.03	2.67	3.71	4.13	4.51
August	0.85	0.87	0.95	1.50	2.24	3.14	4.32	4.67	4.88
September	0.15	0.18	0.22	0.86	1.52	1.85	2.54	2.89	3.06
October	0.00	0.04	0.07	0.21	0.88	1.94	2.71	2.29	3.12
November	0.07	0.08	0.08	0.36	0.55	0.83	1.60	3.00	4.06
December	0.00	0.00	0.08	0.20	0.56	1.25	1.85	2.34	2.65
Annual	8.32	8.73	9.27	10.96	12.91	15.46	18.91	19.22	19.57
Winter	0.68	0.75	0.82	1.36	1.70	2.82	3.84	5.11	6.66
Spring	0.09	0.44	1.02	1.48	2.19	3.39	3.72	5.79	8.21
Summer	1.66	2.06	2.54	4.31	5.41	6.66	8.54	8.71	8.92
Fall	1.12	1.14	1.33	1.95	3.03	4.25	6.07	7.05	7.21

large snowfalls in Los Alamos because westerly winds must descend the east side of the mountains, thereby warming and drying the air.

Monthly mean snowfall amounts are shown in Fig. 3.4 and Table 3.6. Snowfall is greatest during December and January, averaging 11.4 and 10.7 in. (28.9 and 27.2 cm), respectively. Snowfall is also heavy in March, with a mean of 9.7 in. (24.7 cm). Note the obvious snowfall minimum in February, with only 7.3 in. (18.5 cm). Water equivalent is also light in February, making it the driest month of the year.

In December, the median is quite a bit lower than the mean. December is characterized by frequent occurrences of small amounts of snowfall and several occurrences of very heavy snowfall. The medians are near zero in April, May, September, October, and November. Just a few snowfalls during these months inflate the averages; otherwise, snowfall is most often light, or even nil, during these months.

The ratio of snowfall to water equivalent averages about 20 to 1 from November to February, although the ratio frequently reaches 30 or higher. The large ratio is typical of mountain areas, where the air at higher elevations is thinner and generally colder than at sea level and therefore can hold less water vapor than at sea level. The ratio generally is lower in the other months, averaging 15 to 1 or so. Some very wet snows can give ratios of 10 to 1 or even lower.

Table 3.4. Los Alamos mean number of days of precipitation for specified amounts, maximum number of days in which precipitation exceeded the specified amount, and latest year the maximum occurred (mean based on 1951–1980 period).

	0.01 in.			0.05 in.			0.10 in.			0.25 in.		
	Mean	Max	Year of Max	Mean	Max	Year of Max	Mean	Max	Year of Max	Mean	Max	Year of Max
January	5.4	15	1949	3.3	12	1949	2.2	10	1949	1.2	7	1916
February	6.0	12	1960	3.5	8	1987	2.1	7	1920	0.7	5	1987
March	7.0	17	1958	4.4	12	1958	3.0	8	1958	1.3	5	1984
April	5.5	14	1977	3.4	13	1915	2.4	12	1915	1.0	8	1915
May	6.9	15	1987	4.3	12	1979	3.1	11	1926	1.4	7	1929
June	6.0	18	1986	4.0	13	1912	2.9	13	1912	1.5	7	1986
July	14.4	22	1964	9.9	20	1911	7.6	17	1911	1.8	6	1919
August	14.5	23	1957	10.9	18	1957	8.7	15	1952	4.9	13	1952
September	7.9	17	1927	5.2	16	1927	3.9	15	1927	2.4	7	1969
October	5.5	17	1972	4.0	11	1986	3.0	11	1941	1.7	9	1941
November	4.3	13	1982	3.3	9	1957	2.4	8	1957	1.2	7	1978
December	5.1	12	1983	3.7	10	1967	2.6	9	1967	1.2	5	1940
Annual	88.6	130	1957	59.9	84	1941	43.9	74	1941	20.3	44	1941

	0.50 in.			0.75 in.			1.00 in.		
	Mean	Max	Year of Max	Mean	Max	Year of Max	Mean	Max	Year of Max
January	0.3	5	1916	0.2	3	1916	0.0	2	1916
February	0.3	2	1987	0.1	1	1987	0.0	1	1915
March	0.2	3	1919	0.1	2	1973	0.1	2	1973
April	0.5	3	1942	0.1	2	1985	0.1	1	1985
May	0.5	3	1952	0.2	2	1952	0.1	2	1952
June	0.6	6	1986	0.3	3	1937	0.0	2	1913
July	1.8	6	1919	0.9	5	1919	0.5	3	1919
August	2.5	9	1952	1.3	7	1952	0.7	4	1952
September	1.0	5	1941	0.4	3	1975	0.1	3	1941
October	1.2	6	1957	0.7	4	1957	0.3	2	1959
November	0.5	6	1978	0.3	4	1978	0.2	3	1978
December	0.4	3	1984	0.3	2	1961	0.1	1	1984
Annual	9.8	23	1952	4.9	15	1952	2.2	9	1915

Table 3.5. White Rock mean number of days of precipitation for specified amounts, maximum number of days in which precipitation exceeded the specified amount, and latest year the maximum occurred (mean based on 1965–1987 period).

	0.01 in.			0.05 in.			0.10 in.			0.25 in.		
	Mean	Max	Year of Max	Mean	Max	Year of Max	Mean	Max	Year of Max	Mean	Max	Year of Max
January	3.3	7	1987	2.2	5	1977	1.5	4	1987	0.8	3	1965
February	3.8	8	1982	2.6	6	1976	1.6	5	1982	0.7	2	1987
March	5.0	10	1973	3.6	8	1973	2.6	6	1985	1.2	4	1985
April	3.2	8	1985	2.4	6	1986	1.5	6	1985	0.8	3	1986
May	4.6	12	1985	3.2	10	1987	2.6	8	1987	1.3	4	1987
June	4.7	14	1986	3.5	10	1986	2.5	9	1986	1.5	4	1986
July	8.9	15	1970	7.4	15	1970	5.7	11	1970	3.0	6	1976
August	9.3	16	1987	7.6	11	1970	5.5	9	1987	3.4	7	1968
September	6.3	12	1986	4.7	10	1972	3.9	10	1972	2.0	6	1986
October	5.0	16	1972	4.0	15	1972	2.8	11	1972	1.7	5	1972
November	4.2	9	1986	3.2	9	1986	2.3	9	1986	0.9	4	1978
December	4.3	10	1984	3.1	9	1984	2.4	7	1984	1.1	4	1984
Annual	62.6	103	1986	47.5	73	1986	34.9	57	1986	18.4	31	1986

	0.50 in.			0.75 in.			1.00 in.		
	Mean	Max	Year of Max	Mean	Max	Year of Max	Mean	Max	Year of Max
January	0.1	1	1983	0.0	1	1971	0.0	1	1971
February	0.2	1	1985	0.0	1	1975	—	—	—
March	0.2	2	1985	0.1	1	1985	0.0	1	1985
April	0.3	2	1985	0.1	1	1985	0.1	1	1985
May	0.5	2	1985	0.0	1	1972	0.0	1	1972
June	0.6	2	1986	0.3	2	1969	0.1	1	1986
July	1.2	4	1971	0.5	2	1976	0.1	1	1975
August	1.4	4	1987	0.8	3	1987	0.3	1	1987
September	0.8	3	1975	0.2	1	1985	0.1	1	1981
October	0.7	3	1985	0.2	1	1985	0.1	1	1985
November	0.5	3	1978	0.1	1	1982	—	—	—
December	0.3	2	1984	0.1	1	1984	0.0	1	1965
Annual	6.8	13	1985	2.4	5	1984	0.8	3	1985

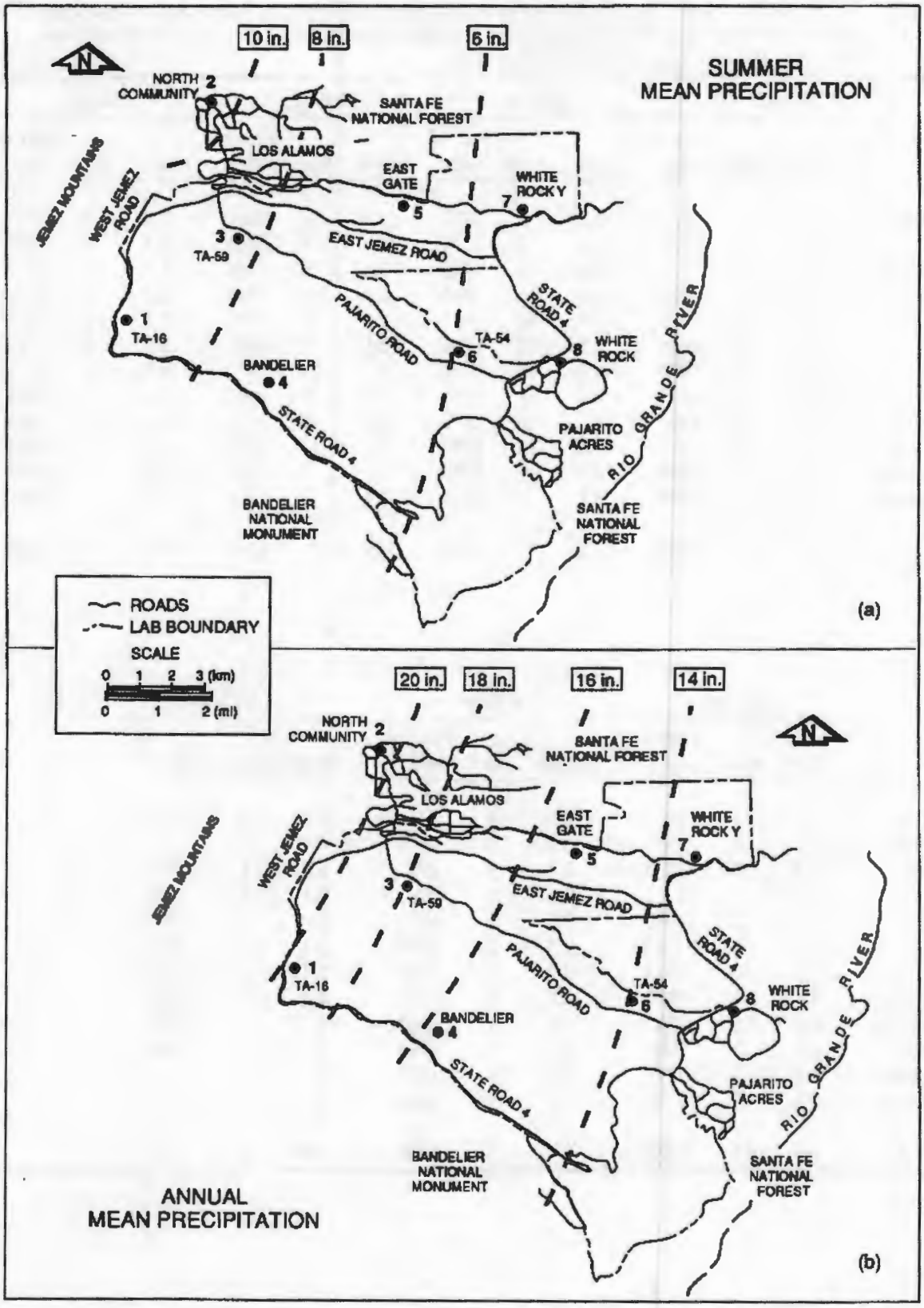

Fig. 3.3. (a) Summer (June–August) mean precipitation and (b) annual mean precipitation at Los Alamos.

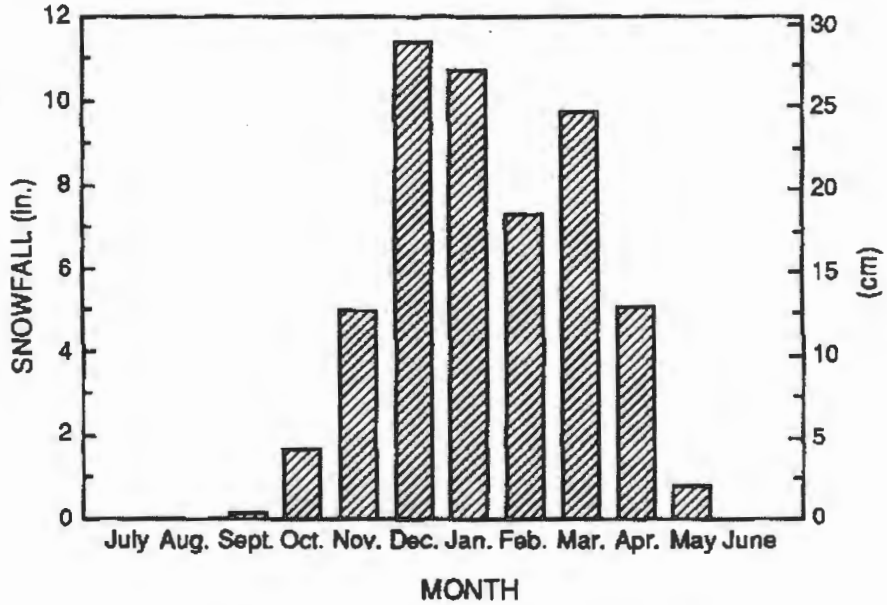

Fig. 3.4. Los Alamos monthly normal snowfall.

3.2.2 Monthly Snowfall Probabilities

Los Alamos snowfall-amount probabilities were calculated by month, season, and year. The results are shown in Table 3.7. Note that even during the snowy months, probabilities are relatively favorable for light snow. For example, 10% of the time, the months December through March have less than 1 in. (2.54 cm) of snow, whereas 25% of the time, those months have less than 4 in. (10 cm). The 50% probability shows that December has the third highest median, even though it has the highest average. However, December and March have increased frequencies of very heavy snowfall. January and February have relatively low probabilities of heavy snowfall, in spite of the record 1987 snowfalls of 64.8 and 48.5 in. (164.6 and 113.2 cm), respectively.

Table 3.6. Los Alamos monthly and annual snowfall means and medians.

	Jan.	Feb.	Mar.	Apr.	May	June	July	Aug.	Sept.	Oct.	Nov.	Dec.	Annual
Snowfall (in.)													
Mean	10.7	7.3	9.7	5.1	0.8	—	—	—	0.1	1.7	5.0	11.4	51.8
Median	9.8	5.5	8.5	2.0	0.0	—	—	—	0.0	0.0	3.1	7.2	50.0

Table 3.7. Los Alamos snowfall probabilities, 1911–1987. Column headings represent the percentage of time snowfall is less than, or equal to, the specified amount for a given month, season, or year.

	Low	5%	10%	25%	50%	75%	90%	95%	High
Snowfall (in.)									
September	0.0	0.0	0.0	0.0	0.0	0.0	0.0	0.9	6.0
October	0.0	0.0	0.0	0.0	0.0	1.0	6.5	9.0	20.0
November	0.0	0.0	0.0	0.5	3.1	7.7	12.4	17.4	34.5
December	0.2	0.8	1.1	3.5	7.2	13.2	26.1	33.2	41.3
January	0.0	0.0	0.8	3.4	9.8	15.8	19.8	29.9	64.8
February	0.0	0.0	0.6	2.0	5.5	12.4	19.0	23.2	48.5
March	0.0	0.0	0.5	4.0	8.5	15.2	27.0	33.3	36.0
April	0.0	0.0	0.0	0.0	2.0	5.5	13.8	14.9	33.6
May	0.0	0.0	0.0	0.0	0.0	0.1	2.3	4.0	17.0
Season	9.3	18.3	24.5	32.4	48.3	72.0	98.8	121.8	153.2
Annual	8.9	21.3	25.6	30.5	50.6	67.6	90.8	99.5	178.4

3.2.3 Specified Daily Snowfall Amounts

Mean and maximum daily snowfalls were calculated for specific amounts and are listed in Table 3.8. The 0.1-in. (0.25-cm) snowfall is the smallest snowfall amount that can be measured. Snowfalls of less than 2 in. (5 cm) are considered light; a moderate snowfall is generally 2–4 in. (5–10 cm). A snowfall exceeding 6 in. (15 cm) is considered heavy, and a 4-in. (10-cm) snowfall within a 12-hour period is also considered heavy. It is interesting to see that the mean for 0.1- and 0.5-in. (0.25- and 1.27-cm) snowfalls is slightly higher for March than for other winter months. Heavy snows are quite evenly distributed, with slightly more occurring in December, January, and March.

Table 3.8. Los Alamos mean number of days of snowfall for specified amounts, maximum number of days in which snowfall exceeded the specified amount, and latest year maximum occurred (mean based on 1951–1980 period).

	0.1 in.			0.5 in.			1.0 in.			2.0 in.		
	Mean	Max	Year of Max	Mean	Max	Year of Max	Mean	Max	Year of Max	Mean	Max	Year of Max
January	4.6	13	1949	3.5	12	1949	2.9	11	1949	1.9	9	1916
February	4.4	11	1960	3.3	10	1960	2.4	8	1960	1.2	6	1987
March	4.9	13	1958	3.7	12	1958	2.8	10	1958	1.8	6	1958
April	2.2	9	1958	1.7	8	1958	1.4	6	1958	0.9	4	1958
May	0.4	3	1978	0.3	3	1978	0.2	3	1978	0.2	3	1978
June	—	—	—	—	—	—	—	—	—	—	—	—
July	—	—	—	—	—	—	—	—	—	—	—	—
August	—	—	—	—	—	—	—	—	—	—	—	—
September	0.1	1	1971	0.0	1	1971	0.0	1	1971	0.0	1	1936
October	0.8	6	1984	0.6	6	1984	0.4	6	1984	0.3	4	1984
November	2.2	8	1957	2.0	7	1957	1.5	7	1957	1.0	7	1957
December	4.2	12	1983	3.5	10	1967	2.7	9	1967	1.9	8	1967
Season	23.8	45	1957–58	18.6	37	1957–58 1984–85	14.3	31	1984–85	9.2	9	1957–58 1986–87

	4.0 in.			6.0 in.			8.0 in.			10.0 in.		
	Mean	Max	Year of Max	Mean	Max	Year of Max	Mean	Max	Year of Max	Mean	Max	Year of Max
January	0.9	6	1949	0.4	3	1987	0.2	2	1987	0.1	2	1987
February	0.7	5	1987	0.2	2	1987	0.1	2	1987	0.1	2	1975
March	0.8	5	1984	0.4	3	1958	0.2	2	1973	0.1	2	1973
April	0.4	3	1980	0.2	3	1958	0.1	2	1975	0.1	2	1975
May	0.1	1	1978	0.0	1	1978	0.0	1	1978	0.0	1	1978
June	—	—	—	—	—	—	—	—	—	—	—	—
July	—	—	—	—	—	—	—	—	—	—	—	—
August	—	—	—	—	—	—	—	—	—	—	—	—
September	0.0	1	1936	—	—	—	—	—	—	—	—	—
October	0.2	3	1984	0.1	1	1984	0.0	1	1972	—	—	—
November	0.4	5	1957	0.2	3	1957	0.1	1	1980	0.0	1	1976
December	0.9	4	1971	0.6	3	1961	0.3	2	1984	0.2	2	1984
Season	4.4	14	1986–87	2.1	10	1957–58	1.0	4	1986–87 (3 others)	0.6	4	1974–75

4 Wind

4.1 Wind Roses

Mean wind-speed and wind-direction frequencies were calculated for daytime, nighttime, and total time (24 hours) at five sites for the months of January, April, July, and October. The frequencies are presented as wind roses, which are circles with spokes extending from the center representing the direction from which the wind blows. The length of each spoke is proportional to the frequency at which the wind blows *from* the indicated direction. Each direction is 1 of 16 primary compass points (N and NNE, for example) and is shown centered on a 22.5° sector of the circle. Each spoke consists of different line widths representing wind-speed classes. The frequency of calm winds (winds having a speed less than 1 mph [0.5 m/s]) is given in the circle's center. Day and night are defined by sunrise and sunset.

The wind roses represent winds at five sites (elevations above sea level [ASL] are in parentheses): TA-59 (7373 ft [2248 m]), TA-50 (7270 ft [2216 m]), Bandelier (7040 ft [2146 m]), East Gate (7019 ft [2140 m]), and Area G (6688 ft [2039 m]). Surface winds were measured at a height of about 39 ft (11–12 m) above ground level (AGL) at all sites except TA-59, where the measuring height is 75 ft (23 m). The TA-59 measuring height is higher because the tower is adjacent to the Laboratory one-story OH-1 building, and the effects of a nearby building on airflow are assumed to be minimal at the 75-ft measuring height. At TA-50, winds were also measured at the 300-ft (92-m) level.

Annual surface wind roses for day, night, and total at TA-50, Bandelier, East Gate, and Area G are shown on maps in Fig. 4.1(a)–(c). Day and night wind roses for the four seasons are shown in Figs. 4.2–4.5. Total (day and night) wind roses for January, April, July, and October are shown in Figs. 4.6–4.9, respectively. Note that the TA-50 (92 m) wind roses are displaced on the maps and are shown far to the right, with an arrow pointing to the TA-50 location. The Bandelier site is located farthest to the south, East Gate is east-northeast of TA-50, and Area G is just west of White Rock.

The TA-50 (upper-left) wind rose (Figs. 4.1–4.9) has been chosen to represent the western Laboratory area; wind roses for TA-59 (not shown on these figures because of space limitation) are shown separately in Figs. 4.10–4.14 at the end of this section. The two sites are located very close to each other, and winds are similar at both sites. Wind data for all these sites were available for the following periods (ending in early 1988): 8 years at TA-59 and Area G, 6 years at East Gate, 3 years at TA-50, and 1 year at Bandelier.

Los Alamos annual surface winds are generally light, with an average speed of nearly 7 mph (3 m/s). Wind speeds greater than 11 mph (5 m/s) occur with frequencies ranging from 10% at TA-50 to 20% or so at East Gate. The S'ly and SW'ly winds tend to be stronger because the Los Alamos Canyon, located just south of East Gate, presents less friction to winds. Many of the strong Los Alamos winds occur during the spring. More than 40% of the surface winds at all sites have speeds less than 5.5 mph (2.5 m/s). The

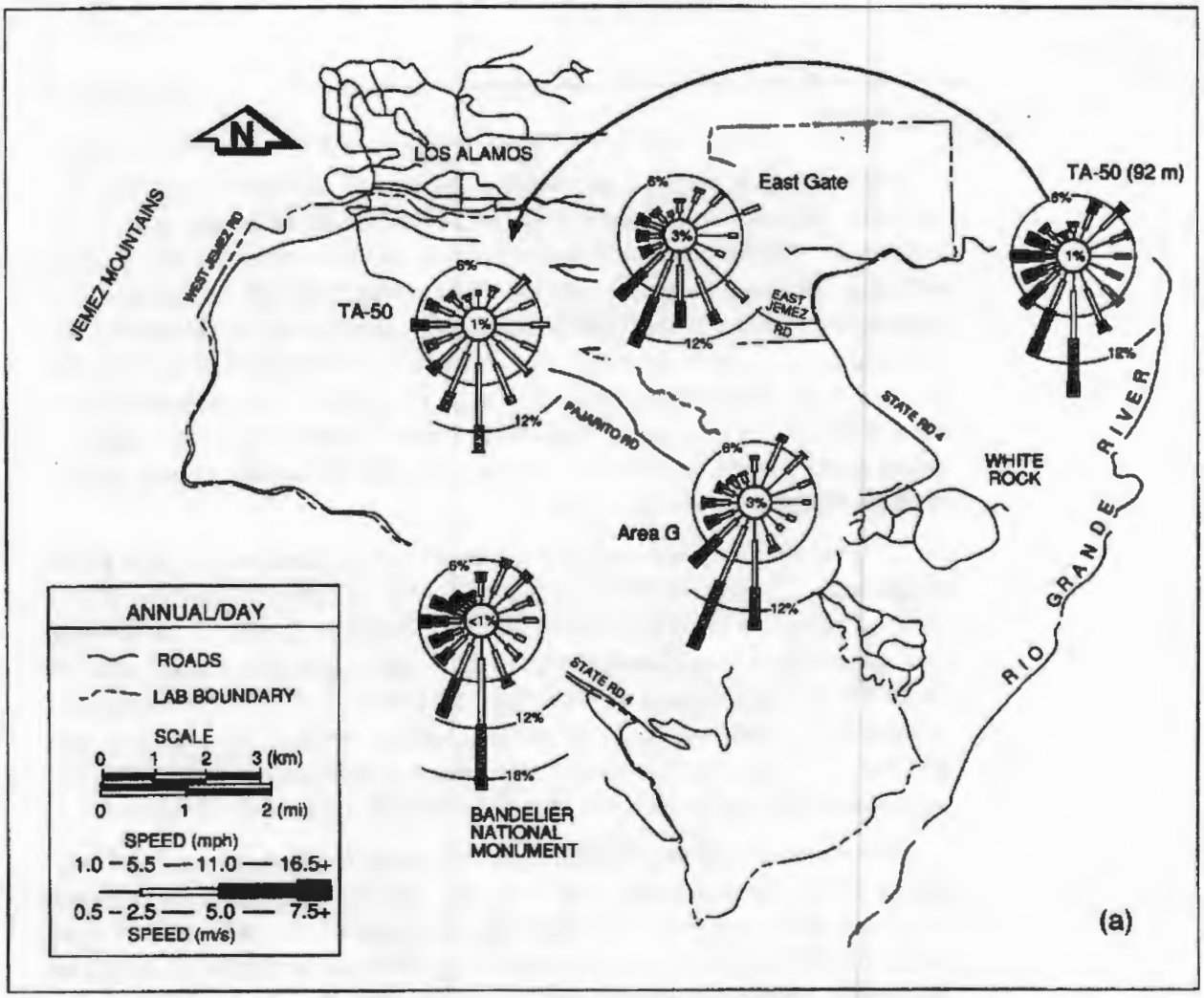

Fig. 4.1(a)–(c). Annual wind roses for (a) daytime, (b) nighttime, and (c) total (day and night) for Los Alamos sites at TA-50, East Gate, Area G, and Bandelier. Winds were measured at a height of about 39 ft (11–12 m) for all the sites and also at the 300-ft (92-m) level at TA-50.

average wind speed increases to over 9 mph (4 m/s) at the TA-50, 300-ft (92-m) level. At this higher level, wind speeds greater than 11 mph (5 m/s) occur one-third of the time, and wind speeds less than 5.5 mph (2.5 m/s) occur almost one-third of the time.

Wind distribution varies with site, height above ground, and time of day, primarily because of the Los Alamos terrain features. On days with sunshine and light, large-scale winds, a deep, thermally driven upslope wind develops over the Pajarito Plateau. Note the high frequency of SE'ly through S'ly winds during the day at TA-50 (both levels) and at East Gate during the year. The upslope wind is even more frequent at TA-59

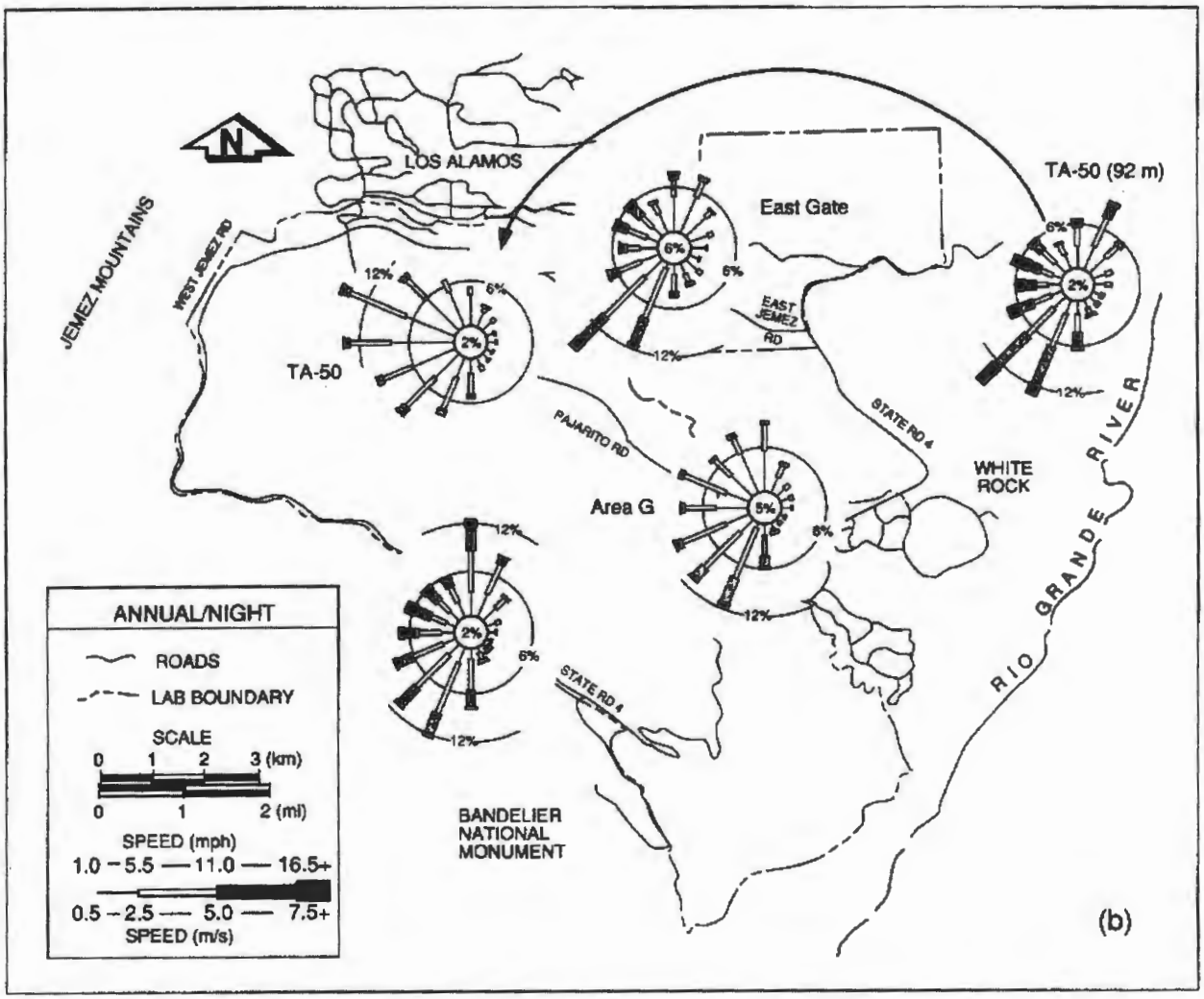

Fig. 4.1 (Continued)
(b) Annual nighttime wind roses at Los Alamos.

(not shown). Upslope winds are generally light, less than 5.5 mph (2.5 m/s). Winds become more SSW'ly at Area G (that is, at lower elevations). The winds here are more affected by the Rio Grande Valley than by the plateau. Regional-scale wind channeling by the valley contributes to the high frequency of SSW'ly and NNE'ly or NE'ly winds. In addition, a thermally driven up-valley wind may cause some of the SSW'ly winds at Area G that are less than 5.5 mph (2.5 m/s).

Winds reverse during the night. A shallow, cold-air drainage wind often forms and flows down the plateau on clear nights along with the light, large-scale winds. Drainage

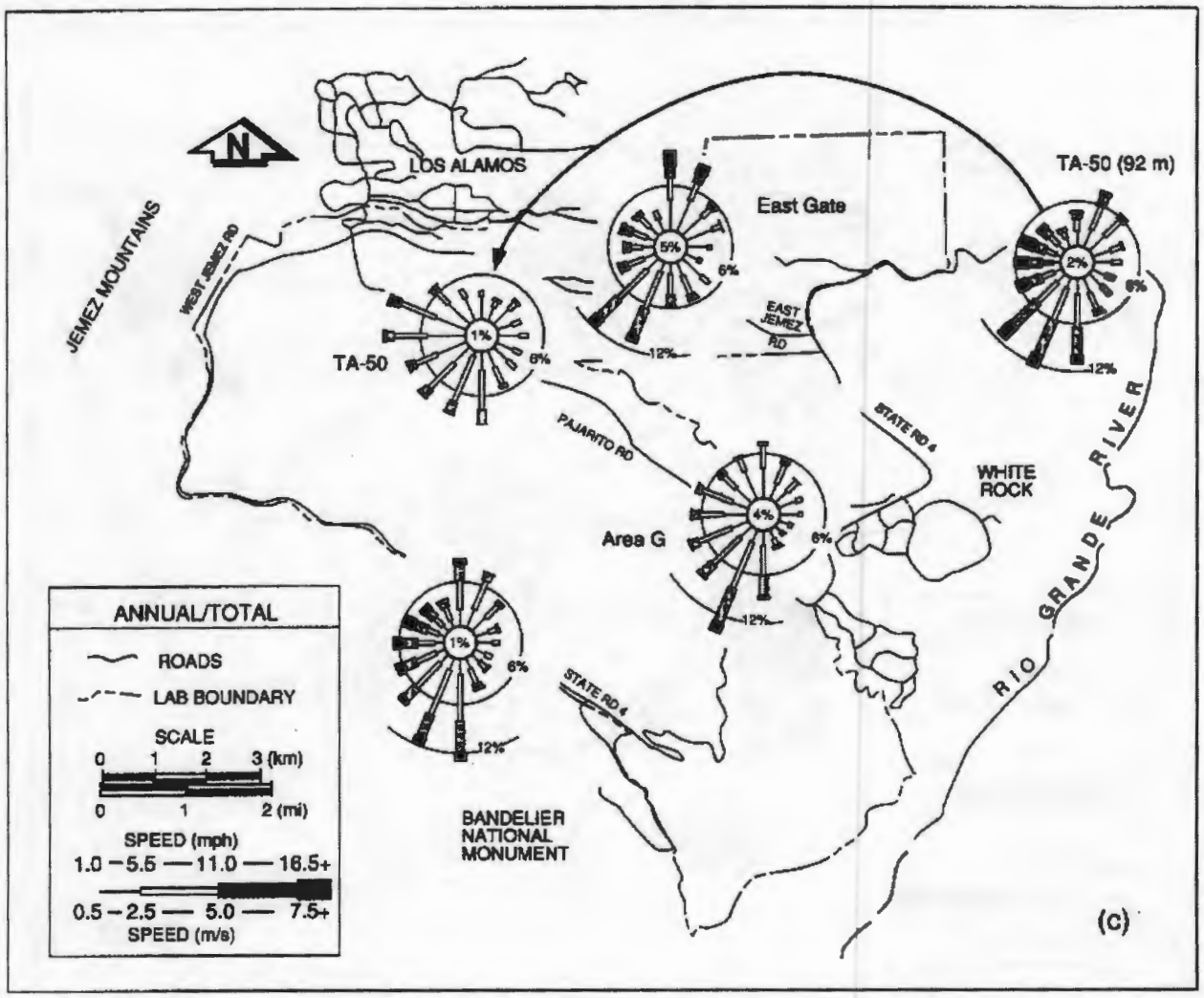

Fig. 4.1 (Continued)
(c) Annual total wind roses at Los Alamos.

winds are generally less than 7 mph (3 m/s). Drainage winds most often occur from the NW through the W at TA-50, whereas the drainage winds at Bandelier and Area G are more evenly distributed from the WNW through the N. Drainage winds are much less frequent at East Gate because the Los Alamos Canyon extends to the west of the site. The nighttime TA-50 wind rose at 300 ft (92 m) shows dramatically different winds from those at the surface, with valley-channeled winds dominating. Up-valley (SW'ly and SSW'ly) and down-valley (N'ly through NE'ly) winds occur with high frequency. Less-frequent channeled winds also occur at the lower sites.

Wind patterns are quite different for different times of the year. More N'ly through NE'ly winds occur during the winter (January, for example, in Fig. 4.2). Large-scale pressure patterns during the winter promote a relatively high frequency of N'ly winds in the lower atmosphere. During the day, NE'ly winds are almost as common as SE'ly winds at TA-50 and East Gate and S-SSW'ly winds at Bandelier and Area G. At night, the NE'ly winds are prominent, especially at the upper level at TA-50. At lower heights, the nighttime drainage flow is important. The data show a dramatic difference in winds between the upper and lower heights at TA-50. The large number of NNW'ly through N'ly winds at Bandelier and Area G indicates that the drainage wind and channeled down-valley wind are equally important, resulting in a compromised wind. However, channeled winds, not drainage winds, predominate at East Gate. This site is situated where drainage winds are not common.

April winds, and spring winds in general, are stronger than winds occurring during other times of the year (Fig. 4.3). Strong storms often track west to east across the southern and central Rockies, thereby causing strong winds in New Mexico. The strong winds are important in limiting local plateau winds (upslope and downslope), as well as, to a lesser extent, channeled winds. Note the scarcity of upslope winds at TA-50 during the day and the increase of W'ly winds at all sites during the day.

Winds are also different in April at night. Note the dramatic decrease in down-valley winds, especially at TA-50 at the upper level, when compared with occurrences in January. The weather pattern for large-scale winds has changed by April, giving fewer large-scale N'ly winds and thereby preventing many channeled NNE-NE'ly winds. Also note the reduction in NNW-N'ly winds at Bandelier and Area G from those occurring in January. The drainage winds for these areas are now more prevalent than the channeled, down-valley winds. At TA-50, the drainage wind is now more W'ly and WNW'ly.

Winds become much weaker by summer. Daytime winds in July (see Fig. 4.4) tend to be S'ly at all sites. The upslope winds are less frequent during July at the upper plateau because of increased humidity and shower activity, which reduce the differential heating. Winds are generally similar in October, with only a slight increase in wind speed (see Fig. 4.5).

In Figs. 4.10–4.14, data show that TA-59, located on a steeper slope than the one at TA-50, has more slope winds. When compared with TA-50 (12 m), TA-59 has more daytime SE-SSE'ly winds and more nighttime drainage winds from the W-NW.

4.2 Mean Wind-Direction Frequencies and Wind Speeds

Although wind roses are useful in showing general day and night wind frequencies, they do not show the short-term features in the wind patterns. Mean wind-direction frequencies and wind speeds were calculated at four sites (including the two levels at TA-50). Frequencies and speeds were calculated for the 16 compass points.

Mean wind-direction frequencies and wind speeds are plotted by hour in Figs. 4.15–4.18 for January, April, July, and October. Data from the upper and lower

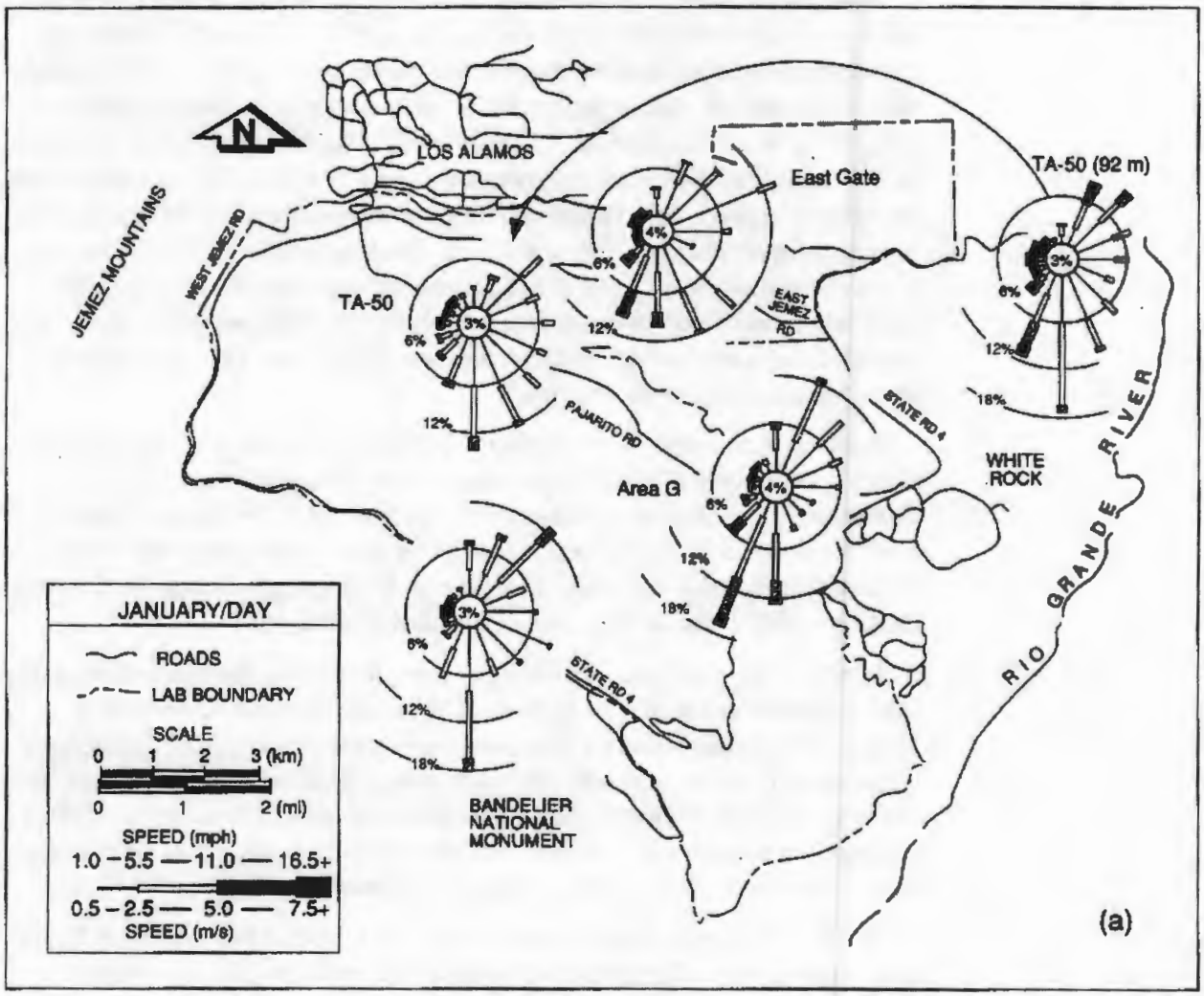

Fig. 4.2(a) and (b).
(a) January day wind roses at Los Alamos.

tower levels at TA-50 and from the towers at East Gate and Area G are shown in figures appearing on opposite pages to allow for easy comparisons. The wind diagrams for TA-59, a site with winds similar to those at TA-50, are shown in Fig. 4.19. Triangles indicate average sunrise and sunset times.

The January analyses show strong maximums of N-NNE'ly winds at TA-50 and Area G during the early morning hours before sunrise and of S-SSW'ly winds during the afternoon. The strong bimodal frequency distribution is caused by channeling of winds near the Rio Grande Valley and above the plateau surface.

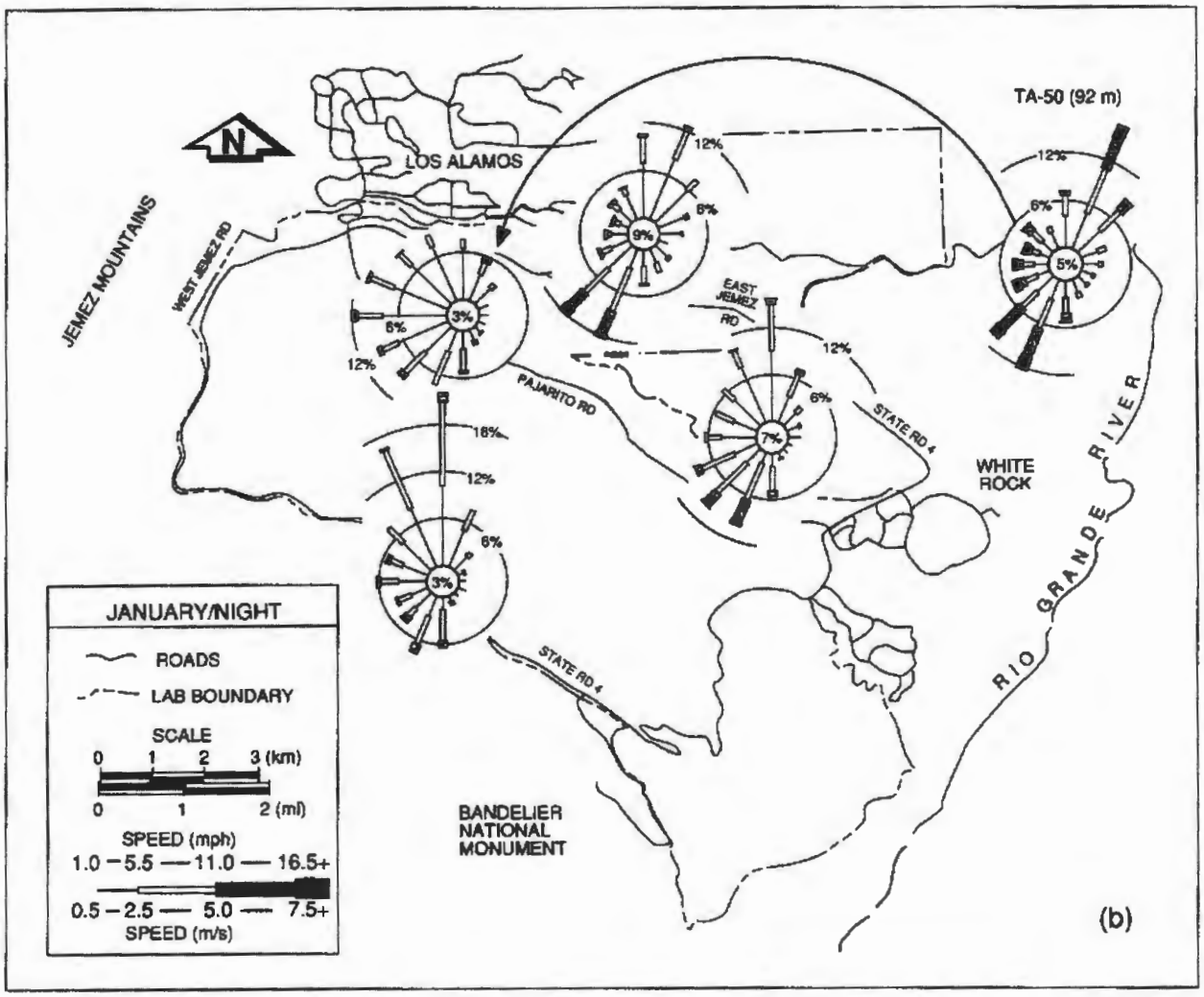

Fig. 4.2 (Continued)
(b) January night wind roses at Los Alamos.

Low-level, large-scale winds are frequently NW'ly during the winter. At night, a surface-based inversion often forms, decoupling surface winds (<100 ft [30 m]) from the winds above. The undisturbed boundary-layer winds (lowest 3000 ft or 1 km) from the NW are often channeled down valley (NNE to SSW) during the night. The pattern changes after sunrise and during the day. The incoming solar radiation heats the ground, which then transfers that heat to the boundary-layer air by turbulence. As a result, the frictional effects of the ground force the boundary-layer winds to slow and turn somewhat counterclockwise (relative to the gradient wind). The turning of the winds, 20°–40°, is just enough to make the wind orientation more toward the up-valley

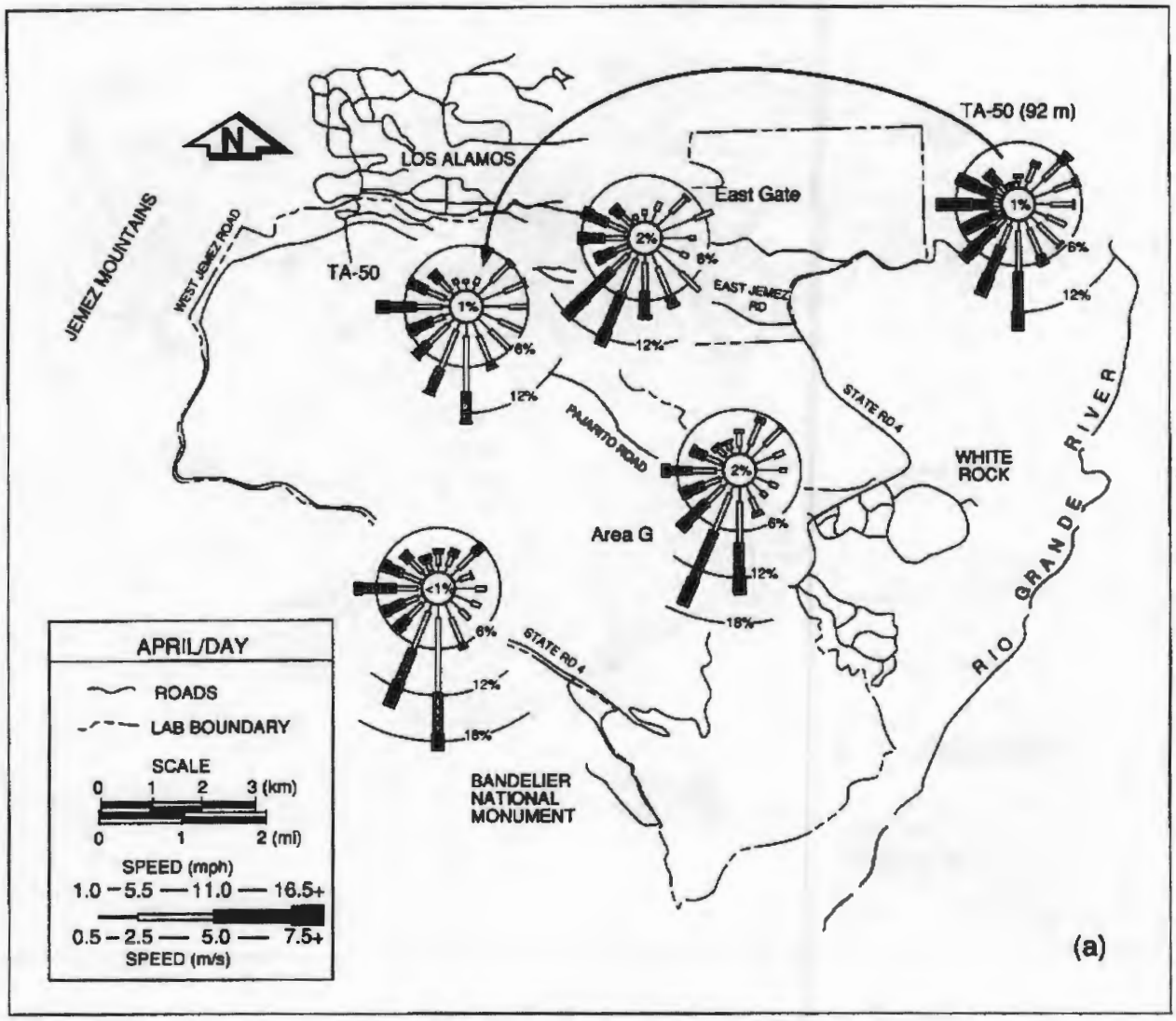

Fig. 4.3(a) and (b).
(a) April day wind roses at Los Alamos.

direction. Therefore, daytime winds (SSW'ly winds) are frequently channeled up valley toward the NNE during the winter.

A slight secondary maximum of SSW-SW'ly winds occurs at TA-50 (92 m), East Gate, and Area G during the early morning. In contrast, W'ly and WNW'ly drainage winds are more frequent from 2200–0100 at TA-50 (12 m). Afterward, a weaker maximum of NNW-NNE'ly winds is apparent at TA-50 (12 m). The mean winds turn clockwise shortly after sunrise at all sites as the vertical mixing increases and the channeling decreases.

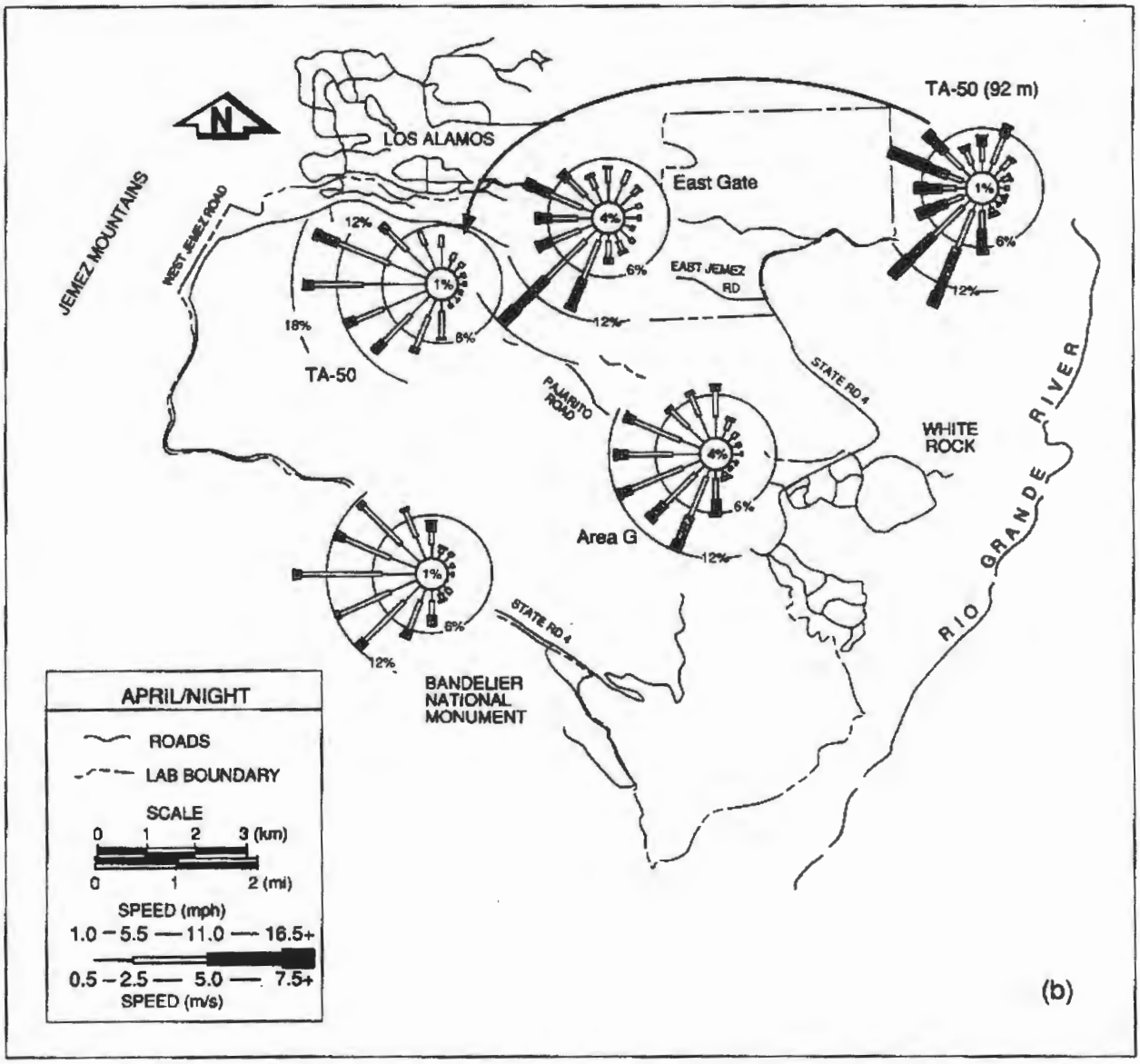

Fig. 4.3 (Continued)
(b) April night wind roses at Los Alamos.

Winds become upslope, up valley, or a combination of the two by noon. Note the frequent southeast orientation of winds at TA-50 (12 m) and East Gate. Even at these two sites, the winds tend to become more S'ly and SW'ly later in the afternoon as channeled valley winds become predominant. Notice the high frequency (30%) of SSW'ly winds at Area G at 1600. After sunset, cold-air drainage gives a brief large maximum of W'ly winds at TA-50 (12 m). The drainage wind decreases in frequency

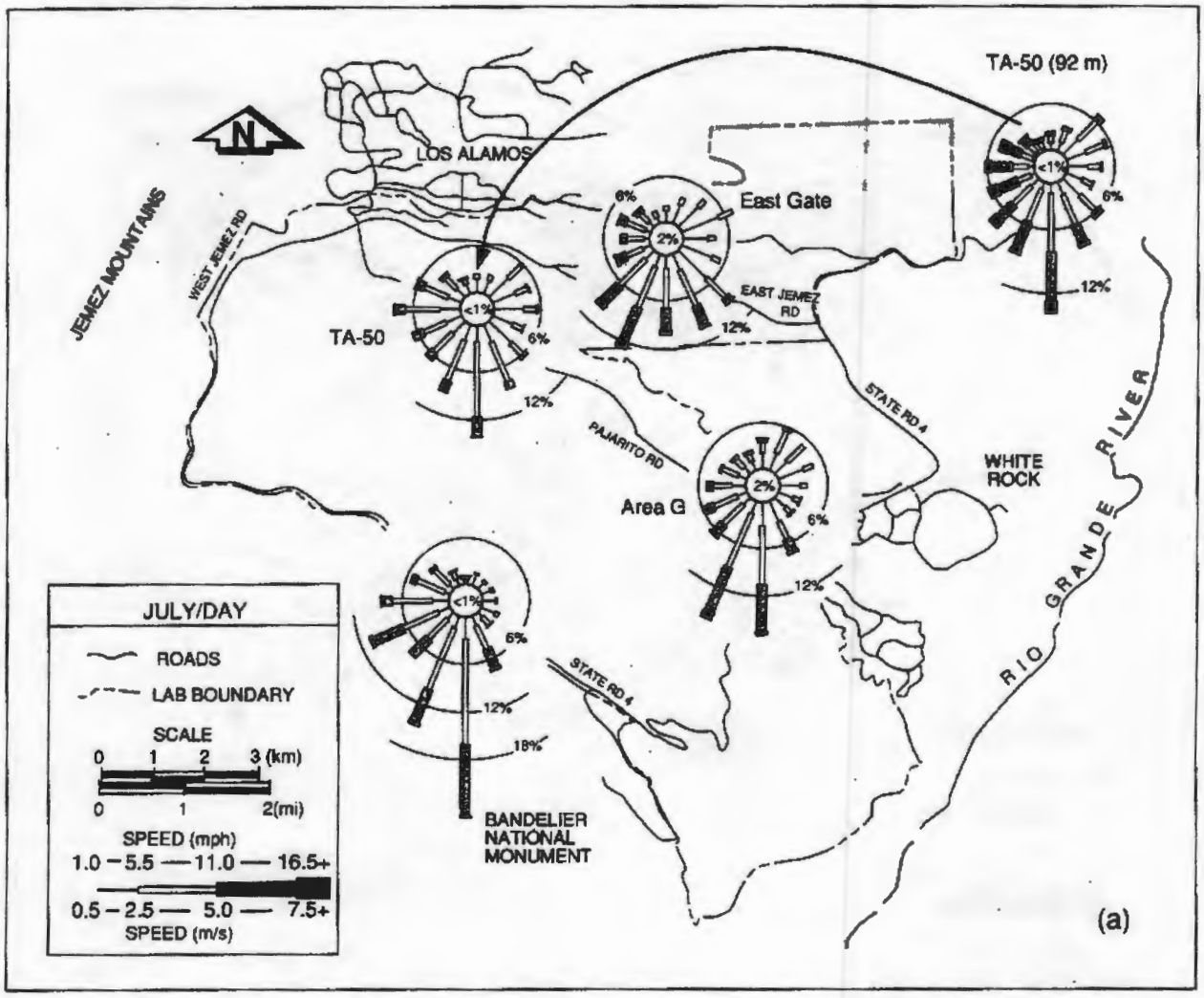

Fig. 4.4(a) and (b).
(a) July day wind roses at Los Alamos.

later in the evening. At TA-50 (92 m), East Gate, and Area G, the up-valley winds decrease and down-valley winds increase.

Wind speeds are generally the greatest in midafternoon, when maximum vertical mixing allows the greatest amount of momentum transfer down toward the ground. Wind speeds are lowest in the morning hours. At TA-50 (92 m), a wind-speed maximum occurs in the evening. During this time, a surface inversion forms, decoupling the surface from the higher (92-m) level and thereby allowing slightly higher wind speeds. For the same reason, the diurnal wind-speed change is less at the higher level than at the lower level.

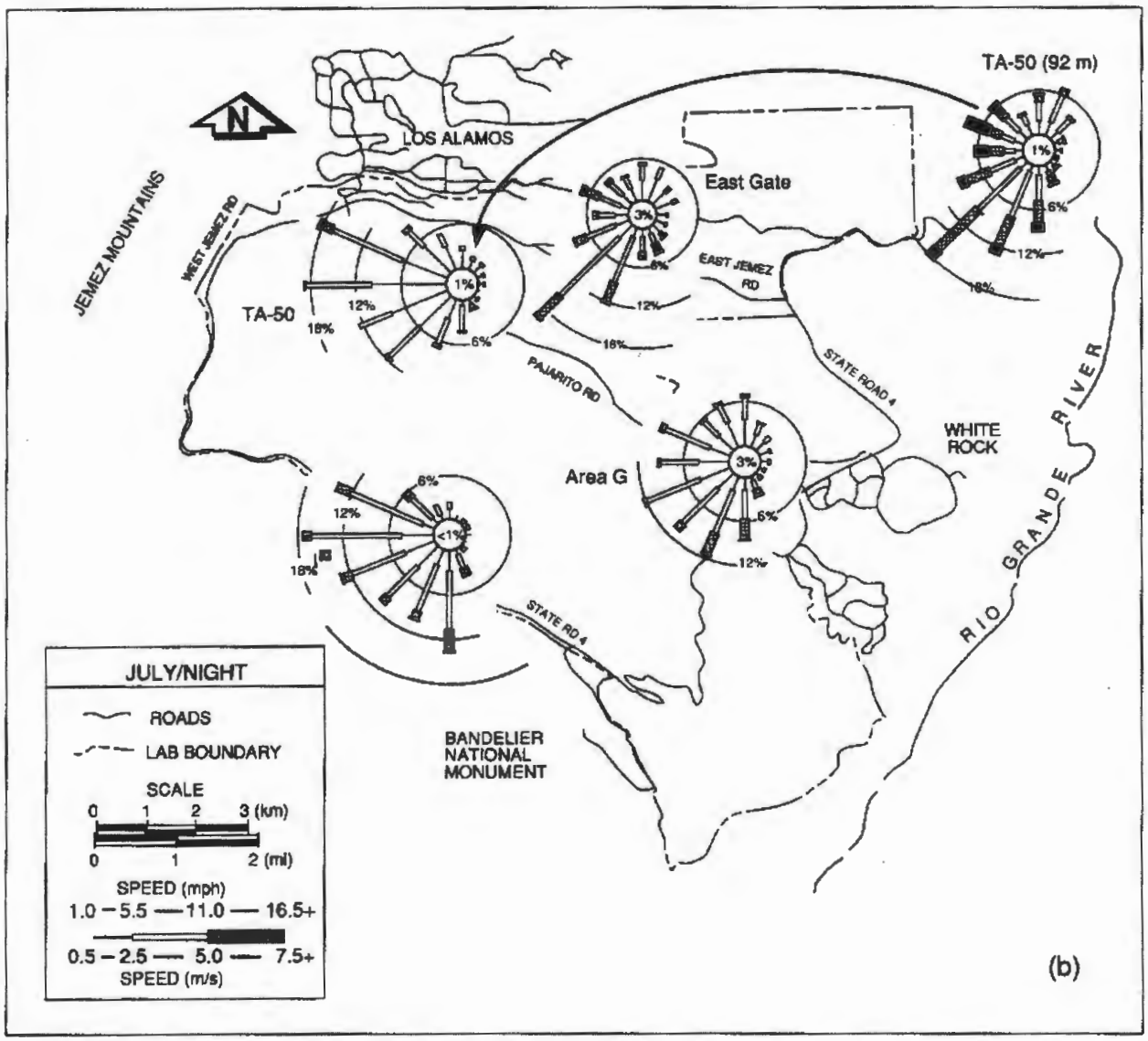

Fig. 4.4 (Continued)
(b) July night wind roses at Los Alamos.

Strong storms during spring (April) produce the strongest winds and, therefore, winds that are least affected by the local terrain. In addition, winds during April are more S'ly and less N'ly than during January. There is a sharp reduction of early morning, down-valley winds at all sites from those occurring in January. Channeled, down-valley NE'ly winds at TA-50 (92 m) become frequent at 0300, reaching a peak after sunrise. Channeled up-valley winds are frequent during the early morning hours, especially at

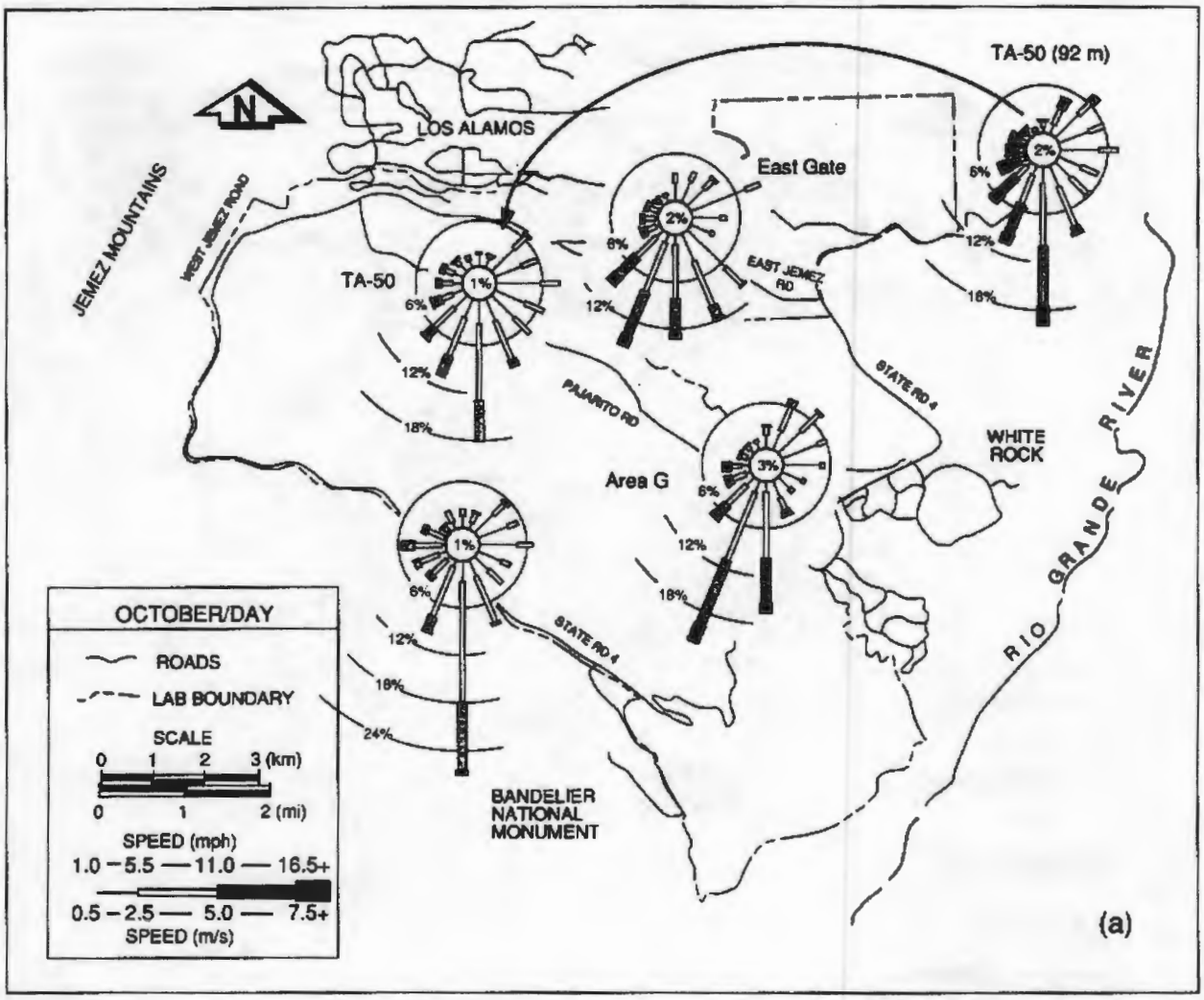

Fig. 4.5(a) and (b).
(a) October day wind roses at Los Alamos.

TA-50 (92 m) and East Gate. An early morning maximum of W-WNW'ly winds at the TA-50 lower level is shown in the figure, representing cold-air drainage.

Another important difference in April is the large number of W-NW'ly winds, including those occurring at the upper level at TA-50 during the afternoon and evening hours and peaking about 2000. Strong W'ly winds, common at upper levels during spring, mix down toward the surface during the afternoon when vertical mixing is the greatest. The fact that W-NW'ly wind frequency lags behind solar heating so much indicates that the winds are brought down from relatively high levels. Drainage winds at

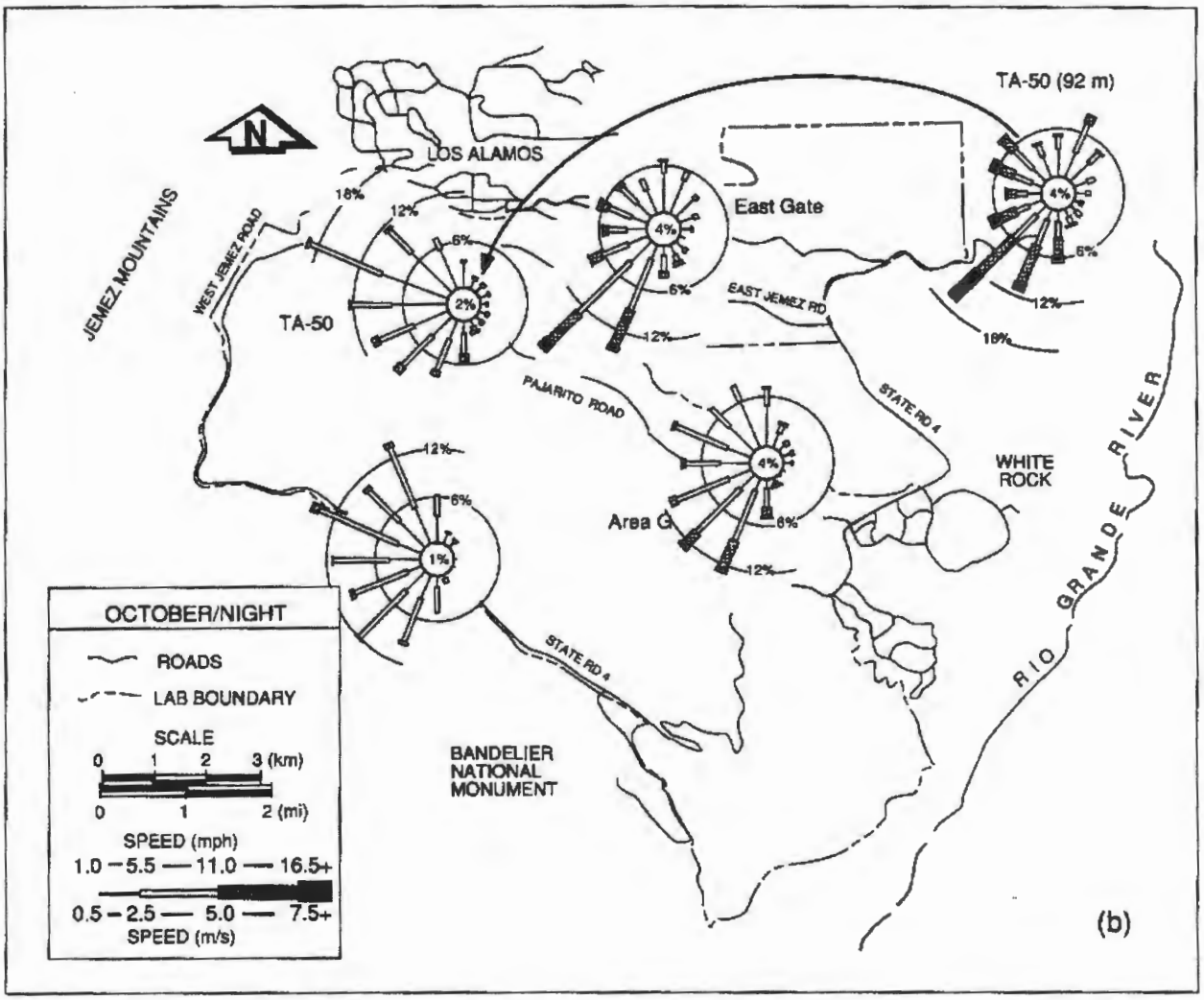

Fig. 4.5 (Continued)
(b) October night wind roses at Los Alamos.

the low level (11–12 m AGL) also contribute to the peak shortly after sunset. The W-NW'ly winds decrease dramatically by 2200.

Local winds, especially slope winds, are more frequent during the summer when large-scale winds are weak (Fig. 4.17). Wind-direction distributions are strongly bimodal at TA-50 (92 m) during the night. Up-valley channeling becomes frequent at sunset and continues through the early morning hours. A secondary maximum of NNE'ly winds begins shortly after midnight, reaching a peak several hours after sunrise. Summer winds more often have a S'ly rather than a N'ly component. Winds above the plateau generally have a S'ly or SW'ly component and at night are channeled to cause a

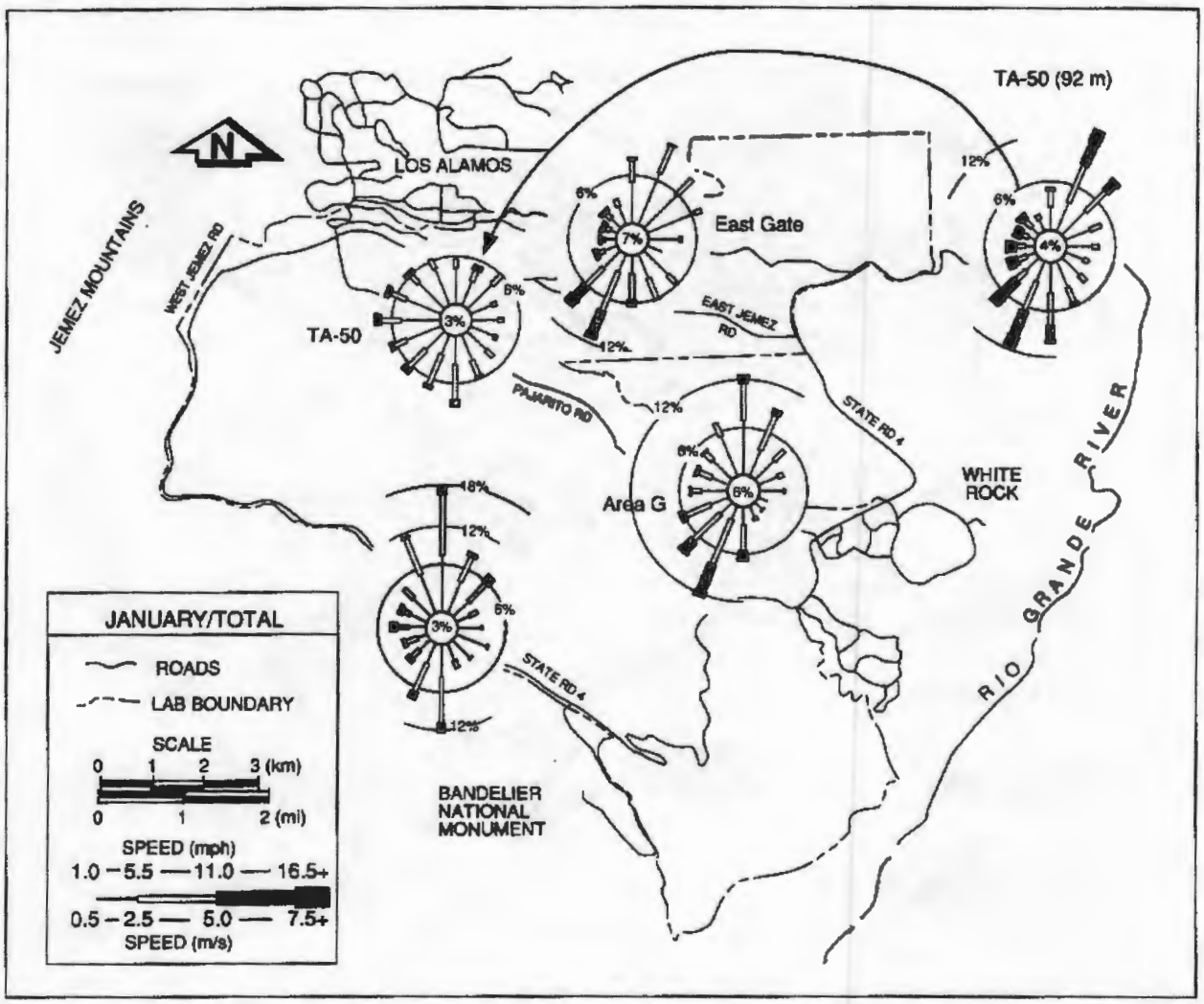

Fig. 4.6. January total wind roses at Los Alamos.

SSW'ly wind. There is a large frequency of NE'ly and E'ly winds at 0800 just after sunrise. The NE'ly and E'ly winds probably represent a balance between a channeled down-valley wind and a thermally driven upslope wind.

The winds are also the lightest at this time, indicating the high frequency of direction transition. As the solar heating intensifies, the NE'ly winds give way to SE'ly through SSW'ly winds. The combination of upslope and channeled up-valley winds creates S'ly winds at TA-50, which become most frequent during the early afternoon. Note the late afternoon and early evening secondary W-WNW'ly wind maximum at TA-50. These

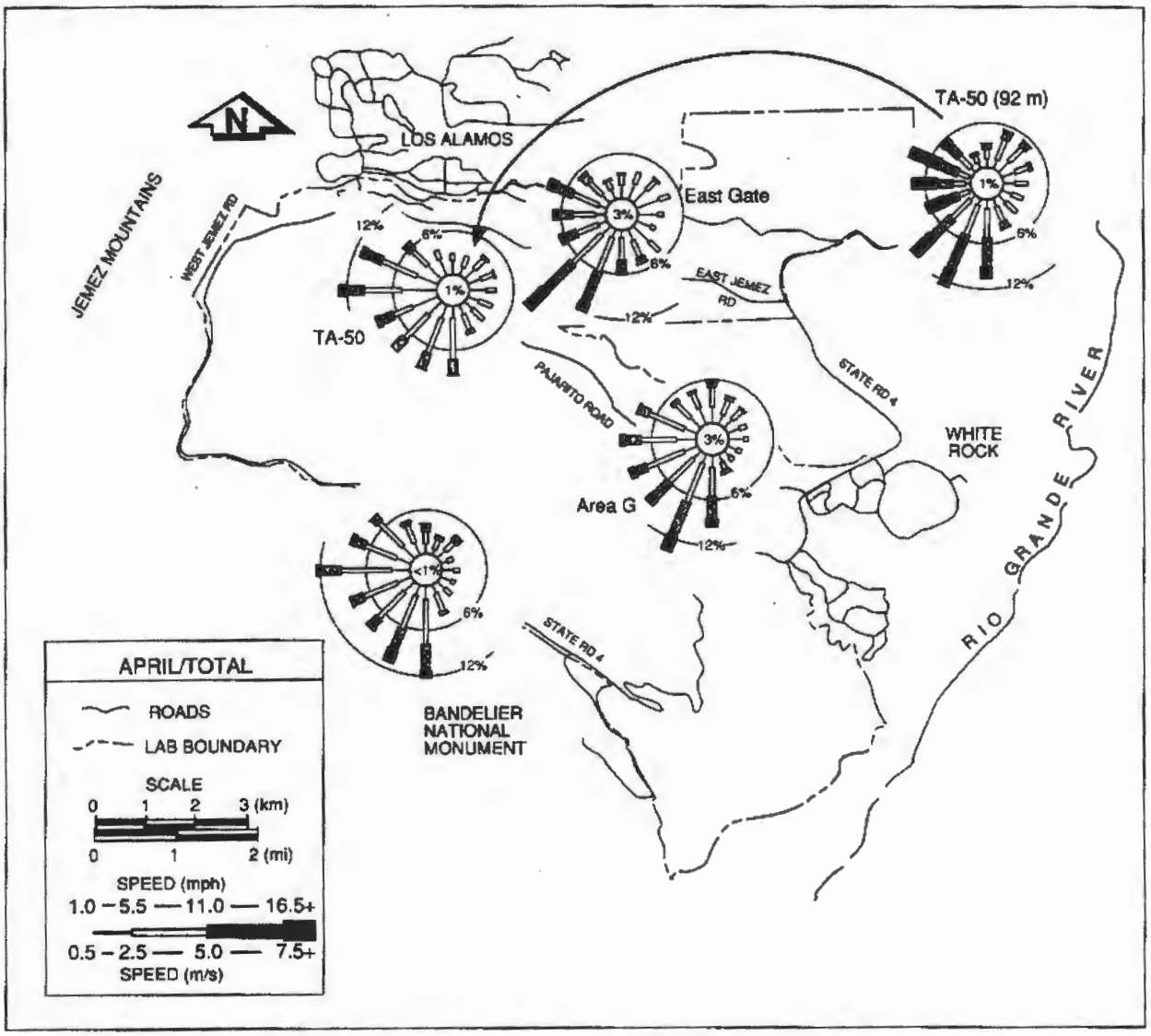

Fig. 4.7. April total wind roses at Los Alamos.

winds are probably from outflows caused by frequent mountain thundershowers and clouds. The clouds are usually concentrated over or near the mountains, allowing differential heating because there is more sunshine toward the valley. A W-WNW'ly wind frequently forms from this imbalance.

Winds at TA-50 (12 m) during the summer are quite different from the higher-level (92 m) winds. Note the large frequency of W-NW'ly winds at night and early evening, representing the drainage wind. The wind direction at 12 m is frequently 90° clockwise

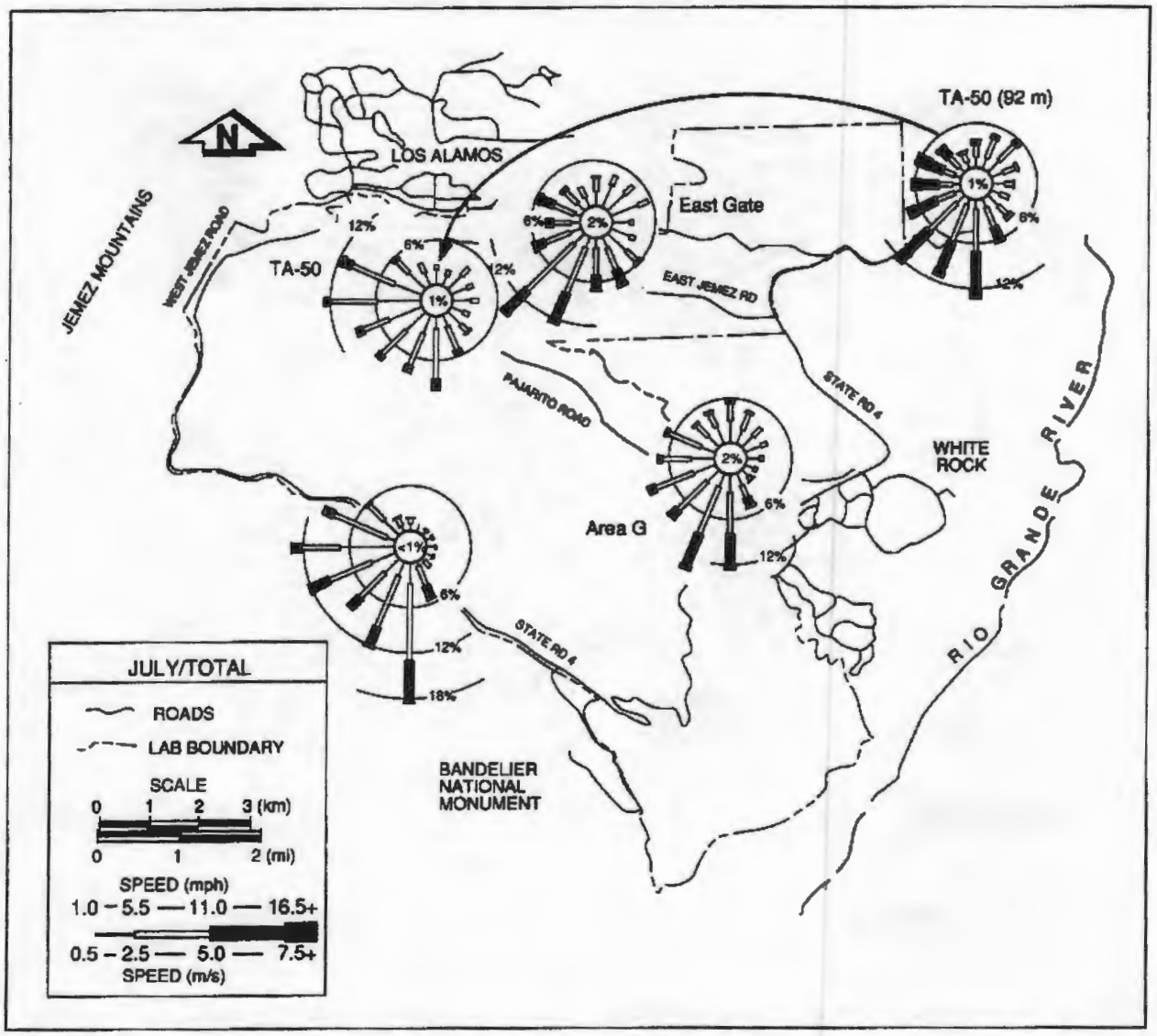

Fig. 4.8. July total wind roses at Los Alamos.

from the wind direction at 92 m. Also, the NE'ly wind maximum after sunrise is smaller at the 12-m level. East Gate winds are similar to those at TA-50 (92 m) at night, with up-valley winds that form at sunset giving way to frequent down-valley winds after sunrise. A slight maximum of WNW'ly (drainage) winds appears several hours after sunset. A pronounced SE'ly wind maximum occurs between 0800 and 1200, caused by thermally driven, upslope winds. Even until late afternoon, upslope and up-valley winds are equally common here. Daytime up-valley winds are the most frequent at Area G, with a

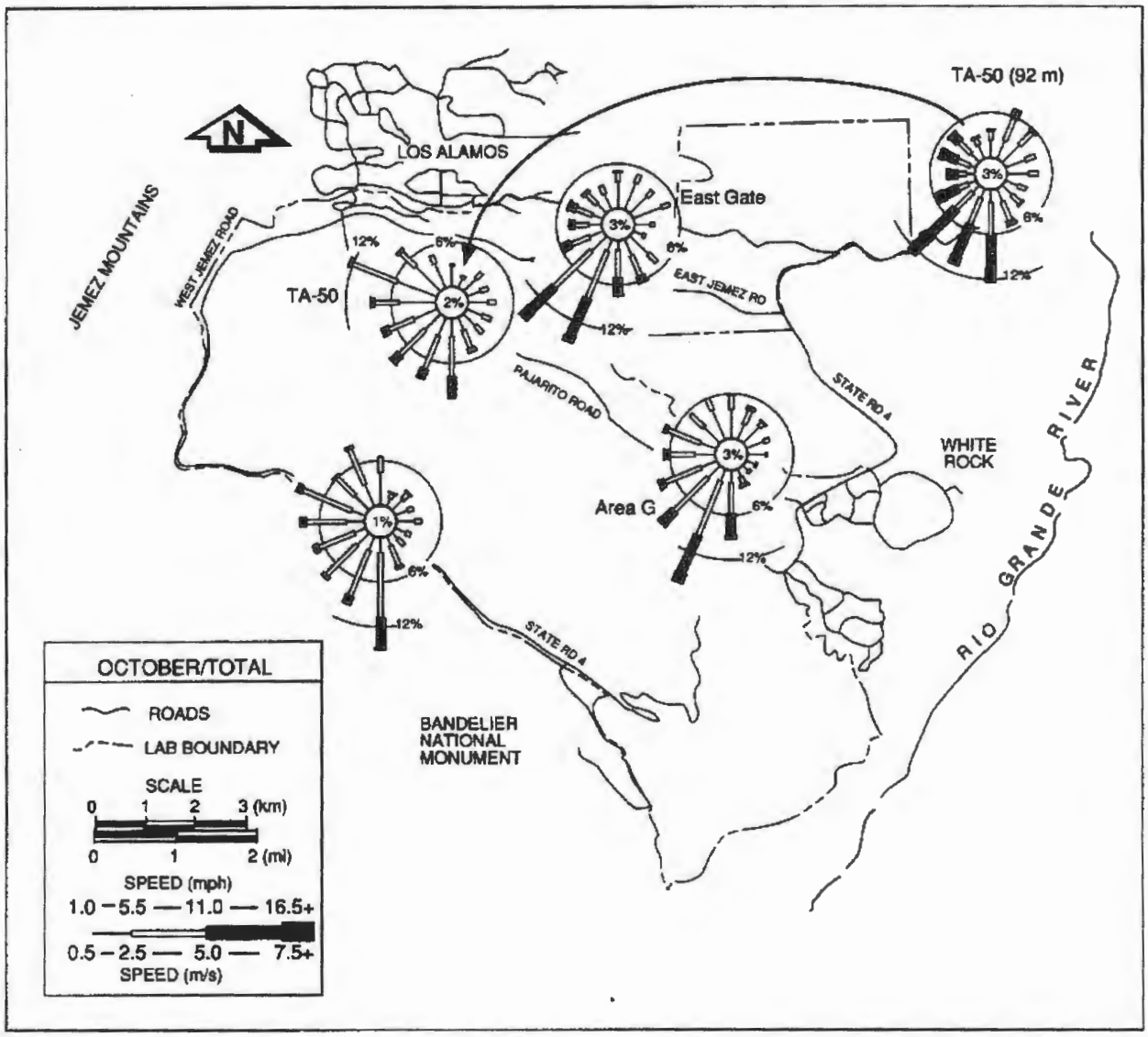

Fig. 4.9. October total wind roses at Los Alamos.

prevalence of SSW'ly winds during the entire day. After sunset, frequencies are similar for the up-valley and downslope winds. The winds become more NE'ly after midnight, and especially after sunrise.

Winds are generally similar during October, except that channeled winds are more frequent. Note the high frequency of SSW'ly daytime and SW'ly nighttime winds at both TA-50 levels. Winds are also frequently SW'ly during the night at East Gate. However, SE-SSE'ly upslope winds are evident there from late morning to early

afternoon. Up-valley winds are especially frequent at Area G, reaching 30% for 3 hours late in the afternoon. The channeled up-valley winds, however, are less frequent at night than at other sites. N'ly winds become the most frequent at Area G after midnight, reaching a peak at sunrise. A secondary maximum of NW'ly winds exists for several hours after sunset at all sites. These strong winds result from imbalances caused by the formation of a low-level inversion shortly after sunset. There is an accompanying secondary wind-speed maximum at all sites during this time. Maximum wind speeds and gusts often occur shortly after sunset.

Wind-frequency diagrams for TA-59 are shown in Fig. 4.19. Winds here are similar to those at TA-50 (12 m). TA-59 is located on a steeper slope and farther away from the valley than is TA-50. Therefore, slope flows are more frequent and valley winds are less frequent at TA-59. Afternoon winds in January have a SE'ly component, indicating upslope winds. During the morning and early afternoon hours, SE'ly winds are evident for all months. The later afternoon winds often become S'ly, closely paralleling those in the valley, except during April. During April, the most frequent winds are downslope winds, especially during the night. Many of the W-NW'ly winds are induced by strong, large-scale spring winds, but some are from cold-air drainage. Winds during July are very similar at TA-59 and TA-50 (12 m), with a more upslope component of daytime winds at TA-59. During October, TA-59 winds are generally along the slope, whereas TA-50 (12 m) winds are more valley oriented.

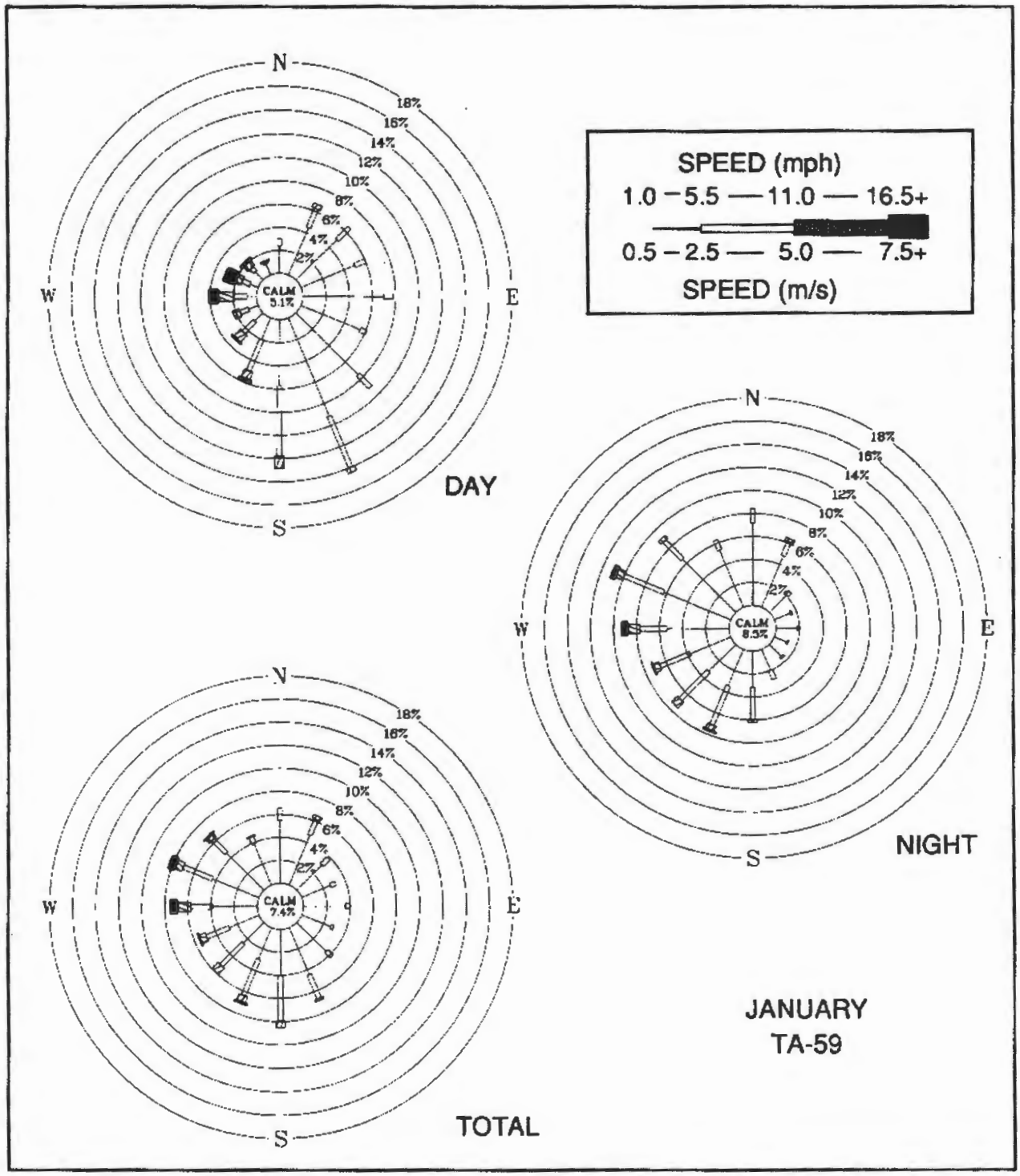

Fig. 4.10. January day, night, and total wind roses at TA-59.

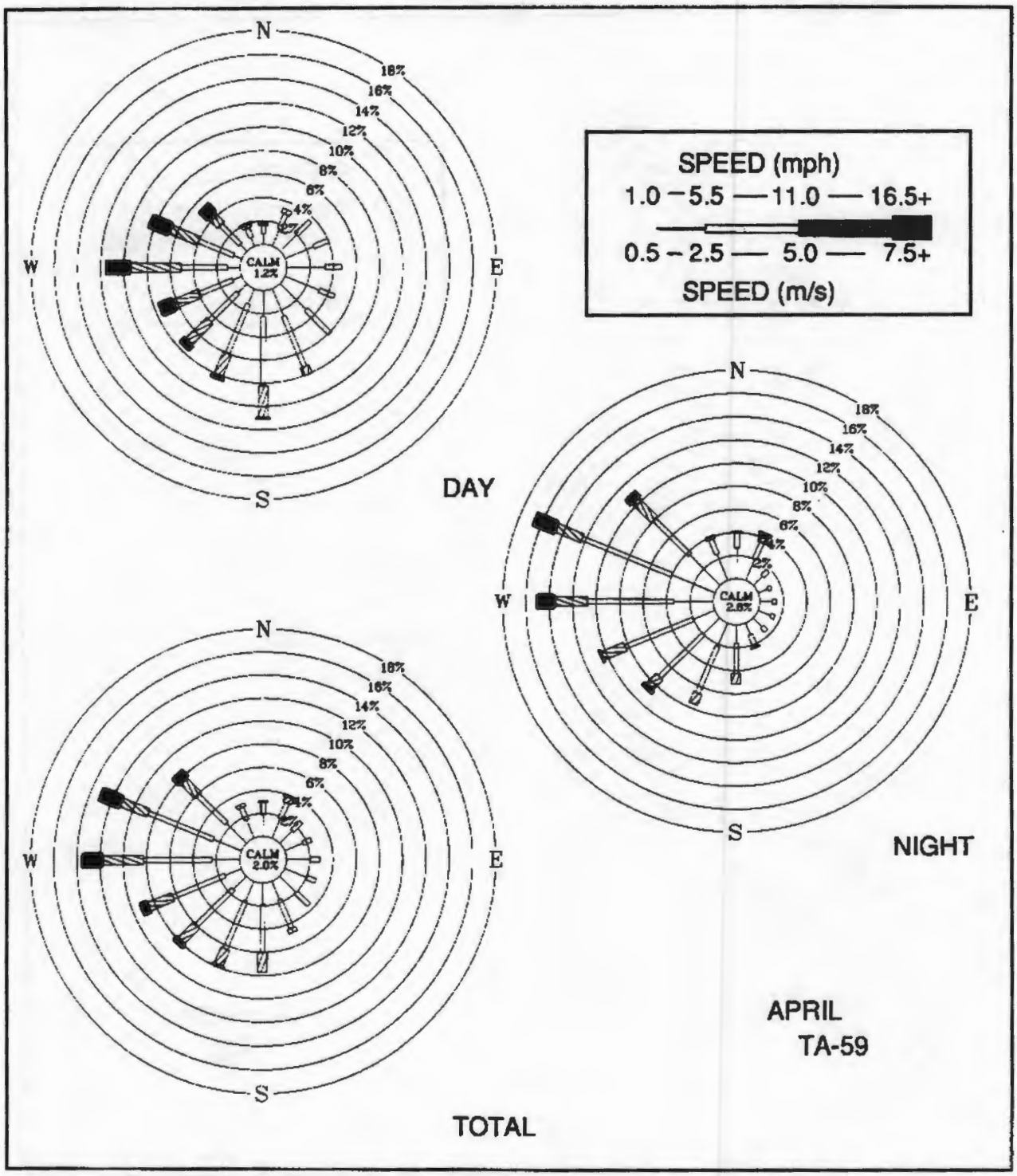

Fig. 4.11. April day, night, and total wind roses at TA-59.

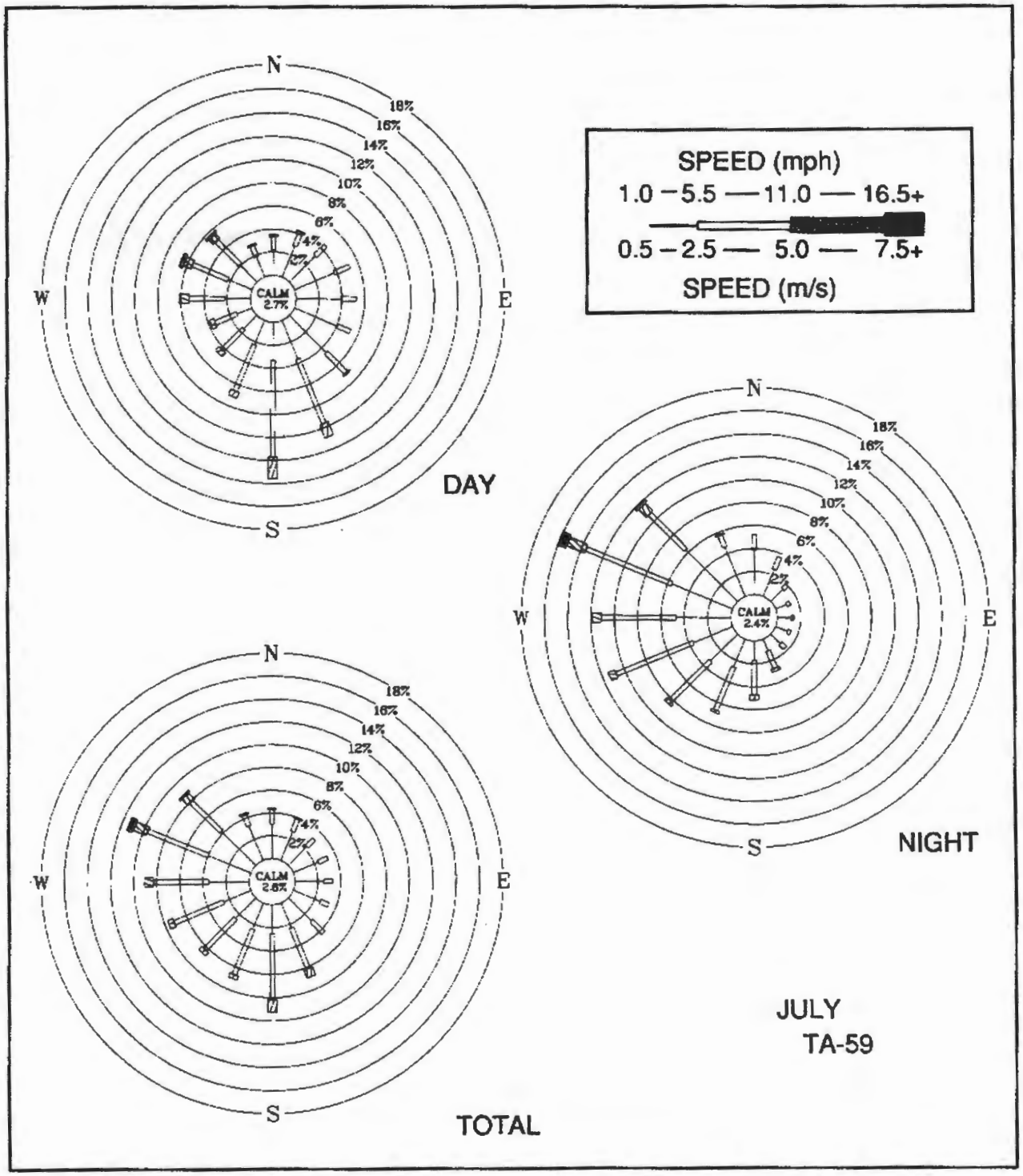

Fig. 4.12. July day, night, and total wind roses at TA-59.

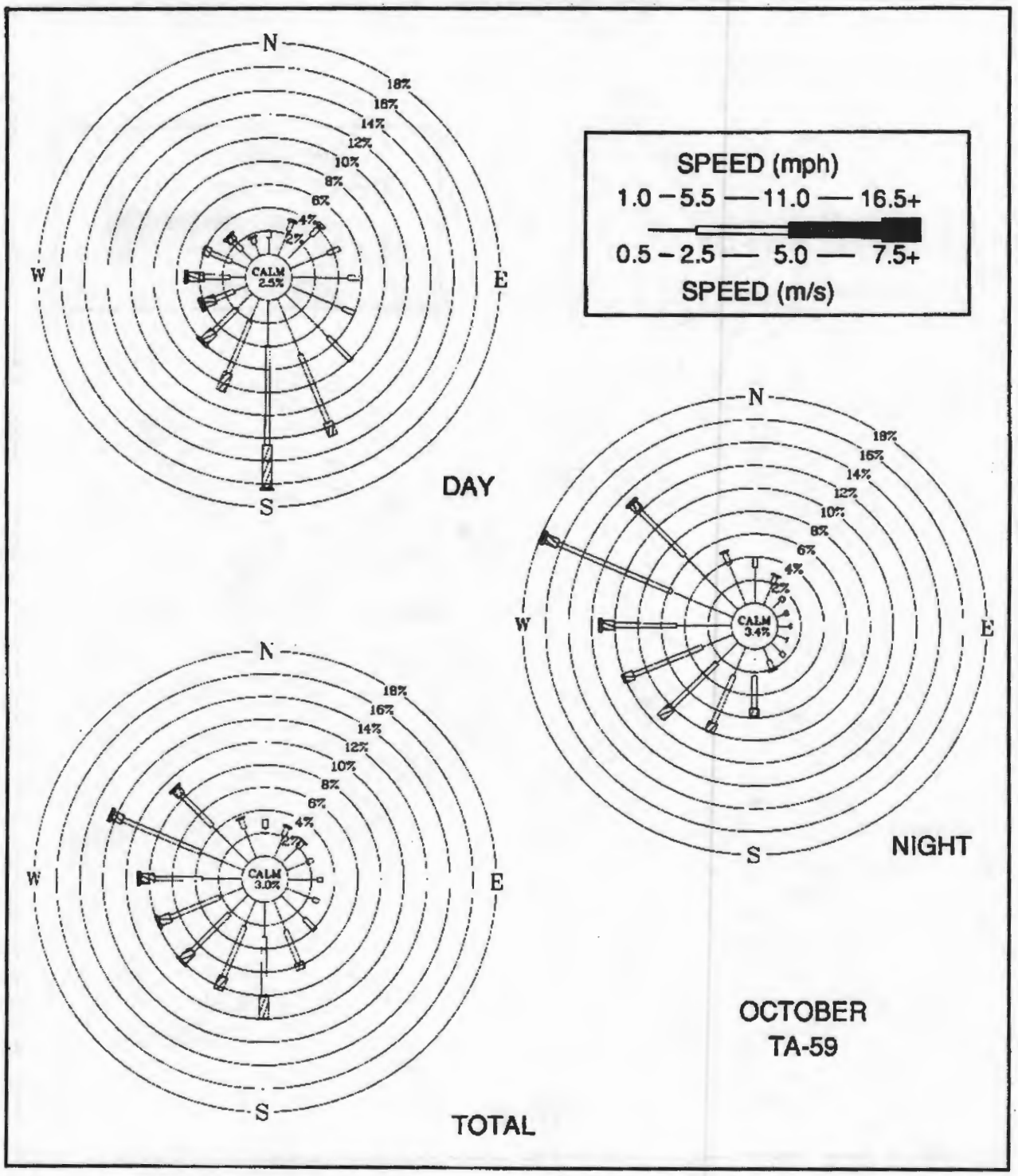

Fig. 4.13. October day, night, and total wind roses at TA-59.

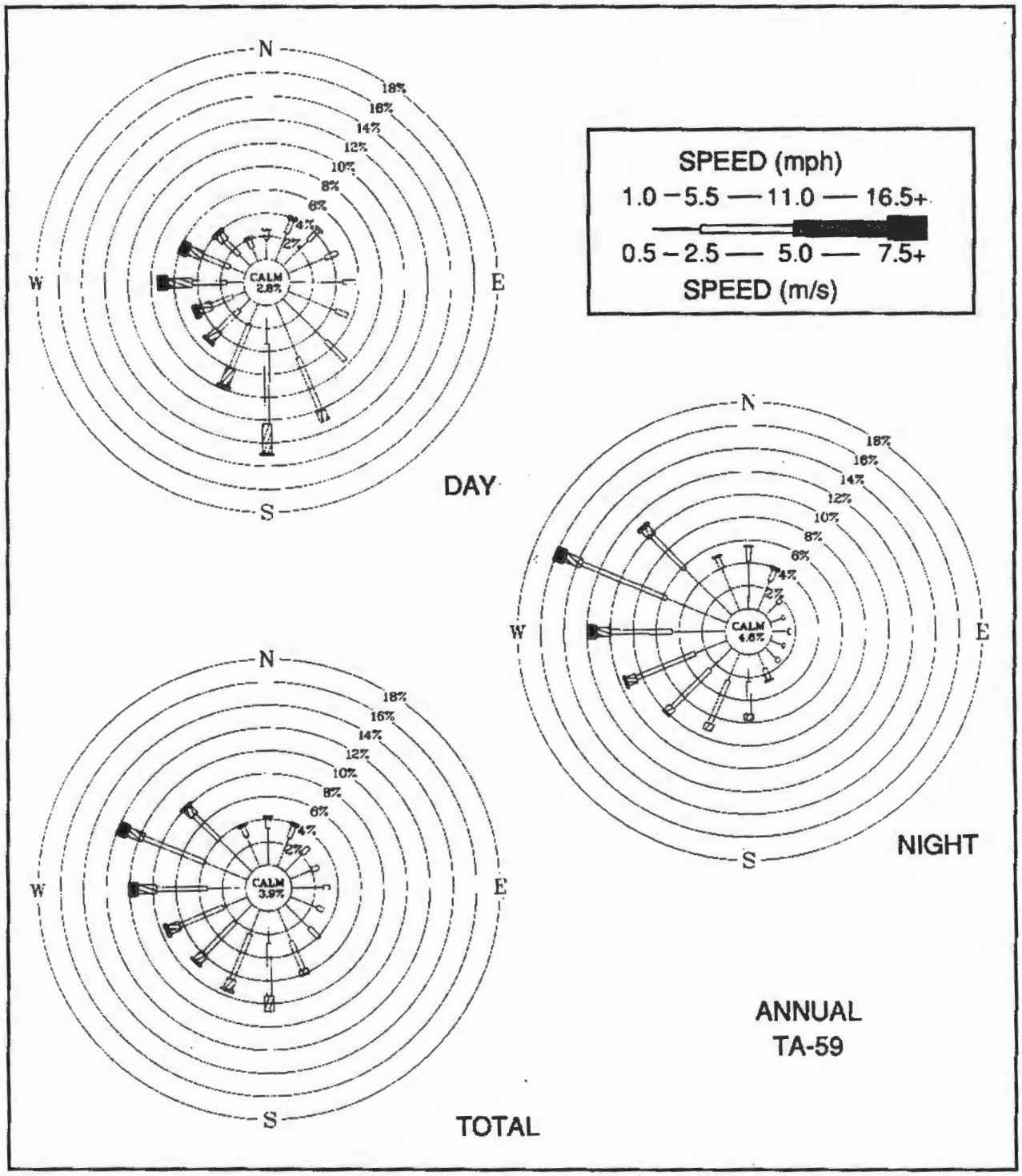

Fig. 4.14. Annual (1980–1987) day, night, and total wind roses at TA-59.

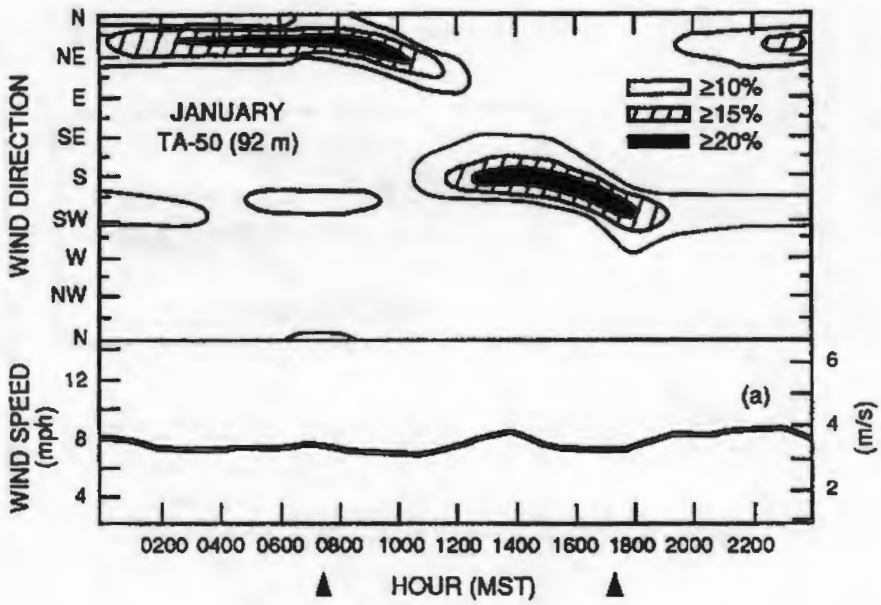

Fig. 4.15(a)–(d). January hourly wind-direction frequencies and mean wind speeds at (a) TA-50, 92-m level, and (b) TA-50, 12-m level; (c) East Gate, 12-m level; and (d) Area G, 11-m level. (Triangles denote mean sunrise and sunset times.)

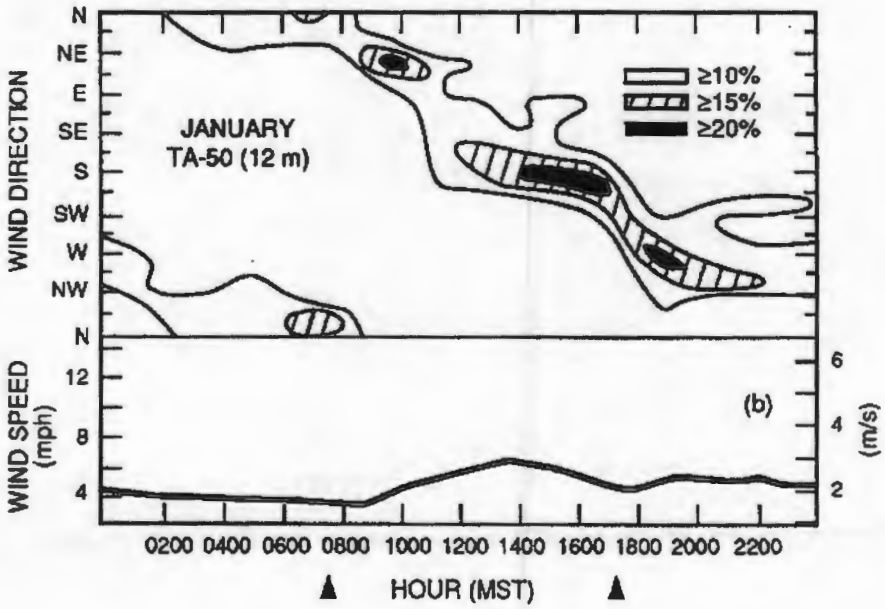

Fig. 4.15 (Continued)

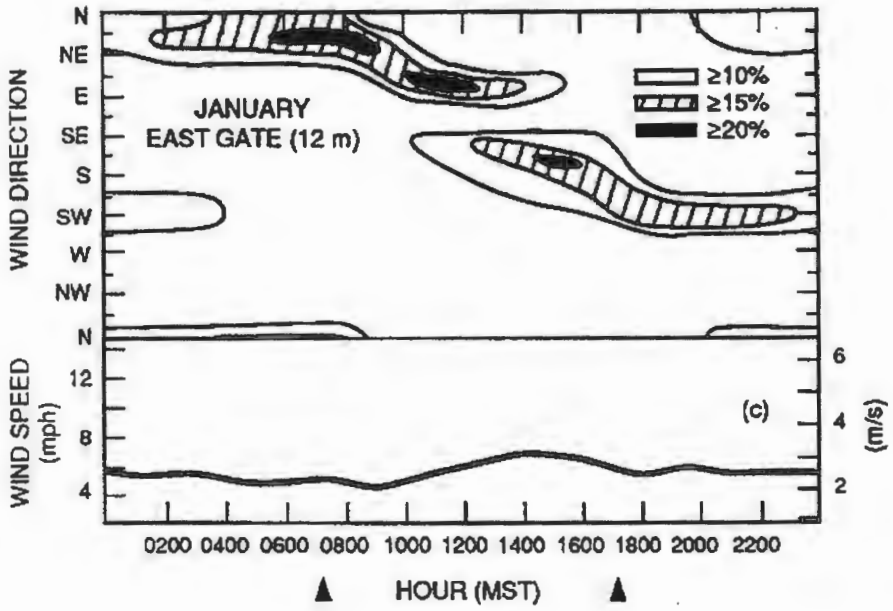

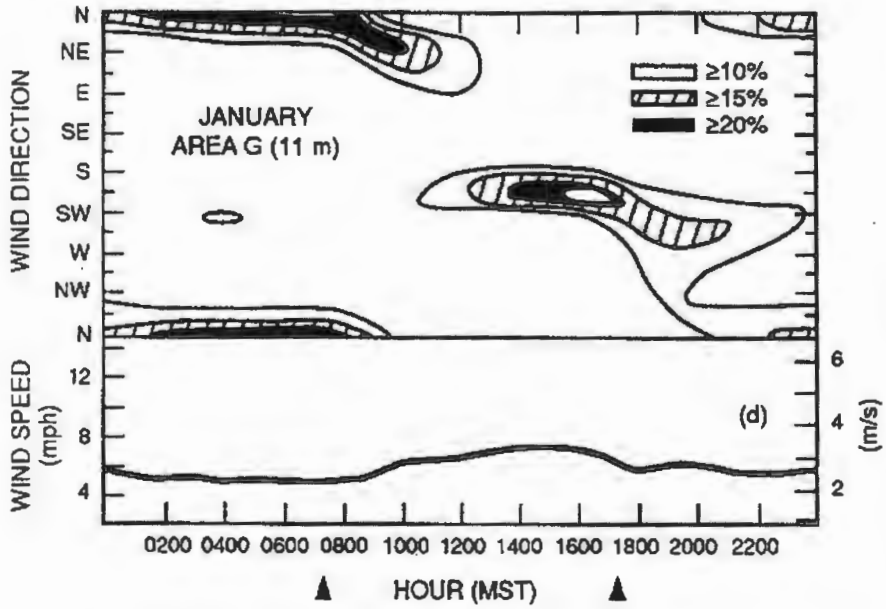

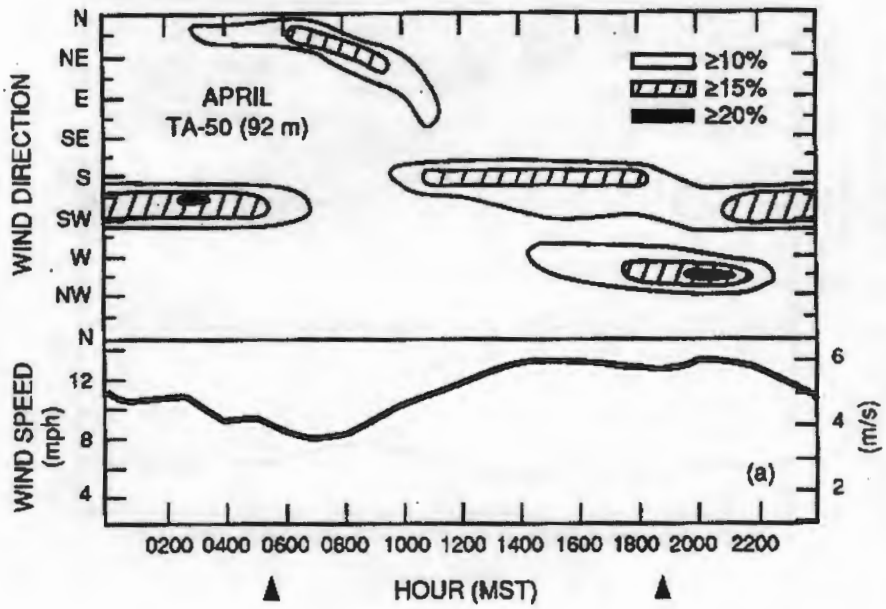

Fig. 4.16(a)–(d). April hourly wind-direction frequencies and mean wind speeds at (a) TA-50, 92-m level, and (b) TA-50, 12-m level; (c) East Gate, 12-m level; and (d) Area G, 11-m level. (Triangles denote mean sunrise and sunset times.)

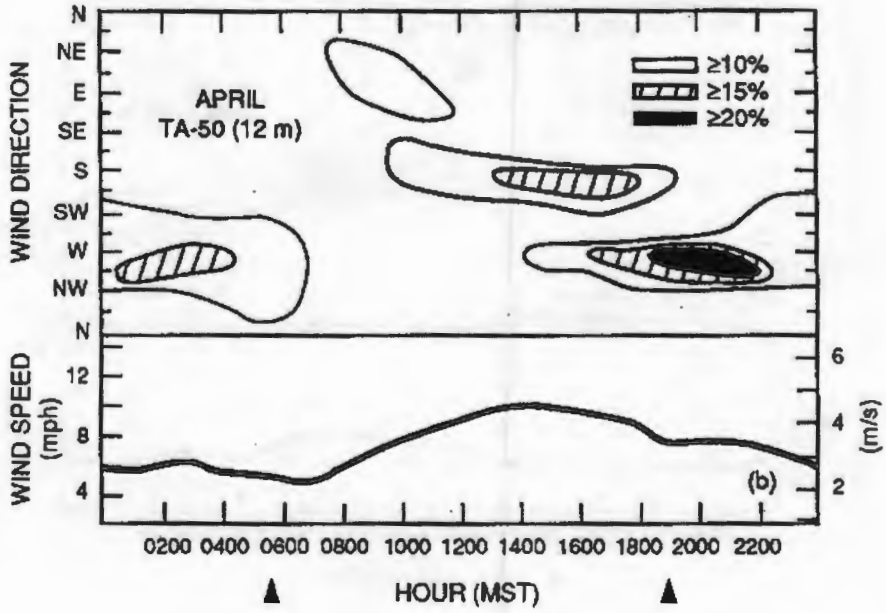

Fig. 4.16 (Continued)

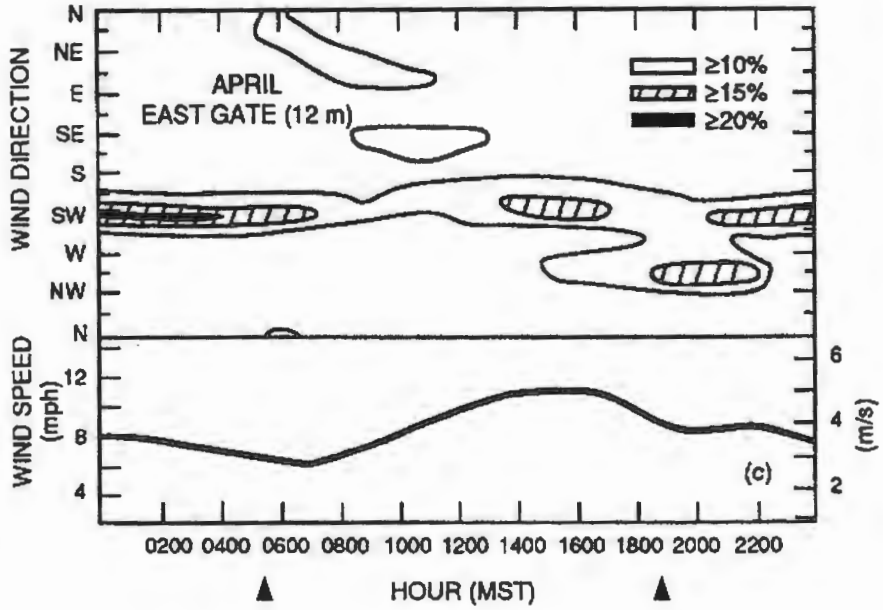

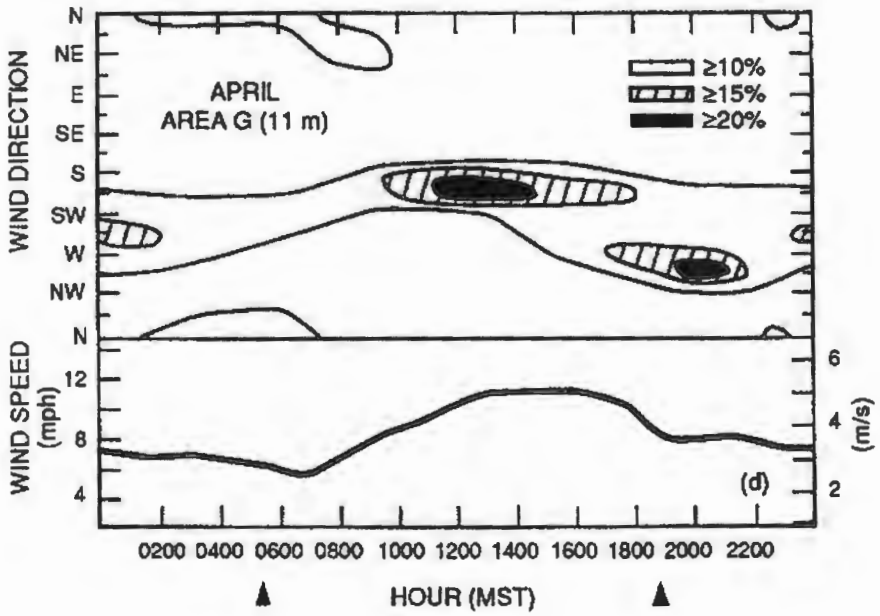

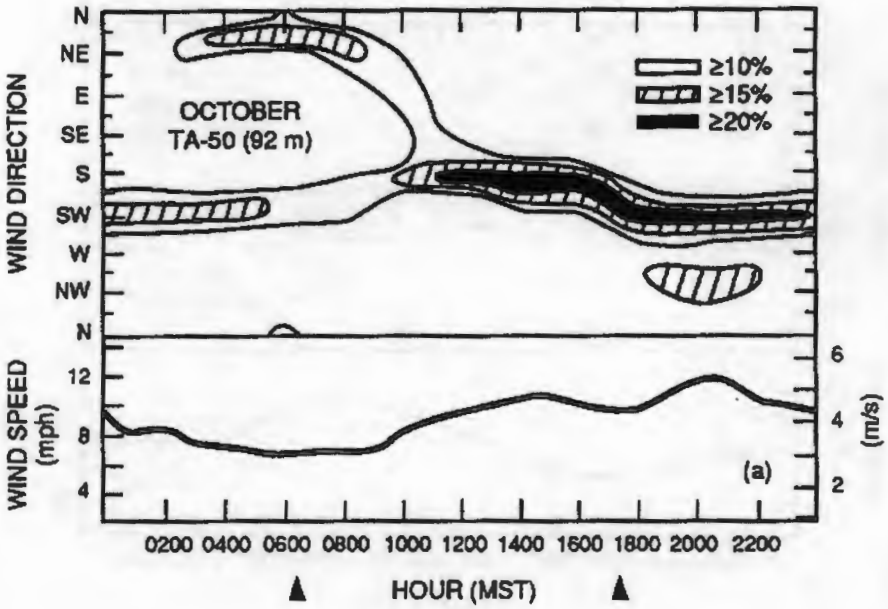

Fig. 4.18(a)–(d). October hourly wind-direction frequencies and mean wind speeds at (a) TA-50, 92-m level, and (b) TA-50, 12-m level; (c) East Gate, 12-m level; and (d) Area G, 11-m level. (Triangles denote mean sunrise and sunset times.)

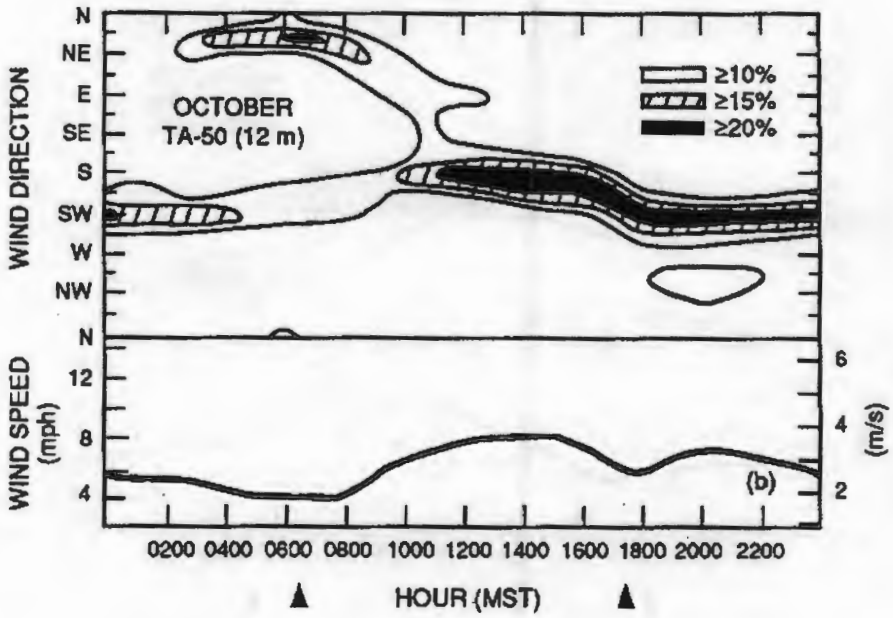

Fig. 4.18 (Continued)

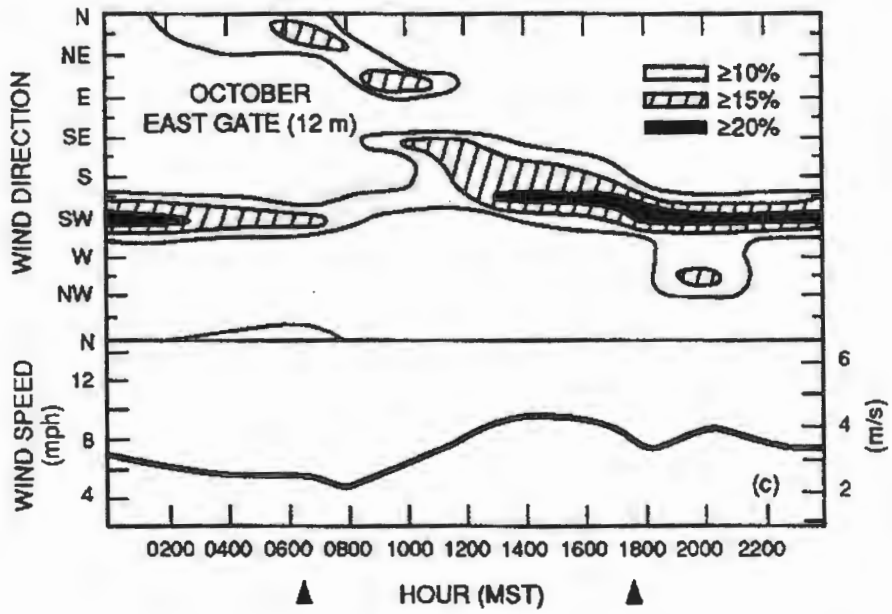

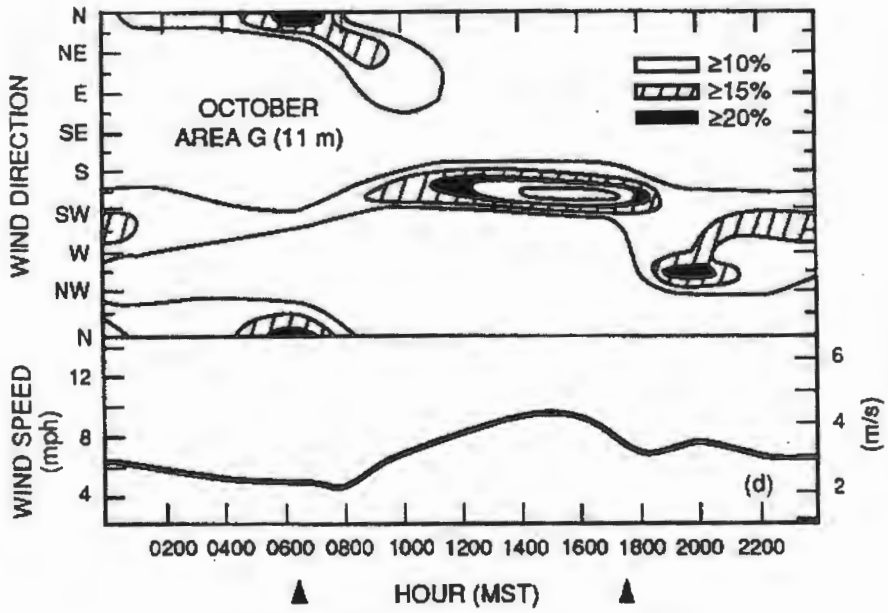

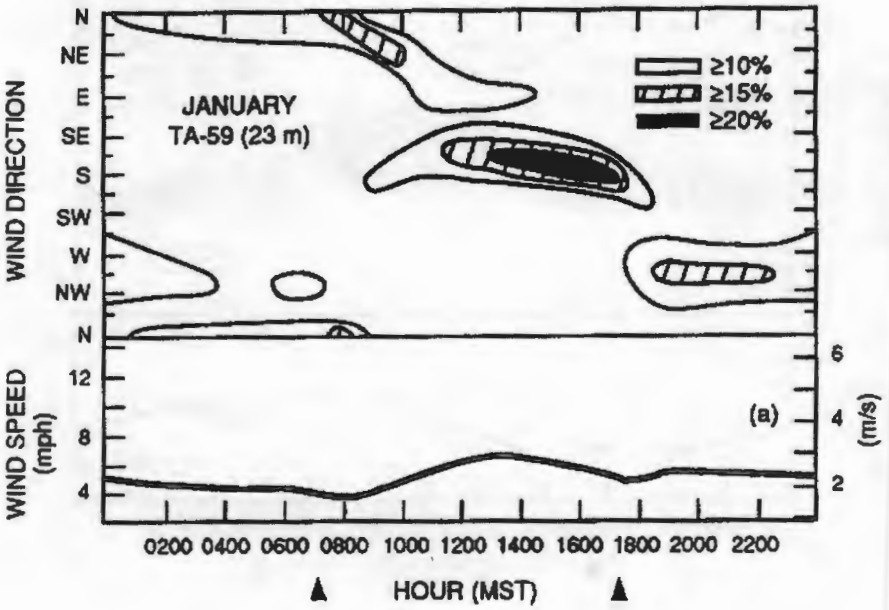

Fig. 4.19(a)–(d). Hourly mean wind-direction frequencies and mean wind speeds at TA-59, 23-m level, during (a) January, (b) April, (c) July, and (d) October. (Triangles denote mean sunrise and sunset times.)

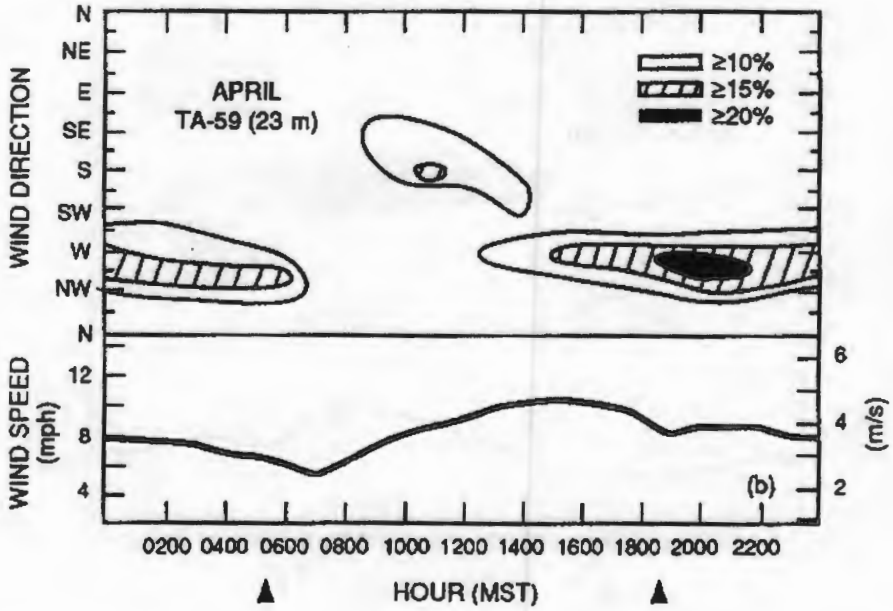

Fig. 4.19 (Continued)

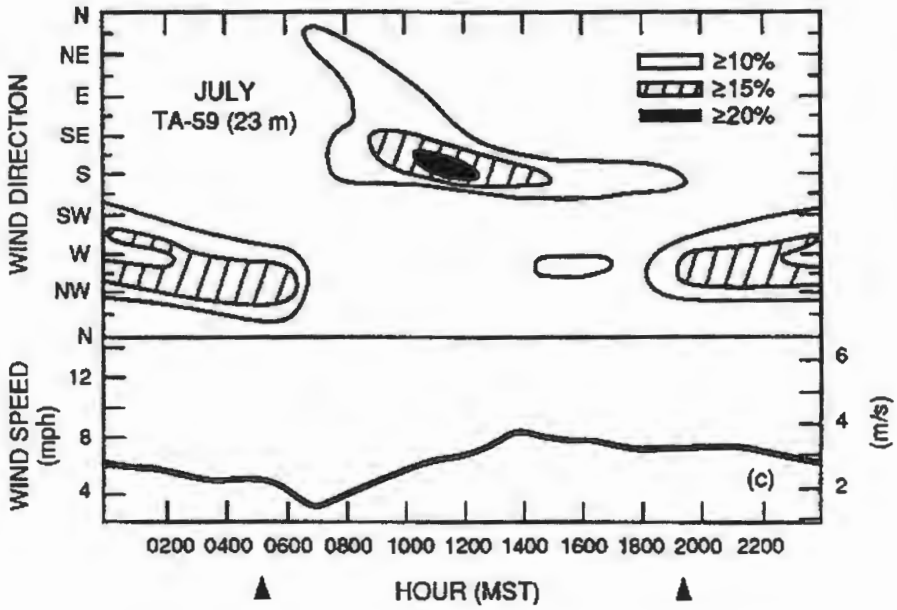

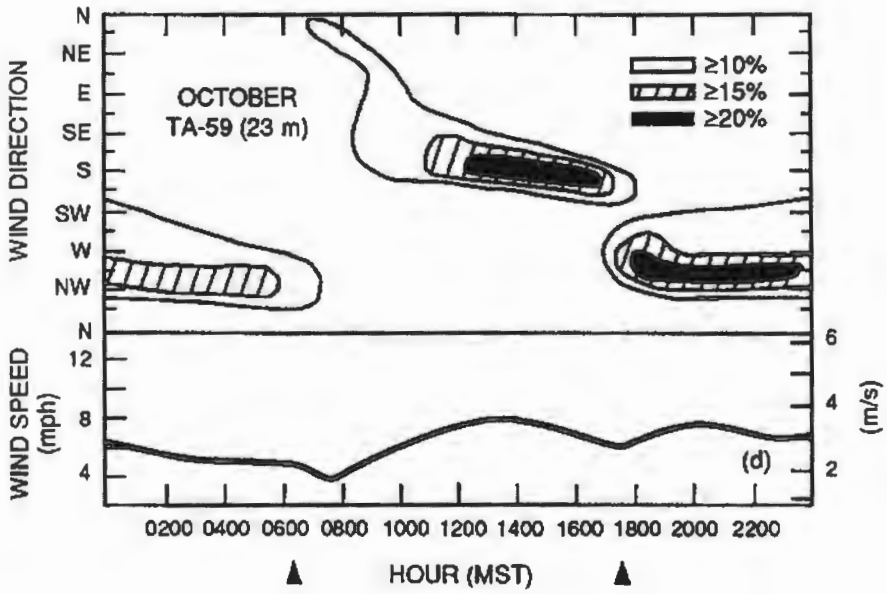

5 Atmospheric Pressure

Atmospheric pressure has been recorded continuously at TA-59 since 1979. Fifteen-minute-averaged pressure data were analyzed by hour and month for the 1979–1988 period. Results are shown in this section, along with a discussion of atmospheric pressure and density.

5.1 Monthly and Daily Pressure

Atmospheric pressure is a measure of the force that air exerts over a unit area in any direction. Pressure is simply the product of the mass of air in an overhead column and the acceleration of gravity. Because the acceleration of gravity is nearly constant (32 ft^2/s or 9.8 m^2/s) through the lower atmosphere, station pressure is proportional to the overhead column mass. The overhead column mass is affected by temperature changes and/or convergence or divergence of air. For example, high temperatures and/or horizontal divergence in the air column lower pressure, whereas lower temperatures and/or horizontal convergence in the air column increase pressure.

The normal atmospheric pressure at sea level for a standard atmosphere is 29.92 in. of mercury (Hg) (a mass of mercury equals the mass of an air column of equal diameter) or 1013.3 mbar (Berry, Bollay, and Beers 1945). However, the atmosphere quickly thins out with height, especially in the first 20 000 ft (6000 m). The standard atmospheric pressure is about 22.73 in. (770.0 mbar) at TA-59's elevation, 7375 ft (2248 m) above sea level (ASL). (Calculations were made using tables from List [1951]). In other words, air pressure at Los Alamos is 76% of normal sea-level pressure.

Monthly mean atmospheric-pressure statistics are shown in Fig. 5.1 and Table 5.1. The data in Fig. 5.1 show that Los Alamos station pressure has a definite annual cycle,

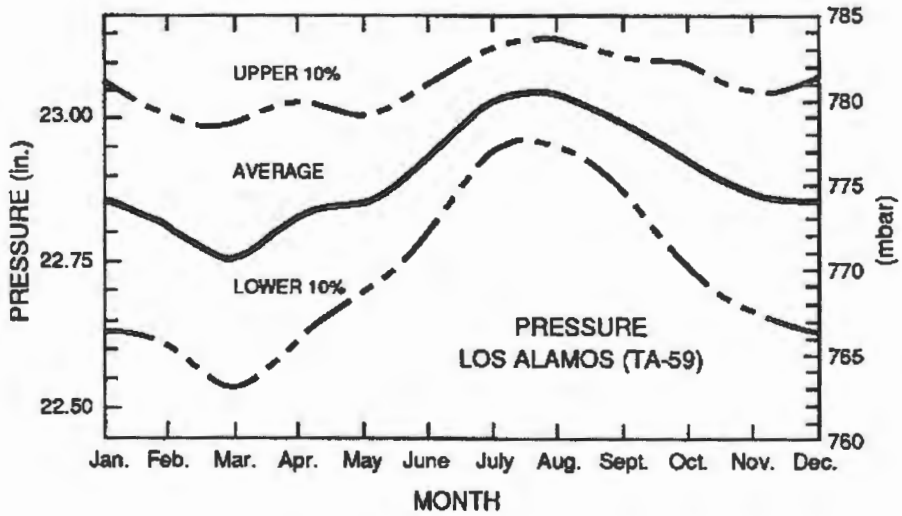

Fig. 5.1. Monthly mean atmospheric pressure at Los Alamos (TA-59).

Table 5.1. Monthly atmospheric pressure, means, and extremes.

				Extremes			Adjusted to Sea Level Extremes		
	Mean	Monthly Std Dev	Mean Daily Range	High	Low	Highest Daily Range	Mean	High	Low
Atmospheric Pressure (in. Hg)									
January	22.86	0.17	0.14	23.30	22.16	0.70	30.12	30.70	29.17
February	22.83	0.16	0.11	23.24	22.41	0.43	30.07	30.53	29.49
March	22.77	0.18	0.14	23.26	22.23	0.42	29.90	30.54	29.19
April	22.84	0.15	0.13	23.22	22.30	0.43	29.83	30.33	29.13
May	22.86	0.12	0.11	23.21	22.53	0.32	29.75	30.20	29.32
June	22.96	0.11	0.10	23.27	22.60	0.27	29.69	30.10	29.25
July	23.03	0.07	0.09	23.23	22.80	0.19	29.70	30.01	29.44
August	23.04	0.08	0.08	23.25	22.76	0.21	29.79	30.05	29.42
September	23.00	0.10	0.08	23.27	22.54	0.23	29.82	30.18	29.23
October	22.94	0.14	0.10	23.30	22.30	0.64	29.95	30.41	29.13
November	22.87	0.15	0.13	23.27	22.31	0.40	30.04	30.53	29.30
December	22.86	0.17	0.12	23.23	22.23	0.48	30.08	30.57	29.25
Annual	22.91	0.13	0.11	23.30	22.23	0.70	29.89	30.70	29.13
Atmospheric Pressure (mbar)									
January	774.1	5.6	4.8	788.9	750.5	23.7	1020.1	1039.5	988.0
February	773.1	5.4	3.9	787.1	758.7	14.5	1018.4	1033.7	998.5
March	771.2	6.1	4.9	787.7	752.7	14.1	1012.5	1034.1	988.2
April	773.4	5.2	4.6	786.4	755.0	14.7	1010.3	1027.3	986.2
May	774.2	4.2	3.8	786.1	762.9	11.0	1007.4	1022.8	992.7
June	777.5	3.6	3.3	788.0	765.5	9.0	1005.4	1019.2	990.2
July	779.8	2.3	3.0	786.8	772.1	6.5	1005.9	1015.9	996.8
August	780.3	2.5	2.8	787.2	770.6	7.0	1008.7	1017.5	996.1
September	778.8	3.3	2.8	787.9	763.3	7.8	1009.8	1021.8	989.8
October	776.9	4.8	3.3	788.9	754.9	21.7	1014.2	1029.9	986.2
November	774.7	5.1	4.2	788.1	755.6	13.6	1017.3	1034.0	992.2
December	774.3	5.6	4.1	786.8	752.7	16.3	1018.6	1035.0	990.3
Annual	775.7	4.5	3.8	788.9	752.7	23.7	1012.4	1039.5	986.2

Conversions:

1 standard atmosphere (std atm) = 29.92 in. of Hg
= 760 mm (torr) of Hg
= 76.0 cm of Hg
= 1.0133 bar
= 1013.3 mbar
= 101.33 kPa
= 101 325 Pa
= 14.69 lb/in.^{2}

with a summer maximum and a spring minimum. The spring minimum is caused by frequent storms. The summer higher pressures result when the middle- and upper-atmosphere westerlies move to the north and weaken while subtropical high-pressure systems move northward toward the southern United States. Variations from the mean are greatest in the spring and winter seasons and least during the summer. The March upper 10% and lower 10% values are displaced from the mean twice as much as displacements during July and August. The monthly standard deviations and mean daily ranges given in Table 5.1 also show increased variability during winter and spring.

Even though the mean pressure is highest during summer, the maximums then are lower than during the winter months. The highest recorded pressure in the 9-year record occurred in January. Winter high-pressure readings can result from cold, low-level high-pressure systems. Extreme high pressure in the summer results from middle- and upper-level high-pressure systems. The difference in extremes for the cold season reaches about 1.00 in. (34 mbar), or about 4.5% of the mean value, about twice the difference in summer extremes. One strong October storm caused a 0.64-in. (21.7-mbar) change in 1 day alone.

Caution should be used when applying data on pressure extremes. Because the data record has been kept for only 9 years, the listed values underestimate extremes that would be recorded over a longer time period.

Pressures adjusted to sea level were also calculated from estimated temperature and humidity profiles for elevations below those at Los Alamos (Table 5.1). Unlike actual station pressures, pressures adjusted to sea level are related to temperatures, reaching a peak in January and a minimum in July. The sea-level pressure follows the annual temperature cycle, whereby a theoretical atmospheric-pressure profile lower than that at Los Alamos would show reduced pressure (and density) because of atmospheric heating. Indeed, during the summer months, a low-level "heat low" is a common feature on weather maps in the deserts of southern California, Nevada, Arizona, New Mexico, and northern Mexico.

5.2 Los Alamos Pressure Adjustment

Sometimes it is necessary to estimate atmospheric pressure at a height slightly different from a measured height. The pressure change with height can be estimated if the average temperature is known. In the standard atmosphere, pressure *rises (falls)* 0.087 in. (2.94 mbar) for each 100-ft (30.5-m) *decline (ascent)* in elevation, or 0.029 in. (0.96 mbar) for each 32.8-ft (10-m) *decline (ascent)* in elevation. The TA-59 site, with an elevation of 7375 ft (2248 m) ASL, can be used as a reference.

If more accuracy is desired, this correction can be adjusted for average air temperature. The air at TA-59's elevation has about a 0°C (273 K) temperature in the

standard atmosphere. The elevation correction can be multiplied by the ratio of the air temperature T (K) and 273 K,

$$\text{Pressure correction} = 0.087 \text{ in.} / 100 \text{ ft} \times (273/T),$$
$$\text{or } 2.94 \text{ mbar}/30.5 \text{ m} \times (273/T),$$

or (for 10 m)

$$\text{Pressure correction} = 0.029 \text{ in.} / 32.8 \text{ ft} \times (273/T).$$
$$\text{or } 0.96 \text{ mbar}/10 \text{ m} \times (273/T).$$

5.3 Hourly Pressure

Hourly station pressure is plotted in Fig. 5.2 for January, April, July, and October. Note the distinct diurnal cycle during all months, with a maximum occurring during the late morning (0900–1100 Mountain Standard Time [MST]) and a minimum during late afternoon (1530–1800 MST). The diurnal cycle is associated with alternate heating and cooling of the atmosphere. Because cold air is denser, pressure increases when the lower atmosphere is colder. The maximum atmospheric cooling from the prior evening occurs late in the morning, well after sunrise. The maximum pressure occurs earlier in the morning during the summer when the sunrise is the earliest. Conversely, mean pressure reaches a minimum in the afternoon, lagging behind the strongest sunshine and surface heating. January's minimum pressure occurs relatively early in the afternoon, at 1530. The diurnal range of hourly mean pressure is similar in all months, 0.06–0.07 in. (2.0–2.4 mbar). Most of the diurnal range of hourly mean values is caused by the diurnal atmospheric heating and cooling cycle.

The Los Alamos diurnal variation of pressure agrees well with other continental stations in the low to mid latitudes in both amplitude and time (Berry, Bollay, and Beers

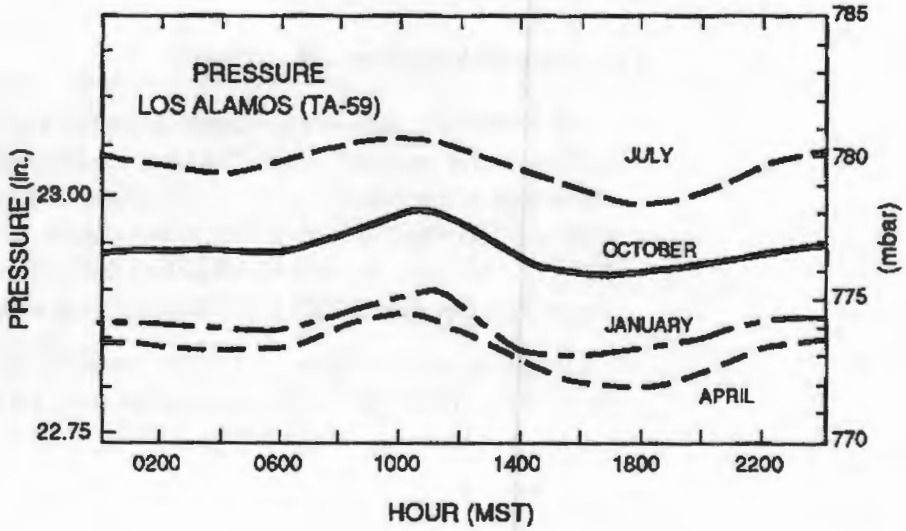

Fig. 5.2. Hourly mean atmospheric pressure at Los Alamos (TA-59) during January, April, July, and October.

1945). Maximum and minimum pressures generally occur at 1000 and 1600, respectively, at other stations. A secondary cycle with a smaller amplitude can be seen in Los Alamos, especially during July. This cycle peaks at 2300–0100 and reaches a minimum at 0400–0600. These times are similar to the average maximum (2200) and minimum (0400) times reported by other low- to mid-latitude stations. No entirely satisfactory explanations have been developed to explain the secondary diurnal pressure cycle.

5.4 Air Density

Air density, like pressure, decreases with height above sea level. In the standard atmosphere, air density equals 1.29 kg/m^3 (0.081 lb/ft^3) at sea level.

Air density varies with pressure and temperature according to the equation of state for an ideal gas:

$$\rho = P / TR ,$$

where

$$\rho = \text{density (kg/m}^3\text{)} ,$$

$$P = \text{pressure (mbar)} , \tag{5.1}$$

$$T = \text{absolute temperature (K)} ,$$

and

$$R = \text{gas constant for dry air (2.870 J/kg-K)} .$$

As the air at Los Alamos averages only 0.5% water vapor, the assumption of dry air is a good one.

If the equation of state is strictly applied to humid air, the density must be adjusted downward depending on the water-vapor concentration or mixing ratio w. The lower air density results from the lower density of water vapor in dry air. One way to account for water vapor in the equation of state is to use an adjusted temperature—virtual temperature (T_v). The virtual temperature is higher than actual temperature by an amount that a specific quantity of water vapor would lower air density. Virtual temperature can be approximated by

$$T_v \cong T\,(1 + 0.61\,w) , \tag{5.2}$$

where

$$T_v = \text{virtual temperature (K)} ,$$

$$T = \text{actual temperature (K)} ,$$

and

$$w = \text{mixing ratio (grams of water vapor/gram of air)}.$$

The relatively dry Los Alamos atmosphere generally results in negligible temperature and density adjustments. The humid air during August results in only a 0.5% downward adjustment of density (0.005 kg/m^3).

Calculations indicate a mean air density of 0.958 kg/m^3, slightly less than 75% of sea-level density. The mean surface density is based on a mean pressure of 22.91 in. (775.2 mbar) and a mean temperature of 48.2°F (9.0°C).

Atmospheric density changes are primarily caused by temperature changes. Pressure changes are relatively small, thereby affecting density less. Monthly mean densities are shown in Table 5.2. Virtual temperatures were used to account for the small (≤0.5%) effect of water vapor. Note that the December and January densities are largest when the mean temperature is lowest. Conversely, density is at a minimum during the summer when temperatures are highest. The monthly mean density has a mean range of 7.0%, nearly equal to the 7.4% annual range of the mean absolute temperature (282 K). In comparison, monthly mean pressure has a mean range of only 1.2%. Density has relatively large extremes, similar to temperature extremes, whereas pressure has much smaller extremes. The largest temperature and density changes occur near the ground because of strong heating and cooling. Pressure includes mass changes of the entire overhead air column. Only the very lowest part of the atmosphere near the ground is affected by the intense diurnal cycle of temperature (density).

5.5 Atmospheric Composition

Atmospheric motion keeps the atmosphere well mixed up to a height of 50 miles (80 km) above ground level. The percentages of gases in the dry atmosphere are shown in Table 5.3. Nitrogen and oxygen account for 99% of the atmosphere by volume. The listed carbon dioxide percentage is an average, as carbon dioxide varies in the atmosphere. The percentage of water vapor in the atmosphere varies from 0.3% during cold winter weather to nearly 2.0% by volume for the most humid summer day.

Table 5.2. Monthly mean atmospheric density at Los Alamos (TA-59).

Month	Atmospheric Density (kg/m^3)	Month	Atmospheric Density (kg/m^3)
January	0.991	July	0.924
February	0.985	August	0.929
March	0.972	September	0.939
April	0.959	October	0.960
May	0.945	November	0.977
June	0.928	December	0.989
		Annual	0.958

Table 5.3. Proportions of gases composing dry air in lower atmosphere (up to 80 km).

Gas	Percentage by Volume	Percentage by Mass
Nitrogen (N_2)	78.08	75.51
Oxygen (O_2)	20.95	23.15
Argon	0.93	1.28
Carbon dioxide	0.03	0.046
Neon	0.0018	0.00125
Helium	0.00052	0.000072
Methane	0.00014	0.000078
Krypton	0.00010	0.000289
Water vapor[a]	0.3–2.0	0.2–1.2

[a]Percentage of moisture in the atmosphere at Los Alamos.

6 Insolation (Sunshine)

Insolation (defined as *in*coming *sol*ar rad*iation*) has been continuously measured at TA-59 and Area G since 1979. Measured by a pyranometer, insolation is the energy that strikes a plane parallel to the earth's surface.

Solar energy strikes the top of the earth's atmosphere at a rate of 2 langleys/min (or 1.4 kW/m^2) on a surface perpendicular to the sun's rays (1 langley[ly] = 1 calorie[cal]/cm^2). This rate (1.4 kW/m^2) is referred to as the solar constant.

Several factors affect the amount of radiation that reaches the earth. First, the angle of the sun above the horizon has a great effect. At the summer solstice (~June 21), the local noon sun is closest to its zenith (highest position in the sky) and therefore provides the maximum possible surface radiation. Also, the angle of the sun during the summer at high elevations results in longer days, contributing to the increased total insolation. In contrast, at the winter solstice, the low sun angles and short days give relatively little solar radiation. Second, the thickness of the atmosphere, clouds, and aerosols also affect the amount of solar radiation received at the ground.

The atmosphere is an excellent scatterer of incoming sunlight. As sunlight reaches farther down into the atmosphere, direct-beam radiation is reduced while the downward-scattered (diffuse) radiation increases. In addition, an increasing amount of solar radiation is lost to upward scattering (backscattering) as sunshine approaches sea level. Similarly, direct-beam sunlight is reduced if it must pass through a greater part of the atmosphere. For example, direct sunlight is greatly reduced shortly before sunset and after sunrise because the beam effectively must pass through several atmospheres. Since Los Alamos is above almost one-fourth of the atmosphere, sunshine is relatively intense compared with sunshine at sea-level elevations. Because of the relatively high elevation and low latitude at Los Alamos, precautions should be taken to avoid excessive sunshine exposure, especially during the summer.

Aerosols in the atmosphere can decrease the amount of solar radiation received at the ground. Days with haze, blowing dust, or high humidity have slightly reduced solar radiation when compared with days with clean and dry air. Clouds, composed of water droplets or ice crystals, are efficient sunshine reflectors, thereby reducing incident solar radiation. However, during brief periods, ground-level solar radiation on partly cloudy days can actually exceed the maximum possible radiation occurring on clear days because sunlight is reflected by surrounding clouds.

6.1 Monthly Insolation

Daily average insolation at Los Alamos and Area G was computed by month and is plotted in Fig. 6.1. The maximum possible radiation, which was determined by taking daily maximum insolation measurements on clear days, is also shown. Clear days were determined subjectively by manually scanning daily insolation summaries for full

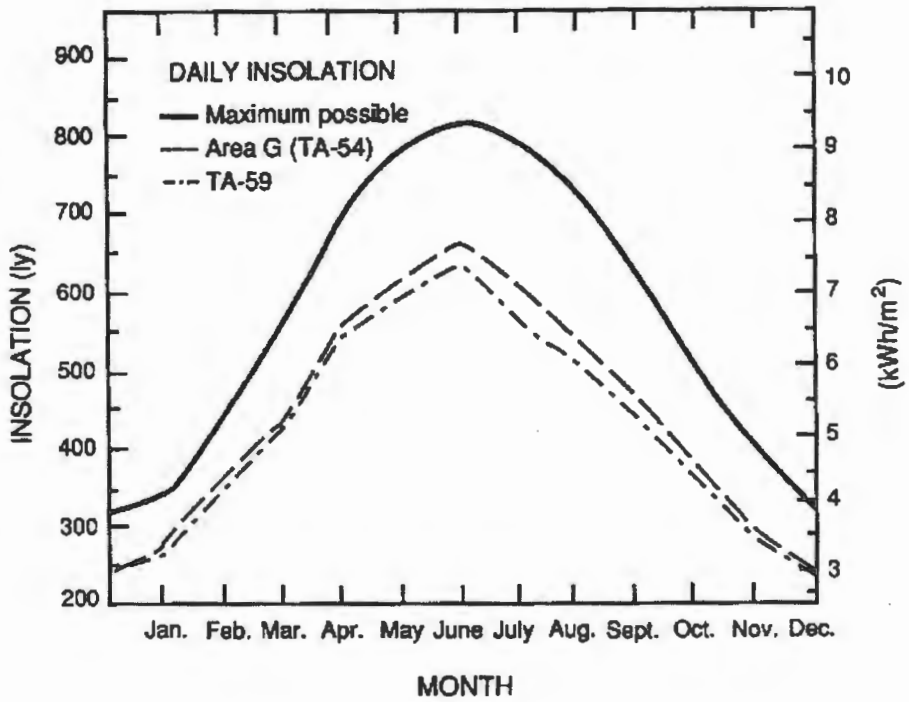

Fig. 6.1. Daily mean and maximum possible insolation at TA-59 and Area G, plotted by month.

Gaussian traces. The solar insolation at both sites follows the seasonal march of the sun, with the greatest radiation occurring in June and the least in December. Solar radiation at Area G is greater than at TA-59 for all months, but especially during July and August, when thundershowers often affect TA-59 more than Area G. The effect of increased clouds at TA-59 is less during the other months.

Monthly insolation statistics are summarized in Table 6.1. The percentage of possible insolation reaches a maximum at both sites during January and February. The high frequency of March storms produces clouds and reduces the percentage of possible insolation during the month. The gap between the percentage of possible insolation at TA-59 and that at Area G widens in the summer months, peaking at nearly 6% in August. Thundershowers often affect TA-59 and areas near the mountains while not affecting Area G and other areas farther away from the mountains. Note that the minimum percentage of possible insolation is reached at TA-59 in August. Because August thundershowers and associated clouds affect Area G less, the percentage of possible radiation at Area G reaches a minimum in March.

Percentages of possible solar radiation given in this section should not be confused with percentages of possible sunshine, which is another indicator. Possible sunshine indicates times of sunshine without interference by clouds. The percentage of possible sunshine is generally lower than the percentage of insolation because radiation in the latter instance is received even during times when the sun is attenuated by clouds. The difference between the two percentages can be especially great during the summer when solar radiation is the most intense. The annual mean percentage of possible sunshine is

Table 6.1. Monthly insolation statistics.

	Maximum Possible		TA-59			Area G		
	Daily	Monthly	Daily	Monthly	% Possible	Daily	Monthly	% Possible
Radiation (ly):								
January	340	10 540	273.4	8 476	80.4	281.34	8 722	82.7
February	445	12 570	358.5	10 038	80.6	370.03	10 361	83.2
March	575	17 825	427.4	13 248	74.3	434.50	13 469	75.6
April	708	21 246	548.9	16 466	77.5	561.80	16 854	79.4
May	780	24 180	590.3	18 300	75.7	614.19	19 040	78.7
June	810	24 300	636.2	19 087	78.6	662.96	19 889	81.8
July	785	24 335	567.9	17 604	72.3	604.65	18 744	77.0
August	715	22 165	510.7	15 831	71.4	551.83	17 091	77.2
September	608	18 246	446.8	13 405	73.5	468.28	14 048	77.0
October	490	15 190	369.5	11 455	75.4	381.01	11 811	77.8
November	382	11 466	283.0	8 460	74.1	292.79	8 784	76.6
December	320	9 920	239.9	7 436	75.0	243.64	7 553	76.1
Annual	580	211 965	437.5	159 806	75.4	455.50	166 366	78.5

estimated to be 65% at TA-59 and 68% at Area G, or about 10% lower than the percentage of possible radiation at these sites.

6.2 Hourly Insolation

Hourly insolation rates at TA-59 and Area G are plotted in Fig. 6.2(a)–(d) for January, April, July, and October, respectively. Insolation at TA-59 is generally slightly less than at Area G. The percentage difference between the maximum possible and the actual radiation received is rather constant throughout the day for most of the year, with early afternoon clouds having an increased effect on insolation. However, the July insolation patterns are dramatically different during the monsoon thundershower season. Note the drop-off in solar radiation after 1100, especially at TA-59. The percentage of possible solar radiation in July drops from more than 90% at 1100 to less than 60% at 1330. The insolation reduction is somewhat less at Area G because of its greater distance from the Jemez Mountains.

6.3 Sunrise, Sunset, and Twilight

6.3.1 Sunrise and Sunset

Los Alamos daily sunrise and sunset times (Mountain Standard Time) and twilight durations are listed in Table 6.2. The data were calculated using *Tables of Sunrise,*

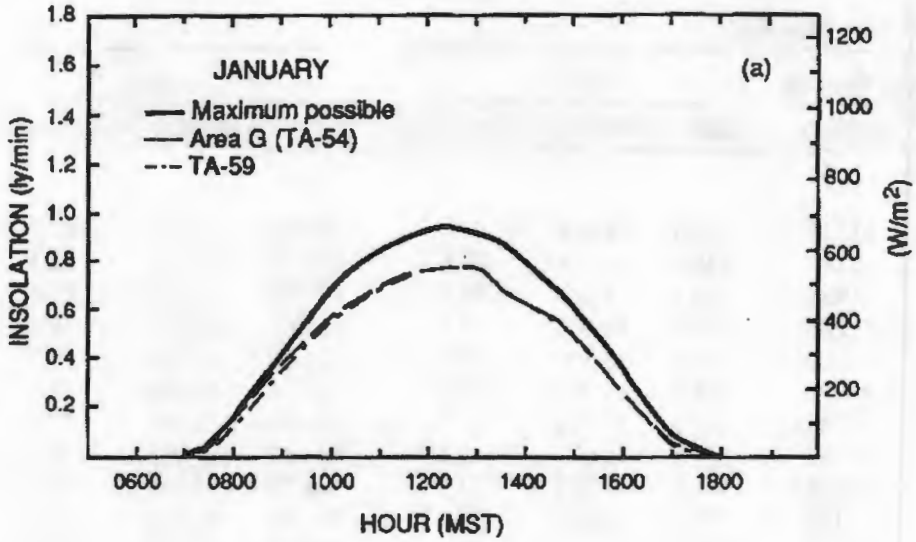

Fig. 6.2(a)–(d). Hourly mean and maximum possible insolation at TA-59 and Area G for (a) January, (b) April, (c) July, and (d) October.

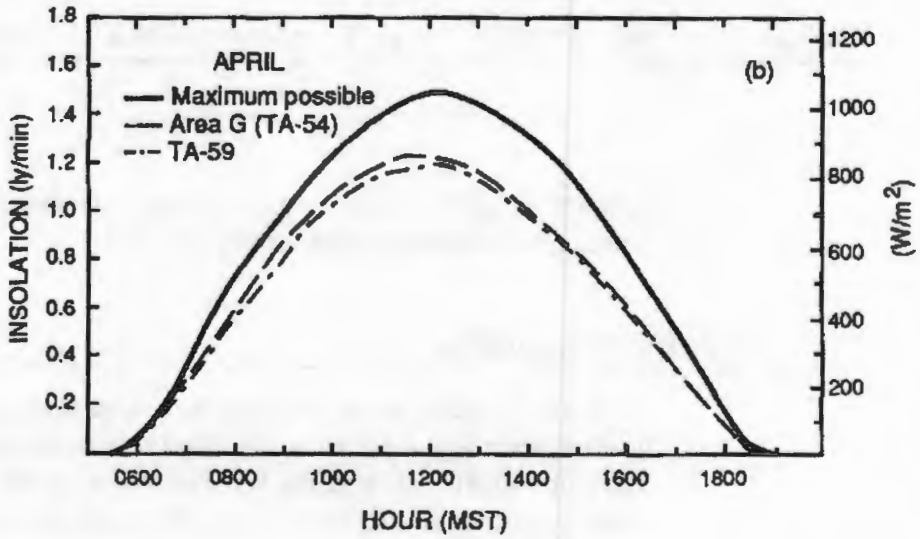

Sunset, and Twilight from the U.S. Naval Observatory (1962). The sunrise and sunset times were calculated for the year 1990; therefore, the listed values are not exactly correct for other years. However, this error amounts to less than 4 minutes and averages less than 1 minute through the year 2030.

The sunrise and sunset times listed in Table 6.2 are the civil times at which the upper edge of the sun's disk would actually be seen on a regular and unobstructed horizon, under normal atmospheric conditions, by an observer on a level region at zero elevation above the earth's surface. At Los Alamos, however, the Sangre de Cristo Mountains to the east obstruct the sunrise and the Jemez Mountains to the west obstruct the sunset. Sunrise and sunset corrections were calculated for TA-59 (located 5.5 miles east of the 10 200-ft [3100-m] summit of Cerro Grande). On average, 5 minutes should be added to

Fig. 6.2 (Continued)

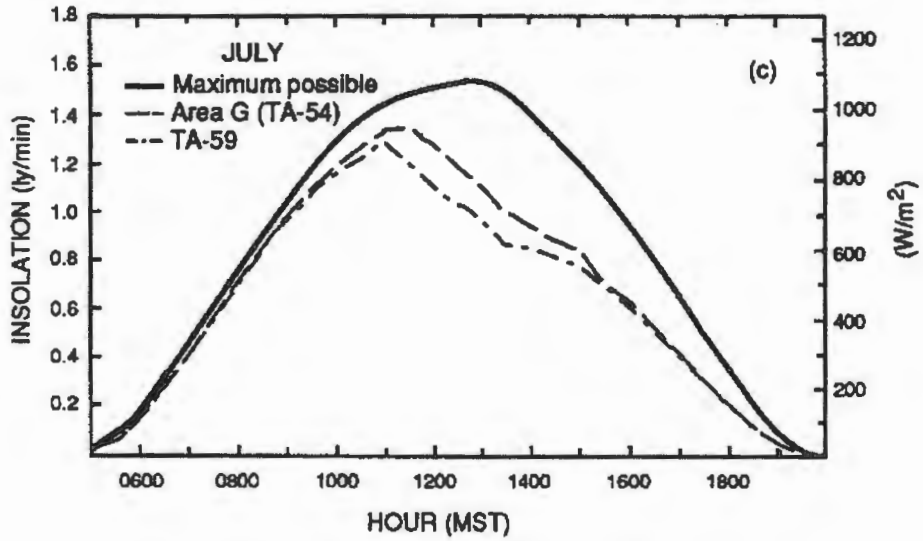

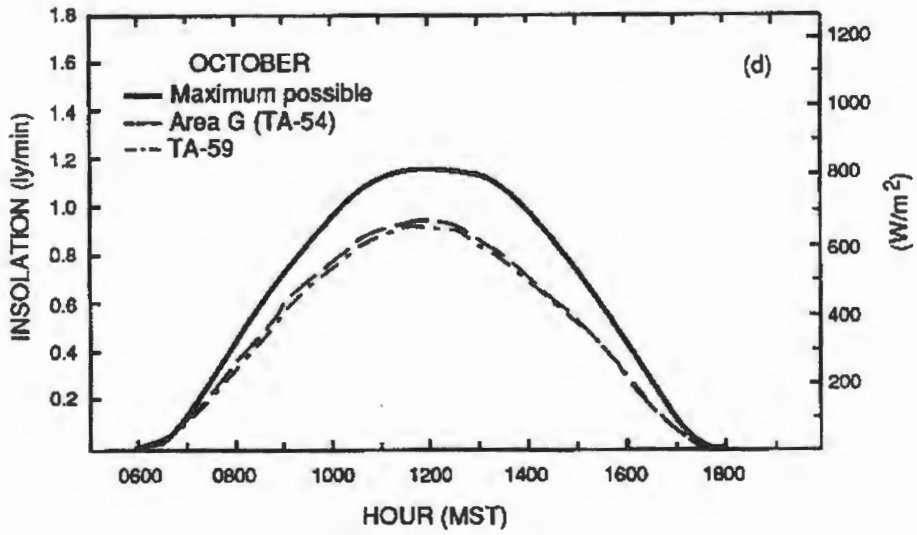

the sunrise time and 21 minutes should be subtracted from the sunset time if the terrain is taken into account. Sunset corrections are considerably greater for areas closer to the Jemez Mountains and are less for areas further east.

6.3.2 Twilight

Monthly averages of the three kinds of twilight are given in Table 6.2. Civil, nautical, and astronomical twilight durations are the intervals of time between sunrise or sunset and the instant when the center of the sun is 6°, 12°, and 18°, respectively, below the horizon. When applying twilight duration, sunrise and sunset times that assume flat terrain should be used.

Table 6.2. Los Alamos (TA-59) sunrise and sunset times (MST) and twilight durations. The sunrise and sunset times are exact for 1990, with the average error less than 1 minute for the years 1950–2030. The sunrise and sunset times assume flat terrain. On average, corrections of 5 and 21 minutes, respectively, should be applied to sunrise and sunset times to allow for the elevated terrain.

	January		February		March		April		May		June	
Day	Rise	Set	Rise	Set	Rise	Set	Rise	Set	Rise	Set	Rise	Set
1	0716	1702	0706	1732	0636	1800	0552	1827	0513	1852	0450	1916
2	0716	1703	0705	1733	0634	1801	0550	1828	0512	1853	0449	1917
3	0716	1703	0704	1734	0633	1802	0549	1828	0511	1854	0449	1917
4	0716	1704	0704	1735	0632	1803	0548	1829	0510	1854	0449	1918
5	0716	1705	0703	1736	0630	1803	0546	1830	0509	1855	0448	1919
6	0716	1706	0702	1737	0629	1804	0545	1831	0508	1856	0448	1919
7	0716	1707	0701	1738	0628	1805	0543	1832	0507	1857	0448	1920
8	0716	1708	0700	1739	0626	1806	0452	1832	0506	1858	0448	1920
9	0716	1708	0659	1740	0625	1807	0541	1833	0505	1859	0448	1921
10	0716	1709	0658	1741	0623	1808	0539	1834	0504	1900	0448	1921
11	0716	1710	0657	1742	0622	1809	0538	1835	0503	1900	0448	1922
12	0716	1711	0656	1743	0621	1810	0536	1836	0502	1901	0448	1922
13	0716	1712	0655	1744	0619	1811	0535	1837	0501	1902	0448	1923
14	0715	1713	0654	1745	1618	1811	0543	1838	0500	1903	0448	1923
15	0715	1714	0653	1746	0616	1812	0532	1838	0500	1904	0448	1923
16	0715	1715	0652	1747	0615	1813	0531	1839	0459	1904	0448	1924
17	0715	1716	0650	1748	0614	1814	0530	1840	0458	1905	0448	1924
18	0714	1717	0649	1749	0612	1815	0528	1841	0457	1906	0448	1924
19	0714	1718	0648	1750	0611	1816	0527	1842	0456	1907	0448	1924
20	0713	1719	0647	1751	0609	1817	0526	1843	0456	1908	0448	1925
21	0713	1720	0646	1752	0608	1817	0525	1844	0455	1908	0448	1925
22	0712	1721	0645	1753	0606	1818	0523	1844	0454	1909	0448	1925
23	0712	1722	0643	1754	0605	1819	0522	1845	0454	1910	0449	1925
24	0711	1723	0642	1755	0603	1820	0521	1846	0453	1911	0449	1925
25	0711	1724	0641	1756	0602	1821	0520	1847	0453	1911	0449	1926
26	0710	1726	0640	1757	0600	1822	0518	1848	0452	1912	0450	1926
27	0710	1727	0638	1758	0559	1823	0517	1849	0452	1913	0450	1926
28	0709	1728	0637	1759	0558	1823	0516	1849	0451	1913	0450	1926
29	0708	1729	0636	1800	0556	1824	0515	1850	0451	1914	0451	1926
30	0707	1730	—	—	0555	1825	0514	1851	0450	1915	0451	1926
31	0707	1731	—	—	0553	1826	—	—	0450	1916	—	—
Mean twilight duration (min)												
Civil	28		26		26		27		29		30	
Nautical	59		57		55		58		63		68	
Astronomical	90		86		86		91		101		108	

Table 6.2 (Continued)

	July		August		September		October		November		December	
Day	Rise	Set	Rise	Set	Rise	Set	Rise	Set	Rise	Set	Rise	Set
1	0452	1926	0512	1910	0535	1832	0559	1748	0626	1709	0657	1651
2	0452	1926	0513	1909	0536	1831	0600	1747	0627	1708	0658	1651
3	0453	1925	0514	1908	0537	1829	0600	1745	0628	0707	0659	1651
4	0453	1925	0514	1907	0538	1828	0601	1744	0629	1706	0700	1651
5	0454	1925	0515	1906	0538	1826	0602	1742	0630	1705	0700	1651
6	0454	1925	0516	1905	0539	1825	0603	1741	0631	1704	1701	1651
7	0455	1925	0517	1904	0540	1823	0604	1740	0632	1703	0702	1651
8	0455	1925	0517	1903	0541	1822	0605	1738	0633	1702	0703	1651
9	0456	1924	0518	1902	0542	1821	0605	1737	0634	1701	0704	1651
10	0456	1924	0519	1901	0542	1819	0606	1735	0636	1701	0705	1651
11	0457	1924	0520	1900	0543	1818	0607	1734	0636	1700	0705	1651
12	0458	1923	0521	1859	0544	1816	0608	1733	0637	1659	0706	1651
13	0458	1923	0522	1858	0545	1815	0609	1731	0638	1658	0707	1652
14	0459	1922	0522	1857	0545	1813	0610	1730	0639	1658	0708	1652
15	0459	1922	0523	1855	0546	1812	0611	1729	0640	1657	0708	1652
16	0500	1922	0524	1854	0547	1810	0611	1727	0641	1656	0709	1652
17	0501	1921	0525	1853	0548	1809	0612	1726	0643	1656	0709	1653
18	0502	1920	0525	1852	0549	1807	0613	1725	0644	1655	0710	1653
19	0502	1920	0526	1850	0549	1806	0614	1724	0645	1655	0711	1654
20	0503	1919	0527	1849	0550	1804	0615	1722	0646	1654	0711	1654
21	0504	1919	0528	1848	0551	1803	0616	1721	0647	1654	0712	1654
22	0504	1918	0529	1847	0552	1801	0617	1720	0648	1653	0712	1654
23	0505	1917	0529	1845	0552	1800	0618	1719	0649	1653	0713	1655
24	0506	1917	0530	1844	0553	1758	0619	1717	0650	1653	0713	1656
25	0507	1916	0531	1843	0554	1757	0620	1716	0651	1652	0714	1657
26	0507	1915	0531	1841	0555	1756	0621	1715	0652	1652	0714	1657
27	0508	1914	0532	1840	0556	1754	0621	1714	0653	1652	0714	1658
28	0509	1914	0532	1839	0556	1753	0622	1713	0654	1651	0715	1659
29	0501	1913	0533	1837	0557	1751	0623	1712	0655	1651	0715	1659
30	0510	1912	0534	1836	0558	1750	0624	1711	0656	1651	0715	1700
31	0511	1911	0535	1834	—	—	0625	1710	—	—	0715	1701
Mean twilight duration (min)												
Civil	29		27		26		26		27		29	
Nautical	65		60		56		56		58		61	
Astronomical	105		94		86		85		89		92	

Civil twilight covers the somewhat indefinite periods before sunrise and after sunset when enough natural light exists for ordinary outdoor activities. However, the light available when the sun is less than 6° below the horizon can vary greatly according to weather conditions, especially during times of cloudiness and haze. The astronomical twilight limits are times when complete darkness (besides moonlight or starlight) ends in the morning and begins in the evening. Nautical twilight represents a period of intermediate light.

7 Other Weather Phenomena

7.1 Tornadoes and Dust Devils

Historically, no tornadoes have ever been reported in Los Alamos County. However, a funnel cloud was reported near White Rock on August 23, 1983. Also, numerous funnel clouds were reported near Santa Fe on August 24–25, 1987. A relatively strong tornado did occur in Albuquerque on September 20, 1985. The storm caused damage to the state fairgrounds and to the near, northeast side of Albuquerque. Specifically, several roofs on homes collapsed, several trees were uprooted, and utility poles were knocked down. Although property damage was significant, few, if any, injuries were caused by the tornado.

Because tornadoes occur more often at lower elevations, a tornado would be more likely toward the Rio Grande Valley than in Los Alamos. Besides being less likely in Los Alamos, tornadoes that might occur at the townsite or in the Jemez Mountains would be weaker than ones at lower elevations. Fujita (1972) predicts a maximum wind speed of 200 mph (89 m/s) should a tornado occur in the Los Alamos area. The design wind speed was obtained by adding a 50-mph (22-m/s) safety factor to 150 mph (67 m/s), the upper wind-speed range of an "F2 tornado" that is possible, but unlikely, to occur in Los Alamos. The design tornado is estimated to have a maximum pressure drop of ~1.5 in. of mercury (40 mbar), a maximum pressure-change rate of 0.67 in./s (23 mbar/s), and a maximum rotational wind diameter of 100 ft (30.5 m). Generally, tornadoes occur most often in the afternoon, especially early afternoon, during the warm season.

Dust devils are more likely to cause locally damaging winds in Los Alamos. Fujita (1972) states that dust devils theoretically could develop uppermost F1 winds of 112 mph (50 m/s). Strong dust devils can commonly produce 75-mph (34-m/s) winds. Several have been reported that caused damage in Los Alamos. A strong dust devil on April 24, 1973, knocked a trailer off its supports and rolled it one complete revolution at Los Alamos Meson Physics Facility (LAMPF), causing extensive damage. Dust devils occur during sunny, warm days with light winds.

7.2 Thunderstorms, Lightning, and Hail

Thunderstorms are quite common at Los Alamos, with 58 occurring in an average year. Average thunderstorm days, by month, are shown in Fig. 7.1. A thunderstorm day is defined as a day in which either a thunderstorm occurs or thunder is heard nearby. Most thunderstorm days occur during July and August, the so-called monsoon season. During this time of year, large-scale southerly and southeasterly winds import moist air into New Mexico, primarily from the Gulf of Mexico. The combination of moist air, strong sunshine, and warm surface temperatures encourages the formation of afternoon and evening thundershowers, especially over the Jemez Mountains. Upper winds often move the thunderstorms over Los Alamos.

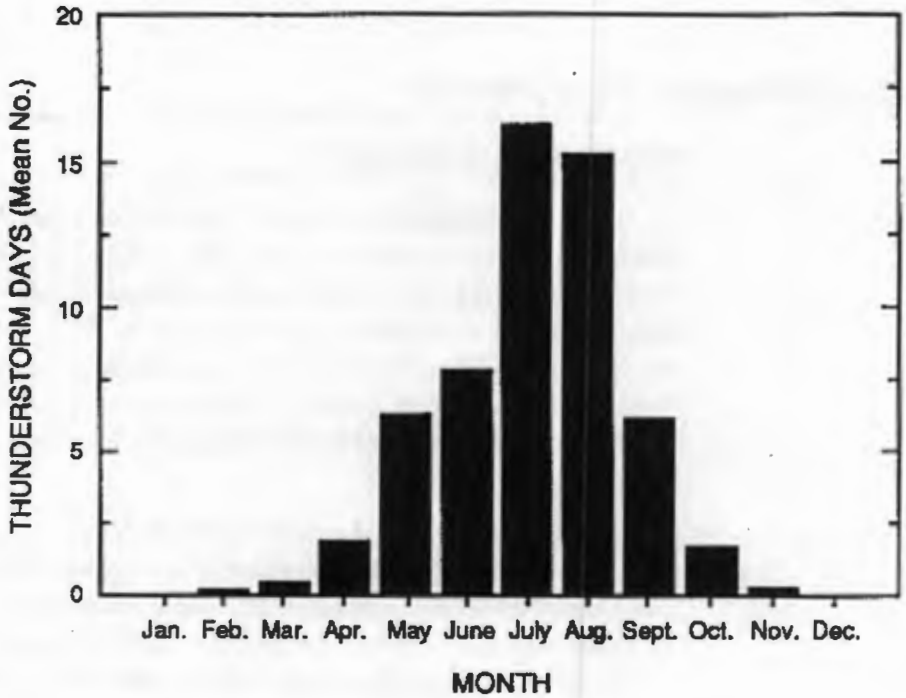

Fig. 7.1. Monthly normal thunderstorm days at Los Alamos (TA-59).

Lightning in Los Alamos can be frequent and intense during some thunderstorms, and people should avoid being outdoors during lightning activity. Because lightning can cause occasional brief power outages, lightning protection is, and should be, an important design factor for most facilities at the Laboratory and the surrounding area.

Hail is also very common at Los Alamos. In fact, the area around Los Alamos has the most frequent hailstorms in New Mexico (NOAA 1977). Most often, the hailstones have diameters of about 0.25 in. (0.6 cm), with a few somewhat larger. Some storms produce measurable accumulation on the ground. Infrequently, hailstorms cause significant damage to property and plants. For example, a thunderstorm on August 11, 1982, dropped about 3 in. (7.6 cm) of hail near the Los Alamos airport, primarily damaging windshields and vegetation in the area. Thunderstorms on May 9, 1989, dropped hailstones up to 1 in. (2.5 cm) in diameter at White Rock and the White Rock Y, causing damage to cars, roofs, and vegetation. The same storms left 2 in. (5 cm) of hail accumulation in the North Community.

7.3 Floods

Large-scale flooding is not common in New Mexico. However, flash floods from heavy thunderstorms are possible in susceptible areas, such as arroyos and canyons. During heavy thunderstorms, these areas should be avoided. Severe flooding has never been observed in Los Alamos, but the northeast heights of Albuquerque experienced

severe flash flooding on July 16, 1988, from a thunderstorm that dropped 5.5–7.5 in. (13.8–18.8 cm) of rain in less than 2 hours. Extensive damage and one death occurred from flooding of these normally dry arroyos and streets. Flooding from a heavy thunderstorm could also occur in Los Alamos in canyons or low spots.

Flooding is possible in the spring from snowmelt, although snowmelt flooding is usually confined to the larger rivers in the state. However, snowmelt can cause muddy conditions in the Los Alamos area, along with minor flooding of streams in the Jemez Mountains.

7.4 Winter Storms

Snowfalls of 4 in. (10 cm) or more are common in Los Alamos during the winter. Storms with winds above 15 mph (7 m/s) can be associated with cold temperatures, resulting in dangerous wind-chill/apparent temperatures, considerable drifting, and low visibility. The combination of heavy snowfall and restricted visibility makes driving conditions dangerous, if not impossible. Occasionally, snowstorms cause heavy snowfall in the mountains, while little snow falls in Los Alamos. Drivers should be prepared for winter storms, especially when traveling in mountainous areas.

7.5 Ice

Ice storms do not occur in Los Alamos and surrounding areas. However, freezing rain occasionally falls in valley areas, such as in Albuquerque. Melted snow or rain may freeze on roadways and sidewalks after a temperature drop, but these occurrences do not cause large ice accumulations on utility lines or trees.

Rime icing occasionally occurs on cold nights when fog droplets come in contact with objects, such as trees, utility lines, and roads. Rime icing occurs more frequently in low spots where cold air settles.

The accumulation of snow on trees, followed by strong winds, may result in downed trees and utility lines, especially after a wet snow, which is common in the late fall and during spring months.

7.6 Heavy Snow Loading

The potential exists for heavy snows to accumulate on roofs, stressing them and even caving them in. In the record snowfall of January 1987, snow from a single storm totaled 4 ft (1.2 m) at TA-59 and 5–6 ft (1.5–1.8 m) in North Community. Another 4 ft (1.2 m) of snow fell at TA-59 during February. The snow's weight damaged or collapsed several roofs in Los Alamos. The water equivalent from the 1987 snowfall totaled 3.43 in. (8.71 cm) in January and 3.44 in. (8.74 cm) in February.

A short, but heavy, snowfall can also be damaging to structures. Generally, wet snowstorms during the spring have the most water equivalent. The heaviest in recent history was a 32-in. (81-cm) snowfall on April 10–12, 1975, with 30 in. (76 cm) falling on the 11th and 12th. The water equivalent totaled 3.12 in. (7.92 cm) during the storm. The January 1987 and April 1975 cases represent levels near the 100-year estimates for snow loading over a period of time and from one storm. Much of the snow in January–February 1987 melted soon after accumulation.

7.7 Wind

Although Los Alamos winds are generally light, strong winds with gusts exceeding 50 mph (22 m/s) are common and widespread during the spring. Occasionally, the strong winds cause some damage to structures and trees. Brief, gusty winds are also common in and near thunderstorms.

7.8 Dust, Haze, and Smoke

Strong spring winds pick up and blow dust in the atmosphere. Visibility is reduced during blowing dust, especially near the Rio Grande Valley where the ground is open. Blowing dust can also be caused by thunderstorms. Haboob is the name given to a dust storm produced by thunderstorm downdrafts in desert regions.

Haze occasionally restricts visibility to 20 miles (32 km) or less, in some cases to as close as 10 miles (16 km). The haze is caused by aerosols with diameters less than 10 μm. Sulfate or nitrate aerosols, which are products of power plants, motor vehicle exhaust, smelters, and other industrial sources, can be transported from faraway places and can severely limit the usually good visibility (approximately 60 miles [96 km]). Haze has been observed in Los Alamos when brisk southwesterly winds occur over the southwestern United States. The brisk winds usually follow times of light winds over southern Arizona and the adjacent Mexico region. Haze is probably caused by emissions from large cities (including automobile exhaust) and large industrial plants located toward the southwest in southern Arizona and northwestern Mexico. There also have been several haze occurrences when a deep easterly wind flow was present over New Mexico, suggesting possible haze transport from Texas.

Distant forest fires also can cause haze in Los Alamos. Hazy conditions persisted in Los Alamos and much of New Mexico for nearly a week in September 1987 when forest fires burned out of control in many of the western states, including California, Nevada, Arizona, and Utah. Westerly upper-air winds transported the aerosols toward the east during and after the fires.

Nearby forest fires, of course, also cause reduced visibility. Heavy smoke was present in the Los Alamos air and other nearby areas during June 18–21, 1977, when the La Mesa fire was burning.

On rare occurrences, distant volcanoes can cause haze by spewing ash into the atmosphere. The eruptions of the Mount St. Helens volcano (Washington) on May 18, 1980, and shortly thereafter caused widespread haze over much of the United States, including Los Alamos.

7.9 Fog

General fog seldom occurs in Los Alamos. Fog days over a 27-year period ending in 1988 are shown in Fig. 7.2. The greatest number of fog days, by far, occurs during December; the average number then is slightly more than 1.5. Fog most often forms on clear nights following snow or rain (radiational fog), sometimes with an upslope wind. Fog formation is greatest in December because nights are longest then. The other cold months average <1 fog day per month. The warm months have even less fog, with no fog days reported in August. Fog tends to be more frequent in the valley and in local low spots.

7.10 Drought

Extended periods of extreme dryness are uncommon in Los Alamos, largely because of the reliable summer thundershowers. Los Alamos escaped the drought of the "dustbowl '30s" and received adequate precipitation. The worst drought occurred during 1956 when only 6.80 in. (17.3 cm) of precipitation fell during the entire year, 38% of

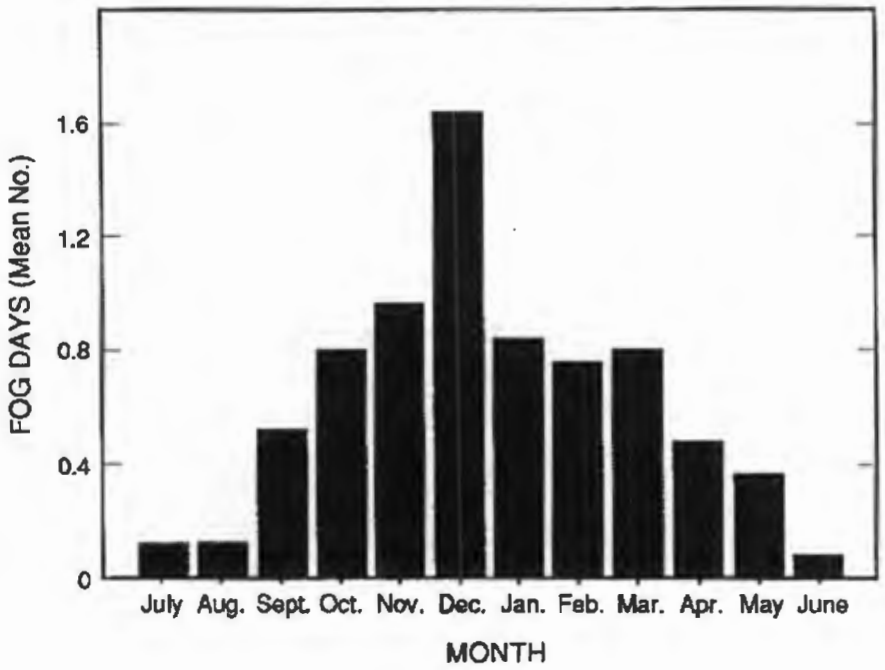

Fig. 7.2. Monthly mean number of fog days at Los Alamos over a 27-year period.

normal. The drought was especially severe toward the end of the year, with only 0.32 in. (0.81 cm) from August 24, 1956, through January 2, 1957. More recently, very dry weather occurred during the summer of 1980. Rainfall totaled only 0.35 in. (0.89 cm) in June and July and 2.32 in. (5.89 cm) during the entire summer (June–August), the driest summer on record.

7.11 Heat Waves

Extreme heat in Los Alamos is very rare, and even when it does occur, low relative humidities make it tolerable. A heat wave can be defined as 3 consecutive days with the temperature reaching 90°F or higher. Los Alamos averages only 2 days per year with temperatures reaching 90°F. The summer of 1980 stands out as the hottest summer on record: 22 times during 1980 the temperature reached 90°F, including 20 times in June and July. Previously, the most 90°F days (7) occurred in 1936. More recently, 9 days at 90°F occurred during summer 1989. Temperatures in 1980 reached 90°F or higher on the last 8 days of June and 3 times on 3 consecutive days during July. Temperatures at White Rock reach 90°F more often than at Los Alamos and occasionally climb above 95°F. The highest recorded Los Alamos temperature was 95°F on July 11, 1935, and June 22, 1981; the highest recorded White Rock temperature was 100°F on July 12, 1971, and June 21, 1981.

7.12 Cold Waves

Frigid weather occasionally occurs in Los Alamos when polar or Siberian air masses settle over the region. Normally, the temperature drops to 0°F or below only once or twice a year. Los Alamos cold waves can be defined as times when the temperature drops to −10°F or lower or when the temperature drops to 0°F or below for at least 2 consecutive days. Cold waves are usually preceded by a fresh snowfall. The lowest temperatures generally occur with clear skies, light winds, and snow cover. Cold-air drainage gives more sub-0°F days and lower temperatures at White Rock than at Los Alamos. However, when clouds or moderate winds are present, temperatures at Los Alamos are colder than at White Rock.

Probably the most severe cold wave occurred during the week beginning January 3, 1971. Temperatures plunged after a snowstorm dropped 10 in. (25.5 cm) of snow on Los Alamos and 15 in. (38 cm) on White Rock. Los Alamos low temperatures reached −9°F, −13°F, −16°F, −15°F, and −9°F, respectively, on 5 consecutive mornings beginning on the 3d. High temperatures only reached 4°F, 8°F, 8°F, and 9°F on January 4–8. White Rock low temperatures were considerably colder, reaching −5°F, −25°F, −29°F, −18°F, and 0°F on January 4–9. The low of −29°F represents the all-time low at White Rock.

Earlier Los Alamos cold waves included one that dropped temperatures to −8°F, −10°F, and −9°F on December 23–25, 1924, and one that occurred in January 1963. Low temperatures in 1963 dropped to −4°F, −11°F, −18°F, −4°F, and 0°F on January 11–15.

The –18°F reading represents the coldest temperature ever recorded at Los Alamos. The high temperature was only 6°F on the 12th. Note that records were not yet available at White Rock in 1963.

Another notable cold wave occurred at the end of November 1976. This cold wave was unusual in that it occurred so early. Los Alamos temperatures dipped to –11°F, –14°F, –12°F, and –5°F on November 27–30. Daytime highs managed to reach 19°F, 17°F, 23°F, and 33°F on those days. White Rock saw low temperatures of –11°F, –14°F, and –4°F on the 27th 28th, and 29th, respectively.

The most recent severe cold wave occurred in early December 1978, when the Los Alamos temperature dropped to –2°F, –8°F, and –13°F during December 7–9. White Rock temperatures were considerably colder, dropping to –6°F, –13°F, –17°F, 0°F, –1°F, and 0°F during December 6–12. The longest string (13 days) of temperatures at 0°F or below occurred in White Rock from December 28, 1966, through January 9, 1967. Low temperatures included –11°F on 1 day and –9°F on 2 days. Another string (10 days) of temperatures at 0°F or below occurred in White Rock from December 30, 1970, through January 8, 1971.

7.13 Optical Phenomena

Rainbows occur frequently during the summer monsoon season. Thundershowers are often scattered or isolated, causing alternate areas of rain and sunshine, which is necessary for rainbow formation. Lightning, sometimes intense, is quite frequent. Virga, precipitation that falls from clouds but evaporates before reaching the ground, occurs frequently because of the relatively dry atmosphere. Halos around the sun and moon and sun dogs (parhelia) can be brilliant at Los Alamos because of the dry, thin, and unpolluted mountain air. A rare display of various optical phenomena occurred in much of northern New Mexico, including Los Alamos, on February 25, 1988. The viewing of meteors, stars, and planets is excellent because of the clear, thin air. The northern lights (aurora borealis) appear infrequently and lack the brilliance observed in areas farther north.

8 Historical Climate Trends

8.1 Los Alamos

Los Alamos annual temperature, precipitation, and snowfall values have been plotted for the years of record. Bar charts representing annual mean temperature and precipitation values are shown in Figs. 8.1 and 8.2, respectively; another, representing seasonal snowfall, is shown in Fig. 8.3.

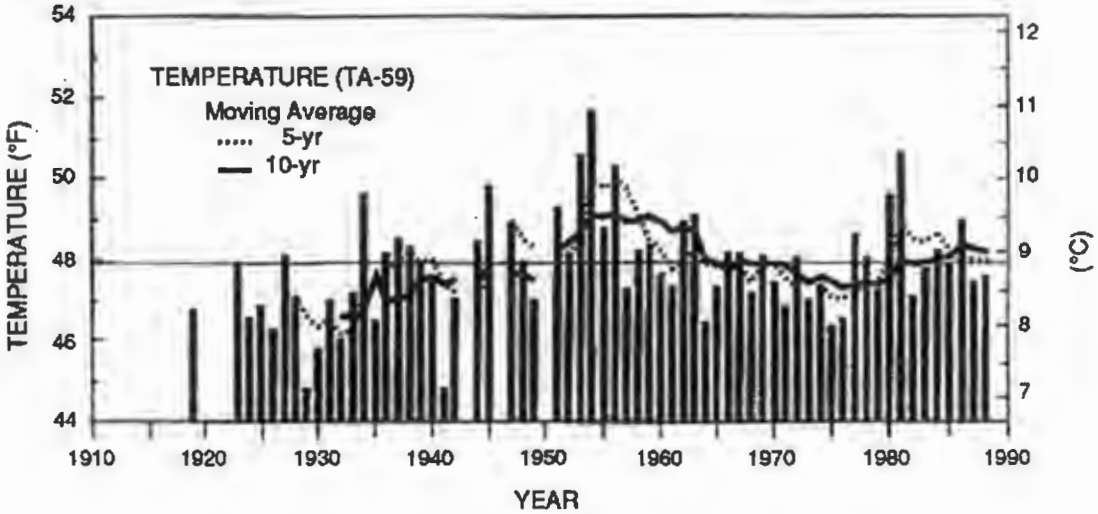

Fig. 8.1. Los Alamos (TA-59) historical annual mean temperatures.

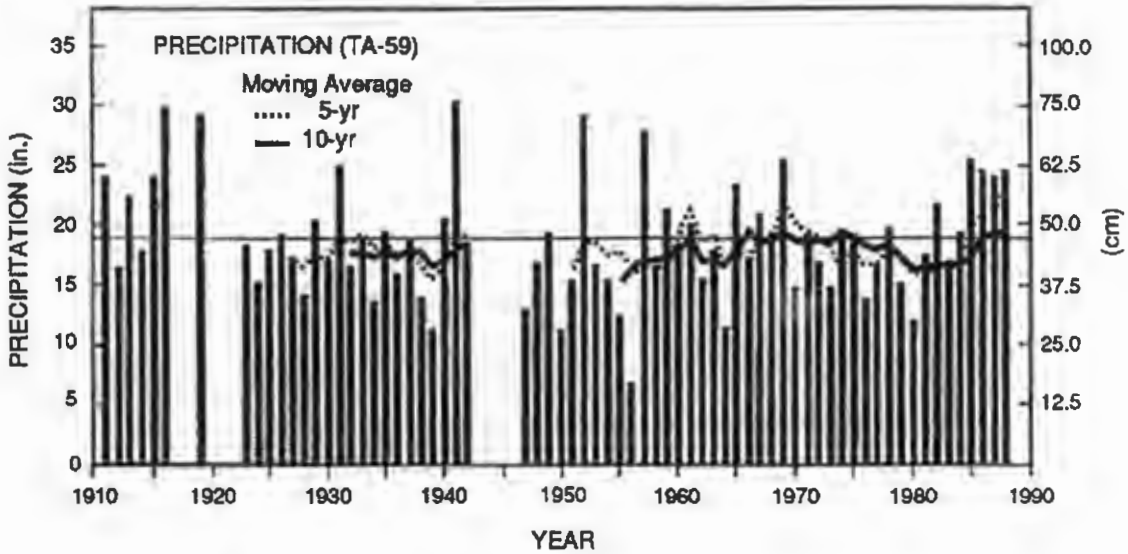

Fig. 8.2. Los Alamos (TA-59) historical annual precipitation.

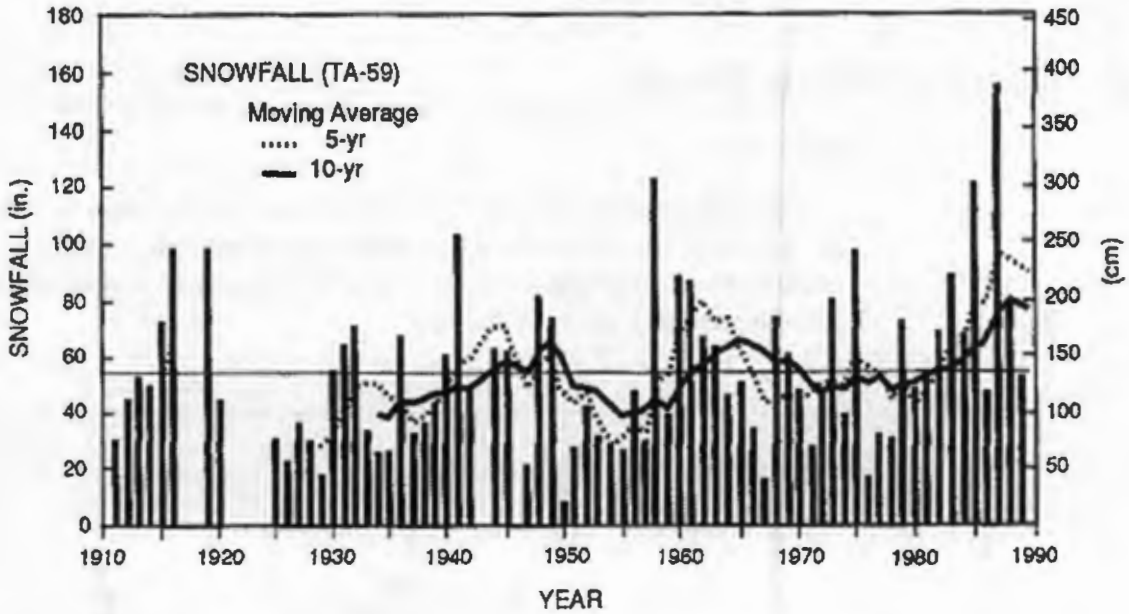

Fig. 8.3. Los Alamos (TA-59) historical seasonal snowfall (year indicates ending year of season).

Available precipitation and snowfall records began in late 1910, whereas temperature records began during 1919. Gaps in precipitation and snowfall data appear during 1917–1918, and all data are unavailable for several years in the early 1920s. Data are also unavailable for some years during World War II, and temperature data are unavailable during 1950.

Note the obviously warm mid-1950s period, with the warmest year on record occurring in 1954 and the second and fourth warmest years in 1953 and 1956, respectively. The third warmest year was 1981. Other warm years were 1934 (during the dust bowl years) and 1945. Cold years occurred in 1929, 1930, and 1941. The 5- and 10-year moving-average lines indicate maximum temperature trends during the 1950s, with minimum temperature trends occurring during the late 1920s, early 1930s, and mid-1970s. A very cool summer helped make 1929 a cold year, and heavy precipitation during 1941 kept temperatures cool that year. The 1980s have seen an increase in temperatures from the 1970s.

Annual precipitation is plotted in Fig. 8.2. Precipitation totals vary dramatically from year to year, ranging from 6.80 in. (17.30 cm) in 1956 to 30.34 in. (77.06 cm) in 1941. Note the heavy precipitation for the 4 years 1985–1988. The 5-year trend line reached its highest point on record at the end of 1988.

Comparison of annual temperature and precipitation records reveals a somewhat negative correlation. The very wet years tend to be cooler than normal, such as in 1941 and 1957. In contrast, very dry years tend to be quite warm, such as the years 1956 and 1980. The negative correlation is weak, however, with many years of exceptions. The negative

correlation of temperature and precipitation is stronger for shorter periods, such as months, but becomes more tenuous for periods of years.

In Fig. 8.3, seasonal snowfall is plotted and designated by the ending year of the winter season. For example, snowfall for the 1980 winter season indicates the total snow from late 1979 through early 1980. The seasonal snowfall has more clearly defined cycles than the cycles for temperature and precipitation, as indicated by the 5- and 10-year trend lines. There is a dramatic rise in snowfall during the 1980s, giving the highest 5- and 10-year snowfall trends ending in 1988. Note the spike of more than 153 in. (389 cm) in the winter of 1986–1987, the largest on record. Except for 1986, the seven winter seasons ending in 1988 all had snowfall above normal. Snowfall was very light during the late 1920s and the early 1950s. Only 8.9 in. (22.6 cm) fell during the winter of 1949–1950.

Los Alamos annual mean temperatures, precipitation, snowfall, and seasonal snowfall are given in Table 8.1. These four variables were also averaged for 30-year periods and are shown in Table 8.2, along with standard deviation, median, and number of cases. Thirty-year periods are often used as short-term climate periods from which normals are calculated. Temperatures were the coldest before 1950 and warmed afterward. Temperature standard deviation, representing year-to-year variables, was the lowest for the 1911–1940 and 1961–1988 periods. Precipitation was the greatest for the 1911–1940 period and second greatest for the 1961–1988 period. The precipitation standard deviation is lowest for the 1961–1988 period and highest for the 1931–1960 and 1941–1970 periods. Both annual and seasonal snowfalls indicate a dramatic peak during the 1961–1988 period, with snowfall amounts 12% higher than their respective totals for the entire record. Snowfall standard deviations are greatest during the 1961–1988 period, reflecting the heavy snows that fell later in the 1980s.

In summary, the climate during the 1961–1988 period had temperatures and precipitation comparable with the entire 1911–1988 record, with less annual variation. The striking characteristic of the 1961–1988 period is the large snowfall of that period compared with that of the entire record. If the weather trends continue in 1989 and 1990, the 1961–1990 normal period will be somewhat cooler and will have 1 in. (2.5 cm) more annual precipitation and 10 in. (25 cm) more annual snowfall than occurred during the 1951–1980 normal period.

Table 8.1. Los Alamos annual mean temperatures, precipitation, snowfall, and seasonal snowfall. Seasonal snowfall is snowfall ending in the indicated year.

Year	Temp. (°F)	Precip. (in.)	Annual Snowfall (in.)	Seasonal Snowfall (in.)	Year	Temp. (°F)	Precip. (in.)	Annual Snowfall (in.)	Seasonal Snowfall (in.)
1911	—	23.89	41.0	31.7	1951	49.3	15.31	33.8	28.4
1912	—	16.52	35.5	45.3	1952	48.3	29.31	39.7	43.0
1913	—	22.39	85.0	54.5	1953	50.5	16.70	30.2	32.4
1914	—	17.88	27.9	51.4	1954	51.9	15.40	26.6	29.2
1915	—	24.02	94.8	76.0	1955	48.8	12.45	24.2	26.7
1916	—	29.87	67.0	99.0	1956	50.3	6.80	41.3	48.3
1917	—	—	—	—	1957	47.3	28.03	66.8	31.2
1918	—	—	63.7	—	1958	48.3	16.73	100.0	123.6
1919	46.8	29.25	73.9	99.1	1959	48.4	21.55	65.1	39.7
1920	—	—	—	45.0	1960	47.6	18.38	87.3	88.6
1921	—	—	—	—	1961	47.4	20.22	90.6	86.3
1922	—	—	—	—	1962	49.0	15.48	40.5	66.5
1923	48.0	18.57	—	—	1963	49.1	17.83	51.1	63.9
1924	46.6	15.15	52.0	—	1964	46.5	11.26	55.7	45.3
1925	46.9	17.46	16.0	31.8	1965	47.4	23.70	52.8	51.8
1926	46.3	19.10	29.0	24.0	1966	48.2	17.48	28.9	34.3
1927	48.2	17.32	30.7	37.0	1967	48.2	20.80	50.0	16.8
1928	47.1	14.11	26.2	31.4	1968	47.3	19.55	39.5	76.0
1929	44.8	20.50	42.5	18.5	1969	48.1	25.67	62.9	53.8
1930	45.9	16.92	41.0	56.0	1970	47.5	14.93	51.8	48.8
1931	47.0	24.92	91.1	65.7	1971	46.9	19.29	67.9	27.5
1932	46.1	16.63	58.7	71.9	1972	48.1	16.99	29.2	47.6
1933	47.2	18.75	25.5	35.5	1973	47.1	14.98	58.7	80.7
1934	49.7	13.54	16.3	22.8	1974	47.4	18.69	51.2	39.8
1935	46.6	19.36	50.2	27.5	1975	46.4	19.32	90.9	97.8
1936	48.3	15.74	49.2	69.4	1976	46.6	13.95	23.5	17.3
1937	48.6	18.30	29.9	34.2	1977	48.7	16.72	22.6	32.6
1938	48.4	13.82	39.5	37.7	1978	48.1	20.06	62.0	31.8
1939	48.0	11.15	50.0	44.5	1979	47.3	15.22	52.9	72.1
1940	47.5	20.54	90.0	61.0	1980	49.6	11.96	55.6	48.1
1941	44.8	30.34	84.7	104.0	1981	50.7	17.71	34.6	54.2
1942	47.1	18.45	33.2	51.2	1982	47.2	21.67	99.8	68.1
1943	—	—	—	—	1983	47.7	16.67	67.4	88.5
1944	48.4	—	55.7	63.1	1984	48.3	19.41	112.9	67.8
1945	49.7	—	—	62.4	1985	47.8	25.57	76.5	121.5
1946	—	—	—	—	1986	49.0	24.12	49.2	47.5
1947	49.0	12.95	30.4	23.1	1987	47.5	23.62	178.4	153.2
1948	48.0	16.84	64.9	82.2	1988	47.6	24.33	49.3	80.2
1949	47.1	19.33	74.9	74.4	1989				52.6
1950	—	11.36	8.9	9.3					
					Mean	47.9	18.74	54.3	55.0
					Highest	51.9	30.34	178.4	153.2
					Lowest	44.8	6.80	8.9	9.3

Table 8.2. Los Alamos annual temperature, precipitation, snowfall, and seasonal snowfall statistics.

Year	Temperature	Precipitation	Annual Snowfall	Seasonal Snowfall
1911–1940				
Mean ± std dev	47.3 ± 1.1 (°F)	19.03 ± 4.63 (in.)	49.1 ± 23.6 (in.)	48.8 ± 22.4 (in.)
Median	47.1°F	18.09 in.	41.7 in.	44.7 in.
Number of cases	19	25	25	24
1921–1950				
Mean ± std dev	47.4 ± 1.3 (°F)	17.55 ± 4.18 (in.)	45.4 ± 23.1 (in.)	47.4 ± 23.6 (in.)
Median	47.1°F	17.39 in.	41.7 in.	41.1 in.
Number of cases	25	24	24	24
1931–1960				
Mean ± std dev	48.2 ± 1.5 (°F)	17.80 ± 5.61 (in.)	50.7 ± 25.2 (in.)	50.8 ± 27.0 (in.)
Median	48.3°F	16.78 in.	49.2 in.	42.1 in
Number of cases	27	26	27	28
1941–1970				
Mean ± std dev	48.3 ± 1.4 (°F)	18.34 ± 5.67 (in.)	51.5 ± 22.6 (in.)	53.4 ± 27.3 (in.)
Median	48.2°F	17.65 in.	51.1 in.	50.0 in.
Number of cases	27	26	27	28
1951–1980				
Mean ± std dev	48.2 ± 1.3 (°F)	17.83 ± 4.78 (in.)	51.8 ± 21.2 (in.)	50.7 ± 25.8 (in.)
Median	48.1°F	17.23 in.	51.5 in.	46.4 in.
Number of cases	30	30	30	30
1961–1988				
Mean ± std dev	47.9 ± 1.0 (°F)	18.83 ± 3.91 (in.)	60.9 ± 31.9 (in.)	61.1 ± 30.0 (in.)
Median	47.7°F	18.99 in.	52.9 in.	53.8 in.
Number of cases	28	28	28	29
1911–1988				
Mean ± std dev	47.9 ± 1.3 (°F)	18.74 ± 4.81 (in.)	54.3 ± 27.9 (in.)	55.0 ± 28.0 (in.)
Median	47.8°F	18.30 in.	50.7 in.	48.3 in.
Number of cases	64	69	70	71

8.2 White Rock

As previously stated, weather statistics for White Rock have only been kept since 1965. Annual mean temperatures and precipitation for White Rock during 1965–1988 are given in Table 8.3. Statistics for the entire period are also shown.

Table 8.3. White Rock annual mean temperatures and precipitation.

Year	Temperature (°F)	Precipitation (in.)	Year	Temperature (°F)	Precipitation (in.)
1965	48.5	16.76	1981	52.3	10.48
1966	48.8	10.15	1982	49.2	13.85
1967	49.1	13.52	1983	50.0	11.85
1968	47.7	14.13	1984	49.2	12.05
1969	50.2	18.99	1985	50.6	19.57
1970	49.1	9.75	1986	51.1	18.87
1971	48.6	15.79	1987	49.4	15.88
1972	49.7	15.46	1988	50.1	15.61
1973	48.8	11.65			
1974	48.5	12.13			
1975	47.5	12.30			
1976	47.9	10.96	Mean	49.3	13.53
1977	50.3	9.01	Std dev	1.1	3.22
1978	48.8	14.33	Median	49.1	13.52
1979	48.2	8.12	Highest	53.2	19.57
1980	—	—	Lowest	47.5	8.12

9 Extremes

9.1 Extreme Value Analysis

Annual extreme weather variables are analyzed in order to estimate return periods for specific values. The 50- and 100-year precipitation magnitudes, for example, are useful for estimating stream run-off and structural design. Snowfall, snow depth, maximum wind gusts, and minimum temperatures, along with precipitation, are all analyzed for annual extreme values.

The extreme value analyses for different meteorological variables are presented in the following probability plots (for example, see Fig. 9.1). A special Gaussian probability scale is used on the graphs to represent the cumulative probability. In Fig. 9.1, the ordinate represents annual precipitation; the abscissa, the cumulative probability. After the annual extreme values are ranked, they are plotted for cumulative probability versus the value. A best-fit line is then drawn through the points. The data will form a straight line if the extreme value distribution is Gaussian (normal). Departures from the best-fit line are a measure of either the lack of data (small data set) or the non-Gaussian behavior of variables. In the figures, the "return period" is the number of years, on average, that will elapse before a given annual precipitation amount will recur, based on the best-fit line. Some values, such as precipitation and snow depth, have more log-normal distributions. Relatively long return periods of specific values, such as 50 and 100 years, can be estimated from the best-fit lines. Reliability of the return-period estimates increases with the size of the data set.

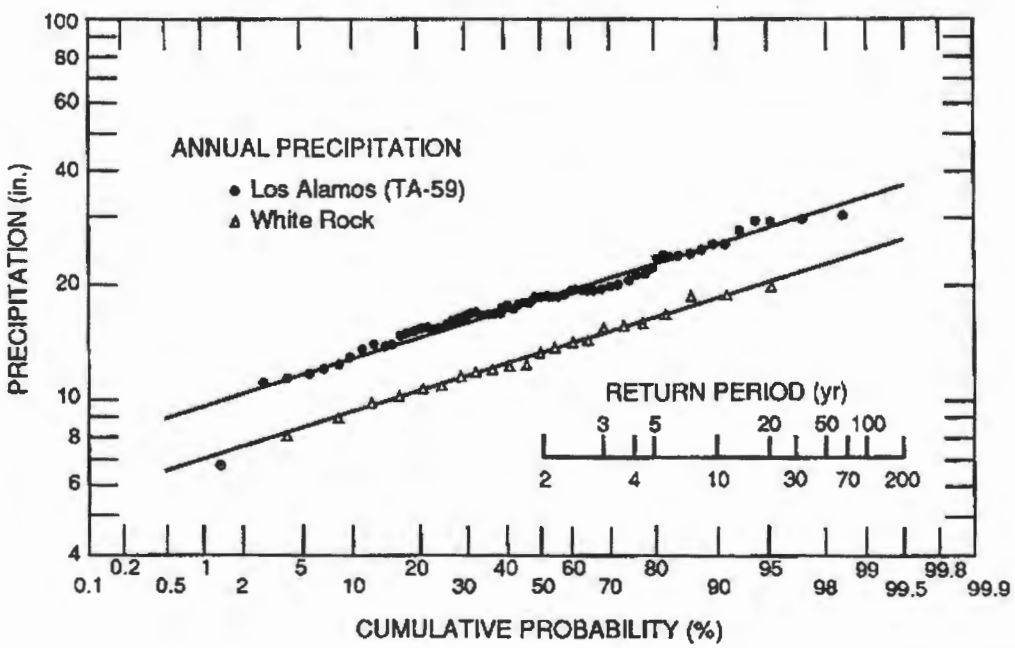

Fig. 9.1. Annual extreme precipitation analyses for Los Alamos (1911–1987) and White Rock (1965–1987).

9.1.1 Precipitation

Annual extreme precipitation values are plotted in Fig. 9.1 for Los Alamos and White Rock. The Los Alamos extreme values are significantly higher than those at White Rock. For example, the maximum annual precipitation representing a 100-year return period (T_R = 100 years) is about 10 in. (25 cm) greater at Los Alamos than at White Rock. Both the Los Alamos and White Rock data coincide very well with their respective best-fit lines. An exception is the data point for the lowest annual precipitation at Los Alamos, which is quite far from the best-fit line, representing an extremely low annual precipitation.

Daily extreme precipitation values have also been analyzed for Los Alamos and White Rock and are shown in Fig. 9.2. As with annual precipitation, daily extreme precipitation values exhibit a near-normal distribution. Again, the daily extreme precipitation amounts for Los Alamos are considerably higher than those for White Rock, and the best-fit lines represent both Los Alamos and White Rock data very well. Note that the daily precipitation values represent calendar days and not 24-hour periods overlapping 2 calendar days.

Extreme precipitation values for shorter time periods (12 hours, 1 hour, and 15 minutes) are shown in Figs. 9.3 and 9.4 for TA-59 and Area G (TA-54), respectively. Area G short-term precipitation values are used because comparable data are unavailable for White Rock. The Area G precipitation amounts are expected to closely approximate, or slightly exceed, the White Rock amounts. The extreme values of the shorter time

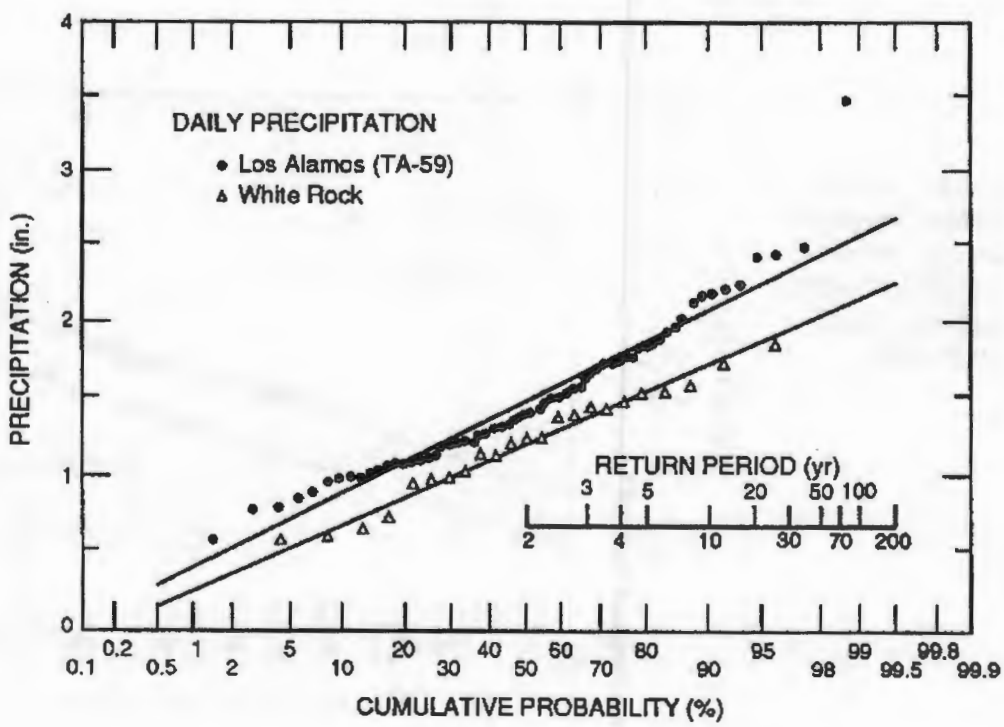

Fig. 9.2. Daily extreme precipitation values for Los Alamos (1911–1987) and White Rock (1965–1987).

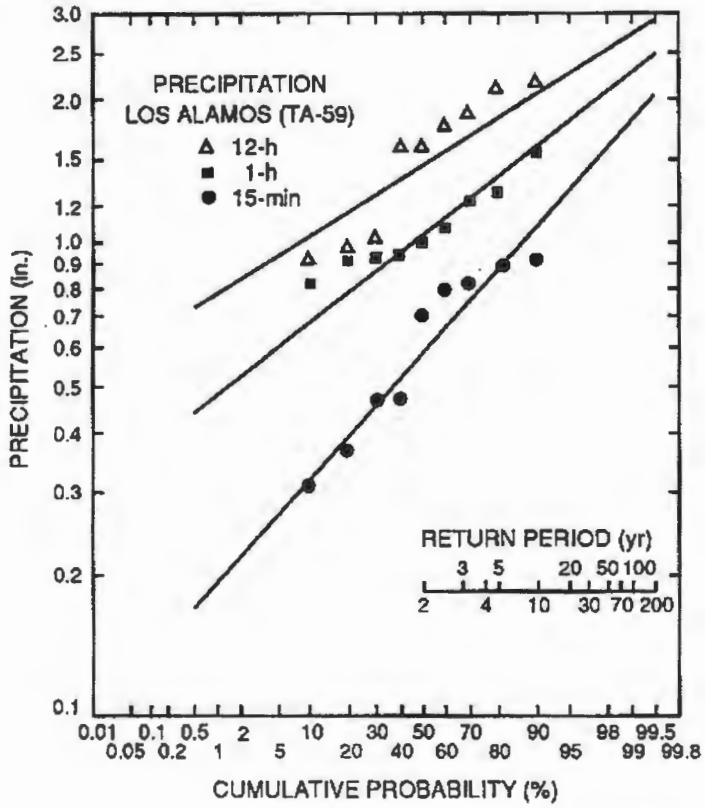

Fig. 9.3. Shorter-period extreme precipitation values for Los Alamos (TA-59) during 1980–1988.

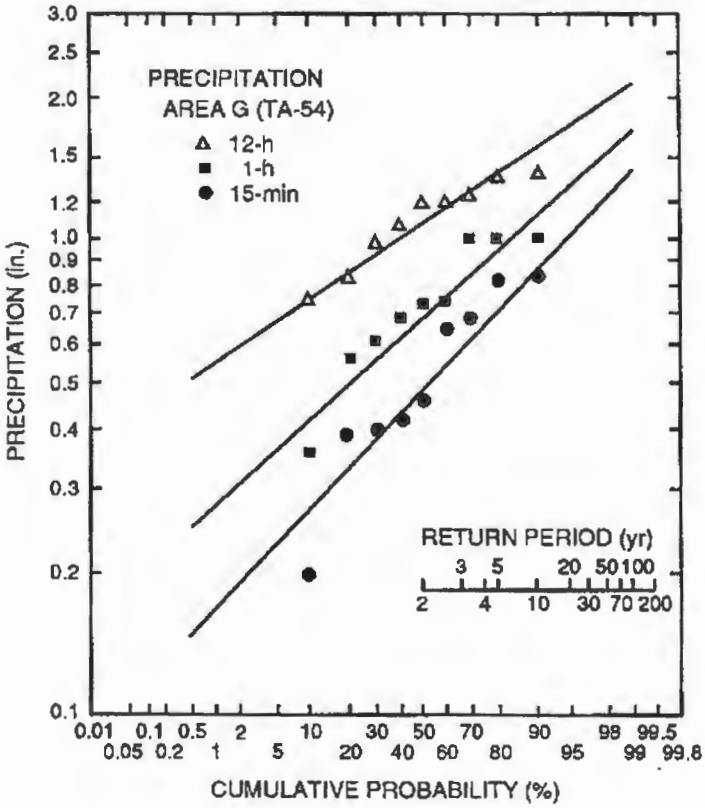

Fig. 9.4. Shorter-period extreme precipitation values for Area G (TA-54) during 1980–1988.

periods are based on tower data available since 1980 at both sites; therefore, only 9 years of extreme values are available at both sites.

Los Alamos extreme precipitation amounts for shorter periods are generally higher than those at White Rock. The shortest periods have the greatest year-to-year variations, as indicated by the increased slope of the best-fit lines for the 15-minute and 1-hour data.

Return periods from 2 to 100 years are listed in Table 9.1 for various precipitation durations at TA-59 and Area G/White Rock. The daily and annual return periods are based on a greater number of years and therefore are the most reliable. However, the shorter periods, based on only 9 years of data, appear to be very consistent. The daily precipitation values represent calendar days and not maximum 24-hour periods. Extreme values for 24-hour periods are probably slightly higher than values for calendar days because heavy-precipitation events sometimes extend over 2 calendar days. Note the heavier precipitation amounts at Los Alamos for all return periods. Also note that the difference in precipitation amounts between return periods decreases slightly with longer durations.

9.1.2 Snowfall

Los Alamos seasonal extreme snowfall values are shown in Fig. 9.5. Only limited snowfall data are available for White Rock; therefore, an analysis could only be made for

Table 9.1. Precipitation for various return periods and time periods at Los Alamos (TA-59) and Area G (TA-54)/White Rock.

	Precipitation (in.)						
T_R (yr)	15 min	30 min	1 h	3 h	12 h	Daily	Annual
TA-59							
2	0.59	0.84	1.03	1.24	1.47	1.45	18.10
5	0.88	1.15	1.38	1.60	1.84	1.90	22.90
10	1.09	1.35	1.59	1.83	2.07	2.18	25.80
25	1.37	1.61	1.86	2.10	2.35	2.54	29.00
50	1.59	1.80	2.06	2.32	2.55	2.80	31.70
100	1.82	2.00	2.25	2.52	2.74	3.06	34.00
Area G [a]							
2	0.49	0.62	0.69	0.81	1.06	1.18	13.10
5	0.73	0.88	0.96	1.08	1.36	1.55	16.40
10	0.90	1.05	1.15	1.27	1.55	1.78	18.40
25	1.12	1.27	1.38	1.50	1.78	2.08	21.00
50	1.28	1.45	1.56	1.68	1.95	2.31	22.90
100	1.46	1.62	1.75	1.86	2.11	2.52	24.40

[a] Daily and annual Area G values are White Rock values.

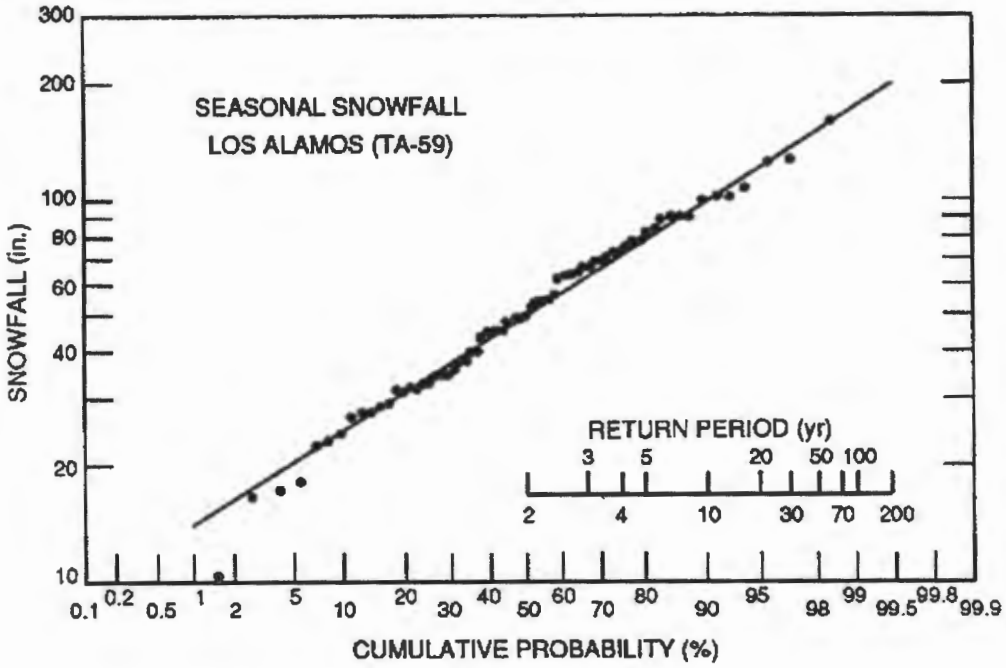

Fig. 9.5. Seasonal extreme snowfall analyses for Los Alamos (TA-59) during 1911–1988.

Los Alamos. A straight line fits the data very well. The record snowfall of 153 in. (389 cm) in the winter of 1986–1987 represents a return period of nearly 65 years.

Los Alamos extremes for monthly and daily snowfall values are plotted in Fig. 9.6. A best-fit line fits the data very well for both monthly and daily snowfall. The maximum monthly snowfall of nearly 65 in. (165 cm) in January 1987 represents a return period of nearly 140 years, according to the best-fit line.

Extreme snow-depth values by year are plotted in Fig. 9.7. Again, a best-fit line fits the data well. The record 42 in. (107 cm) of snow depth in January 1987 represents a 120-year return period. This record snow depth resulted from the 48 in. (122 cm) of snow that fell during January 15–17, 1987. Note that the snow depth is actually less than the snowfall because of compaction and settling during and after a snowfall.

9.1.3 Maximum Wind Gusts

Although Los Alamos can be considered a light-wind site, maximum, instantaneous wind gusts exceeding 50 mph (22 m/s) are common during the spring. Extreme values of annual peak wind gusts at TA-59 are shown in Fig. 9.8. Because only 9 years of data were available for this analysis, the general trend should be stressed, and precise values of return periods should be used cautiously. The 100-year return value is modest at about 77 mph (34 m/s). The maximum wind speed of 69 mph (31 m/s) at TA-59 was recorded during the afternoon of March 6, 1986. Most of the peak gusts for the 9-year period took place during March and April. In addition, the peak gusts usually were southwesterly to northwesterly and occurred during the afternoon and evening hours. The highest

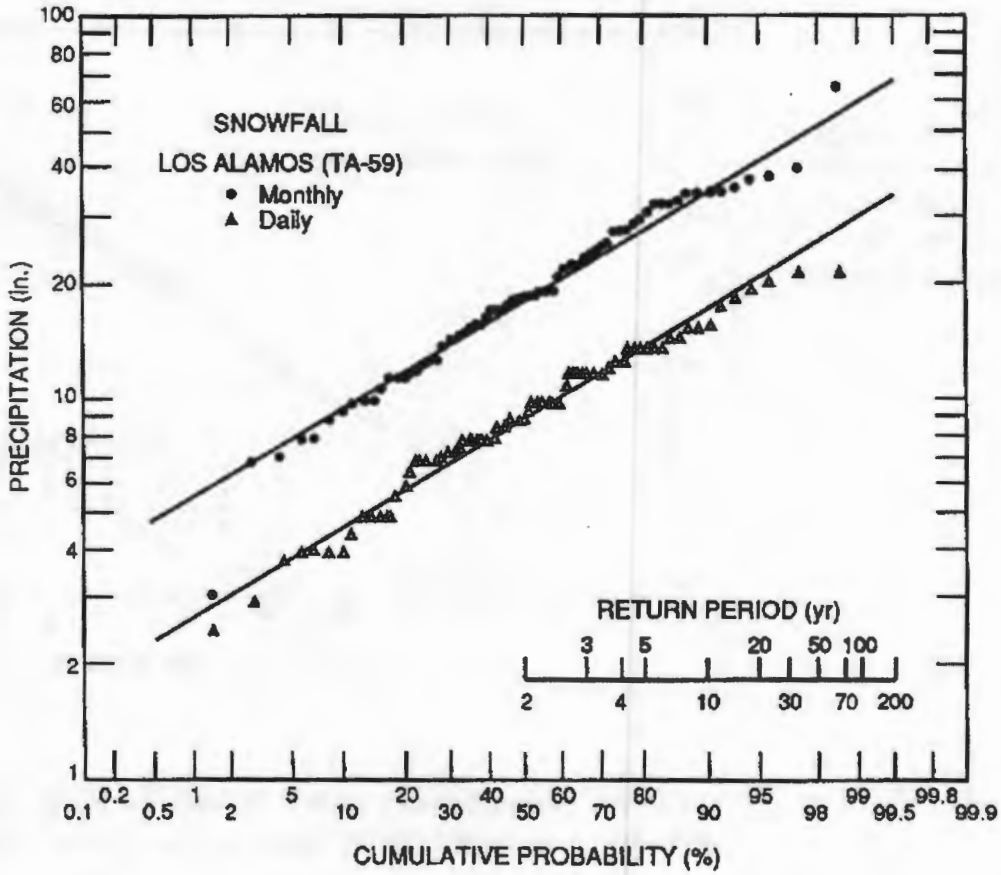

Fig. 9.6. Monthly and daily extreme snowfall values for Los Alamos (TA-59) during 1911–1988.

recorded wind gust in recent history was 77 mph (34 m/s) from the south-southwest at East Gate on November 15, 1988. Other gusts of 76 mph (34 m/s) from the southeast resulted from thunderstorms at East Gate and Area G on May 9 and 27, 1989, respectively.

The peak gusts were measured at a 23-m height at TA-59. The gusts are estimated to be 10%–15% lower at a standard measurement height of 10–12 m above the ground. Conversely, wind gusts are up to 15% higher at a height of 92 m, according to the 4 years of TA-50 wind data. A maximum wind gust of 78 mph (35 m/s) was recorded at the 92-m level at TA-50 on March 9, 1986.

Designers should realize that peak gusts have a relatively smaller force when compared with equal gusts at sea level. Because the air density is approximately three-fourths that at sea level, a peak gust of, say, 60 mph (27 m/s) at Los Alamos is equal in momentum to a 45-mph (20-m/s) gust at sea level.

9.1.4 Minimum Temperatures

Extreme temperatures are very important in the design of buildings, roads, and heating and cooling equipment. Maximum annual temperatures fall in a small range

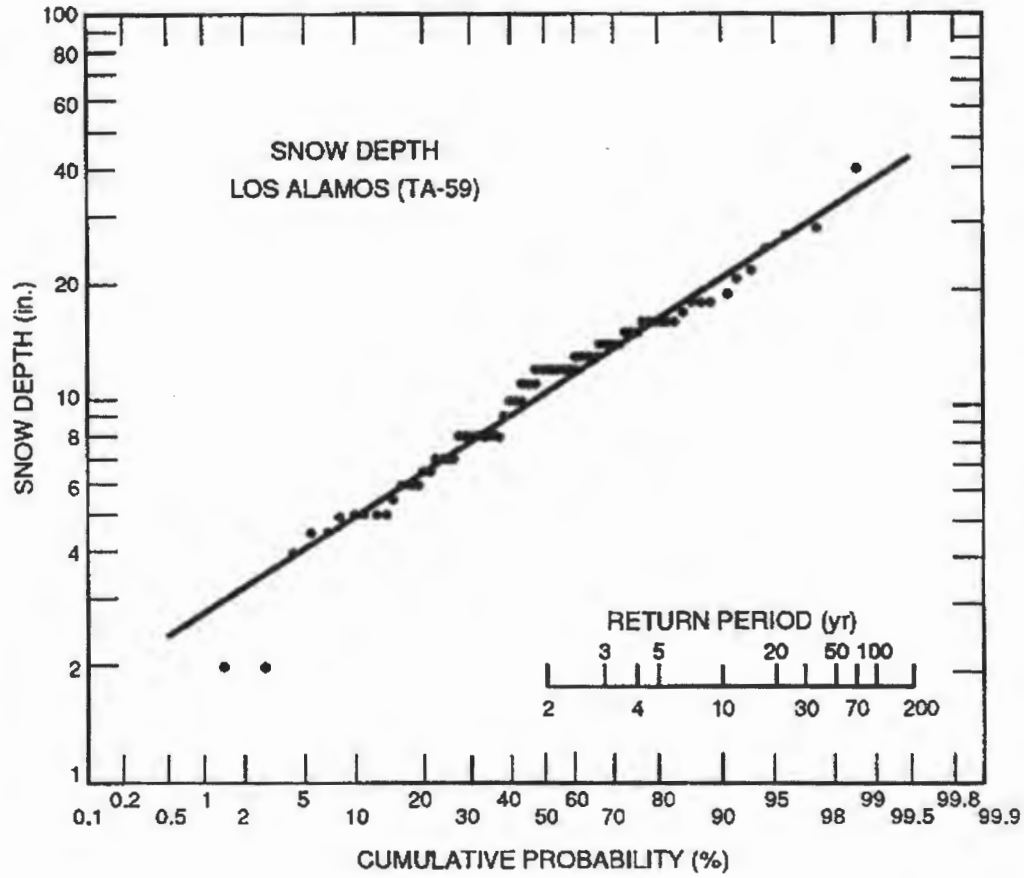

Fig. 9.7. Extreme snow-depth values for Los Alamos (TA-59) during 1911–1988.

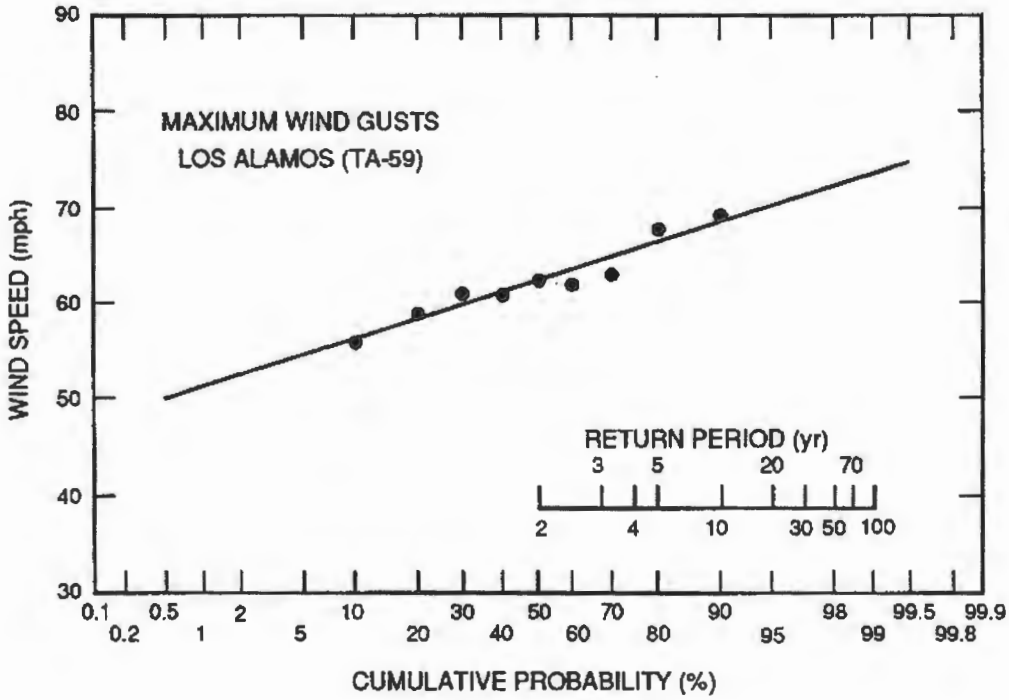

Fig. 9.8. Extreme instantaneous wind-gust values (measured at a 23-m height) for Los Alamos (TA-59) during 1981–1989.

from year to year, ranging from the upper 80s (°F) to 95°F in Los Alamos and from the mid-90s to the lower 100s (°F) at White Rock.

Minimum temperatures show considerably more variation from year to year. Extreme minimum-temperature values are plotted and analyzed for Los Alamos and White Rock in Fig. 9.9. The White Rock annual minimum temperatures are generally several degrees (Fahrenheit) colder than at Los Alamos. Most of the coldest annual temperatures occur on clear nights with light, large-scale winds, allowing cold air to drain toward lower areas. The data at both sites correlate well with the best-fit lines. Note that the coldest White Rock temperature of −29°F is quite far from the best-fit line and represents a return period of more than 200 years, based on the best-fit line. Also note that the −29°F temperature was recorded at a site other than the current fire station location and that this temperature is lower than the coldest temperature ever recorded at the fire station.

9.2 Daily Weather Extremes

Daily records at Los Alamos (TA-59) of maximum and minimum temperatures, precipitation, and snowfall, along with monthly extremes, are shown by month in Tables 9.2–9.13. Note that the precipitation and snowfall records began in late 1910, whereas the temperature records began in 1919.

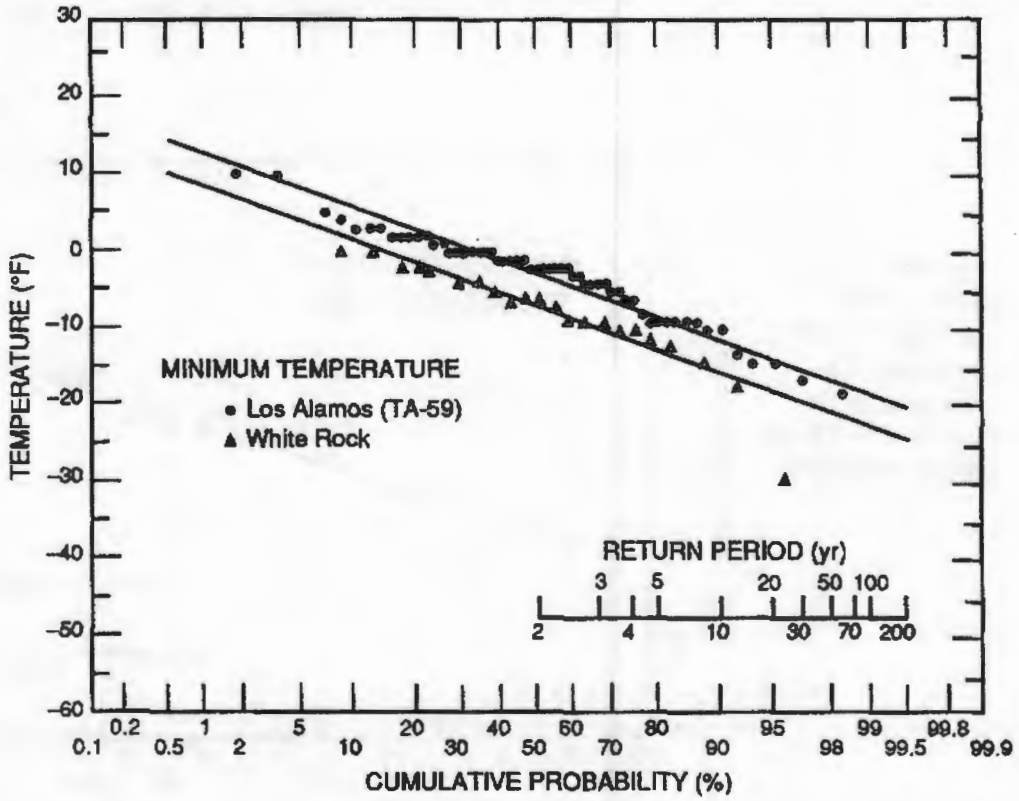

Fig. 9.9. Extreme minimum-temperature values for Los Alamos (1919–1987) and White Rock (1965–1987).

Table 9.2. Los Alamos (TA-59) weather extremes for January.

	Temperature (°F)				Maximum Precipitation	
	Maximum		Minimum		Water Equivalent	Snowfall
Day	High	Low	High	Low	(in.)	(in.)
1	52 (1981)[a]	16 (1979)	30 (1982)[a]	−5.4 (1978)	0.54 (1919)	10.0 (1982)[a]
2	55 (1964)	17 (1974)	27 (1955)	−9 (1978)	0.50 (1936)	5.0 (1936)
3	54 (1927)	13 (1919)	31 (1955)	−4 (1974)	0.75 (1971)	10.0 (1971)
4	55 (1927)	4 (1971)	38 (1955)	−9 (1971)	0.34 (1989)	3.0 (1920)
5	54 (1981)[a]	8 (1971)	31 (1981)[a]	−13 (1971)	1.53 (1913)	15.0 (1913)
6	59 (1933)	8 (1971)	32 (1927)	−16 (1971)	1.01 (1935)	4.2 (1988)
7	55 (1969)	9 (1971)	36 (1965)	−15 (1971)	0.41 (1987)	7.0 (1987)
8	53 (1969)	18 (1930)	35 (1954)	−9 (1971)	0.68 (1965)	6.5 (1965)
9	53 (1981)[a]	21 (1977)	31 (1956)	0 (1977)	0.81 (1957)	4.0 (1939)
10	59 (1953)	25 (1975)	34 (1953)	−1 (1920)	0.47 (1949)	5.1 (1949)
11	58 (1956)	20 (1975)	34 (1960)	−9 (1962)	0.40 (1911)	4.0 (1957)
12	64 (1953)	6 (1963)	33 (1953)	−11 (1963)	0.47 (1960)	4.5 (1960)
13	60 (1953)	14 (1963)	35 (1949)	−18 (1963)	0.25 (1954)	5.5 (1984)
14	58 (1928)	19 (1963)	38 (1957)	−4 (1963)	0.98 (1952)	8.5 (1984)
15	55 (1945)	25 (1932)	37 (1945)	0 (1963)	0.70 (1915)	22.0 (1987)
16	54 (1945)	18 (1987)[a]	33 (1938)	3 (1947)	0.57 (1987)	21.0 (1987)
17	54 (1976)	22 (1987)	39 (1945)	4 (1947)	0.38 (1979)	5.0 (1987)
18	55 (1976)	19 (1960)	38 (1945)	−6 (1960)	1.00 (1916)	8.0 (1988)
19	60 (1986)	18 (1960)	33 (1945)	−2 (1963)	0.95 (1916)	10.0 (1958)
20	60 (1971)	20 (1987)	33 (1950)	−3 (1963)	0.58 (1916)	4.5 (1949)
21	58 (1953)	20 (1966)	37 (1950)	−5 (1935)	0.44 (1974)	4.5 (1954)
22	56 (1970)	18 (1930)	35 (1950)	−4 (1966)	0.15 (1962)	3.0 (1956)
23	57 (1986)	22 (1955)	35 (1972)	0 (1940)	0.40 (1939)	8.0 (1945)
24	57 (1953)	26 (1988)[a]	41 (1950)	−1 (1926)	0.26 (1949)	7.0 (1945)
25	63 (1953)	20 (1929)	35 (1970)	0 (1932)	0.96 (1962)	7.5 (1962)
26	61 (1975)	26 (1950)	39 (1969)	1 (1932)	0.60 (1916)	6.0 (1979)
27	61 (1953)	24 (1948)	38 (1951)	4 (1979)	2.45 (1916)	11.5 (1989)
28	59 (1986)	8 (1948)	39 (1951)	2 (1979)	0.15 (1979)	2.0 (1979)
29	57 (1986)	13 (1948)	32 (1986)[a]	−4 (1932)	0.91 (1979)	10.0 (1979)
30	59 (1986)	10 (1949)	37 (1954)	−5 (1949)	0.69 (1975)	6.0 (1975)
31	62 (1971)	14 (1985)	34 (1965)	−3 (1985)	0.80 (1983)	12.0 (1983)
Month	51.1 (1986)	29.0 (1985)	27.0 (1956)	11.4 (1925)	6.75 (1916)	64.8 (1987)

Average temperature (1951–1980) Maximum: 39.7°F, Minimum: 18.5°F, Mean: 29.1°F

Temperatures		*Precipitation*	
Warmest January	37.6°F (1986)	Most days precipitation ≥0.01 in.	15 (1949)
Coldest January	20.9°F (1930)	Most days precipitation ≥0.10 in.	10 (1920)
Most days ≤32°F	31 (many)	Most snows ≥1 in.	11 (1949)
Fewest days ≤32°F	25 (1932)	Most snows ≥4 in.	5 (1949)
Most days ≤0°F	7 (1963)	Most snow on ground	40 in. (January 17, 1987)
		Least January precipitation	0.00 in. (1928, 1912)
		Least January snow	0.0 in. (1928)[a]

[a]Latest occurrence.

Table 9.3. Los Alamos (TA-59) weather extremes for February.

	Temperature (°F)				Maximum Precipitation	
	Maximum		Minimum		Water Equivalent	Snowfall
Day	High	Low	High	Low	(in.)	(in.)
1	60 (1963)	15 (1985)	36 (1963)	–4 (1951)	0.21 (1982)	7.2 (1919)
2	60 (1943)	10 (1951)	33 (1989)	–19 (1985)	0.76 (1913)	7.5 (1939)
3	60 (1953)	16 (1956)	33 (1953)	–3 (1929)	0.58 (1964)	5.3 (1964)
4	60 (1963)	18 (1982)	34 (1954)	–1 (1923)	0.61 (1982)	19.0 (1982)
5	62 (1953)	22 (1955)	38 (1950)	0 (1985)	0.55 (1989)	10.0 (1989)
6	61 (1963)	13 (1989)	36 (1963)	–4 (1989)	0.68 (1964)	7.0 (1964)
7	61 (1963)	20 (1974)	43 (1944)	–1 (1964)	0.46 (1986)	8.0 (1986)
8	58 (1963)	11 (1929)	35 (1951)	–14 (1933)	0.80 (1966)	6.0 (1956)
9	60 (1954)	20 (1929)	39 (1976)	3 (1929)	0.22 (1986)	6.5 (1986)
10	59 (1962)	20 (1933)	31 (1962)	–5 (1933)	0.54 (1963)	8.0 (1965)
11	64 (1962)	22 (1963)	41 (1951)	–2 (1933)	0.81 (1948)	12.3 (1948)
12	60 (1951)	12 (1948)	38 (1951)	–9 (1948)	0.47 (1964)	5.0 (1964)
13	59 (1979)	15 (1948)	34 (1970)	–5 (1948)	0.46 (1976)	6.5 (1931)
14	60 (1979)	25 (1978)	41 (1967)	1 (1966)	0.40 (1980)	4.1 (1968)
15	57 (1981)	25 (1965)	34 (1986)	3 (1964)	0.96 (1975)	10.5 (1975)
16	59 (1981)	24 (1978)	35 (1971)	1 (1966)	0.27 (1987)	4.5 (1987)
17	60 (1970)	25 (1942)	37 (1971)	5 (1942)	0.35 (1946)	6.5 (1946)
18	60 (1986)[a]	24 (1960)	34 (1955)	2 (1978)	0.30 (1987)	6.0 (1911)
19	65 (1981)	28 (1987)	37 (1986)	3 (1942)	0.97 (1987)	20.0 (1987)
20	63 (1972)	17 (1955)	32 (1986)[a]	3 (1955)	0.14 (1980)	3.5 (1940)
21	63 (1982)	19 (1955)	34 (1972)	5 (1955)	0.65 (1975)	10.0 (1975)
22	60 (1982)	22 (1955)	32 (1972)	3 (1971)	0.40 (1963)	4.0 (1963)
23	62 (1946)	24 (1955)	35 (1972)	–4 (1975)	0.39 (1985)[a]	5.5 (1985)[a]
24	68 (1986)	24 (1960)	39 (1956)	3 (1960)	0.61 (1912)	4.0 (1941)
25	69 (1986)	16 (1960)	39 (1946)	0 (1960)	0.43 (1948)	3.4 (1948)
26	68 (1976)	29 (1955)	38 (1988)	–4 (1935)	0.63 (1987)	9.0 (1987)
27	62 (1980)	28 (1962)	36 (1988)	6 (1939)	0.50 (1961)	7.0 (1930)
28	64 (1980)	25 (1971)	33 (1985)[a]	4 (1962)	0.36 (1968)	6.0 (1913)
29	62 (1976)	41 (1960)	37 (1940)	19 (1964)	0.08 (1916)	1.0 (1916)
Month	53.2 (1954)	34.6 (1964)	29.8 (1954)	11.0 (1939)	2.27 (1987)	48.5 (1987)

Average temperature (1951–1980) Maximum: 43.0°F, Minimum: 21.5°F, Mean: 32.3°F

Temperatures		*Precipitation*	
Warmest February	41.5°F (1954)	Most days precipitation ≥0.01 in.	12 (1960)
Coldest February	23.0°F (1939)	Most days precipitation ≥0.10 in.	7 (1920)
Most days ≤32°F	29 (many)	Most snows ≥1 in.	8 (1960)
Fewest days ≤32°F	17 (1954)	Most snows ≥4 in.	5 (1987)
Most days ≤0°F	3 (1933)	Most snow on ground	24 in. (February 1, 1979)
		Least February precipitation	0.00 in. (1943, 1954)
		Least February snow	0.0 in. (1976)[a]

[a]Latest occurrence.

Table 9.4. Los Alamos (TA-59) weather extremes for March.

	Temperature (°F)				Maximum Precipitation	
	Maximum		Minimum		Water Equivalent	Snowfall
Day	High	Low	High	Low	(in.)	(in.)
1	64 (1986)	23 (1971)	43 (1946)	1 (1929)	0.48 (1978)	5.0 (1960)
2	64 (1986)[a]	20 (1965)	36 (1982)[a]	5 (1929)	0.60 (1981)	8.0 (1915)
3	61 (1972)[a]	17 (1965)	39 (1955)	2 (1971)	0.44 (1978)	5.0 (1978)
4	62 (1972)	25 (1969)	39 (1972)[a]	2 (1965)	0.37 (1958)	6.0 (1958)
5	65 (1986)	19 (1948)	38 (1956)	1 (1939)	0.92 (1940)	14.0 (1940)
6	67 (1972)	32 (1935)	38 (1972)	3 (1939)	0.87 (1931)	13.0 (1931)
7	65 (1972)	26 (1947)	44 (1934)	3 (1931)	0.29 (1941)	4.0 (1913)
8	67 (1989)	31 (1969)	38 (1925)	10 (1969)	0.70 (1938)	10.0 (1938)
9	72 (1989)	30 (1973)	42 (1946)	9 (1942)[a]	1.64 (1973)	14.0 (1973)
10	71 (1989)	20 (1969)	40 (1989)[a]	9 (1958)	0.92 (1974)	8.5 (1969)
11	73 (1989)	19 (1948)	43 (1989)	−3 (1948)	1.00 (1981)	15.0 (1981)
12	70 (1989)	20 (1958)	44 (1972)	7 (1932)	1.33 (1985)	11.0 (1985)
13	66 (1972)	22 (1962)	39 (1989)	6 (1962)	0.43 (1982)	2.0 (1962)
14	64 (1935)	28 (1954)	38 (1972)	8 (1962)	0.35 (1941)	5.5 (1941)
15	64 (1961)	33 (1985)	38 (1966)	10 (1969)	0.55 (1942)	9.0 (1942)
16	66 (1926)	32 (1924)	41 (1984)	14 (1959)	0.64 (1924)	13.0 (1924)
17	67 (1967)	30 (1988)	44 (1972)	11 (1943)	0.30 (1988)	7.5 (1988)
18	67 (1941)	31 (1924)	41 (1950)	9 (1988)	0.54 (1983)	5.3 (1985)
19	67 (1941)	32 (1951)	42 (1974)[a]	6 (1928)	1.00 (1951)	10.0 (1961)
20	64 (1988)	29 (1970)	41 (1975)[a]	8 (1965)	0.63 (1989)[a]	6.5 (1989)
21	65 (1988)[a]	32 (1968)	40 (1943)	9 (1944)	0.60 (1919)	8.5 (1919)
22	65 (1945)	27 (1952)	42 (1951)	8 (1952)	1.03 (1944)	9.0 (1919)
23	70 (1986)	23 (1952)	46 (1950)	5 (1952)	0.48 (1954)	8.0 (1912)
24	66 (1986)	31 (1973)[a]	44 (1971)	12 (1936)[a]	0.61 (1941)	4.0 (1919)
25	67 (1986)[a]	36 (1936)	48 (1950)	12 (1911)	0.66 (1931)	11.0 (1931)
26	71 (1971)	29 (1926)	48 (1956)[a]	7 (1955)	0.60 (1984)	10.0 (1984)
27	71 (1986)	26 (1975)	45 (1971)	7 (1931)	0.68 (1970)	5.0 (1984)
28	70 (1986)[a]	31 (1987)	53 (1933)	12 (1975)	0.40 (1925)	5.5 (1984)
29	70 (1986)[a]	27 (1987)	42 (1974)[a]	6 (1944)	1.15 (1973)	12.0 (1973)
30	71 (1946)	26 (1926)	43 (1950)	4 (1926)	2.25 (1916)	18.0 (1916)
31	69 (1986)[a]	34 (1988)	42 (1956)	10 (1985)	0.49 (1988)	8.0 (1988)[a]
Month	58.5 (1972)	42.0 (1952)	33.2 (1972)	20.0 (1942)	4.11 (1973)	36.0 (1973)

Average temperature (1951–1980) Maximum: 48.7°F, Minimum: 26.5°F, Mean: 37.6°F

Temperatures		*Precipitation*	
Warmest March	45.8°F (1972)	Most days precipitation ≥0.01 in.	17 (1958)
Coldest March	31.5°F (1958)	Most days precipitation ≥0.10 in.	12 (1915)
Most days ≤32°F	31 (1973)	Most snows ≥1 in.	10 (1958)
Fewest days ≤32°F	17 (1954)	Most snows ≥4 in.	5 (1984)
Most days ≤0°F	1 (1948)	Most snow on ground	28 in. (March 4–5, 1915)
		Least March precipitation	0.00 in. (1934)
		Least March snow	0.0 in. (1977)[a]

[a]Latest occurrence.

Table 9.5. Los Alamos (TA-59) weather extremes for April.

	Temperature (°F)				Maximum Precipitation	
	Maximum		Minimum		Water Equivalent	Snowfall
Day	High	Low	High	Low	(in.)	(in.)
1	66 (1940)	33 (1988)	42 (1969)[a]	14 (1980)	0.46 (1965)	3.0 (1949)
2	69 (1966)	24 (1949)	44 (1928)	15 (1938)	0.35 (1986)[a]	4.0 (1980)
3	71 (1946)	29 (1977)	45 (1947)	18 (1972)	1.02 (1916)	4.0 (1916)
4	70 (1954)	26 (1983)	50 (1935)	10 (1983)	0.65 (1983)	10.0 (1983)
5	72 (1972)	35 (1983)	47 (1954)	8 (1983)	0.83 (1928)	12.0 (1928)
6	72 (1959)	32 (1983)	48 (1972)	12 (1936)	0.41 (1942)	3.0 (1942)
7	75 (1989)	34 (1964)	48 (1989)	15 (1973)[a]	0.55 (1951)	2.5 (1951)
8	74 (1989)	27 (1928)	47 (1989)[a]	11 (1973)	0.60 (1961)	6.0 (1961)
9	72 (1977)	36 (1961)	45 (1946)	5 (1928)	0.57 (1958)	8.5 (1958)
10	74 (1972)	38 (1975)	45 (1972)[a]	12 (1920)	0.80 (1944)	11.0 (1944)
11	73 (1971)[a]	32 (1975)	54 (1972)	16 (1951)	1.45 (1969)	10.0 (1975)
12	78 (1937)	31 (1975)	47 (1946)	15 (1940)	2.00 (1975)	20.0 (1975)
13	71 (1988)	34 (1927)	43 (1946)	18 (1980)	0.30 (1958)	3.0 (1958)
14	72 (1962)[a]	40 (1972)	46 (1954)[a]	7 (1933)	0.60 (1916)	4.0 (1916)
15	77 (1937)[a]	44 (1973)	49 (1937)	17 (1961)	0.81 (1945)	10.0 (1945)
16	74 (1937)	33 (1976)	51 (1925)	21 (1945)	1.22 (1988)	0.9 (1969)
17	77 (1937)	33 (1976)	50 (1925)	16 (1976)	1.30 (1915)	3.0 (1969)
18	75 (1919)	38 (1920)	49 (1984)[a]	21 (1920)	0.73 (1935)	2.0 (1935)
19	75 (1954)	35 (1973)	51 (1954)	14 (1920)	0.97 (1949)	2.5 (1986)
20	78 (1989)	35 (1973)	53 (1954)	9 (1920)	0.57 (1977)	0.2 (1970)
21	79 (1989)	43 (1984)	52 (1953)	20 (1941)[a]	0.50 (1952)	4.0 (1941)
22	77 (1965)	33 (1982)	53 (1989)	19 (1928)	0.85 (1942)	1.0 (1982)
23	80 (1950)	40 (1968)	48 (1965)[a]	19 (1937)	1.20 (1919)	3.0 (1941)
24	72 (1989)[a]	43 (1980)	50 (1954)	26 (1968)	0.54 (1980)	4.0 (1980)
25	74 (1974)	42 (1924)	51 (1954)	22 (1935)	0.60 (1945)	5.0 (1945)
26	73 (1927)	34 (1984)	53 (1949)	21 (1964)	1.12 (1922)	6.5 (1920)
27	72 (1946)	38 (1965)	50 (1956)[a]	18 (1920)	0.25 (1962)	1.5 (1932)
28	71 (1953)	46 (1985)	47 (1954)	22 (1924)	1.45 (1985)	
29	75 (1982)	44 (1970)[a]	48 (1936)	25 (1940)	0.46 (1915)	
30	77 (1928)	41 (1967)	49 (1986)	24 (1975)[a]	0.39 (1914)	
Month	65.7 (1946)	51.1 (1973)	42.9 (1954)	28.2 (1973)	4.64 (1915)	33.6 (1958)

Average temperature (1951–1980) Maximum: 57.6°F, Minimum: 33.7°F, Mean: 45.7°F

Temperatures		*Precipitation*	
Warmest April	54.3°F (1954)	Most days precipitation ≥0.01 in.	14 (1977)
Coldest April	39.7°F (1973)	Most days precipitation ≥0.10 in.	12 (1915)
Most days ≤32°F	22 (1920)	Most snows ≥1 in.	6 (1958)
Fewest days ≤32°F	2 (1954)	Most snows ≥4 in.	3 (1980)
Most days ≤0°F	—	Most snow on ground	27 in. (April 12, 1975)
		Least April precipitation	0.00 in. (1967)
		Least April snow	0.0 in. (1979)

[a]Latest occurrence.

Table 9.6. Los Alamos (TA-59) weather extremes for May.

	Temperature (°F)				Maximum Precipitation	
	Maximum		Minimum		Water Equivalent	Snowfall
Day	High	Low	High	Low	(in.)	(in.)
1	79 (1936)	41 (1970)	58 (1945)	24 (1976)	0.66 (1941)	0.2 (1960)
2	79 (1947)	36 (1978)	51 (1965)	25 (1967)	1.24 (1978)	12.0 (1978)
3	79 (1947)	41 (1935)	58 (1945)	28 (1978)[a]	0.85 (1935)	8.0 (1935)
4	80 (1947)	33 (1935)	55 (1952)	25 (1942)[a]	0.53 (1968)[a]	
5	77 (1922)	27 (1978)	57 (1947)	28 (1946)	0.80 (1982)	2.0 (1978)
6	78 (1989)[a]	33 (1978)	54 (1952)	24 (1935)	0.57 (1976)	1.5 (1938)
7	81 (1989)[a]	43 (1969)	53 (1956)	24 (1978)	0.60 (1917)	8.0 (1917)
8	83 (1989)[a]	43 (1976)	56 (1989)	25 (1936)	0.84 (1940)	9.0 (1917)
9	81 (1934)	47 (1930)	60 (1956)	24 (1938)	0.75 (1989)	
10	83 (1934)	46 (1946)	59 (1934)	30 (1953)	1.10 (1947)	
11	82 (1984)	39 (1946)	57 (1962)	23 (1946)	0.58 (1932)	
12	83 (1984)	41 (1926)	54 (1956)	27 (1980)	0.90 (1949)	
13	87 (1941)	41 (1953)	57 (1960)	25 (1942)[a]	0.95 (1920)	0.6 (1953)
14	80 (1988)[a]	45 (1961)	66 (1936)	27 (1985)	0.65 (1923)	
15	82 (1988)[a]	48 (1980)	58 (1936)	27 (1933)	0.66 (1914)	
16	83 (1941)	51 (1953)	55 (1941)	29 (1957)	0.81 (1988)	
17	87 (1937)	51 (1953)[a]	55 (1937)	30 (1983)	1.35 (1952)	4.0 (1952)
18	81 (1937)	38 (1952)	58 (1970)	28 (1983)	1.05 (1952)	
19	81 (1946)	46 (1955)	57 (1956)	32 (1971)[a]	0.55 (1919)	
20	81 (1984)[a]	40 (1946)	55 (1925)	27 (1960)	0.71 (1979)	3.0 (1915)
21	85 (1936)	44 (1946)	53 (1989)[a]	31 (1983)	1.80 (1929)	
22	86 (1984)	53 (1975)	56 (1984)	33 (1975)[a]	0.53 (1926)	
23	84 (1989)[a]	54 (1928)	57 (1989)[a]	29 (1930)	0.59 (1987)	
24	86 (1984)	54 (1987)	61 (1989)	32 (1919)	0.39 (1956)	
25	82 (1984)	55 (1965)	59 (1984)	30 (1980)	0.62 (1941)	
26	82 (1984)[a]	52 (1979)	53 (1953)[a]	33 (1965)	0.59 (1926)	
27	88 (1951)	59 (1948)	60 (1951)	34 (1965)	0.46 (1958)	
28	88 (1951)	52 (1962)	59 (1951)[a]	36 (1971)	1.18 (1934)	
29	89 (1935)	52 (1979)[a]	62 (1951)	32 (1929)	0.42 (1937)	
30	86 (1977)	48 (1979)	62 (1951)	35 (1975)	0.75 (1930)	
31	85 (1935)	45 (1964)	60 (1951)	30 (1934)	0.71 (1914)	
Month	74.9 (1984)	61.1 (1957)	50.2 (1956)	37.8 (1980)	4.47 (1929)	17.0 (1917)

Average temperature (1951–1980) Maximum: 67.0°F, Minimum: 42.8°F, Mean: 54.9°F

Temperatures		*Precipitation*	
Warmest May	60.5°F (1956)	Most days precipitation ≥0.01 in.	15 (1979)
Coldest May	50.1°F (1957)	Most days precipitation ≥0.10 in.	11 (1926)
Most days ≤32°F	8 (1953)	Most snows ≥1 in.	3 (1978)
Fewest days ≤32°F	3 (1933)	Most snows ≥4 in.	2 (1917)
Most days ≤0°F	0	Most snow on ground	12 in. (May 2, 1978)
		Least May precipitation	0.00 in. (1945, 1940)
		Least May snow	0.0 in. (many)

[a]Latest occurrence.

Table 9.7. Los Alamos (TA-59) weather extremes for June.

	Temperature (°F)				Maximum Precipitation	
	Maximum		Minimum		Water Equivalent	Snowfall
Day	High	Low	High	Low	(in.)	(in.)
1	85 (1935)	57 (1979)	57 (1953)	29 (1919)	0.64 (1979)	No snow
2	84 (1977)	52 (1963)	54 (1953)	30 (1919)	0.95 (1963)	recorded in
3	87 (1938)	61 (1952)	58 (1924)	28 (1919)	1.58 (1986)	June
4	85 (1938)	59 (1970)	60 (1956)	37 (1934)[a]	0.68 (1938)	
5	83 (1977)	60 (1984)[a]	58 (1956)	40 (1973)[a]	0.85 (1970)	
6	82 (1980)[a]	58 (1978)	66 (1933)	31 (1942)	0.70 (1912)	
7	87 (1985)	62 (1972)	60 (1964)	36 (1954)	2.16 (1987)	
8	87 (1985)[a]	59 (1974)	65 (1935)	38 (1974)	0.84 (1972)	
9	87 (1952)[a]	58 (1979)	62 (1952)	32 (1979)	0.44 (1960)	
10	88 (1947)	51 (1931)	65 (1946)	36 (1968)	2.51 (1913)	
11	88 (1946)	55 (1965)	63 (1950)	32 (1975)	1.36 (1913)	
12	89 (1959)[a]	61 (1927)	62 (1924)	37 (1976)	1.50 (1927)	
13	91 (1939)	55 (1927)	64 (1950)	35 (1928)	0.57 (1933)	
14	90 (1939)	63 (1989)	65 (1945)	38 (1983)[a]	0.38 (1911)	
15	89 (1977)[a]	61 (1969)[a]	69 (1952)	33 (1976)	0.80 (1933)	
16	90 (1977)	60 (1961)	57 (1985)	39 (1927)	0.78 (1969)	
17	90 (1980)[a]	67 (1961)	68 (1950)	38 (1957)	1.17 (1969)	
18	90 (1983)[a]	70 (1969)[a]	68 (1954)	42 (1939)	0.87 (1953)	
19	92 (1989)	65 (1947)	66 (1950)	39 (1939)	0.74 (1965)	
20	90 (1954)[a]	66 (1947)	67 (1951)	43 (1920)	0.39 (1957)	
21	90 (1937)	61 (1933)	64 (1974)	45 (1982)[a]	0.40 (1911)	
22	95 (1981)	63 (1933)	59 (1919)	36 (1947)	0.67 (1925)	
23	90 (1980)[a]	62 (1948)	66 (1943)	46 (1948)[a]	0.78 (1932)	
24	90 (1980)	57 (1986)	65 (1978)	41 (1976)	1.09 (1912)	
25	94 (1980)	61 (1986)	68 (1978)	40 (1969)	0.61 (1986)	
26	93 (1980)	68 (1969)	65 (1919)	43 (1958)	1.10 (1937)	
27	90 (1980)[a]	57 (1920)	64 (1919)	45 (1985)	1.26 (1920)	
28	91 (1980)	65 (1988)	67 (1968)[a]	46 (1985)[a]	0.59 (1943)	
29	94 (1980)	62 (1978)	64 (1919)	50 (1978)	1.08 (1944)	
30	92 (1980)	64 (1924)	66 (1960)	47 (1935)	0.98 (1966)	
Month	84.5 (1980)	71.2 (1949)	58.3 (1956)	45.2 (1941)	5.67 (1986)	

Average temperature (1951–1980) Maximum: 77.8°F, Minimum: 52.4°F, Mean: 65.1°F

Temperature		*Precipitation*	
Warmest June	69.4°F (1980)	Most days precipitation ≥0.01 in.	8 (1979)
Coldest June	60.4°F (1965)	Most days precipitation ≥0.10 in.	6 (1979)
Most days ≤32°F	3 (1919)	Most snows ≥1 in.	—
Fewest days ≤32°F	0 (many)	Most snows ≥4 in.	—
Most days ≥90°F	9 (1980)	Most snow on ground	—
		Least June precipitation	0.00 in. (1980, 1951, 1929, 1916)
		Least June snow	—

[a]Latest occurrence.

Table 9.8. Los Alamos (TA-59) weather extremes for July.

	Temperature (°F)				Maximum Precipitation	
	Maximum		Minimum		Water Equivalent	Snowfall
Day	High	Low	High	Low	(in.)	(in.)
1	90 (1989)[a]	62 (1929)	71 (1946)	45 (1942)	0.69 (1984)	No snow
2	93 (1989)	67 (1932)	68 (1953)	43 (1942)	0.55 (1919)	recorded in
3	91 (1989)[a]	62 (1919)	68 (1960)	44 (1942)	0.80 (1919)	July
4	93 (1957)	69 (1940)	65 (1957)	45 (1979)	1.13 (1953)	
5	93 (1980)	59 (1968)	66 (1953)	45 (1940)	1.32 (1926)	
6	92 (1985)	57 (1924)	64 (1953)	45 (1931)	0.83 (1960)	
7	92 (1985)	65 (1926)	65 (1951)[a]	37 (1924)	1.00 (1911)	
8	90 (1989)[a]	68 (1933)[a]	66 (1951)	40 (1926)	1.35 (1967)	
9	93 (1935)	64 (1986)	68 (1951)	47 (1944)[a]	1.76 (1963)	
10	92 (1935)	65 (1929)	68 (1951)	47 (1944)	1.75 (1916)	
11	95 (1935)	62 (1926)	66 (1951)	48 (1944)[a]	0.71 (1926)	
12	92 (1958)	64 (1964)	63 (1970)[a]	44 (1926)	1.19 (1941)	
13	91 (1971)[a]	68 (1949)	63 (1988)	43 (1944)	0.77 (1957)	
14	90 (1948)[a]	58 (1924)	65 (1948)[a]	45 (1976)	1.98 (1930)	
15	94 (1925)	65 (1952)[a]	63 (1971)	45 (1944)[a]	1.20 (1952)	
16	94 (1937)	68 (1986)[a]	65 (1963)	48 (1935)	1.25 (1919)	
17	92 (1980)	67 (1967)[a]	64 (1974)	48 (1986)[a]	1.46 (1969)	
18	91 (1989)[a]	68 (1953)	62 (1966)[a]	48 (1940)[a]	0.91 (1972)	
19	92 (1925)	71 (1972)	65 (1923)	48 (1920)	1.09 (1941)	
20	90 (1984)[a]	69 (1971)	64 (1963)	48 (1935)	0.95 (1971)	
21	90 (1982)	69 (1957)	64 (1945)	49 (1944)	1.70 (1915)	
22	92 (1937)	58 (1918)	67 (1945)	45 (1941)	1.05 (1930)	
23	92 (1937)	60 (1918)	69 (1931)	47 (1941)	1.56 (1983)	
24	93 (1936)	63 (1918)	62 (1963)	47 (1971)	1.57 (1969)	
25	91 (1936)	64 (1989)	62 (1966)	43 (1928)	1.53 (1934)	
26	90 (1980)	65 (1957)	64 (1966)	48 (1935)[a]	1.87 (1915)	
27	92 (1946)	73 (1925)	64 (1954)	49 (1942)	1.17 (1955)	
28	94 (1946)	67 (1955)[a]	64 (1945)	47 (1941)	0.48 (1966)	
29	94 (1946)	66 (1985)	65 (1960)	48 (1962)	1.15 (1982)	
30	90 (1986)	66 (1971)	65 (1969)	47 (1974)	1.05 (1968)	
31	90 (1972)	65 (1968)	61 (1972)	48 (1976)	2.47 (1968)	
Month	87.3 (1980)	75.9 (1919)	60.7 (1951)	50.5 (1926)	7.98 (1919)	

Average temperature (1951–1980) Maximum: 80.4°F, Minimum: 56.1°F, Mean: 68.3°F

Temperatures		*Precipitation*	
Warmest July	71.4°F (1980)	Most days precipitation ≥0.01 in.	22 (1964)
Coldest July	63.3°F (1926)	Most days precipitation ≥0.10 in.	14 (1954)
Most days ≤32°F	—	Most snows ≥1 in.	—
Fewest days ≤32°F	—	Most snows ≥4 in.	—
Most days ≥90°F	11 (1980)	Most snow on ground	—
		Least July precipitation	0.13 in. (1980)
		Least July snow	—

[a]Latest occurrence.

Table 9.9. Los Alamos (TA-59) weather extremes for August.

	Temperature (°F)								Maximum Precipitation	
	Maximum				Minimum				Water Equivalent	Snowfall
Day	High		Low		High		Low		(in.)	(in.)
1	91	(1980)	58	(1965)	64	(1944)	46	(1934)	2.26 (1951)	No snow
2	89	(1938)[a]	66	(1985)[a]	60	(1944)[a]	47	(1976)[a]	1.29 (1966)	recorded in
3	90	(1977)	52	(1974)	72	(1945)	45	(1925)	0.90 (1928)	August
4	90	(1980)	67	(1929)	62	(1922)	44	(1976)	1.00 (1933)	
5	88	(1980)	67	(1933)[a]	62	(1944)[a]	46	(1978)	0.60 (1942)	
6	91	(1977)	67	(1946)	64	(1977)	46	(1976)[a]	0.68 (1948)	
7	88	(1979)	59	(1929)	64	(1956)	45	(1930)	1.21 (1931)	
8	88	(1961)[a]	60	(1929)	65	(1944)	45	(1971)	0.78 (1931)	
9	89	(1937)	61	(1929)	62	(1956)[a]	46	(1939)	1.13 (1959)	
10	92	(1937)	65	(1967)	63	(1956)[a]	43	(1927)	2.05 (1925)	
11	89	(1937)	58	(1967)	64	(1922)	47	(1926)	1.47 (1929)	
12	86	(1978)	61	(1977)	65	(1920)	44	(1927)	1.28 (1924)	
13	89	(1944)	65	(1920)	64	(1951)	45	(1940)	0.83 (1963)	
14	89	(1944)[a]	61	(1979)	62	(1973)[a]	43	(1920)	1.43 (1946)	
15	90	(1936)	62	(1918)	65	(1944)	42	(1947)	1.29 (1595)	
16	88	(1932)	68	(1979)[a]	65	(1946)	40	(1947)	0.79 (1970)	
17	88	(1986)	69	(1979)	70	(1946)	44	(1942)	1.23 (1974)	
18	89	(1986)	65	(1978)	66	(1936)	46	(1979)	1.72 (1965)	
19	90	(1986)	66	(1979)[a]	63	(1936)	46	(1979)	1.35 (1927)	
20	90	(1986)	65	(1923)	64	(1954)	46	(1979)[a]	1.92 (1952)	
21	88	(1937)	68	(1975)[a]	60	(1969)	45	(1940)[a]	0.93 (1912)	
22	89	(1938)	64	(1958)	61	(1960)[a]	45	(1989)	1.76 (1955)	
23	88	(1937)[a]	64	(1987)	70	(1937)	41	(1923)	2.23 (1957)	
24	91	(1922)	60	(1946)	72	(1936)	42	(1920)	1.54 (1982)	
25	89	(1944)[a]	64	(1987)	72	(1936)	46	(1976)[a]	1.30 (1952)	
26	88	(1922)	61	(1972)	70	(1936)	44	(1940)	1.00 (1987)	
27	88	(1927)	58	(1988)	67	(1945)	42	(1940)	0.85 (1952)	
28	86	(1948)	60	(1988)	67	(1945)	44	(1920)	1.60 (1952)	
29	89	(1948)	64	(1987)	66	(1945)	44	(1987)	1.53 (1915)	
30	88	(1948)	65	(1973)[a]	66	(1945)	43	(1978)[a]	1.66 (1957)	
31	87	(1948)	61	(1967)	62	(1945)[a]	42	(1932)	1.88 (1967)	
Month	83.4 (1944)		69.5 (1929)		59.1 (1936)		49.4 (1976)		11.18 (1952)	

Average temperature (1951–1980) Maximum: 77.4°F, Minimum: 54.3°F, Mean: 65.9°F

Temperatures		*Precipitation*	
Warmest August	70.3°F (1936)	Most days precipitation ≥0.01 in.	23 (1957)
Coldest August	60.9°F (1929)	Most days precipitation ≥0.10 in.	14 (1959)
Most days ≤32°F	—	Most snows ≥1 in.	—
Fewest days ≤32°F	—	Most snows ≥4 in.	—
Most days ≥90°F	2 (1980, 1977)	Most snow on ground	—
		Least August precipitation	0.51 in. (1972)
		Least August snow	—

[a]Latest occurrence.

Table 9.10. Los Alamos (TA-59) weather extremes for September.

	Temperature (°F)				Maximum Precipitation	
	Maximum		Minimum		Water Equivalent	Snowfall
Day	High	Low	High	Low	(in.)	(in.)
1	87 (1930)	64 (1967)	68 (1946)	41 (1943)	0.83 (1942)	
2	84 (1983)[a]	66 (1977)[a]	61 (1961)	45 (1932)	0.79 (1969)	
3	90 (1948)	65 (1938)	61 (1951)[a]	36 (1961)	0.50 (1937)	
4	89 (1948)	57 (1975)	62 (1951)	33 (1961)	1.85 (1916)	
5	87 (1948)	58 (1975)	62 (1959)	38 (1961)	0.60 (1972)	
6	88 (1946)	59 (1929)	57 (1959)	42 (1930)[a]	0.73 (1987)	
7	86 (1948)[a]	63 (1927)	59 (1959)	42 (1942)	0.47 (1919)	
8	86 (1977)	62 (1969)[a]	58 (1964)	44 (1942)[a]	0.93 (1975)	
9	87 (1984)	57 (1976)	56 (1944)	32 (1941)	0.87 (1972)	
10	86 (1979)	58 (1976)	58 (1984)	38 (1935)	1.86 (1971)	
11	94 (1934)	55 (1929)	59 (1974)	35 (1986)[a]	1.10 (1975)[a]	
12	86 (1934)	53 (1975)	57 (1958)	40 (1975)	0.93 (1988)	
13	86 (1935)	53 (1975)	61 (1923)	39 (1989)	1.66 (1958)	
14	84 (1956)	55 (1974)	57 (1922)	34 (1989)[a]	0.63 (1972)	
15	85 (1956)	57 (1974)	61 (1956)	38 (1979)	1.05 (1931)	
16	87 (1956)	57 (1939)	59 (1953)	38 (1951)[a]	0.69 (1946)	
17	87 (1956)	53 (1923)	57 (1956)[a]	35 (1968)	0.90 (1926)	
18	82 (1980)	37 (1971)	58 (1954)	30 (1971)	0.69 (1982)	1.5 (1971)
19	83 (1984)[a]	49 (1971)	54 (1970)	26 (1971)	0.70 (1931)	
20	83 (1956)[a]	52 (1965)	58 (1951)	33 (1971)[a]	1.00 (1914)	
21	82 (1956)	50 (1975)	59 (1950)	25 (1983)	0.74 (1969)	
22	82 (1944)	48 (1974)	56 (1944)	30 (1919)	1.00 (1941)	0.2 (1970)
23	80 (1922)	51 (1952)	59 (1953)	33 (1985)[a]	1.61 (1941)	
24	81 (1979)	45 (1986)	55 (1947)	33 (1941)	1.15 (1931)	
25	80 (1953)	52 (1978)	62 (1947)	33 (1941)	1.74 (1915)	6.0 (1913)
26	82 (1947)	41 (1984)	56 (1966)[a]	31 (1970)	1.00 (1940)	
27	82 (1953)	49 (1935)	52 (1953)	29 (1924)	0.82 (1944)	
28	81 (1953)	42 (1936)	60 (1953)	24 (1936)	0.50 (1936)	4.0 (1936)
29	81 (1949)	51 (1936)	53 (1954)[a]	23 (1936)	1.80 (1941)	
30	81 (1980)	56 (1959)[a]	55 (1925)	25 (1985)	0.45 (1930)	
Month	80.0 (1956)	67.3 (1967)	52.6 (1954)	43.3 (1942)	5.79 (1941)	6.0 (1913)

Average temperature (1951–1980) Maximum: 72.1°F, Minimum: 48.4°F, Mean: 60.3°F

Temperatures		*Precipitation*	
Warmest September	65.8°F (1956)	Most days precipitation ≥0.01 in.	17 (1927)
Coldest September	56.2°F (1965)	Most days precipitation ≥0.10 in.	15 (1927)
Most days ≤32°F	3 (1935, 1924)	Most snows ≥1 in.	1 (1971)
Fewest days ≤32°F	0 (many)	Most snows ≥4 in.	1 (1936, 1913)
Most days ≥90°F	1 (1948, 1934)	Most snow on ground	3 in. (September 28, 1936)
		Least September precipitation	0.00 in. (1956, 1953)
		Least September snow	0.0 in. (many)

[a]Latest occurrence.

Table 9.11. Los Alamos (TA-59) weather extremes for October.

	Temperature (°F)				Maximum Precipitation	
	Maximum		Minimum		Water Equivalent	Snowfall
Day	High	Low	High	Low	(in.)	(in.)
1	84 (1980)	43 (1959)	53 (1989)	30 (1929)	0.55 (1930)	
2	78 (1979)	46 (1959)	58 (1954)	28 (1927)	0.93 (1959)	
3	77 (1987)[a]	48 (1984)	54 (1951)	30 (1971)	0.59 (1984)[a]	
4	77 (1922)	44 (1959)[a]	54 (1954)[a]	28 (1941)	1.10 (1911)	
5	78 (1980)[a]	47 (1989)	54 (1954)	25 (1932)	3.48 (1911)	
6	77 (1979)[a]	53 (1986)	53 (1954)	30 (1969)	0.74 (1974)	
7	79 (1928)	50 (1976)	50 (1979)[a]	24 (1979)	0.86 (1946)	
8	78 (1979)	48 (1970)	52 (1979)[a]	26 (1970)	1.43 (1939)	
9	76 (1980)	52 (1973)	50 (1954)[a]	27 (1982)	0.96 (1954)	
10	78 (1942)	41 (1973)	52 (1947)	25 (1982)	1.26 (1931)	
11	77 (1979)	47 (1986)[a]	52 (1955)	26 (1986)	0.61 (1986)	2.5 (1986)
12	76 (1979)	28 (1986)	51 (1951)	21 (1986)	1.38 (1960)	4.5 (1986)[a]
13	74 (1955)[a]	41 (1957)	53 (1954)	20 (1986)[a]	1.70 (1916)	0.2 (1942)
14	77 (1932)	44 (1957)	57 (1922)	24 (1928)	0.30 (1925)	
15	72 (1955)	36 (1984)	50 (1938)	25 (1984)[a]	0.59 (1984)	4.0 (1984)[a]
16	82 (1930)	38 (1970)	50 (1930)	21 (1984)	0.92 (1960)	4.0 (1960)
17	73 (1947)	40 (1960)	48 (1964)	24 (1948)	2.20 (1945)	0.7 (1966)
18	74 (1938)	38 (1965)	48 (1953)[a]	20 (1968)	0.89 (1960)	1.0 (1965)
19	75 (1936)	42 (1972)	48 (1988)	15 (1976)	2.06 (1957)	
20	80 (1918)	39 (1984)	50 (1979)[a]	20 (1976)	1.29 (1957)	
21	82 (1918)	36 (1984)	49 (1951)[a]	20 (1976)	1.29 (1957)	6.0 (1984)
22	73 (1954)	37 (1984)	49 (1961)	26 (1936)[a]	0.69 (1932)	1.5 (1984)
23	69 (1973)	33 (1984)	44 (1946)	20 (1936)	0.60 (1941)	3.5 (1984)
24	70 (1979)	30 (1935)	44 (1956)[a]	18 (1974)	0.85 (1953)	4.0 (1984)
25	72 (1979)	42 (1935)	45 (1988)[a]	17 (1935)	1.33 (1971)	1.0 (1978)
26	73 (1979)	40 (1957)[a]	45 (1951)[a]	23 (1935)	1.10 (1918)	1.1 (1918)
27	70 (1934)	35 (1970)	46 (1952)	22 (1918)	0.69 (1951)	5.5 (1980)
28	72 (1952)	33 (1976)	43 (1926)	16 (1970)	0.50 (1941)	
29	73 (1934)	35 (1929)	49 (1946)	18 (1980)	0.63 (1971)	7.5 (1929)
30	70 (1937)	34 (1971)	46 (1964)	18 (1989)[a]	1.38 (1959)	3.0 (1959)
31	70 (1937)	31 (1972)	43 (1951)	19 (1972)	1.17 (1959)	9.0 (1972)
Month	67.0 (1952)	52.7 (1984)	43.5 (1954)	30.2 (1971)	5.77 (1957)	20.0 (1984)

Average temperature (1951–1980) Maximum: 62.0°F, Minimum: 38.7°F, Mean: 50.3°F

Temperatures		*Precipitation*	
Warmest October	54.7°F (1963)	Most days precipitation ≥0.01 in.	17 (1917)
Coldest October	42.8°F (1984)	Most days precipitation ≥0.10 in.	11 (1941)
Most days ≤32°F	21 (1976)	Most snows ≥1 in.	6 (1984)
Least days ≤32°F	0 (1951)	Most snows ≥4 in.	3 (1984)
Most days ≤0°F	None	Most snow on ground	7 in. (October 31, 1977)
		Least October precipitation	0.00 in. (1952)
		Least October snow	0.0 in. (many)

[a]Latest occurrence.

Table 9.12. Los Alamos (TA-59) weather extremes for November.

	Temperature (°F)				Maximum Precipitation	
	Maximum		Minimum		Water Equivalent	Snowfall
Day	High	Low	High	Low	(in.)	(in.)
1	72 (1950)	32 (1972)	46 (1952)	11 (1929)	0.57 (1987)	2.0 (1969)
2	69 (1924)	35 (1969)	47 (1932)	11 (1929)	0.54 (1911)	8.0 (1911)
3	67 (1983)	30 (1956)	43 (1932)	10 (1936)	1.09 (1978)	3.0 (1946)[a]
4	66 (1949)	28 (1946)	42 (1918)	17 (1936)	0.27 (1986)	5.0 (1946)
5	68 (1949)	30 (1961)	43 (1918)	14 (1935)	0.91 (1957)	9.0 (1933)
6	66 (1988)[a]	33 (1946)	45 (1940)	15 (1959)	1.11 (1953)	4.0 (1957)
7	66 (1983)[a]	30 (1938)	40 (1950)[a]	5 (1938)	1.03 (1929)	9.5 (1929)
8	67 (1980)	34 (1929)[a]	42 (1950)	5 (1938)	0.33 (1929)	5.5 (1929)
9	71 (1980)	33 (1977)	41 (1973)	10 (1948)[a]	0.33 (1966)	3.5 (1966)
10	68 (1980)	28 (1950)	42 (1958)	5 (1950)	0.74 (1982)	0.1 (1950)
11	67 (1980)	32 (1950)	40 (1985)	10 (1940)	1.35 (1978)	2.5 (1935)
12	64 (1973)[a]	26 (1976)	42 (1967)[a]	13 (1929)	0.66 (1978)	1.5 (1972)
13	65 (1967)	35 (1976)	41 (1973)	4 (1929)	0.48 (1928)	2.0 (1961)
14	62 (1967)[a]	36 (1980)	40 (1962)	6 (1929)	0.78 (1978)	6.0 (1978)
15	68 (1941)	27 (1980)	40 (1967)	7 (1925)	0.25 (1962)	3.0 (1961)
16	64 (1975)[a]	28 (1980)	41 (1966)	8 (1955)	0.38 (1957)	7.6 (1957)
17	64 (1975)	31 (1944)	42 (1967)	10 (1980)	0.35 (1972)	5.5 (1958)
18	60 (1976)[a]	27 (1962)[a]	36 (1950)	6 (1958)	0.87 (1964)	7.0 (1964)
19	62 (1942)	30 (1985)	39 (1977)	6 (1948)	1.04 (1940)	10.0 (1930)
20	60 (1989)[a]	27 (1953)	38 (1950)	8 (1956)	0.50 (1972)[a]	9.0 (1972)
21	62 (1955)	24 (1929)	39 (1950)	6 (1966)	0.13 (1931)	2.0 (1957)
22	66 (1924)	24 (1957)	41 (1950)	−4 (1957)	1.46 (1931)	14.0 (1931)
23	60 (1943)[a]	22 (1929)	38 (1966)	5 (1957)	0.63 (1931)	6.4 (1922)
24	61 (1954)	21 (1952)	35 (1926)	−2 (1931)	0.62 (1913)	8.0 (1980)
25	61 (1970)	26 (1952)	38 (1949)	5 (1931)	1.77 (1979)	8.0 (1935)
26	60 (1977)[a]	23 (1952)	40 (1949)	6 (1975)[a]	0.70 (1935)	7.0 (1935)
27	62 (1933)	17 (1976)	37 (1950)[a]	−11 (1976)	1.00 (1976)	12.0 (1976)
28	60 (1950)[a]	11 (1976)	39 (1950)[a]	−14 (1976)	0.28 (1913)	2.0 (1931)
29	60 (1950)	24 (1976)	38 (1949)	−4 (1976)	0.35 (1939)	5.0 (1939)
30	59 (1924)	27 (1975)	37 (1950)	5 (1934)	0.31 (1962)	2.0 (1985)
Month	55.5 (1942)	39.6 (1972)	34.2 (1949)	18.3 (1929)	6.60 (1972)	26.2 (1931)

Average temperature (1951–1980) Maximum: 48.7°F, Minimum: 27.1°F, Mean: 37.9°F

Temperatures		*Precipitation*	
Warmest November	44.4°F (1949)	Most days precipitation ≥0.01 in.	12 (1961)
Coldest November	30.5°F (1972)	Most days precipitation ≥0.10 in.	12 (1961)
Most days ≤32°F	30 (1972)	Most snows ≥1 in.	7 (1957)
Fewest days ≤32°F	11 (1949)	Most snows ≥4 in.	5 (1957)
Most days ≤0°F	3 (1976)	Most snow on ground	17 in. (November 28, 1931)
		Least November precipitation	0.00 in. (1956)[a]
		Least November snow	0.0 in. (1970)[a]

[a]Latest occurrence.

Table 9.13. Los Alamos (TA-59) weather extremes for December.

	Temperature (°F)				Maximum Precipitation	
	Maximum		Minimum		Water Equivalent	Snowfall
Day	High	Low	High	Low	(in.)	(in.)
1	61 (1926)	23 (1952)	37 (1942)	9 (1931)	0.95 (1933)	6.0 (1962)
2	60 (1942)[a]	30 (1971)[a]	36 (1951)	11 (1976)	0.33 (1955)	5.0 (1955)
3	59 (1977)	29 (1978)[a]	36 (1969)	6 (1968)[a]	0.19 (1955)	3.0 (1955)
4	60 (1987)[a]	26 (1955)	38 (1954)	5 (1925)	1.11 (1925)	8.5 (1913)
5	60 (1939)	30 (1955)[a]	36 (1946)	9 (1931)	0.54 (1926)	8.0 (1926)
6	58 (1939)	25 (1978)	40 (1966)[a]	5 (1983)	1.60 (1978)	22.0 (1978)
7	61 (1981)	16 (1978)	38 (1946)	−2 (1978)	0.39 (1974)	6.0 (1974)
8	60 (1981)	13 (1978)	30 (1970)	−8 (1978)	1.19 (1971)	16.0 (1971)
9	60 (1981)	22 (1924)	37 (1958)	−13 (1978)	0.84 (1982)	10.0 (1960)
10	58 (1981)	23 (1960)	35 (1938)	−3 (1951)	1.35 (1965)	10.0 (1985)
11	59 (1939)	25 (1985)	37 (1981)	2 (1919)	0.96 (1961)	7.0 (1961)
12	63 (1938)	16 (1949)	31 (1919)	−9 (1961)	0.30 (1943)[a]	4.5 (1987)
13	57 (1942)	22 (1967)[a]	31 (1981)[a]	−4 (1931)	0.82 (1967)	16.0 (1967)
14	55 (1946)[a]	23 (1987)	32 (1970)[a]	2 (1931)	1.09 (1984)	21.0 (1984)
15	55 (1980)[a]	20 (1965)	35 (1946)[a]	3 (1987)	0.28 (1965)	5.0 (1915)
16	57 (1980)	25 (1932)	31 (1980)[a]	0 (1940)[a]	1.12 (1961)	16.0 (1961)
17	60 (1980)	23 (1927)	33 (1980)	4 (1961)	0.48 (1918)[a]	7.0 (1967)
18	59 (1939)	23 (1927)	33 (1980)[a]	−1 (1927)	0.47 (1987)	6.0 (1987)
19	59 (1942)	23 (1928)	31 (1980)	0 (1927)	0.40 (1914)	7.0 (1914)
20	59 (1939)	19 (1929)	34 (1955)	2 (1928)	0.45 (1914)	7.0 (1914)
21	56 (1955)	22 (1951)	35 (1944)	−1 (1967)	0.40 (1923)	4.0 (1923)
22	52 (1985)[a]	20 (1968)	32 (1948)	−2 (1967)	0.41 (1965)	4.0 (1959)
23	55 (1955)	22 (1949)	35 (1971)[a]	−8 (1924)	0.76 (1924)	14.0 (1924)
24	58 (1958)	11 (1924)	36 (1946)	−10 (1924)	0.47 (1987)	12.0 (1987)
25	55 (1955)	18 (1924)	35 (1955)	−9 (1924)	0.45 (1942)	7.0 (1987)
26	61 (1980)	14 (1987)	37 (1969)	0 (1918)	1.10 (1915)	18.0 (1915)
27	64 (1980)	17 (1987)	34 (1980)	0 (1939)	0.74 (1984)	7.0 (1979)[a]
28	58 (1980)	22 (1939)	35 (1980)	0 (1983)	0.80 (1946)	7.0 (1954)
29	53 (1965)	21 (1969)	37 (1951)	0 (1983)	0.42 (1971)	8.5 (1958)
30	53 (1980)	23 (1969)[a]	37 (1951)	2 (1931)	0.65 (1941)	3.0 (1941)
31	58 (1980)	23 (1969)	33 (1980)	2 (1969)	0.51 (1918)	8.0 (1915)
Month	50.1 (1980)	34.7 (1931)	26.7 (1980)	13.8 (1927)	3.21 (1984)	41.3 (1967)

Average temperature (1951–1980) Maximum: 41.4°F, Minimum: 20.3°F, Mean: 30.9°F

Temperatures		*Precipitation*	
Warmest December	38.4°F (1980)	Most days precipitation ≥0.01 in.	10 (1967)
Coldest December	24.6°F (1931)	Most days precipitation ≥0.10 in.	9 (1967)
Most days ≤32°F	31 (many)	Most snows ≥1 in.	9 (1967)
Least days ≤32°F	24 (1955)	Most snows ≥4 in.	5 (1943)
Most days ≤0°F	4 (1924)	Most snow on ground	22 in. (December 5–6, 1978)
		Least December precipitation	0.01 in. (1981)
		Least December snow	0.2 in. (1981)[a]

[a]Latest occurrence.

10 Turbulence and Dispersion

Turbulence is important in determining the dispersion of plumes or puffs from releases of airborne material. For example, greater turbulence promotes dispersion and, therefore, lowers concentrations of airborne pollutants. Turbulence is dependent on vertical thermal stratification and wind speed. With light winds, vertical thermal effects dominate the production or destruction of turbulence. During sunny conditions, the temperature drops quickly with height above ground, creating unstable conditions characterized by relatively large horizontal and vertical turbulence. Conversely, during light-wind, nighttime conditions, a surface inversion forms, creating stable conditions with relatively little vertical motion. Horizontal motions during light winds, however, often show large low-frequency variations (meandering, for example). With greater wind speeds, wind shear becomes more important in determining turbulence intensity. Turbulence caused by strong winds is often sufficient to produce a well-mixed atmosphere in the vertical thermal stratification (a near-neutral temperature lapse rate).

The local terrain plays an important part in the creation of turbulence. Generally, a rougher and more irregular terrain causes more horizontal and vertical turbulence because of increased wind shear. The Los Alamos area, with its irregular and rough terrain, thus has more turbulence and dispersion than smoother areas have. An exception occurs when local, light drainage winds develop in canyons and on the plateau during the nighttime. Turbulence intensity also depends on height above ground. Horizontal turbulence is greatest at ground level and decreases with height. Vertical turbulence decreases with height during neutral and stable conditions, but increases with height during unstable conditions. During the day, sunshine can cause thermals to form near the ground, which then rise and cause large-scale vertical turbulence higher than 1 km above the ground. The large scale of this turbulence causes fewer effects near the ground than well above ground.

Horizontal and vertical turbulence both vary by wind direction, especially in rough terrain like that at Los Alamos. There are several reasons for this. First, certain wind directions are associated with stronger speeds than others. Stronger winds generate greater mechanical mixing. Second, terrain roughness varies in different, upwind directions. Rougher terrain also promotes more mixing. Likewise, the usual turbulence decrease with height is affected by terrain roughness; hence, turbulence intensity at greater heights above the ground is increased by roughness over longer upwind distances.

10.1 Turbulence (by Wind Direction)

Standard deviations of horizontal wind direction (σ_θ) and vertical wind direction (σ_ϕ) are widely used indicators of horizontal and vertical turbulence components. Atmospheric diffusivity is proportional to σ_θ and σ_ϕ. These two variables (from 15-minute-averaged data) are plotted for TA-59 and Area G in Figs. 10.1 and 10.2. These sites represent the western and eastern edges of the Pajarito Plateau, respectively. The local

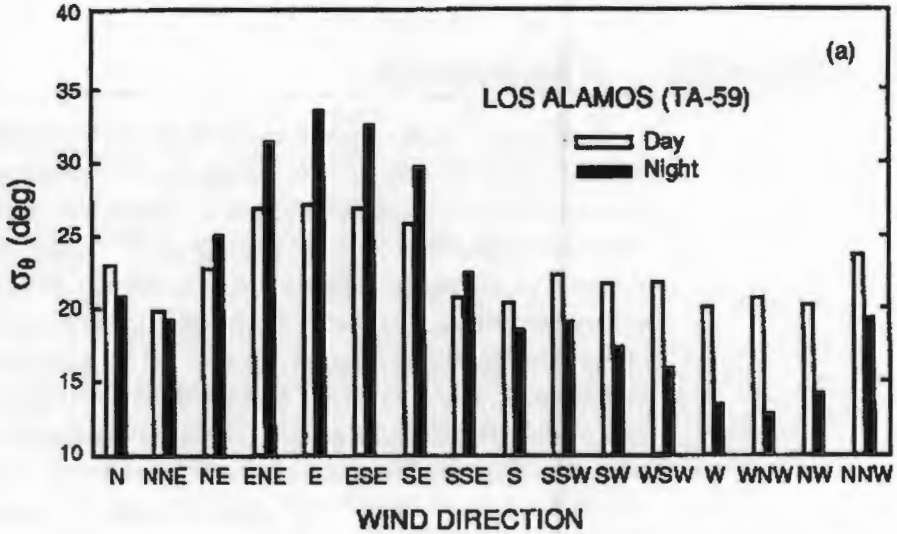

Fig. 10.1(a) and (b). Horizontal wind-direction standard deviation (15-minute-averaged σ_θ) at (a) TA-59 and (b) Area G.

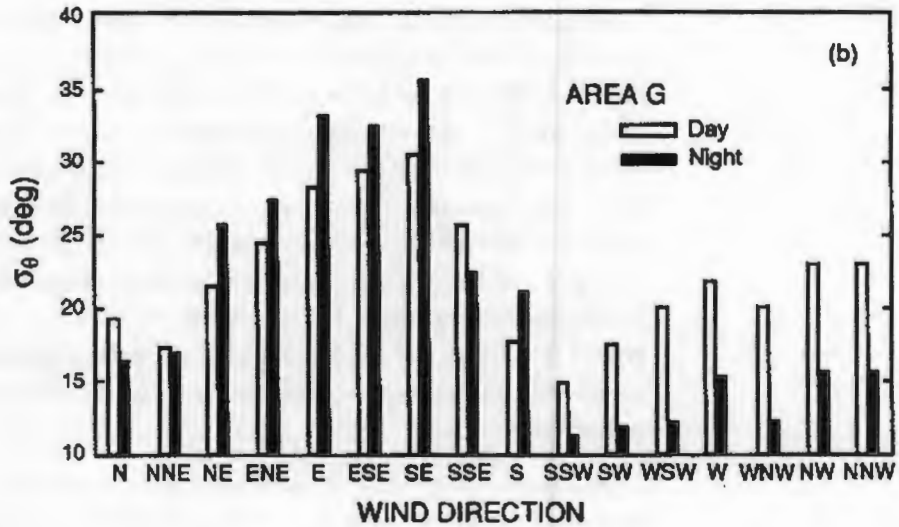

area surrounding TA-59 is quite rough, with buildings, canyons, and Ponderosa pines (up to 20 m high). The Area G tower is located on a smooth mesa, with some short grass and shrubs (about 0.5 m high). The winds are measured at an 11-m height at Area G and a 23-m height at TA-59. Therefore, the Area G horizontal turbulence is slightly overstated when compared with that at TA-59 because of the wind instruments' closer proximity to the ground.

Figures 10.1(a) and 10.1(b) show 15-minute-averaged σ_θ (indicator of horizontal turbulence) by wind direction and day or nighttime occurrence at TA-59 and Area G, respectively. Note that σ_θ is greatest at both sites for NE'ly through SE'ly winds. Winds from these directions tend to be light and quite variable. Also note that σ_θ is generally greater at both sites during the day than at night for all directions except the NE'ly

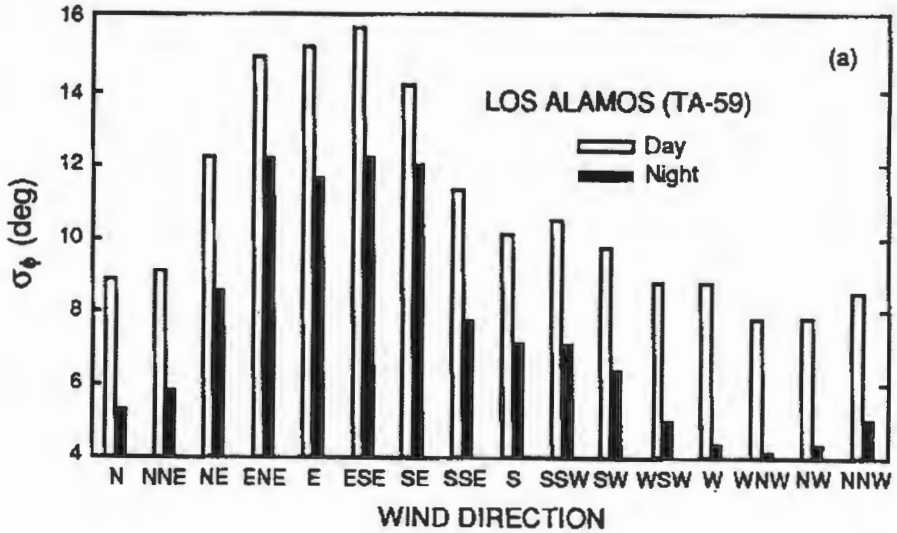

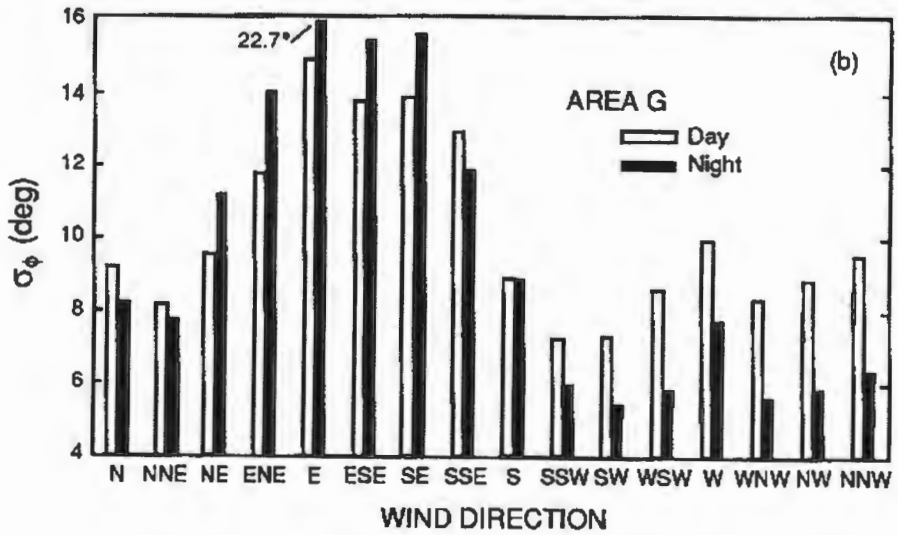

Fig. 10.2(a) and (b). Vertical wind-direction standard deviation (15-minute-averaged σ_ϕ) at (a) TA-59 and (b) Area G.

through SE'ly winds. Data in the figures show that TA-59 has noticeably greater σ_θ for SSW'ly and SW'ly winds than does Area G. These up-valley winds are frequent and brisk. Similarly, σ_θ is greater at TA-59 than at Area G for down-valley winds (N through NNE).

Similar analyses for σ_ϕ (indicator of vertical turbulence) are shown in Figs. 10.2(a) and 10.2(b). Vertical turbulence is also greatest for NE'ly through SE'ly winds. One difference from the σ_θ analysis is that σ_ϕ at TA-59 is less at night than during the day for the NE'ly through SE'ly winds; σ_ϕ at Area G is also noticeably less than at TA-59 for the brisk SSW'ly and SW'ly winds. Another contrast from the σ_θ analysis is that TA-59 has considerably smaller σ_ϕ at night than does Area G for WSW'ly through NNE'ly winds, and σ_ϕ at TA-59 decreases considerably more at night than does σ_θ. Even though TA-59

appears to be a rougher site than Area G, the horizontal turbulence is only slightly greater, and the vertical turbulence is actually less, for most wind directions. It may be that the large-scale roughness of canyons and mesas over the Laboratory area is frequently more important than local roughness. Other turbulence analyses show that East Gate and TA-50 both have horizontal turbulence similar to that at TA-59 and Area G, but both have slightly less vertical turbulence.

10.2 Vertical Profiles of σ_θ and σ_ϕ

Vertical profiles (constructed from data taken at various tower heights) of 15-minute-averaged σ_θ and σ_ϕ at TA-50 for 1985–1987 were calculated for different stability classes, as determined by σ_ϕ and daytime or nighttime occurrence. The profiles are useful in estimating dispersion changes with height. The Pasquill-Gifford (P-G) stability categories A–F, as described by Turner (1969), were determined from σ_ϕ ranges recommended by the United States Environmental Protection Agency (EPA 1981). These σ_ϕ ranges, which are shown in Table 10.1, include a correction for the rough terrain at the Laboratory. The original values were multiplied by the expression $(z_0/15\ \text{cm})^{0.2}$, where z_0 is the average surface-roughness length within a 1- to 3-km radius of the TA-50 tower. Calculations of wind speeds at TA-50 during nearly neutral conditions give a surface roughness of about 38 cm. When 38 cm is substituted into the above expression, a multiplication factor of 1.2 is derived.

Vertical profiles of σ_ϕ for different σ_ϕ-derived stability classes at TA-50 at four heights above ground level (AGL) are shown in Fig. 10.3(a). Note that σ_ϕ tends to increase with height, especially during unstable (A–C) daytime conditions. In fact, σ_ϕ at the 92-m level is typically nearly twice that at the 12-m level. Increases are especially large from the 23- to 46-m levels. The dramatic increase with height is caused by large thermals rising from the ground during sunny and light-wind conditions. Because the

Table 10.1. Estimation of Pasquill-Gifford (P-G) stability categories based on σ_ϕ ranges.[a]

P-G Stability Category	σ_ϕ (deg)
A	≥14.5
B	12.0–14.5
C	9.5–12.0
D	6.0– 9.5
E	2.9– 6.0
F	<2.9

[a]The P-G categories were determined by calculations using σ_ϕ ranges recommended by the EPA (1981). The ranges include corrections for rough terrain at Los Alamos.

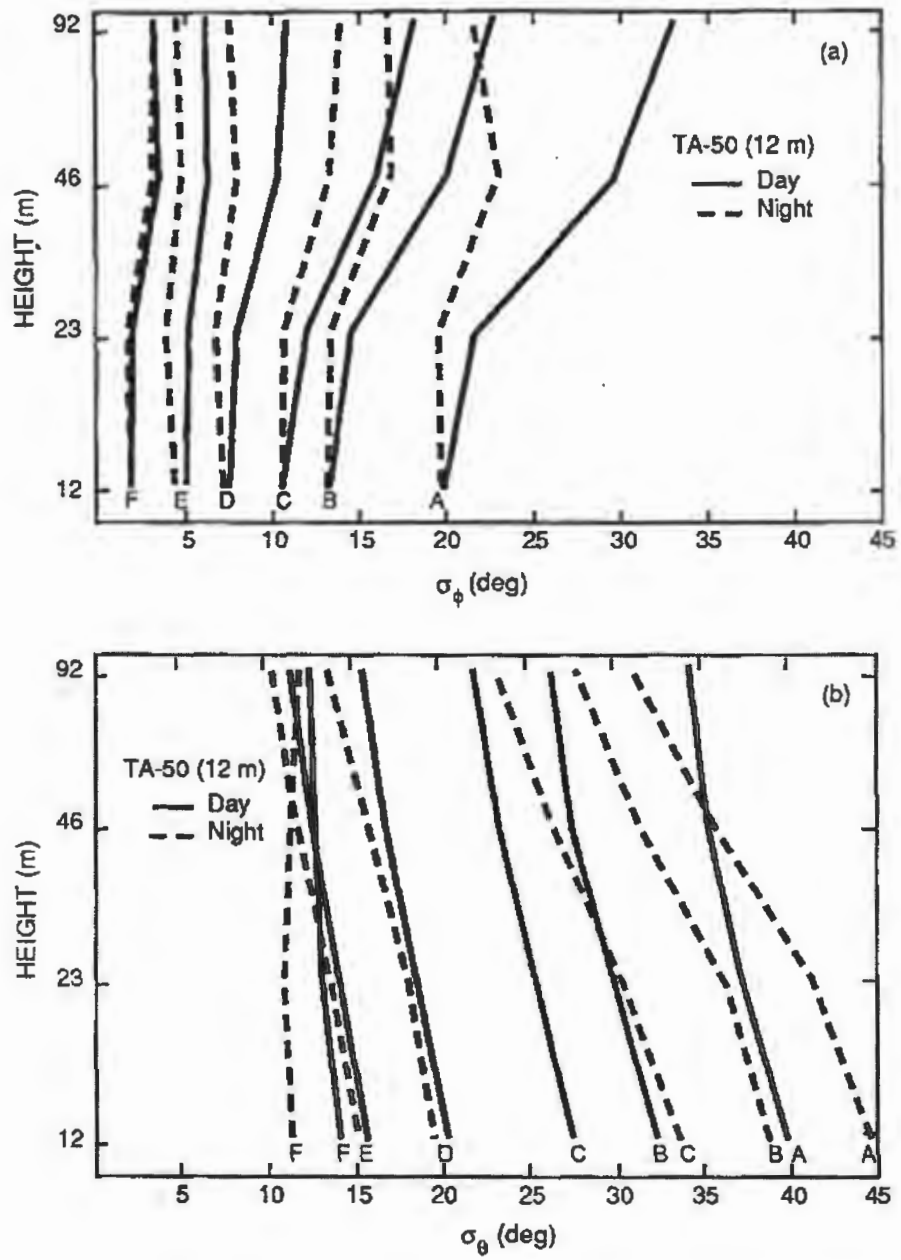

Fig. 10.3(a) and (b). Vertical profiles of (a) σ_ϕ and (b) σ_θ at TA-50 for different stability categories. Stability was derived by 15-minute-averaged σ_ϕ, observed at 12 m AGL.

nearness of the ground inhibits vertical motion, σ_ϕ values are smaller at lower levels. Above the surface, larger-scale vertical motions are more common. It is evident that the increase in σ_ϕ is much smaller during unstable (A–C) conditions at night. Note that the increase in σ_ϕ with height becomes less pronounced during neutral (D) and stable (E–F) conditions.

Vertical profiles of σ_θ are displayed in Fig. 10.3(b), also according to σ_ϕ-derived stability categories at the lowest level (12 m). In contrast to σ_ϕ, the σ_θ generally decreases with height. The decrease is rather smooth with increasing height for most

stabilities. The only exception to the σ_θ decrease with height is during F stabilities at night when σ_θ increases slightly at the 46- and 92-m levels. The F stability contains many instances of surface drainage winds that extend only slightly higher than the 23-m level.

A comparison of Figs. 10.3(a) and 10.3(b) gives interesting insights into the relationship of horizontal and vertical turbulence. One can see that σ_θ is different for day and night for specified categories at 12 m (σ_ϕ is the same by definition). For example, σ_θ is higher at night than during the day for the unstable (A–C) stability categories. The reason can be seen in the vertical turbulence (σ_ϕ) profiles obtained during unstable conditions. The σ_ϕ increases sharply with height during unstable daytime conditions, but only modestly during the night. The daytime increase indicates strong vertical mixing at upper levels during unstable conditions. Rising thermals are largely responsible for the increased σ_ϕ at the higher levels. At night, σ_ϕ at the lower levels is more affected by the rough ground and less affected by the downward mixing of stronger horizontal winds, giving slightly more horizontal diffusion (larger σ_θ). The opposite occurs for very stable (F) conditions: horizontal turbulence (σ_θ) is less at night than during the day, especially at the 12- and 23-m levels.

Vertical wind-speed profiles for TA-50 were calculated by stability category and daytime or nighttime occurrence (Fig. 10.4). The wind-speed increase with height is the greatest during the night. The exception is the F category, when the wind speed increases only slightly with height. These are times when the nocturnal drainage flow predominates in the layer, which includes the 12- and 23-m levels. The wind speed increases very little with height during unstable (A–C) daytime conditions. Weak,

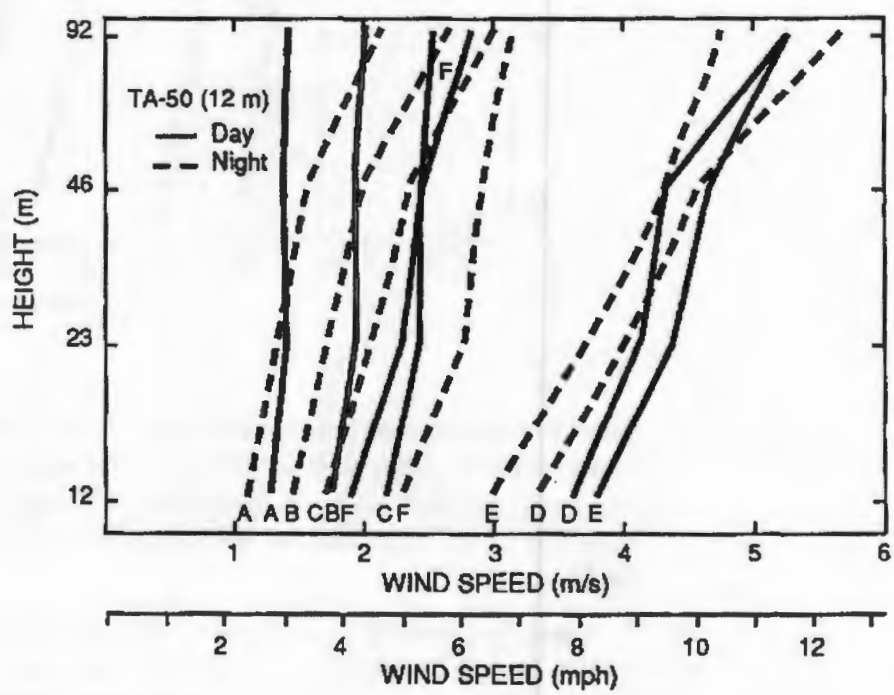

Fig. 10.4. Vertical profiles of wind speeds at TA-50 for different stability categories. Stability was derived by 15-minute-averaged σ_ϕ, observed at 12 m AGL.

upslope winds occur frequently during these times. The profiles show that winds are strongest for the neutral (D) and slightly stable (E) categories at all levels.

10.3 Dispersion

Accurate dispersion predictions are useful in determining downwind concentrations of atmospheric-released pollutants. Dispersion modeling uses wind information (including average direction and speed and horizontal and vertical turbulence), along with release information, to provide estimates of downwind concentrations. Wind data from different sites and heights are necessary for accurate modeling results, especially in complex terrain.

Dispersion modeling is particularly challenging at the Laboratory because of the complex terrain. The terrain forces spatial, temporal, and height-dependent variations of wind direction, speed, and turbulence. Air interaction between the mesa tops and canyons is especially difficult to model. A dynamic model that uses the physics of air flow is the best tool for predicting dispersion at Los Alamos. However, a simpler Gaussian model is widely used in air pollution work:

$$\chi(x,y,z,H) = \frac{Q}{2\pi\sigma_y\sigma_z\overline{U}} \exp\left[-\frac{1}{2}\left(\frac{y}{\sigma_y}\right)^2\right] \times \left\{\exp\left[-\frac{1}{2}\left(\frac{z-H}{\sigma_z}\right)^2\right] + \exp\left[-\frac{1}{2}\left(\frac{z+H}{\sigma_z}\right)^2\right]\right\}, \quad (10.1)$$

where

χ = concentration (g/m^3 or Ci/m^3),

x, y, z = distances downwind, lateral, and above the ground (m), respectively,

Q = source strength (g/s or Ci/s),

$\overline{U}$ = average wind speed (m/s),

σ_y, σ_z = diffusion coefficients in the y and z directions (m),

and

H = effective height of source emission (m).

The equation becomes simpler for ground-level ($z = 0$) concentrations:

$$\chi(x,y,0,H) = \frac{Q}{\pi\sigma_y\sigma_z\overline{U}} \exp\left[-\frac{1}{2}\left(\frac{y}{\sigma_y}\right)^2\right] \exp\left[-\frac{1}{2}\left(\frac{z}{\sigma_z}\right)^2\right]. \quad (10.2)$$

These equations can also be used to calculate the total amount of plume and time for passage (integrated concentration) by substituting total release (grams or curies) for release rate (gram-seconds [or curie-seconds] per cubic meter [g-s/m^3 or Ci-s/m^3]).

The Gaussian model is actually a probability model based on a normal distribution. The assumption is that the plume will spread horizontally and vertically in a normal distribution with downwind distance. The amount of spread is dependent on turbulence and, in turn, on atmospheric stability. The diffusion coefficients σ_y and σ_z represent horizontal and vertical plume spread. Horizontal dispersion is generally greater than vertical dispersion ($\sigma_y > \sigma_z$). Specifically, about 68% of the pollutant molecules are found within 1 std dev of the plume center line (σ_y,σ_z), and 96% within 2 std dev. The concentration at 1 std dev is about 61% of the center-line concentration; at 2 std dev, it is 14%.

The Gaussian model, using on-site turbulence data, is accurate (within a factor of 2) in predicting daily radioactive or nonradioactive levels up to 1 km or so downwind on mesa tops at the Laboratory (Bowen et al. 1987). Recent work shows that accurate predictions can be made to at least 3 km downwind on mesa tops. The predictions are dependent on accurate diffusion coefficients σ_y and σ_z. One method to calculate σ_y and σ_z uses on-site turbulence variables σ_θ and σ_w and downwind travel distance and time ($\sigma_\phi \cong \sigma_w/\overline{U}$). The method, suggested by Draxler (1976), uses the following two equations:

$$\sigma_y = \sigma_\theta X f_1(T/T_i) \tag{10.3}$$

and

$$\sigma_z = \sigma_w \frac{X}{\overline{U}} f_2(T/T_i) \ , \tag{10.4}$$

where

σ_θ = standard deviation of the horizontal wind direction (rad),

σ_w = standard deviation of the vertical wind speed (m/s),

X = downwind distance (m),

$\overline{U}$ = average wind speed (m/s),

f_1, f_2 = functions of downwind distance and thermal stability,

T = downwind travel time (s),

and

T_i = constant, dependent on stability and whether the calculation is for vertical or horizontal dispersion.

It is suggested that at Los Alamos a direct, objective method (such as Draxler's), rather than an indirect, subjective method based on estimates extrapolated from P-G curves (the Turner method), be used with on-site turbulence data to estimate σ_y and σ_z. The P-G curves are more appropriate for flat terrain. In addition, stability curves do not always accurately reflect the actual turbulence, even with flat terrain.

Calculations of σ_y and σ_z, based on the Draxler method, were made at Los Alamos (TA-50, 12 m AGL) for six stability categories, as determined by σ_ϕ (see Table 10.1). Figures 10.5(a) and 10.5(b) show the σ_y and σ_z by downwind distance. These dispersion coefficients are less conservative (greater in value) than values obtained from the widely used P-G curves, especially the σ_y. The increased values of σ_y and, to a lesser extent, σ_z represent the rough terrain at Los Alamos. The σ_θ-derived σ_y coefficients are 2 to 3 times larger than values obtained from P-G curves for A and B categories and up to 4 times larger than those for the other categories. For D and E stability categories, the σ_ϕ-derived σ_z coefficients are also larger than σ_z from P-G by a factor of 2 to 3. For the most stable F category, σ_ϕ-derived σ_z is only slightly larger than the P-G–derived σ_z. However, for the unstable A and B categories, the σ_ϕ-derived σ_z is only larger than the P-G–derived σ_z very close downwind. At greater downwind distances, the P-G–derived σ_z becomes much larger than the σ_ϕ-derived σ_z. For the unstable categories, however, P-G–derived σ_z (using the Turner method) is slightly less than σ_ϕ-derived σ_z (using the Draxler method).

The use of on-site derived dispersion coefficients generally gives concentration estimates that are one-tenth those derived using P-G coefficients for neutral and stable conditions. This holds true because the concentration (χ) is inversely proportional to the product of σ_y and σ_z,

$$\chi \propto \frac{1}{\sigma_y \sigma_z} .$$

The difference in concentration estimates may actually be larger, because the σ_ϕ-derived stability classes were calculated using 15-minute averages of σ_θ and σ_ϕ rather than the 1-hour averages recommended by the EPA (1981); using 1-hour averages would give even larger σ_θ and σ_ϕ and, in turn, larger σ_y and σ_z. Note that σ_y is calculated assuming a 3-m/s wind speed. For example, at a downwind distance of 10 km, the σ_y should be increased by 35% for a 10-m/s wind and decreased by 30% for a 1-m/s wind. Similarly, σ_z should be increased by 40% for a 10-m/s wind and decreased by 35% for a 1-m/s wind. Based on average TA-50 (12 m) wind speeds by stability category (see Fig. 10.4), the average σ_y and σ_z should be reduced 10%–20% for the A–C categories.

10.4. Comparison of Stability Class Methods

Stability classes were calculated at TA-59 and Area G for winter (December–February) and summer (June–August) by both the P-G method (similar to the objective method suggested by Turner [1961]) and the σ_ϕ determination (see Table 10.1). The

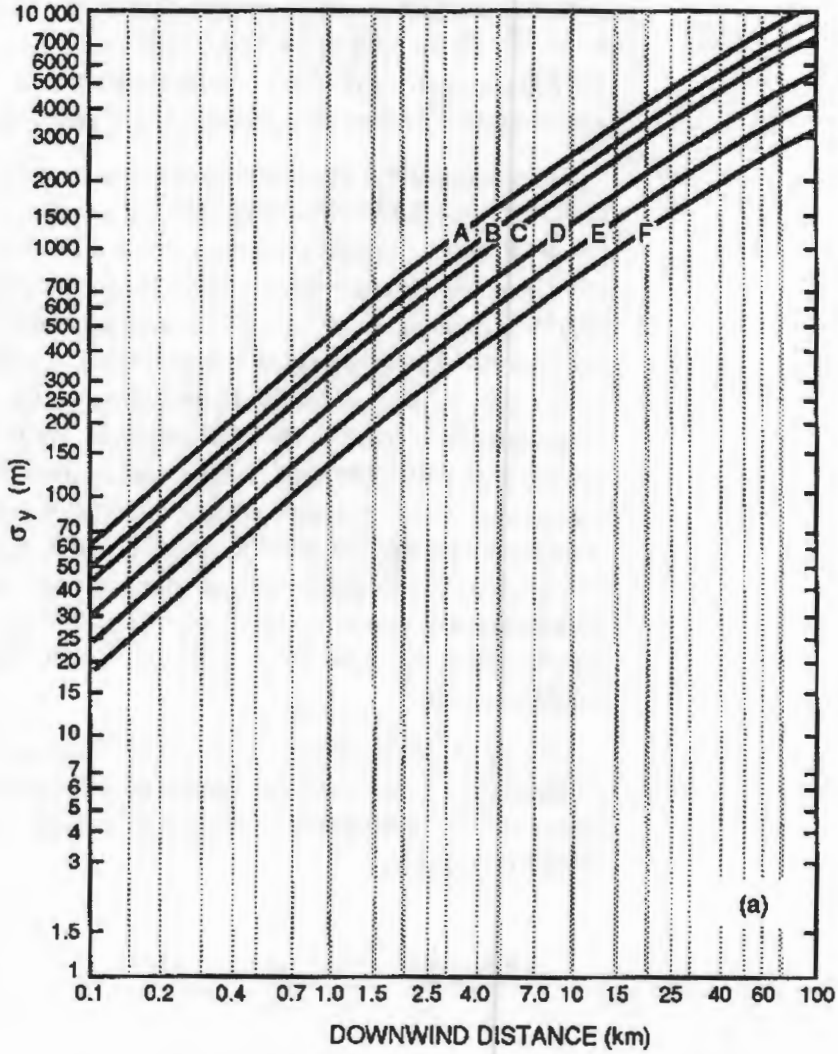

Fig. 10.5(a) and (b). (a) Calculated horizontal-dispersion coefficients (σ_y), based on TA-50 (12 m AGL) σ_ϕ values.

former was used with 15-minute-averaged data to determine P-G categories (the key to the method is shown in Table 10.2). With this method to determine P–G categories, meteorologists use ΔT (the change in temperature from surface to 11–23 m AGL) to determine nighttime stability class instead of relying on observation of cloudiness, as in the widely used subjective method. Similarly, intensity of sunshine is used to determine daytime stability class.

Comparisons of P-G and σ_ϕ-derived stability categories are shown in Tables 10.3 and 10.4 for TA-59 and Area G, respectively. Results are quite different for each site and season. During the winter, Area G has more P-G categories in the nearly neutral (C and E) and neutral (D) categories. This is expected because Area G has slightly stronger average winds and, therefore, fewer extreme stabilities. The stability category distribution based on σ_ϕ shows that TA-59 has higher categories (more unstable) than does Area G. TA-59 has only 49% in σ_ϕ-derived categories D–F, whereas Area G has

Fig. 10.5 (Continued)
(b) Calculated vertical-dispersion coefficients (σ_z), based on TA-50 (12 m AGL) σ_θ values.

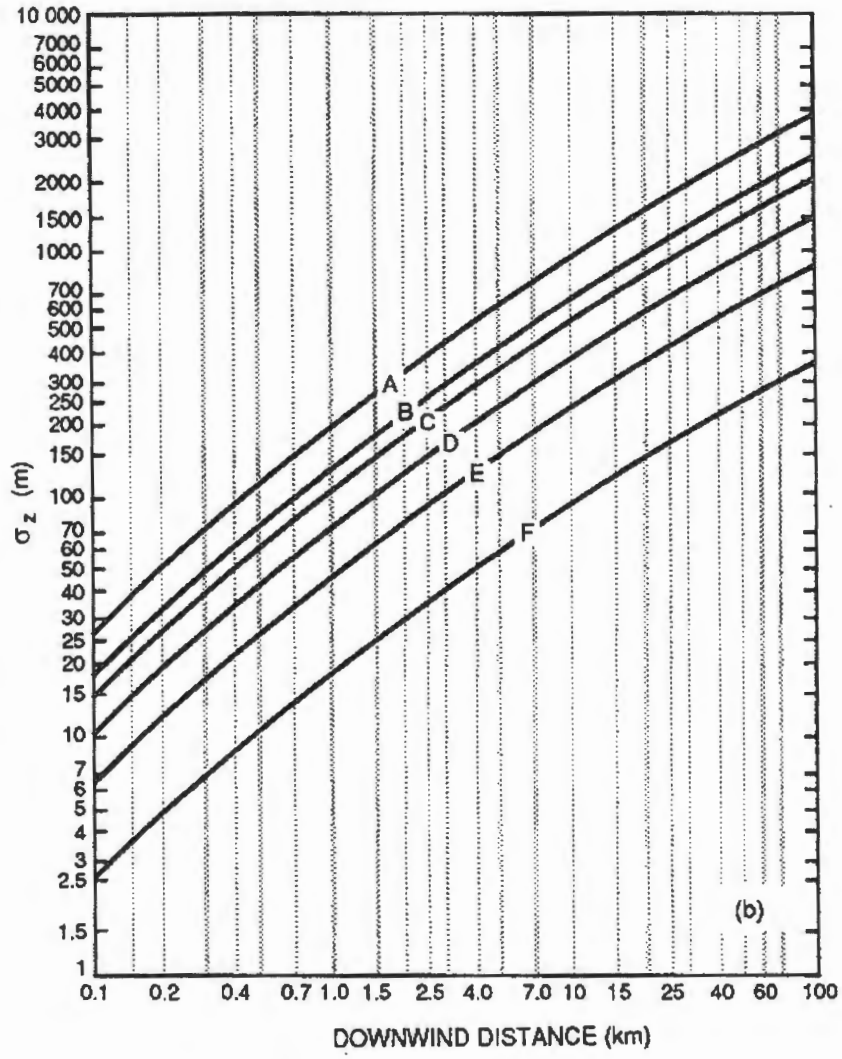

Table 10.2. Key to objective method used to determine P-G stability categories.[a]

Wind Speed (m/s)	Day: Incoming Solar Radiation (ly/min)[b] >1.0 (Strong)	0.5–1.0 (Moderate)	<0.5 (Slight)	Night: ΔT [c] (Negative)	(Positive)
<2	A	A	B	E	F
2–3	A	B	C	E	F
3–5	B	B	C	D	E
5–6	C	C	D	D	D
>6	C	D	D	D	D

[a]Reference Turner (1969).

[b]Incoming solar radiation (insolation) is usually measured in langleys (1 ly/min ≅ 698 W/m^2).

[c]Data on ΔT (change in temperature) were taken from ground level to heights 11–23 m AGL. Negative ΔT indicates temperatures decreasing with height; positive ΔT, temperatures increasing with height.

Table 10.3. Percentage of time of P-G–derived versus σ_ϕ–derived stability categories at Los Alamos (TA-59).

Winter

	P-G Category (%)						Totals
	A	B	C	D	E	F	(%)
σ_ϕ *Category (%)*							
A	6.8	7.2	0.9	0.2	1.2	10.3	26.6
B	0.9	2.8	1.4	1.3	0.7	2.6	9.8
C	0.5	3.6	2.2	3.2	1.5	4.2	15.1
D	0.2	2.9	3.1	3.4	3.1	8.6	21.2
E	0.0	0.8	0.7	0.5	3.4	7.4	12.8
F	0.3	1.0	0.4	0.4	2.1	10.4	14.5
Totals	8.6	18.3	8.6	9.0	12.0	43.5	100.0

Summer

	P-G Category (%)						Totals
	A	B	C	D	E	F	(%)
σ_ϕ *Category (%)*							
A	9.1	6.6	1.0	0.1	0.4	3.1	20.3
B	1.5	3.6	2.4	0.5	0.4	1.1	9.4
C	1.0	4.4	3.6	2.0	1.2	2.2	14.3
D	0.5	3.4	5.0	3.4	4.0	5.4	21.8
E	0.2	1.1	1.8	1.1	5.9	5.0	15.1
F	1.2	2.9	1.7	0.4	4.5	8.3	19.1
Totals	13.5	22.0	15.5	7.6	16.4	25.0	100.0

71% in these categories. The rougher terrain and slightly lighter winds are the probable reasons for the increased σ_ϕ at TA-59 over that at Area G during the winter.

The coincidence of identical stability categories using the two methods is slightly less than 30% at both sites. However, both methods are within one category about 62% and 58% of the time, respectively, at TA-59 and Area G. The least agreement occurs during very stable (F) conditions at both sites. It is evident that the P-G curves often greatly underestimate the diffusivity of the atmosphere at Los Alamos during very stable conditions. The use of P-G curves during very stable conditions produces overly conservative results at the Laboratory; therefore, their use during these times is discouraged.

The correlation of the two stability determination methods increases during the summer. The two methods are within one category about 70% and 65% of the time, respectively, at TA-59 and Area G. Note that the P-G stability categories are shifted toward more instability during the summer at both sites. This is understandable, because

Table 10.4. Percentage of time of P-G–derived versus σ_ϕ–derived stability categories at Area G.

Winter

	P-G Category (%)						Totals
	A	B	C	D	E	F	(%)
σ_ϕ *Category (%)*							
A	4.1	3.1	0.1	0.0	0.9	7.1	15.2
B	0.9	1.6	0.3	0.0	0.2	1.8	4.7
C	1.0	3.0	0.8	0.3	0.6	3.6	9.4
D	0.8	5.3	4.6	5.9	2.5	9.9	29.0
E	0.2	1.5	3.1	4.7	6.8	7.0	23.3
F	0.9	2.1	1.3	1.4	4.4	8.3	18.4
Totals	7.8	16.6	10.2	12.4	15.5	37.5	100.0

Summer

	P-G Category (%)						Totals
	A	B	C	D	E	F	(%)
σ_ϕ *Category (%)*							
A	6.6	2.7	0.1	0.0	0.4	2.6	12.4
B	1.6	1.9	0.3	0.0	0.1	0.9	4.9
C	1.3	4.5	1.7	0.2	0.5	2.1	10.2
D	0.7	6.0	9.4	5.3	3.4	7.3	32.0
E	0.1	1.3	4.0	3.9	7.7	5.4	22.4
F	1.2	2.4	2.7	1.7	5.4	4.7	18.1
Totals	11.5	18.8	18.2	11.0	17.5	23.0	100.0

the increased sunshine and sunshine intensity provide more unstable conditions. Somewhat surprising, however, is an opposite shift toward more stability for σ_ϕ-derived values at both sites during the summer. The slight shift toward more stability evidently occurs during the night (P-G stability categories E and F). The probable reason is that surface inversions are commonly stronger during winter than during summer nights. Ironically, at rough areas like those at Los Alamos, a stronger surface inversion can promote large horizontal and vertical turbulence values near the surface, especially for breezy conditions.

Stability classes were also determined by values of σ_θ for TA-59 and Area G based on a method suggested by the United States Nuclear Regulatory Commission (NRC 1972). A comparison of P-G versus σ_θ-derived stability categories was made. The results are similar to the comparison of P-G and σ_ϕ-derived stability categories. At both sites, greater agreement of the categories is prevalent during the summer. As with the σ_ϕ method, very few F categories are indicated by the σ_θ method.

11 Wind Persistence

Persistence data of wind direction and speed are very useful in emergency-response planning for atmospheric releases of pollutants or other hazardous materials. Persistence is the probability that a variable (such as wind direction or speed) or a combination of variables will remain in a specified range for a certain number of hours after entering that range category. Data on average winds are of limited use for emergency-response planning because accidental releases may occur during times of atypical winds. For extended releases, wind-persistence records provide information needed to predict which wind directions and speeds can be expected to last the longest. The most persistent wind directions and speeds are not necessarily the most frequent.

Fifteen-minute-averaged, near-surface winds were analyzed for wind-direction and -speed persistence at TA-59, TA-50 (two tower heights, 12 and 92 m), East Gate, and Area G. Persistence was calculated for each season. For the sake of brevity, results are shown only for winter and summer seasons.

11.1 Wind-Speed Persistence

11.1.1 Explanation

Following are cumulative frequency analyses of wind-speed classes by directional quadrant for TA-59 (23 m) and Area G (11 m) near-surface winds and for TA-50 (92 m) winds. The analyses are presented for winter (December–February) and summer (June–August) seasons. Persistence is analyzed for the following speed classes:

Light	<2.5 m/s (<5.5 mph),
Moderate	2.5–5.0 m/s (5.5–11 mph),
Strong	5.0–7.5 m/s (11–16.5 mph), and
Very strong	>7.5 m/s (>16.5 mph).

Persistence of all speeds in the quadrant is also presented. Each directional quadrant comprises four compass directions. For example, the NW quadrant (258.75°–348.75°) includes the W, WNW, NW, and NNW directions, and the NE quadrant includes the N, NNE, NE, and ENE directions.

Wind-speed persistence information is useful in determining the dilution the wind can provide for extended periods following a contaminant release to the atmosphere. Wind-speed persistence analyses are also useful to persons involved in forest fire prevention and containment and to those planning and conducting outdoor activities that may be affected by strong winds. Note that high persistence does not imply high frequency or vice versa. For example, strong winds are quite persistent from the NW quadrant during the winter at TA-59, but these winds seldom occur. In other words, strong NW'ly winds are infrequent at TA-59, but when they do occur, they tend to last.

Wind-direction persistence data are shown in Figs. 11.1–11.3. An example of using persistence curves in these figures follows. Figure 11.1(a) shows the winter TA-59

persistence probabilities by directional quadrant. The three lowest wind-speed classes have similar persistence characteristics. All the classes begin with a 100% frequency of 0.25-hour (15-minute) duration. The 15-minute period is the averaging time of all data and, therefore, the minimum persistence duration. The NW-quadrant frequencies for 0.5-hour persistence quickly drop to 65% for the three lowest wind-speed classes, but the frequencies for the very strong wind and all-speeds classes persist 80% of the time for a

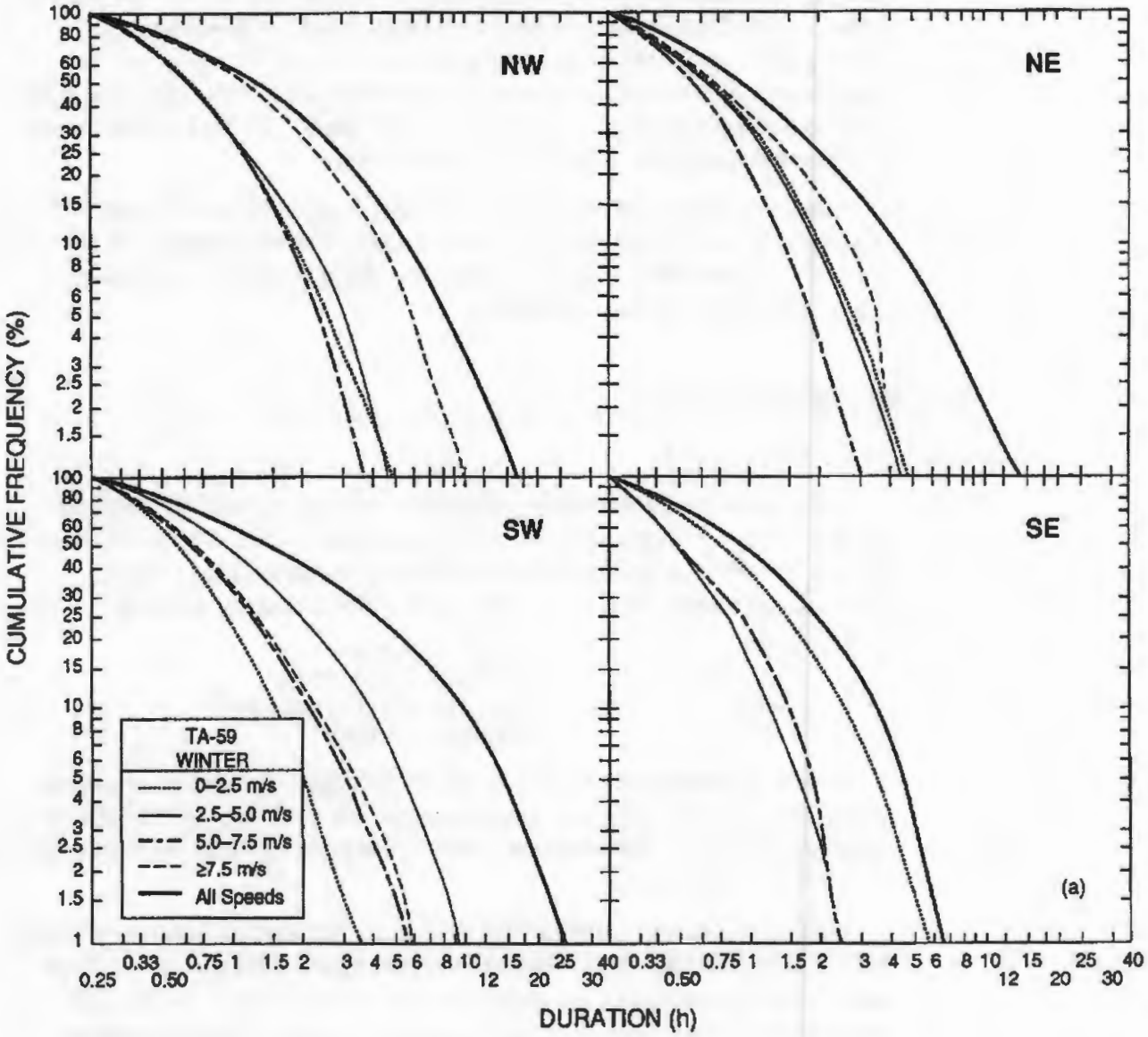

Fig. 11.1(a) and (b).

(a) Winter persistence probabilities at TA-59 of wind-speed classes by directional quadrant. Note the high SW'ly wind persistence, especially for winds with speeds 2.5–5.0 m/s. Strong winds from the NW are also persistent. SE'ly winds are not persistent, except for light winds.

duration of 0.5 hour (persistence includes the initial 0.25-hour time of establishment). The ratio of strong-wind frequency to light-wind frequency increases for longer durations. For a 4-hour duration, the NW-quadrant wind-speed frequencies range from <1% for strong winds, 1.75% for light winds, and 2.2% for moderate winds to 13% for very strong winds and 17% for all wind speeds. Similarly, for a specific frequency, the duration for very strong winds and all winds is longer than for lighter winds. For

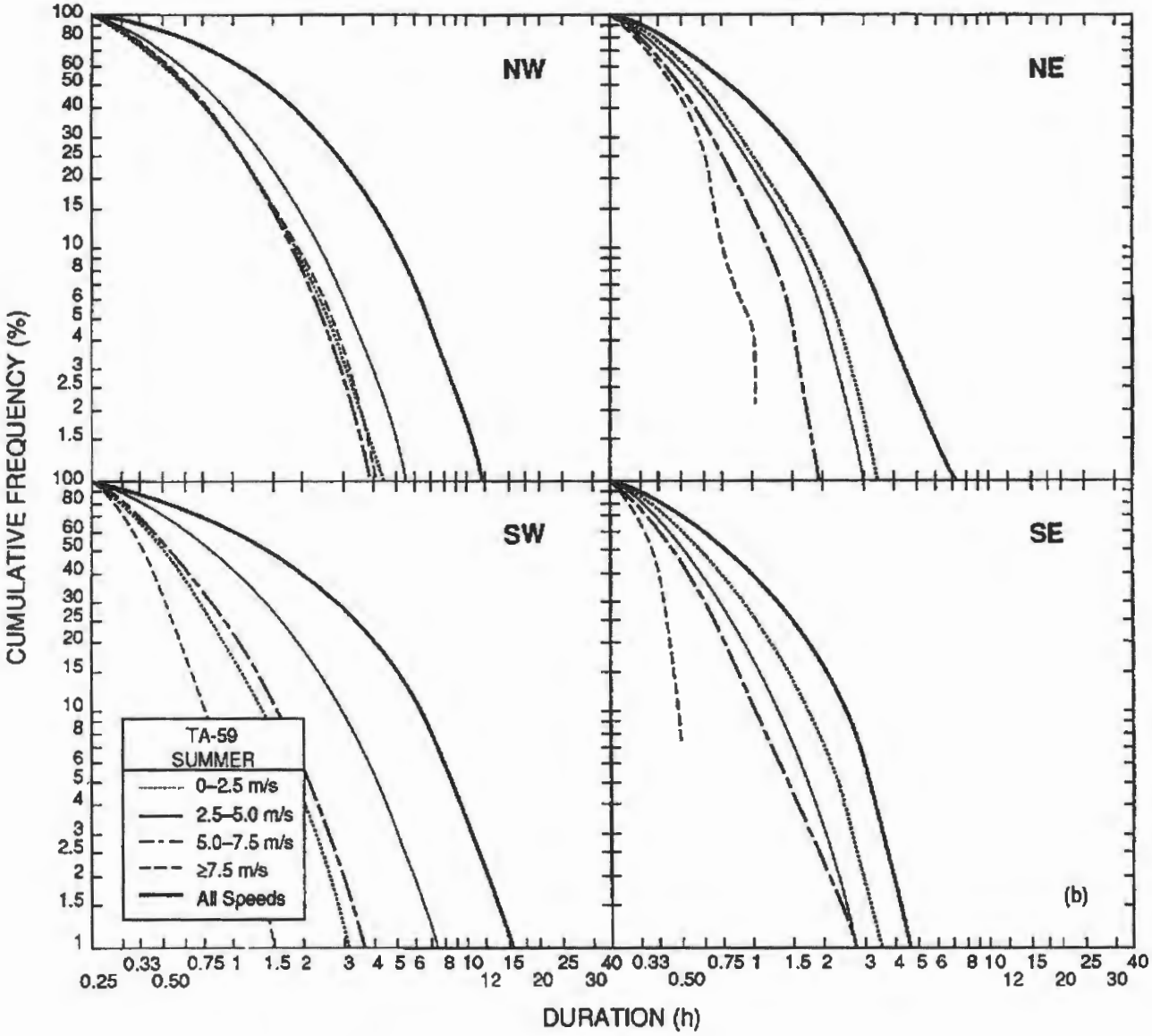

Fig. 11.1 (Continued)

(b) Summer persistence probabilities at TA-59 of wind-speed classes by directional quadrant. Persistence in summer is generally less than in winter. Strong NW'ly winds during summer are not as persistent as those occurring during winter. SW'ly winds are the most persistent, especially for moderate speeds.

example, a 2% frequency is associated with durations of 3–5 hours for the three lowest speed categories, 8 hours for the very strong wind-speed category, and 13 hours for the all-speeds category. These frequency analyses of NW'ly winds indicate that very strong winds are much more persistent than weaker winds and that the three weaker-wind classes are uniformly persistent, except for minor differences at low frequencies. NW'ly winds for all speeds (all-speeds class) are more persistent than winds in each speed class.

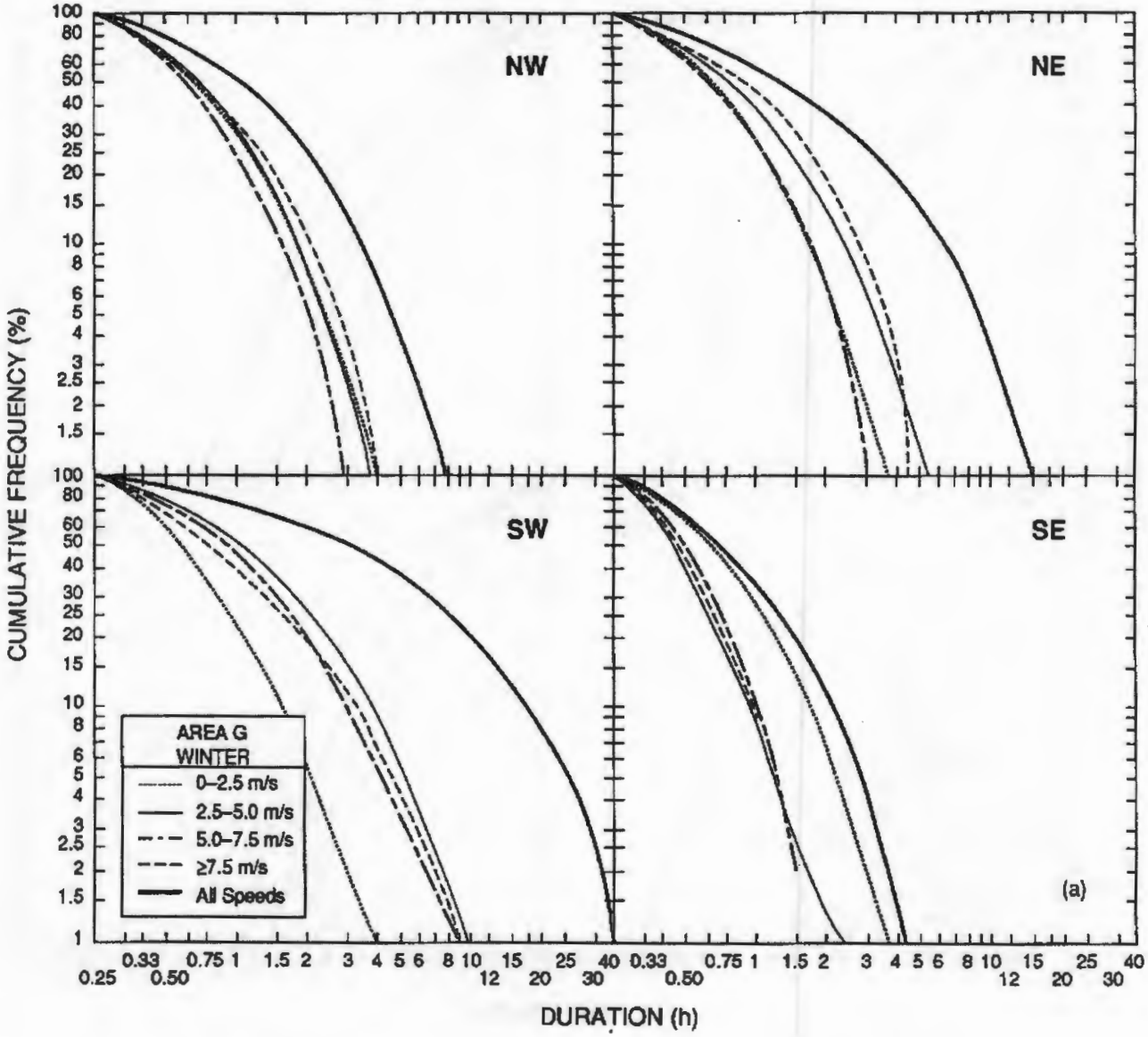

Fig. 11.2(a) and (b).

(a) Winter persistence probabilities at Area G of wind-speed classes by directional quadrant. High persistence of SW'ly winds is apparent for winds at most speeds, with less persistence of light winds. Relatively high persistence is seen for NE'ly winds. NW'ly wind persistence for all classes is much less at Area G than at TA-59.

One must exercise caution in using durations for very low frequencies, especially those below 0.5%. Reasons for this include (1) relatively short wind records, (2) the varying length of data records, and (3) infrequent occurrences of extremes.

Summer TA-59 persistence probabilities are shown in Fig. 11.1(b).

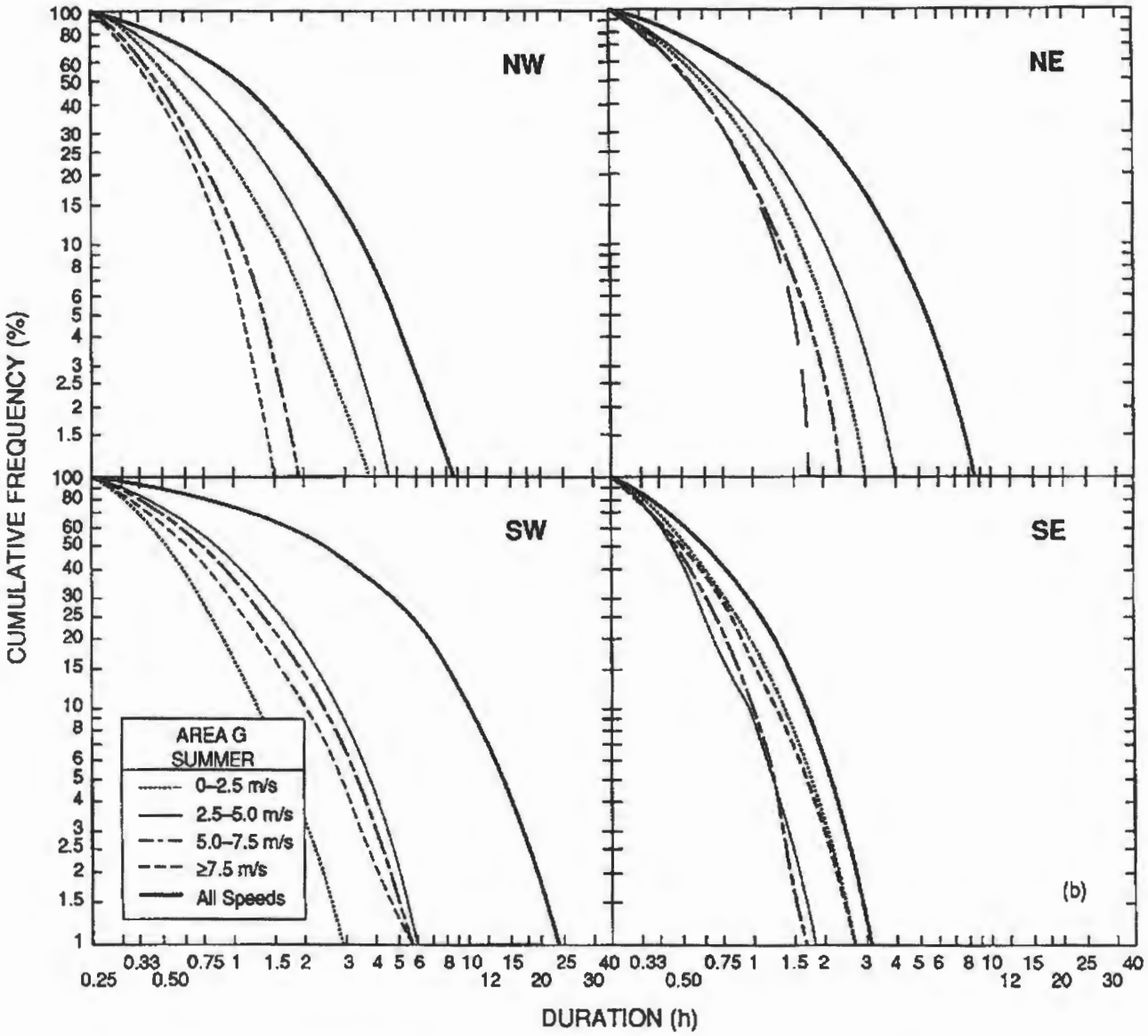

Fig. 11.2 (Continued)

(b) Summer persistence probabilities at Area G of wind-speed classes by directional quadrant. NW'ly wind persistence for moderate and strong wind speeds is less during the summer. Persistence at Area G in the summer is highest for SW'ly winds, but is less than in winter.

11.1.2 Discussion

The cumulative wind-direction persistence data (Figs. 11.1–11.3) for TA-59, Area G, and TA-50 (92 m) indicate differences associated with wind direction, site, elevation, height above ground, and season. Winds from the SW and, to a lesser extent, from the NE are the most persistent, especially in areas toward the valley (Area G) and at greater

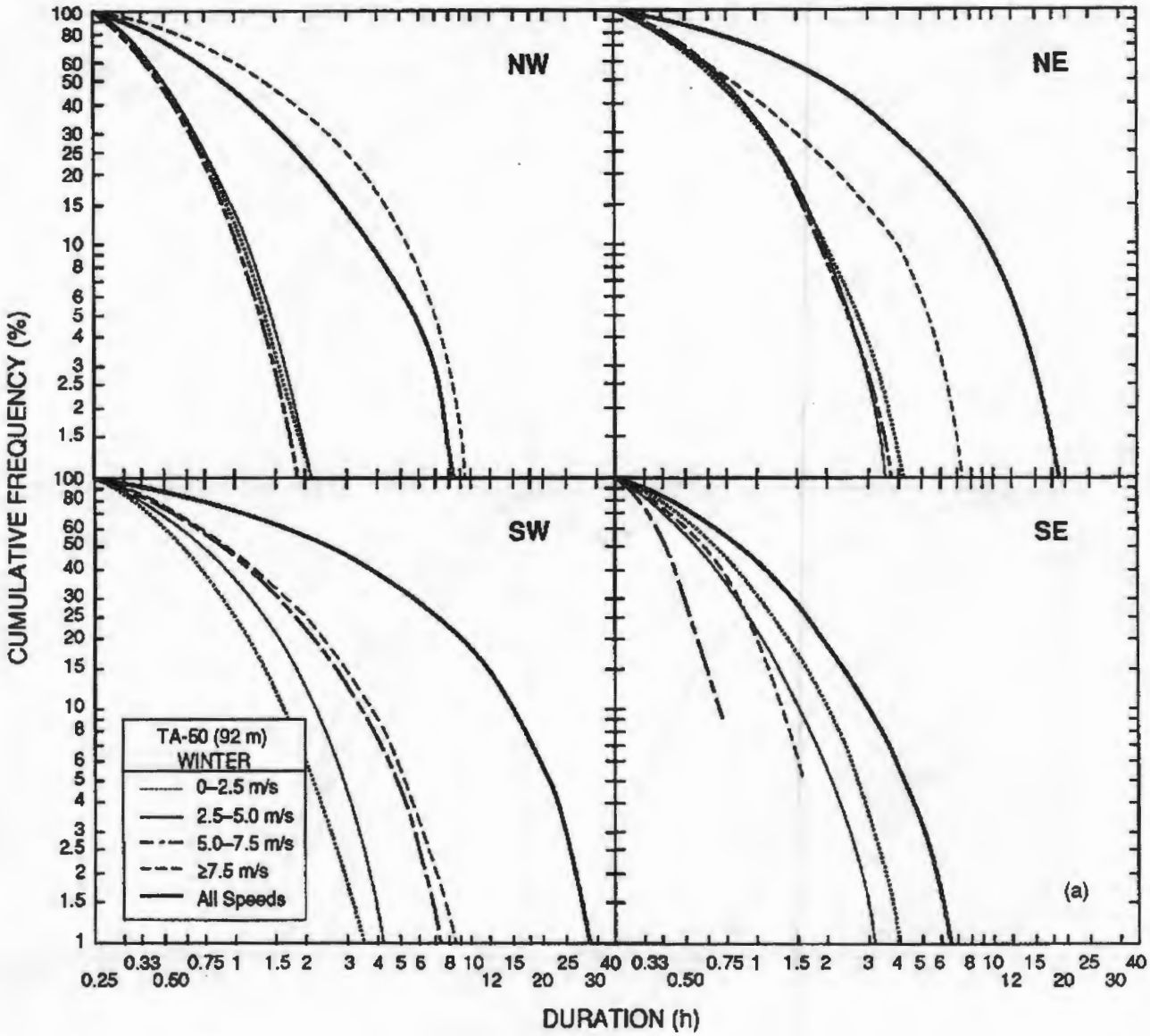

Fig. 11.3(a) and (b).

(a) Winter persistence probabilities at TA-50 (92 m) of wind-speed classes by directional quadrant. Persistence in the winter is less in the NW quadrant at TA-50 higher levels (92 m) than at TA-50 and TA-59 lower levels, except for strong winds. NE'ly wind persistence for strong winds is greater at TA-50 (92 m) than at both TA-59 and Area G. Persistence of stronger winds is noticeable in the SW quadrant, similar to persistence conditions at Area G.

heights above ground (TA-50, 92 m). The high persistence of SW'ly and NE'ly winds is largely because of the high frequency of regional-scale winds channeled by the Rio Grande Valley. The persistence of SW'ly and NE'ly surface winds decreases with increasing elevation (TA-59). Slope winds become increasingly important at TA-59. The 1% persistence for all SW'ly winds reaches 40 hours at Area G during the winter, with

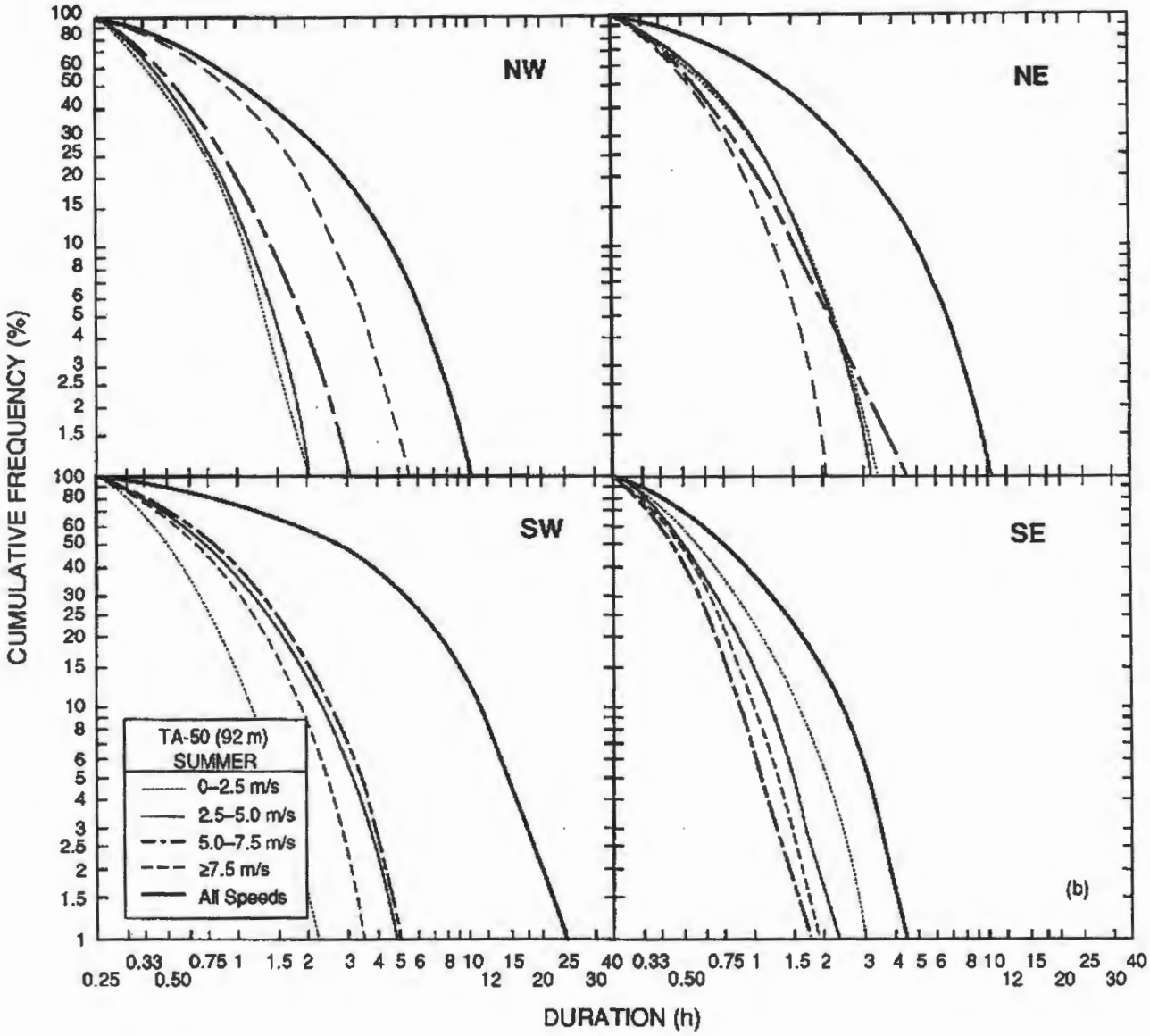

Fig. 11.3 (Continued)

(b) Summer persistence probabilities at TA-50 (92 m) of wind-speed classes by directional quadrant. Wind persistence in the NE and SW quadrants decreases somewhat from that in winter, especially for the stronger winds. Strong NW'ly winds are also less persistent in summer than in winter, but persistence of winds in the NW'ly all-speeds category edges up slightly.

the 5% and 10% frequencies reaching 27 and 18 hours, respectively. Frequencies of winds in the three strongest wind-speed classes are similar and are considerably less than frequencies of winds in the all-speeds class. Light winds are conspicuously less persistent than stronger winds. This is consistent with the fact that few light, up-valley winds occur at Area G. The persistence of SW'ly winds at TA-50 (92 m) is only slightly less than at Area G.

High persistence also occurs for NE'ly winds at all sites and elevations above ground, especially during the winter. The persistence is similar for near-surface winds at all sites, including East Gate and the 12-m level at TA-50 (not shown in the figures), although somewhat greater persistence is indicated at Area G and East Gate. Persistence is generally the highest for moderate winds above the 3% frequency level, and it also increases slightly for winds at higher levels, as at TA-50 (92 m).

Persistence of NW'ly winds varies markedly with site and height above ground. Wind persistence is high from the NW quadrant at TA-59 during the winter, and it is noticeably high for very strong winds . Lighter NW'ly winds, many of which are nighttime drainage winds, are less persistent than are the very strong winds. In contrast, NW'ly winds at Area G are noticeably less persistent. Also, very strong winds are only slightly more persistent than winds in the lower wind-speed classes. Near-surface NW'ly winds at TA-50 (not shown) actually have slightly higher persistence during summer than during winter, and light NW'ly winds at Area G also have slightly higher persistence in the summer. In addition, it is likely that NW'ly wind persistence increases in the summer over that for the winter for sites other than TA-59 because channeled SW'ly and NE'ly winds are less likely during the summer. This is true in spite of the fact that there are many more nighttime hours with NW'ly drainage winds <5.0 m/s in the winter than in the summer.

SE'ly winds are the least-persistent winds at all sites, both near-surface and at 92 m above the ground. Light winds are the most persistent of these SE'ly winds. SE'ly winds at all speeds have approximately 10% frequencies for 3–4 hours persistence and 2% frequencies for 5–6 hours persistence at TA-59 and TA-50 (92 m), as well as at TA-50 (12 m) and East Gate (not shown in the figures). Light winds from the SE have nearly the same frequency as that for winds in the all-speeds class. SE'ly wind persistence is markedly less at Area G, with nearly 50% less persistence than occurs at the other sites. The reason is that thermally driven, upslope winds frequently occur over the plateau during the day. However, Area G is located near the Rio Grande Valley and at the southeastern edge of the plateau. Upslope winds occur less frequently at Area G; hence, SE'ly winds are not very persistent once they form at Area G.

In general, summer winds are less persistent than winter winds in most directions. Stronger winds are especially less persistent during the summer. The difference between the seasons occurs because cyclones and anticyclones are much stronger during winter than during summer. The resulting horizontal pressure differences cause stronger and more-persistent regional winds during the winter season. Summer persistences drop by 30%–40% in the SW quadrant at all sites. NE'ly wind persistence decreases even more,

nearly 50%, from winter to summer at all sites. SW'ly and NE'ly wind persistence is less in the summer because regional-scale winds are very often channeled by the valley. However, regional-scale winds are more often light during summer than during winter. This, in turn, gives fewer channeled winds during the summer. In addition, summer large-scale winds are more frequent from the S than from the N. This explains why NE'ly wind persistence drops from winter to summer more than SW'ly wind persistence does.

At most sites, persistence changes less from winter to summer for NW'ly and SE'ly winds. However, near-surface NW'ly wind persistence at TA-59 drops substantially from winter to summer. The drop in persistence of winds in the all-speeds class is largely because of the large drop in persistence of very strong winds. The light and moderate wind-speed classes (≤5 m/s), largely associated with nighttime drainage winds, remain nearly the same for both seasons. SW'ly wind persistence decreases markedly at TA-50 (12-m level, not shown) and TA-59 (23 m). Note in the figures that the persistence analyses are similar for the TA-50 and TA-59 near-surface winds. Moderate SW'ly winds account for the greatest persistence at all locations, although SW'ly wind persistence generally is less at TA-59. Unlike Area G winds, strong winds at TA-50 and TA-59 are less persistent than are moderate winds.

Analyses of wind-speed persistence for spring and autumn (not shown) indicate that these seasons have persistence more similar to winter's than to summer's. Wind-speed persistence for stronger winds from the NW is even higher during spring than during winter.

In summary,

1. moderate to strong SW'ly winds are the most persistent at all sites and during all seasons, with the most persistence above the plateau and toward the valley;
2. light to moderate NE'ly winds are the next most persistent, especially above the plateau and toward the valley;
3. strong NW'ly winds are quite persistent in the winter, but light to moderate NW'ly winds in the winter are persistent only at near-surface levels, largely because of nighttime drainage winds;
4. the least-persistent winds are SE'ly. Of these winds, light winds are the most persistent, especially high on the plateau (TA-59, TA-50, and East Gate), because of daytime upslope winds; and
5. winds from all quadrants generally are less persistent during summer than during winter. Channeled NE'ly and SW'ly winds are especially less persistent during the summer. NW'ly wind persistence actually is slightly greater during the summer.

11.1.3 Persistence Tables

Wind-speed persistence data for 0.5% frequency probability and for the longest duration of wind-speed persistence on record are given in Tables 11.1 and 11.2 for winter and summer, respectively. Care should be taken in comparing durations among the sites, especially for the longest on record, because the data base varies from 3 years at TA-50 to 8 years at TA-59.

11.2 Wind-Direction Persistence

11.2.1 Explanation

Following are cumulative frequency analyses of wind directions for near-surface winds at TA-59 (23 m), Area G (11 m), and TA-50 (92 m) (Figs. 11.4–11.6). The

Table 11.1. Winter wind-speed persistence (in hours), for 0.5% frequency probability/longest duration on record.

	Wind-Speed Class				
Site	<2.5 m/s	2.5–5.0 m/s	5.0–7.5 m/s	>7.5 m/s	All Speeds
NW Quadrant					
TA-59 (23 m)	6.1/10.0	5.2/ 6.8	4.2/ 5.5	11.1/12.3	20.6/35.3
TA-50 (92 m)	2.5/ 3.3	2.5/ 3.5	2.2/ 2.8	10.2/10.8	9.6/11.8
TA-50 (12 m)	4.7/ 6.3	4.5/ 5.5	3.5/ 3.8	6.1/ 6.3	9.4/11.8
East Gate (12 m)	3.1/ 5.3	3.3/ 4.0	3.5/ 3.5	5.7/ 5.8	13.3/17.5
Area G (11 m)	5.3/14.0	4.1/ 5.8	3.3/ 3.8	4.3/ 4.3	9.5/14.0
NE Quadrant					
TA-59 (23 m)	6.1/12.3	5.2/ 7.0	3.4/ 3.5	4.0/ 4.0	18.7/24.8
TA-50 (92 m)	5.2/ 6.8	4.0/ 6.3	4.2/ 4.8	8.1/ 8.3	22.0/27.8
TA-50 (12 m)	6.2/ 8.3	5.4/ 6.0	7.3/ 7.3	—/—	18.4/22.5
East Gate (12 m)	6.0/ 8.5	5.9/ 7.0	3.8/ 4.0	2.0/ 2.0	18.9/28.5
Area G (11 m)	4.3/ 5.8	6.7/11.8	3.3/ 3.5	4.5/ 4.5	17.4/24.0
SE Quadrant					
TA-59 (23 m)	6.5/ 9.3	2.7/ 3.3	2.3/ 2.3	—/—	7.1/ 9.3
TA-50 (92 m)	4.6/ 6.0	3.4/ 4.0	—/—	—/—	7.1/ 9.5
TA-50 (12 m)	5.6/ 6.8	2.6/ 3.5	—/—	—/—	7.0/ 8.5
East Gate (12 m)	5.9/ 9.8	2.7/ 3.5	—/—	—/—	6.9/ 9.8
Area G (11 m)	4.4/ 7.0	3.1/ 3.5	—/—	—/—	5.0/ 7.0
SW Quadrant					
TA-59 (23 m)	4.1/ 8.0	10.3/14.5	6.2/ 7.3	6.0/ 6.0	30.8/47.0
TA-50 (92 m)	4.0/ 5.3	4.7/ 5.5	7.9/10.0	9.6/11.0	41.2/54.0
TA-50 (12 m)	4.3/ 5.5	11.1/14.0	7.3/ 8.3	—/—	32.9/46.5
East Gate (12 m)	4.1/ 6.5	7.2/12.3	8.2/11.0	10.1/11.5	35.4/53.5
Area G (11 m)	5.6/ 9.8	12.2/17.0	11.1/14.3	10.3/11.0	44.5/54.0

analyses are presented for the winter (December–February) and summer (June–August) seasons. Persistence is analyzed for (and centered on) each compass point (N, NNE, NE, and so forth). Because wind-direction variability limits persistence in one direction, persistence was calculated for a range of three adjacent direction sectors (67.5° total width) centered on one direction. For example, a 3-hour persistence of SSW'ly winds includes SSW'ly as well as SW'ly and S'ly winds. Winds centered on N'ly through ENE'ly directions are listed in the NE quadrant, and E'ly through SSE'ly winds are listed in the SE quadrant.

Wind-direction persistence is useful in determining risks from downwind transport of airborne pollutants or toxic materials from an atmospheric release. For example, a relatively high SW'ly wind persistence indicates an increased chance of a lengthy transport toward the NE. Note that high persistence does not necessarily correlate with high probability; for example, a common wind direction may not be very persistent and vice versa.

Table 11.2. Summer wind-speed persistence (in hours), for 0.5% frequency probability/longest duration on record.

	Wind-Speed Class				
Site	<2.5 m/s	2.5–5.0 m/s	5.0–7.5 m/s	>7.5 m/s	All Speeds
NW Quadrant					
TA-59 (23 m)	4.9/7.5	6.2/ 8.5	4.4/5.0	—/—	13.3/20.0
TA-50 (92 m)	2.3/3.0	2.3/ 2.8	3.5/4.8	6.7/7.8	11.1/13.8
TA-50 (12 m)	4.9/6.3	5.7/ 7.8	2.9/3.3	—/—	10.6/13.8
East Gate (12 m)	2.3/3.0	4.4/ 6.5	3.7/4.8	4.6/4.8	8.0/15.0
Area G (11 m)	4.1/6.8	5.3/ 7.3	2.3/2.8	—/—	10.1/15.0
NE Quadrant					
TA-59 (23 m)	3.8/4.8	3.8/ 5.3	2.0/2.0	—/—	9.0/14.3
TA-50 (92 m)	4.0/5.0	3.7/ 4.0	5.5/6.0	—/—	9.2/12.0
TA-50 (12 m)	3.6/4.5	3.7/ 4.0	—/—	—/—	9.0/13.3
East Gate (12 m)	4.9/6.3	5.7/ 7.5	—/—	—/—	9.1/13.0
Area G (11 m)	3.4/4.5	4.9/ 6.5	2.7/2.8	—/—	9.2/12.0
SE Quadrant					
TA-59 (23 m)	3.9/5.0	3.3/ 5.3	3.2/3.5	—/—	5.4/ 9.8
TA-50 (92 m)	3.4/4.0	2.8/ 4.0	2.0/2.3	—/—	4.9/ 6.0
TA-50 (12 m)	4.1/4.8	3.0/ 3.8	—/—	—/—	5.1/ 7.0
East Gate (12 m)	3.7/5.0	2.2/ 3.5	3.0/3.8	—/—	5.0/ 7.3
Area G (11m)	3.1/3.5	2.2/ 3.5	2.1/2.5	—/—	3.5/ 5.3
SW Quadrant					
TA-59 (23 m)	3.5/5.5	8.6/12.8	3.9/4.5	—/—	18.3/35.8
TA-50 (92 m)	2.4/2.8	5.6/ 7.3	5.4/6.3	3.9/4.5	32.6/41.8
TA-50 (12 m)	5.7/8.5	11.0/16.3	4.5/5.0	—/—	26.9/38.5
East Gate (12 m)	2.5/3.0	7.1/ 9.5	4.9/6.3	3.7/3.7	20.4/34.0
Area G (11 m)	3.6/5.3	7.6/13.5	6.9/9.8	7.4/8.8	30.4/43.8

11.2.2 Discussion

Wind-persistence analyses for near-surface winds at TA-59 and Area G reveal extremes over the Pajarito Plateau. Area G surface winds during the winter are often channeled by the Rio Grande Valley. Note the high persistence of winds from the SSW and adjacent directions. High persistence is also noted from the N and NNE. Wind persistence at TA-59 is less affected by channeled flow and increasingly affected by slope flow. As at Area G, persistence is greatest at TA-59 for SSW'ly winds and winds

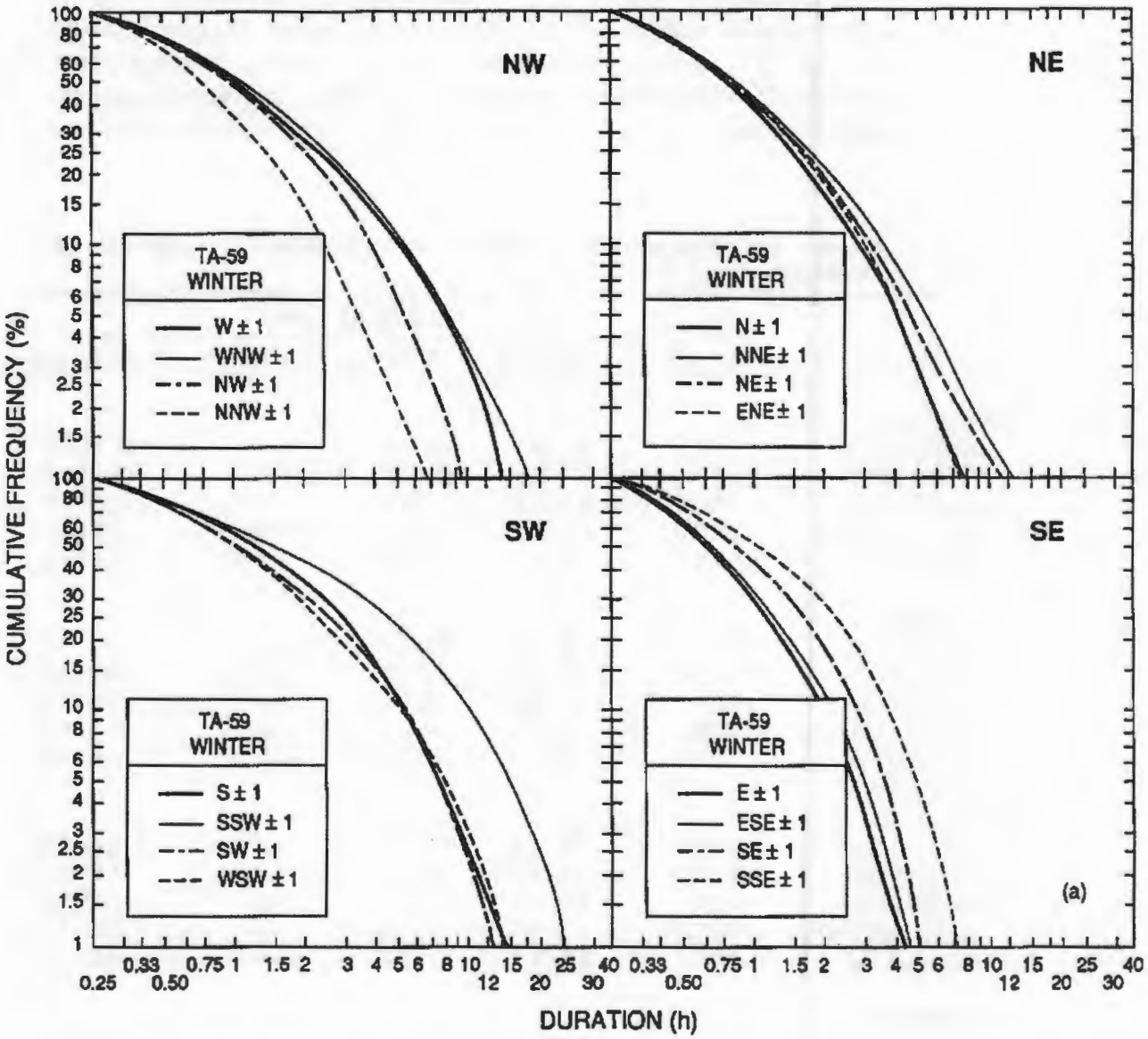

Fig. 11.4(a) and (b).

(a) Winter persistence probabilities at TA-59 of wind directions ±1 direction. SSW'ly wind persistence during winter is highest by far. Persistence is also high for winds from the S, the SW through NW, and the NNE through NE.

from adjacent directions, but W-WNW'ly winds are also persistent. The W-NW'ly winds are much more persistent at TA-59 than at Area G.

Above-surface winds at TA-50 (92 m) have persistence qualities similar to those at Area G. The wind-persistence peaks at TA-50 that are centered on the SSW and NE are even greater than those at Area G. The slight increase in W-WNW'ly wind persistence found at TA-50 (92 m) is not found at Area G. Analyses of near-surface winds at TA-50

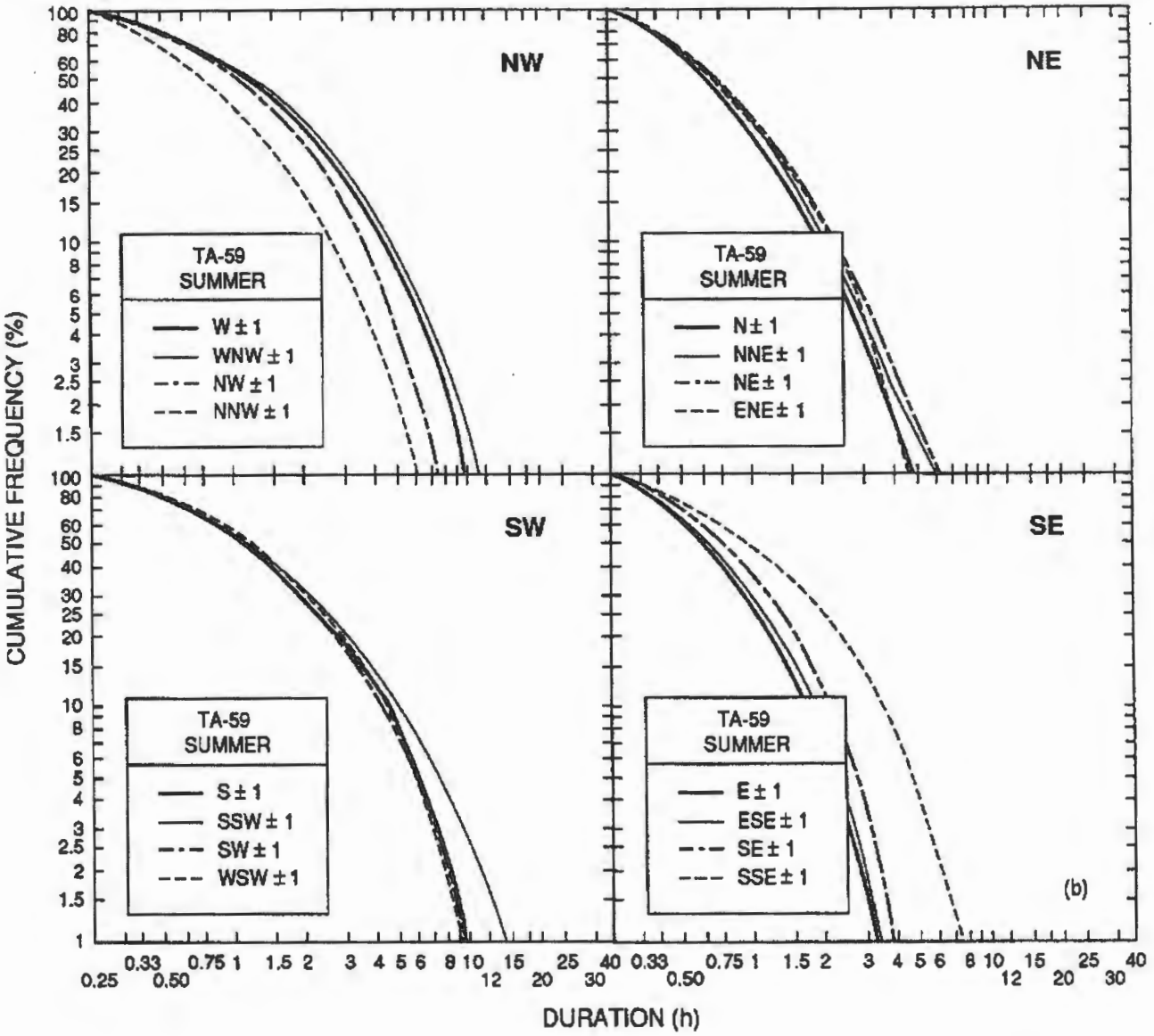

Fig. 11.4 (Continued)

(b) Summer persistence probabilities at TA-59 of wind directions ±1 direction. As during the winter, persistence in the summer peaks from the SSW and is relatively high from the W through the WNW. Unlike persistence in the winter, no secondary peaks are apparent from the NNE and NE.

(12-m level, not shown in the figures) indicate persistence characteristics much closer to those for TA-59 than those for TA-50 (92 m). Specifically, measurements at the TA-50 lower level (12 m) show less channeled (SSW-SW'ly and N-NE'ly) wind persistence and increased W-NW'ly wind persistence. Wind-persistence analyses for East Gate (not shown) generally show an average between persistence levels at TA-59 and those at Area G.

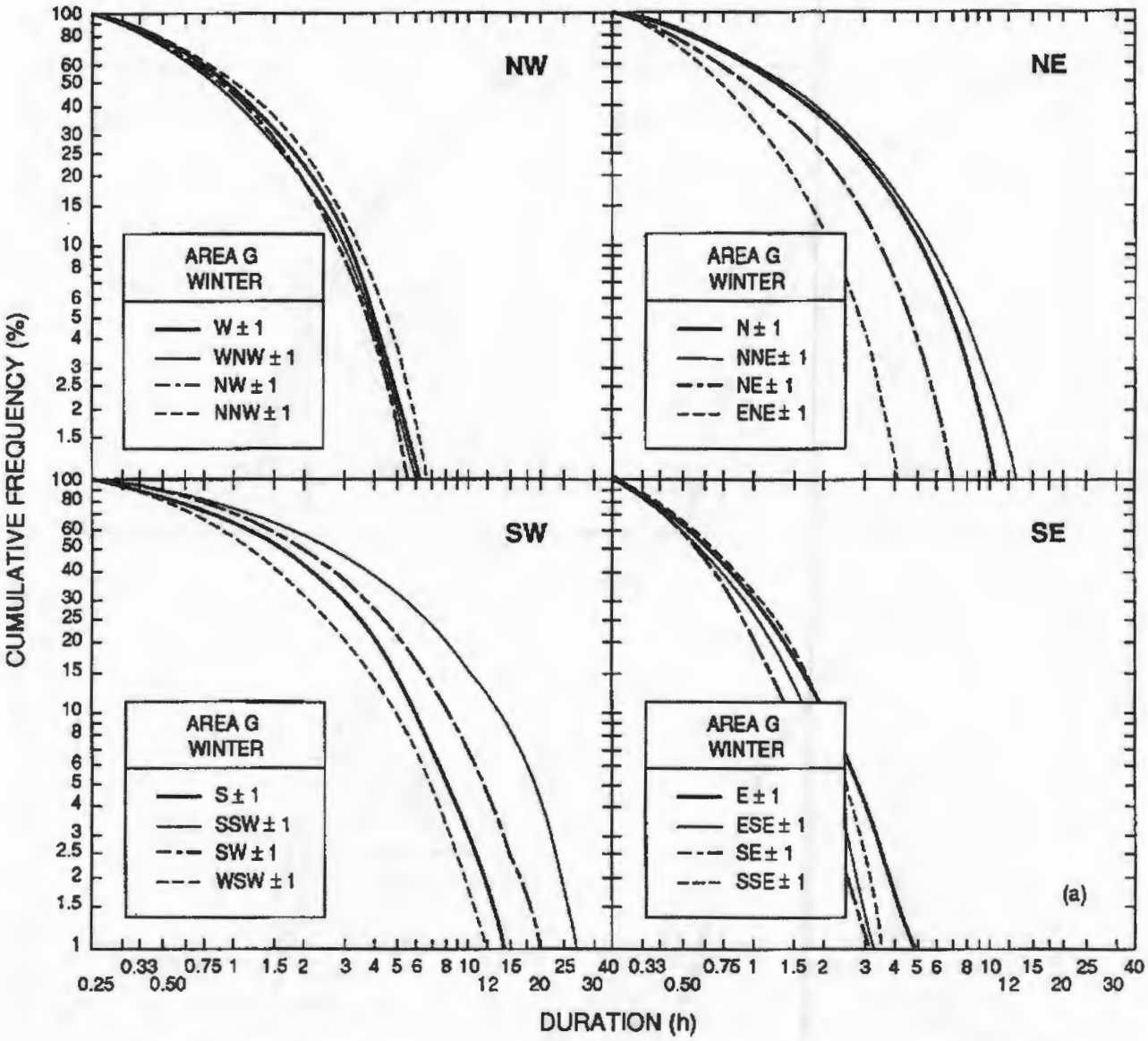

Fig. 11.5(a) and (b).

(a) Winter persistence probabilities at Area G of wind directions ±1 direction. Note the dramatic bimodal peaks in frequency of persistence from the NNE and the SSW. Persistence is also quite high from the S and SW through the WSW and from the N and NE.

Wind persistence during summer is less for winds from channeled directions and especially decreases for N-NE'ly winds. Persistence for S-SW'ly winds shows a smaller decrease. Slope wind persistence generally increases during the summer. W-WNW'ly wind persistence increases at all sites, except at TA-59, and S-SE'ly wind persistence also increases somewhat at all sites.

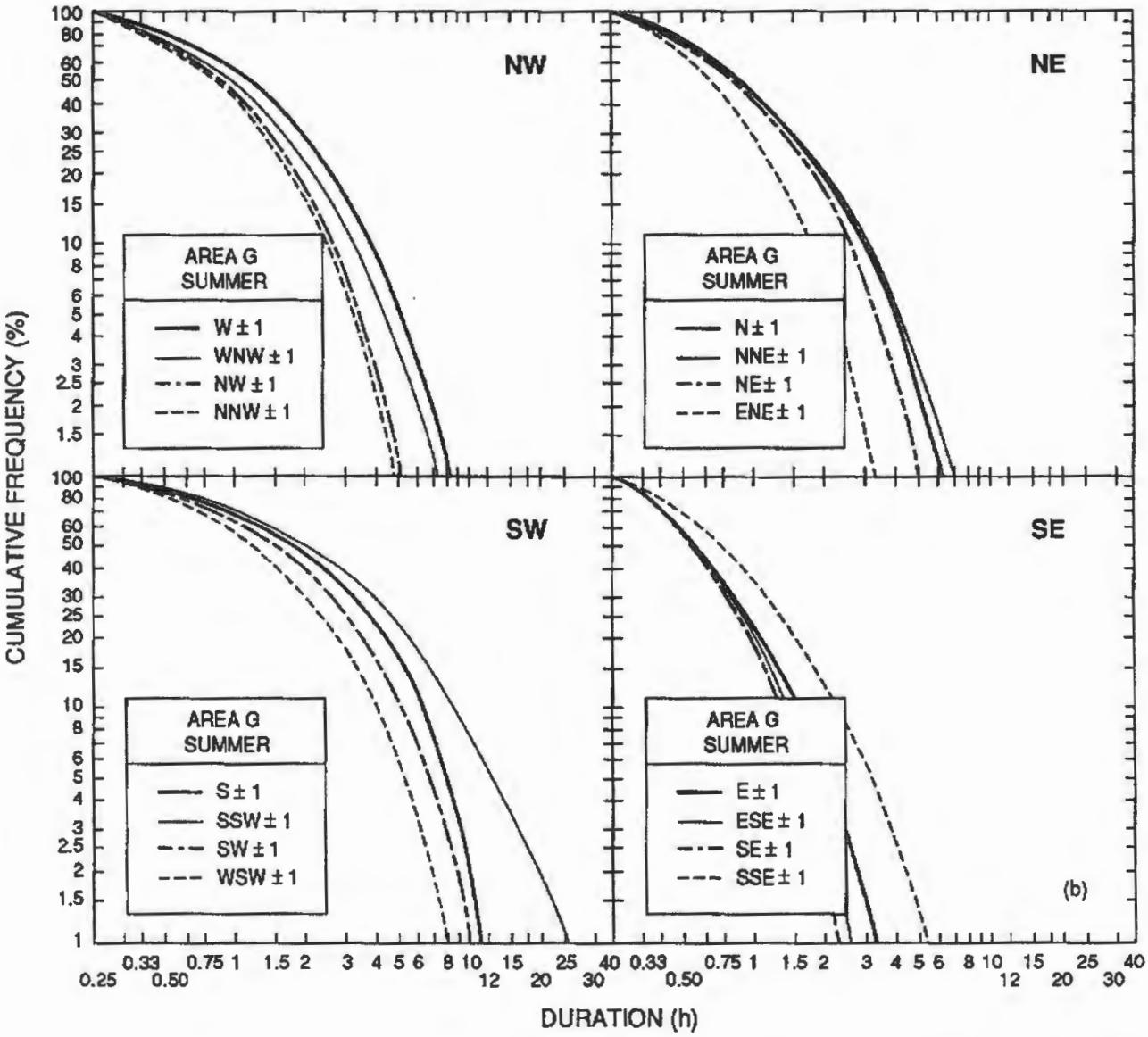

Fig. 11.5 (Continued)

(b) Summer persistence probabilities at Area G of wind directions ±1 direction. The SSW'ly wind persistence in the summer falls off only modestly from persistence levels in the winter in contrast to drops in persistence at other sites. S'ly through WSW'ly wind persistence remains relatively high, but falls off considerably from winter levels. The peak of NNE'ly wind persistence in the summer falls off dramatically from that in the winter. Persistence from the W through the WNW increases slightly from that in the winter.

At most sites, wind persistence during the spring and autumn (not shown) is more similar to persistence during winter than that during summer. Summer, with its light winds, has less-persistent channeled winds, but slope winds are generally slightly more persistent than they are during all other seasons.

In summary,

1. channeled winds from the SSW and adjacent directions are the most persistent at all sites, especially winds above surface and toward the Rio Grande Valley;

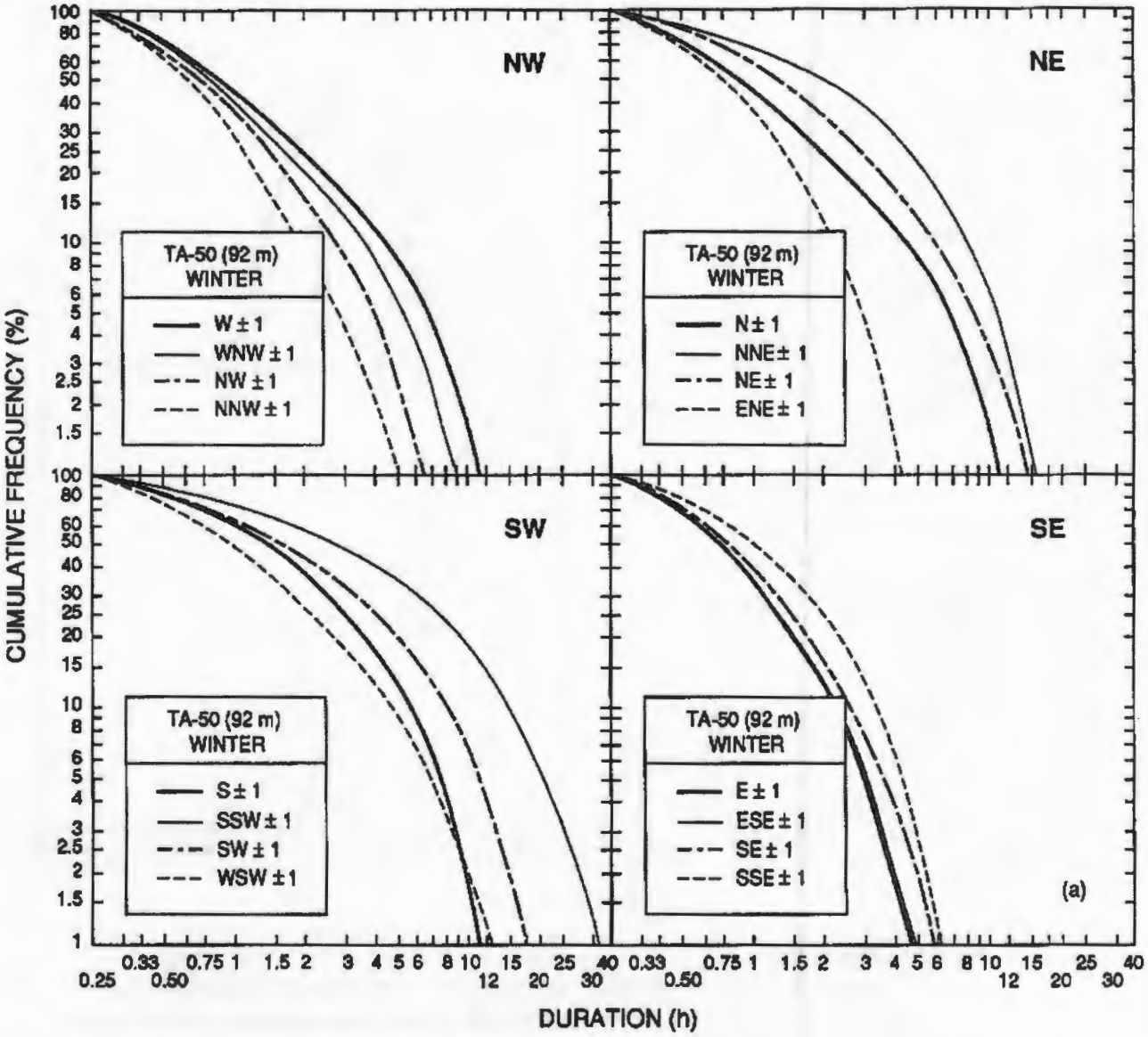

Fig. 11.6(a) and (b).

(a) Winter persistence probabilities at TA-50 (92 m) of wind directions ±1 direction. Persistence peaks from the SSW, with relatively high persistence from the S and SW through W. Persistence is also high from the N through the NE.

2. downslope winds from the W-WNW are more persistent at TA-59 and TA-50 (12 m) because of surface drainage winds at night;

3. channeled winds from the SSW and NNE are less persistent during the summer, especially NNE'ly winds; and

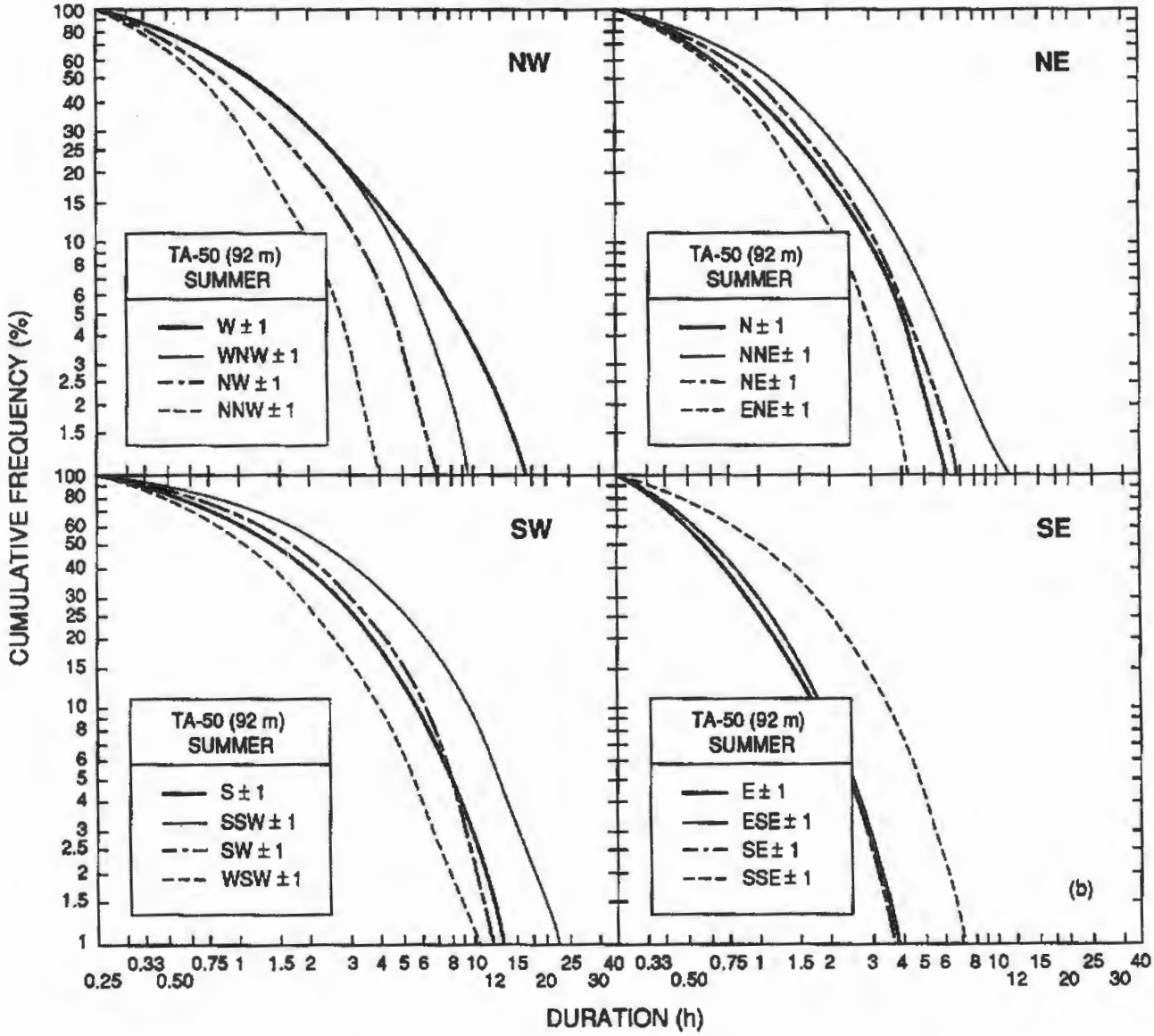

Fig. 11.6 (Continued)

(b) Summer persistence probabilities at TA-50 (92 m) of wind directions ±1 direction. SSW'ly wind persistence is highest, but less so than during the winter. S'ly winds show a slight increase in persistence during summer, but SW'ly through WSW'ly wind persistence is little changed. Note that W'ly wind persistence increases substantially from that in the winter. Also, wind persistence from the N through NE decreases sharply from that in the winter.

4. slope winds generally are more persistent during the summer, except for W-WNW'ly winds at TA-59.

11.2.3 Persistence Tables

Wind-direction persistence data for winter and summer for 0.5% frequency probability and for the longest duration of wind persistence on record are given in Tables 11.3

Table 11.3. Wind-direction persistence (in hours) for a single direction, for 0.5% frequency probability/longest duration on record.

	Winter				Summer			
Site	N	NNE	NE	ENE	N	NNE	NE	ENE
TA-59 (23 m)	19.3/24.8	8.3/13.0	2.5/ 3.8	1.9/ 2.5	2.7/3.8	2.9/5.0	2.4/ 3.8	1.8/2.8
TA-50 (92 m)	7.8/ 9.8	12.0/16.8	3.5/ 4.5	2.5/ 3.8	3.6/4.0	3.9/4.8	2.6/ 4.0	1.7/1.8
TA-50 (12 m)	5.2/ 7.0	6.2/ 7.8	2.9/ 3.3	1.9/ 2.3	2.2/3.0	1.8/1.8	3.6/ 4.0	1.6/2.3
East Gate (12 m)	5.1/11.0	3.4/ 5.3	3.5/ 4.8	3.1/ 5.3	2.7/3.3	2.7/4.0	2.6/ 3.5	2.2/2.8
Area G (11 m)	5.1/ 7.5	3.4/ 4.5	2.7/ 5.0	1.6/ 2.3	3.2/5.0	2.7/4.0	21.9/ 2.3	1.7/2.3
Site	E	ESE	SE	SSE	E	ESE	SE	SSE
TA-59 (23 m)	1.9/ 3.0	1.8/ 2.8	2.5/ 3.5	3.1/ 4.5	1.7/2.0	1.8/2.3	1.7/ 2.3	2.4/3.3
TA-50 (92 m)	2.2/ 2.8	1.6/ 1.8	4.0/ 5.0	2.2/ 3.0	2.4/3.0	1.5/1.8	1.8/ 2.0	2.4/3.3
TA-50 (12 m)	2.0/ 2.8	2.4/ 3.3	2.0/ 3.3	2.2/ 2.3	1.9/2.3	1.4/1.5	1.7/ 2.0	2.2/3.3
East Gate (12 m)	5.1/ 9.3	1.0/ 1.3	2.5/ 3.5	2.7/ 3.5	1.7/2.3	1.7/1.8	2.0/ 2.5	3.6/6.0
Area G (11 m)	3.2/ 5.0	1.5/ 2.0	1.2/ 1.3	1.7/ 2.0	1.2/1.3	1.5/2.0	1.3/ 1.3	2.6/3.8
Site	S	SSW	SW	WSW	S	SSW	SW	WSW
TA-59 (23 m)	6.0/ 8.3	7.3/11.5	4.2/ 7.0	5.4/ 6.8	4.0/7.3	4.5/7.3	2.6/ 3.3	5.2/9.0
TA-50 (92 m)	5.6/ 7.5	7.5/11.5	7.2/ 8.5	2.8/ 3.3	5.7/8.0	4.7/6.8	8.6/10.8	3.1/4.8
TA-50 (12 m)	6.9/ 9.5	5.0/ 6.5	7.0/ 9.5	7.2/10.0	2.9/3.5	2.9/4.3	5.6/ 8.0	3.2/4.3
East Gate (12 m)	12.6/17.9	10.1/16.8	14.6/22.8	3.2/ 4.3	1.9/2.8	4.1/6.5	7.8/11.0	3.2/4.0
Area G (11 m)	9.2/14.3	8.7/13.8	4.9/ 6.5	4.6/ 7.0	4.0/6.3	4.0/5.8	3.6/ 6.0	4.0/5.8
Site	W	WNW	NW	NNW	W	WNW	NW	NNW
TA-59 (23 m)	10.0/16.3	5.3/ 8.0	3.7/ 6.5	2.0/ 4.8	4.3/7.0	6.5/8.8	5.2/ 6.8	2.2/3.0
TA-50 (92 m)	4.9/ 5.8	4.0/ 4.5	4.6/ 5.3	1.4/ 1.5	3.4/4.0	6.3/7.3	4.3/ 5.3	1.9/2.3
TA-50 (12 m)	4.6/ 5.5	4.5/ 5.5	3.2/ 4.8	2.1/ 2.8	4.3/4.8	5.3/7.0	2.3/ 2.8	2.2/2.8
East Gate (12 m)	2.7/ 3.3	5.9/ 8.3	3.3/ 4.5	2.3/ 3.0	3.2/4.0	4.3/5.0	4.4/ 6.8	2.0/2.5
Area G (11 m)	4.2/ 6.0	3.5/ 4.5	3.2/ 5.8	2.4/ 3.3	3.7/5.8	4.4/5.5	2.4/ 3.0	2.3/3.3

and 11.4. Table 11.3 lists persistences of single directions, and Table 11.4 lists persistences of directions ±1 direction (a centered direction and directions on each side). Care should be taken in comparing durations among the sites, especially for the longest on record, because the data base varies from 3 years at TA-50 to 8 years at TA-59.

Table 11.4. Wind-direction persistence (in hours) for a centered direction ±1 direction, for 0.5% frequency probability/longest duration on record.

	Winter				Summer			
Site	N	NNE	NE	ENE	N	NNE	NE	ENE
TA-59 (23 m)	11.2/16.3	17.7/24.5	16.2/22.5	11.3/16.5	6.0/ 9.0	8.0/14.3	8.0/11.8	5.3/ 6.5
TA-50 (92 m)	12.8/17.3	18.2/24.5	16.6/22.5	5.2/ 7.3	7.5/ 9.3	14.5/18.0	7.7/10.0	4.8/ 5.8
TA-50 (12 m)	10.8/15.5	16.3/22.5	9.5/12.0	7.0/ 8.3	4.3/ 5.5	10.0/13.3	6.3/ 7.5	5.5/ 8.3
East Gate (12 m)	11.8/16.8	17.0/26.5	11.7/16.3	7.0/ 9.5	5.9/ 7.5	7.5/ 9.8	8.5/11.5	5.3/ 7.0
Area G (11 m)	12.6/22.3	14.9/21.5	8.2/14.0	4.8/ 6.3	7.8/12.0	8.7/12.0	5.7/ 6.8	3.8/ 5.0
Site	E	ESE	SE	SSE	E	ESE	SE	SSE
TA-59 (23 m)	5.4/ 7.0	5.6/ 7.3	8.0/11.0	8.0/11.0	3.7/ 5.0	3.9/ 6.0	4.4/ 6.3	9.2/12.8
TA-50 (92 m)	5.8/ 7.8	5.8/ 7.0	6.4/ 7.8	7.1/13.8	4.7/ 5.8	4.4/ 5.5	4.0/ 5.0	8.0/ 9.3
TA-50 (12 m)	5.7/ 7.3	6.1/ 8.0	5.3/ 7.5	8.5/13.3	3.8/ 4.8	4.1/ 5.5	4.4/ 7.0	7.3/10.8
East Gate (12 m)	6.3/ 9.3	5.3/ 9.3	5.2/ 7.5	7.0/ 9.8	4.1/ 6.8	4.1/ 5.8	4.1/ 5.5	5.5/ 8.3
Area G (11 m)	5.9/ 8.3	3.7/ 5.0	4.2/ 6.0	4.1/ 5.5	3.7/ 4.8	2.8/ 3.5	2.7/ 4.3	6.7/ 9.8
Site	S	SSW	SW	WSW	S	SSW	SW	WSW
TA-59 (23 m)	18.1/23.8	28.4/35.0	14.1/19.5	15.7/19.3	11.3/15.0	20.3/34.8	11.3/16.8	10.5/13.0
TA-50 (92 m)	12.6/14.5	36.7/43.8	20.5/28.3	17.0/22.5	15.0/20.0	27.8/36.5	13.9/20.0	13.4/16.5
TA-50 (12 m)	24.7/32.3	26.1/31.5	34.1/43.5	22.7/32.3	13.9/17.8	26.0/34.8	9.9/13.8	10.6/16.3
East Gate (12 m)	16.9/20.0	36.4/47.8	18.7/24.3	23.9/28.0	8.9/15.0	15.9/22.0	14.4/20.8	15.0/18.8
Area G (11 m)	17.2/28.5	35.1/42.8	22.3/27.5	13.6/20.0	12.9/18.5	30.3/42.3	12.0/13.8	9.1/12.3
Site	W	WNW	NW	NNW	W	WNW	NW	NNW
TA-59 (23 m)	20.3/29.3	24.5/35.3	10.8/14.0	8.1/12.7	11.6/18.3	12.6/19.3	8.3/12.0	6.9/ 9.8
TA-50 (92 m)	33.3/35.8	10.0/11.5	7.3/ 8.5	6.4/10.0	18.7/20.8	10.6/13.3	8.2/10.0	4.4/ 5.3
TA-50 (12 m)	10.7/16.3	8.4/11.5	6.9/10.0	7.6/11.5	10.2/17.8	9.9/13.3	7.4/10.0	4.5/ 5.3
East Gate (12 m)	12.6/16.5	12.5/15.5	8.7/12.5	6.0/10.8	9.9/12.0	6.5/10.0	6.0/ 8.0	4.3/ 5.0
Area G (11 m)	7.7/11.5	7.5/12.8	6.6/13.0	7.6/10.8	9.7/13.0	9.1/13.2	5.9/ 7.9	5.5/ 7.0

Appendix A

Historical Locations of Weather Stations

Climate record reliability depends on instrument accuracy, data recovery, and siting consistency. The Los Alamos cooperative weather station, in operation since late 1910, has been moved several times. Table A.1 lists historical station site information. Notice that although the Los Alamos station has been moved several times, the elevation and locations have changed very little except for a brief period during 1950–1951 when the site was located farther east at the airport. Airport temperatures are higher and precipitation is lower than at other sites because of the lower elevation and greater distance from the Jemez Mountains. The station was moved to the Laboratory in 1952 at a site only slightly higher in elevation than the sites for 1910–1950. The station was again moved a short distance in 1956, when temperatures were measured on the roof of a building at SM-43 for a 5-month period. Temperatures generally would have had a decreased diurnal range on the roof, with lower high temperatures and higher low temperatures. Later in 1956, the temperatures were measured at the standard ground level (4 to 5 ft above ground). The station was moved again a short distance to TA-59 in late 1978 or early 1979, where it is still located (late 1989). Present plans call for moving the site in early 1990 to a location 0.5 mile (800 m) south of TA-59 at a slightly higher elevation of 7425 ft.

The Los Alamos weather station siting has actually stayed rather uniform, despite the moves. The elevations above sea level have remained within a 100-ft range, and the locations are within a 1-mile (1.6-km) distance, except for the 1950–1951 period. Temperatures probably showed more moderate diurnal ranges during the 5-month period in 1956 when temperatures were measured on the roof. Generally, however, the temperature and precipitation records are thought to be little affected by the different locations, except for the above examples. Data recovery has been good, except for some periods from 1917 to 1923 and 1943 to 1945.

The White Rock station has remained at the same site since it was started in late 1964. Data recovery at this station has been mostly complete, except for 8 months beginning in late 1979 and 2 months in early 1981.

Table A.1. Historical weather station locations (for temperature and precipitation).

Site	Dates	Elevation (ft ASL)	Latitude	Longitude	Comments
Los Alamos Weather Station:					
Ranch School	11/1/1910	7320	35°53′ N	106°18′ W	Temperature records began, 10/19/1918 No data: 11/1916–2/1917, 8/1917–1/1918, 3/1918–7/1918, 9/1920–3/1922, 12/1922–1/1923, 10–11/1923, 1/1943, 4–5/1943, 9/1945
Townsite	3/19/1946–4/30/1950	7320	35°53′ N	106°18′ W	Very close to previous site
Airport	5/1/1950–12/31/1951	7150	35°53′ N	106°16′ W	Temperatures not representative (too high during 1950)
Laboratory Sites:					
H/Ad	1/1/1952–3/20/1956	7410	35°52′ N	106°19′ W	
SM-43	3/21/1956–8/31/1956	7400	35°52′ N	106°19′ W	Temperature measured on roof
SM-43	9/1/1956–1978	7400	35°52′ N	106°19′ W	Thermometer moved to ground
TA-59	1979–1989	7380	35°52′ N	106°19′ W	Station moved to TA-59 in 1978 or 1979
TA-6	1990–	7425	35°51′ N	106°19′ W	Proposed new site
White Rock Weather Station:					
Fire Station	9/21/1964–present	6380	35°50′ N	106°12′ W	Data missing: 11/1979–6/1980; 2/1981–3/1981

Appendix B

Future Plans

Starting in 1990, temperature, relative humidity, and precipitation, which are measured as part of the National Weather Service's Cooperative Weather Observer Program and used as the official Los Alamos weather records, will be taken at TA-6. The new site will be located about 2500 ft (760 m) from the TA-59 site at a nearly identical elevation. Temperatures and relative humidity will be measured electronically with a ventilated thermistor, replacing the maximum/minimum thermometers and hygrothermograph now located in a shelter at TA-59. The White Rock hygrothermograph will also be replaced by electronic sensors in 1990.

Weather normals for the latest 30 years will be updated in early 1991 and will include the years 1961–1990 at the Los Alamos site. White Rock normals will include the years 1964–1990. The comparison of the updated Los Alamos and White Rock normals will be more reliable because the data records at the two sites will be more similar.

The 300-ft (92-m) meteorological tower at TA-50 has been moved to the TA-6 site, and data should be routinely acquired beginning in 1990. Additional instruments are planned to be installed that measure net radiation, ground reflection of insolation, soil temperature, and soil heat conduction. In addition, a Doppler acoustic sodar (*so*und *d*etection *a*nd *r*anging), installed during 1989, will measure winds and turbulence up to a height of 2460 ft (750 m) above the ground.

The East Gate and TA-54 (Area G) towers will be replaced with taller ones so that wind and temperature can be measured at three levels, up to a height of 150 ft (46 m) above ground level (AGL). The towers will be identical to the one at Bandelier. The East Gate tower will be relocated across the Los Alamos Canyon, close to the Los Alamos Meson Physics Facility's release stack, and the Area G tower will be relocated toward White Rock.

Several more rain gauges may be added to the existing network in the next few years. Maximum wind gusts and measurements of wind direction and speed every minute will be recorded at all of the tower sites.

The additional data from the expanded East Gate and Area G towers, together with the Bandelier and TA-6 data, will be analyzed after several years of data have been acquired. A precipitation data base covering a longer period will allow more-accurate regional analysis and will also allow more-accurate analyses of precipitation extremes for specified durations. Wind-speed analyses of extreme gusts will be made when more wind data are available. Normal climate data for the 30 years ending in 1990 will be calculated and made available in early 1991. Finally, analyses of turbulence and wind data recorded at levels up to 2460 ft (750 m) above the ground will be made after several years of Doppler acoustic sodar data are available. An updated climate manual that includes these new data should be published in the future, possibly in 1992–1993.

Appendix C

Data Quality and Accuracy

Regularly scheduled calibrations are made on all instruments, and data are routinely checked for data quality. Quality assurance is given a high priority in order to achieve optimum data accuracy and to comply with state and federal meteorological monitoring standards. An outside contractor audits the instruments once a year. The reader may consult "Meteorological Quality-Assurance Program of the Los Alamos National Laboratory's Environmental Surveillance Group, HSE-8" (Olsen and Dewart 1986) for a complete description of the meteorological data quality-assurance program.

Following are accuracy estimates for the instruments and their systems that produced data used in this report. Note that the accuracy is estimated for the instrument-measuring system and not just for the instrument. For example, a wind vane may be accurate within 1° in a laboratory, but when placed in the field the measurement error may be within several degrees when tower siting, instrument mounting, and data logger uncertainties, as well as other factors, are considered.

Temperature

Thermometers historically have been used in weather shelters to measure maximum and minimum daily temperatures. Observers must reset the thermometers daily. Hygrothermographs, instruments that record temperature and relative humidity for periods up to a week, have also been used to record temperature. Hygrothermographs are less sensitive to temperature changes and thus are less accurate than thermometers. Besides instrument and observer errors, additional errors are possible because temperatures within the shelter do not exactly represent outside temperatures. Errors of 1°F (0.6°C) or more can occur, especially on sunny, warm days when the shelter becomes warmer than the outside air.

Thermistors equipped with solar radiation shields and aspirators are used at the tower sites. These instruments are more accurate and thus better reflect air temperatures. Plans for the near future are to use thermistors and blowers for all temperature measurements.

Temperature: Instruments and Accuracy Characteristics

Thermometers (in shelter)	
Accuracy	+2°F to −1°F
Resolution	1°F
Output units	°F
Hygrothermograph (in shelter)	
Accuracy	±2°F
Resolution	1°F
Output units	°F
Thermistors (with aspirators)	
Accuracy	±0.5°F (0.3°C)
Resolution	0.01°C
Output units	°C

Relative Humidity

Relative humidity historically has been measured and recorded by a hygrothermograph in an instrument shelter. A more-accurate, aspirated electronic instrument, the hygrometer, is used at the tower sites.

Relative Humidity: Instruments and Accuracy Characteristics

Hygrothermograph (in shelter)	
Accuracy	±6%
Resolution	1%
Output units	% of saturation
Hygrometer (with aspirator)	
Accuracy	±3%
Resolution	0.1%
Output units	% of saturation

Dew-Point Temperature

Average dew-point values were calculated or estimated by charts from observed temperature and relative humidity.

Dew Point: Technique Accuracy Characteristics

Accuracy	±1.5°F
Resolution	±1.0°F
Output units	°F or °C

Wind Direction and Speed

Propeller vanes have been used since 1984 to measure both wind direction and speed at the tower sites. Orthogonal wind-propeller (U-V-W) systems were used previously. The propeller vane is very accurate in the laboratory, but accuracy decreases somewhat in the field because of compass orientation uncertainties.

Wind: Propeller Vane Accuracy Characteristics

Wind Direction:	
Accuracy	±5°
Resolution	0.1°
Output units	degrees from true north
Wind Speed:	
Accuracy	±3%
Resolution	0.1%
Output units	m/s

Vertical Wind Speed

Vertical wind speed is measured by a vertically oriented propeller vane. Standard deviation of vertical wind speed is used more than the speed itself to estimate vertical mixing.

Vertical Wind: Propeller Vane Accuracy Characteristics

Accuracy	±10%
Resolution	0.1%
Output units	m/s

Insolation

An Eppley pyranometer measures the total global solar radiation (direct and diffuse) that strikes an area parallel to the ground surface. Errors occasionally can be significant if debris or snow is not wiped from the instrument.

Insolation: Pyranometer Accuracy Characteristics

Accuracy	±2%
Resolution	0.1%
Output units	langleys/min

Precipitation

Tipping buckets have primarily been used to measure rainfall. The tipping buckets are equipped with heaters to measure snowfall water equivalent. Heavy rainfall or snowfall may be underestimated because of spilling. The thermostat setting is important in the winter because a too-warm setting will evaporate melting snow and a too-cold setting will fail to melt the snow (both result in underestimates).

Precipitation: Tipping-Bucket Accuracy Characteristics

Accuracy	+2% to −5%
Resolution	0.01 in.
Output units	hundredths of inches

Atmospheric Pressure

An electronic pressure transducer is used to measure air pressure.

Atmospheric Pressure: Pressure Transducer Accuracy Characteristics

Accuracy	±0.6 mbar
Resolution	0.1 mbar
Output units	millibars

Appendix D

Unit Conversion Factors

The scientific community has adopted the worldwide standard International System of Units (SI) in an effort to simplify technical communication. The United States, however, is only gradually adopting the system. This report generally uses familiar English units, such as degrees Fahrenheit (°F), miles per hour (mph), and inches (in.), because they are the more widely used and because climate data, generally, are still compiled, distributed, and understood in English units.

Many of the figures in this report have a second axis showing SI or metric units. Some meteorological variables occasionally are given only in SI or metric units, depending on the intended use. For example, the meters-per-second (m/s) unit is the primary unit used in the atmospheric-dispersion sections because it is widely used in dispersion calculations.

In addition, some metric units used in this report are not SI units. The units of meters per second (m/s), millibars (mbar), and calories (cal) (or langleys [ly]) are all examples of widely used metric units that are not SI units.

Tables D.1–D.3 give conversion factors for various units of length, speed (wind speed), temperature, lapse rate, atmospheric pressure, energy flux (radiation or vertical insolation flux), and energy per area (radiation or vertical insolation per area). Tables D.4–D.9 give actual conversions for temperature, wind speed, wind direction, atmospheric pressure, and vertical insolation flux.

Table D.1. Length conversion factors.

	Multiply	By	To Obtain
Length	inches	2.54	centimeters
	centimeters	0.3937	inches
	feet	0.3048	meters
	meters	3.281	feet
	inches	0.02540	meters
	meters	39.37	inches
	statute miles	1.6093	kilometers
	kilometers	0.6214	statute miles
	statute miles	0.8690	nautical miles
	nautical miles	1.1508	statute miles
	statute miles	5280	feet
	feet	0.0001894	statute miles
	kilometers	3281	feet
	feet	0.00030479	kilometers
Speed (Wind)	miles per hour (mph)	0.869	knots
	knots	1.151	mph
	mph	0.447	meters per second (m/s)
	m/s	2.237	mph
	mph	1.609	kilometers per hour (km/h)
	km/h	0.621	mph
	m/s	1.944	knots
	knots	0.514	m/s
	m/s	3.6	km/h
	km/h	0.278	m/s
	km/h	0.540	knots
	knots	1.852	km/h

Table D.2. Temperature, lapse rate, and atmospheric pressure conversion factors.

	Multiply	By	To Obtain
Temperature	degrees Fahrenheit (°F) − 32	0.5555	degrees Celsius (°C)
	°C	1.80	°F+ 32
	°F + 459.67	0.5555	kelvins (K)
	K	1.80	°F − 459.67
	°C + 273.15	1.0	K
	K	1.0	°C − 273.15
Lapse Rate	°F/1000 ft	1.83	°C/km
	°C/km	0.55	°F/1000 ft
	°F/1000 ft	3.28	°F/km
	°F/km	0.305	°F/1000 ft
Pressure	1 atmosphere[a]	29.92	inches
	inches	0.03342	atmospheres
	inches	33.865	millibars
	millibars	0.02953	inches
	inches	25.401	millimeters (torr)
	millimeters (torr)	0.03937	inches
	millibars	0.7501	millimeters (torr)
	millimeters (torr)	1.3332	millibars
	millibars	0.1	kilopascals
	kilopascals	10.0	millibars
	inches	0.4910	lb/in.^{2}, pounds per square inch (psi)
	lb/in.^{2} (psi)	2.0368	inches

[a] 1 atmosphere (atm) ≡ 29.92 inches (in.)
≡ 760 millimeters (mm) (torr)
≡ 76.0 centimeters (cm)
≡ 1.0133 bar = 1 013.3 millibar (mbar) = 101.33 kilopascals (kPa)
≡ 1 469 lb/in.

Table D.3. Energy (radiation) flux and energy per area conversion factors.

	Multiply	By	To Obtain
Energy Flux (Insolation flux)	langleys (ly)/min (cal/cm^2-min)	697.64	watts (W)/m^2 [a]
	W/m^2	0.001433	ly/min
	ly/min	4.186	joules (J)/cm^2-min
	J/cm^2-min	0.2389	ly/min
	W/m^2	0.00600	J/cm^2-min
	J/cm^2-min	166.71	W/m^2
	ly/min	3.688	Btu/ft^2-min
	Btu/ft^2-min	0.2711	ly/min
	ly/min	0.08686	horsepower (hp)/ft^2
	hp/ft^2	11.513	ly/min
Energy/Area (Solar energy)	ly (cal/cm^2)	0.011627	kilowatt-hours (kW-h)/m^2
	kW-h/m^2	86.007	ly
	ly	0.04186	10^6 J/m^{-2}
	10^6 J/m^2	23.890	ly
	10^6 J/m^2	0.27785	kW-h/m^2
	kW-h/m^2	3.5991	10^6 J/m^2
	ly	3.688	Btu/ft^2
	Btu/ft^2	0.2711	ly

[a] One watt is equivalent to one joule per second (1 W ≡ 1 J/s).

Table D.4. Temperature conversion chart.

Temperature							
(°F)	(°C)	(°F)	(°C)	(°F)	(°C)	(°F)	(°C)
−40	−40.0	0	−17.8	40	4.4	80	26.7
−39	−39.4	1	−17.2	41	5.0	81	27.2
−38	−38.9	2	−16.7	42	5.6	82	27.8
−37	−38.3	3	−16.1	43	6.1	83	28.3
−36	−37.8	4	−15.5	44	6.7	84	28.9
−35	−37.2	5	−15.0	45	7.2	85	29.4
−34	−36.7	6	−14.4	46	7.8	86	30.0
−33	−36.1	7	−13.9	47	8.3	87	30.6
−32	−35.6	8	−13.3	48	8.9	88	31.1
−31	−35.0	9	−12.8	49	9.4	89	31.7
−30	−34.4	10	−12.2	50	10.0	90	32.2
−29	−33.9	11	−11.7	51	10.6	91	32.8
−28	−33.3	12	−11.1	52	11.1	92	33.3
−27	−32.8	13	−10.6	53	11.7	93	33.9
−26	−32.2	14	−10.0	54	12.2	94	34.4
−25	−31.7	15	−9.4	55	12.8	95	35.0
−24	−31.1	16	−8.9	56	13.3	96	35.6
−23	−30.6	17	−8.3	57	13.9	97	36.1
−22	−30.0	18	−7.8	58	14.4	98	36.7
−21	−29.4	19	−7.2	59	15.0	99	37.2
−20	−28.9	20	−6.7	60	15.6	100	37.8
−19	−28.3	21	−6.1	61	16.1	101	38.3
−18	−27.8	22	−5.6	62	16.7	102	38.9
−17	−27.2	23	−5.0	63	17.2	103	39.4
−16	−26.7	24	−4.4	64	17.8	104	40.0
−15	−26.1	25	−3.9	65	18.3	105	40.6
−14	−25.6	26	−3.3	66	18.9	106	41.4
−13	−25.0	27	−2.8	67	19.4	107	41.7
−12	−24.4	28	−2.2	68	20.0	108	42.2
−11	−23.9	29	−1.7	69	20.6	109	42.8
−10	−23.3	30	−1.1	70	21.1	110	43.3
−9	−22.8	31	−0.6	71	21.7	111	43.9
−8	−22.2	32	0.0	72	22.2	112	44.4
−7	−21.7	33	0.6	73	22.8	113	45.0
−6	−21.1	34	1.1	74	23.3	114	45.6
−5	−20.6	35	1.7	75	23.9	115	46.1
−4	−20.0	36	2.2	76	24.4	116	46.7
−3	−19.4	37	2.8	77	25.0	117	47.2
−2	−18.9	38	3.3	78	25.6	118	47.8

Table D.5. Wind-speed conversion chart.

Wind Speed							
(mph)	(knots)	(m/s)	(km/h)	(mph)	(knots)	(m/s)	(km/h)
1	0.9	0.5	1.7	51	46.5	23.9	86.2
2	1.8	0.9	3.4	52	47.5	24.4	87.9
3	2.8	1.4	5.1	53	48.4	24.9	89.6
4	3.7	1.9	6.8	54	49.3	25.4	91.3
5	4.6	2.3	8.5	55	50.2	25.8	93.0
6	5.5	2.8	10.1	56	51.1	26.3	94.7
7	6.4	3.3	11.8	57	52.0	26.8	96.3
8	7.3	3.8	13.5	58	52.9	27.2	98.0
9	8.2	4.2	15.2	59	53.8	27.7	99.7
10	9.1	4.7	16.9	60	54.8	28.2	101.4
11	10.0	5.2	18.6	61	55.7	28.6	103.1
12	11.0	5.6	20.3	62	56.6	29.1	104.8
13	11.9	6.1	22.0	63	57.5	29.6	106.5
14	12.8	6.6	23.7	64	58.4	30.0	108.2
15	13.7	7.0	25.4	65	59.3	30.5	109.9
16	14.6	7.5	27.0	66	60.3	31.0	111.6
17	15.5	8.0	28.7	67	61.2	31.5	113.3
18	16.4	8.5	30.4	68	62.0	31.9	114.9
19	17.3	8.9	32.1	69	63.0	32.4	116.6
20	18.3	9.4	33.8	70	63.9	32.9	118.3
21	19.2	9.9	35.5	71	64.8	33.3	120.0
22	20.1	10.3	37.2	72	65.7	33.8	121.7
23	21.0	10.8	38.9	73	66.6	34.3	123.4
24	21.9	11.3	40.6	74	67.6	34.7	125.1
25	22.8	11.7	42.3	75	68.5	35.2	126.8
26	23.7	12.2	43.9	76	69.4	35.7	128.5
27	24.6	12.7	45.6	77	70.3	36.2	130.2
28	25.5	13.1	47.3	78	71.2	36.6	131.8
29	26.5	13.6	49.0	79	72.1	37.1	133.5
30	27.4	14.1	50.7	80	73.0	37.6	135.2
31	28.3	14.6	52.4	81	73.9	38.0	136.9
32	29.2	15.0	54.1	82	74.8	38.5	138.6
33	30.1	15.5	55.8	83	75.8	39.0	140.3
34	31.1	16.0	57.5	84	76.7	39.4	142.0
35	32.0	16.4	59.2	85	77.6	39.9	143.7
36	32.9	16.9	60.9	86	78.5	40.4	145.4
37	33.8	17.4	62.5	87	79.4	40.8	147.1
38	34.7	17.8	64.2	88	80.3	41.3	148.7
39	35.6	18.3	65.9	89	81.2	41.8	150.4
40	36.5	18.8	67.6	90	82.1	42.3	152.1
41	37.4	19.2	69.3	91	83.1	42.7	153.8
42	38.3	19.7	71.0	92	84.0	43.2	155.5
43	39.3	20.2	72.7	93	84.9	43.7	157.2
44	40.2	20.7	74.4	94	85.8	44.1	158.9
45	41.1	21.1	76.1	95	86.7	44.6	160.6
46	42.0	21.6	77.8	96	87.6	45.1	162.3
47	42.9	22.1	79.4	97	88.6	45.5	164.0
48	43.8	22.5	81.1	98	89.4	46.0	165.6
49	44.7	23.0	82.8	99	90.3	46.5	167.3
50	45.6	23.5	84.5	100	91.3	47.0	169.0

Table D.6. Wind-direction conversion chart.

Direction	Degrees
N	348.75– 11.25
NNE	11.25– 33.75
NE	33.75– 56.25
ENE	56.25– 78.75
E	78.75–101.25
ESE	101.25–123.75
SE	123.75–146.25
SSE	146.25–168.75
S	168.75–191.25
SSW	191.25–213.75
SW	213.75–236.25
WSW	236.25–258.75
W	258.75–281.25
WNW	281.25–303.75
NW	303.75–326.25
NNW	326.25–348.75

Table D.7. Atmospheric pressure conversion chart.

Atmospheric Pressure					
(in. Hg)	(mbar)	(kPa)	(mm Hg [torr])	(lb/in.^{2})	(atm)
Los Alamos					
22.50	761.9	76.19	571.5	11.05	0.752
22.52	762.6	76.26	572.0	11.06	0.753
22.54	763.3	76.33	572.5	11.07	0.753
22.56	764.0	76.40	573.0	11.08	0.754
22.58	764.6	76.46	573.5	11.09	0.755
22.60	765.3	76.53	574.0	11.10	0.755
22.62	766.0	76.60	574.5	11.11	0.756
22.64	766.7	76.67	575.1	11.12	0.757
22.66	767.4	76.74	575.6	11.13	0.757
22.68	768.0	76.80	576.1	11.14	0.758
22.70	768.7	76.87	576.6	11.15	0.759
22.72	769.4	76.94	577.1	11.15	0.759
22.74	770.1	77.01	577.6	11.16	0.760
22.76	770.7	77.07	578.1	11.17	0.761
22.78	771.4	77.14	578.6	11.18	0.762
22.80	772.1	77.21	579.1	11.19	0.762
22.82	772.8	77.28	579.6	11.20	0.763
22.84	773.5	77.35	580.1	11.21	0.763
22.86	774.1	77.41	580.6	11.22	0.764
22.88	774.8	77.48	581.2	11.23	0.765
22.90	775.5	77.55	581.7	11.24	0.765
22.92	776.2	77.62	582.2	11.25	0.766
22.94	776.8	77.68	582.7	11.26	0.767
22.96	777.5	77.75	583.2	11.27	0.767
22.98	778.2	77.82	583.7	11.28	0.768
23.00	778.9	77.89	584.2	11.29	0.769
23.02	779.5	77.95	584.7	11.30	0.769
23.04	780.2	78.02	585.2	11.31	0.770
23.06	780.9	78.09	585.7	11.32	0.771
23.08	781.6	78.16	586.2	11.33	0.771
23.10	782.3	78.23	586.7	11.34	0.772
23.12	782.9	78.29	587.2	11.35	0.773
23.14	783.6	78.36	587.8	11.36	0.773
23.16	784.3	78.43	588.3	11.37	0.774
23.18	785.0	78.50	588.8	11.38	0.775
23.20	785.6	78.56	589.3	11.39	0.775
23.22	786.3	78.63	589.8	11.40	0.776
23.24	787.0	78.70	590.3	11.41	0.777
23.26	787.7	78.77	590.8	11.42	0.778
23.28	788.4	78.84	591.3	11.43	0.778
23.30	789.0	78.90	591.8	11.44	0.779
23.32	789.7	78.97	592.3	11.45	0.779
23.34	790.4	79.04	592.8	11.46	0.780
23.36	791.1	79.11	593.3	11.47	0.781
23.38	791.7	79.17	593.9	11.48	0.781
23.40	792.4	79.24	594.4	11.49	0.782
23.42	793.1	79.31	594.9	11.50	0.783
23.44	793.8	79.38	595.4	11.51	0.783
23.46	794.4	79.44	595.9	11.52	0.784
23.48	795.1	79.51	596.4	11.53	0.785
23.50	795.8	79.58	596.9	11.54	0.785

Table D.7 (Continued)

Atmospheric Pressure					
(in. Hg)	(mbar)	(kPa)	(mm Hg [torr])	(lb/in.^{2})	(atm)
White Rock					
23.50	795.8	79.58	596.9	11.54	0.785
23.52	796.5	79.65	597.4	11.55	0.786
23.54	797.2	79.72	597.9	11.56	0.787
23.56	797.9	79.79	598.4	11.57	0.787
23.58	798.5	79.85	598.9	11.58	0.788
23.60	799.2	79.92	599.4	11.59	0.789
23.62	799.9	79.99	599.9	11.60	0.789
23.64	800.6	80.06	600.5	11.61	0.790
23.66	801.3	80.13	601.0	11.62	0.791
23.68	801.9	80.19	601.5	11.63	0.791
23.70	802.6	80.26	602.0	11.64	0.792
23.72	803.3	80.33	602.5	11.65	0.793
23.74	804.0	80.40	603.0	11.66	0.793
23.76	804.6	80.46	603.5	11.67	0.794
23.78	805.3	80.53	604.0	11.67	0.795
23.80	806.0	80.60	604.5	11.68	0.795
23.82	806.7	80.67	605.0	11.69	0.796
23.84	807.3	80.73	605.5	11.70	0.797
23.86	808.0	80.80	606.0	11.71	0.797
23.88	808.7	80.87	606.6	11.72	0.798
23.90	809.4	80.94	607.1	11.73	0.799
23.92	810.0	81.00	607.6	11.74	0.799
23.94	810.7	81.07	608.1	11.75	0.800
23.96	811.4	81.14	608.6	11.76	0.801
23.98	812.1	81.21	609.1	11.77	0.801
24.00	812.8	81.28	609.6	11.78	0.802
24.02	813.4	81.34	610.1	11.79	0.803
24.04	814.0	81.40	610.6	11.80	0.803
24.06	814.8	81.48	611.1	11.81	0.804
24.08	815.5	81.55	611.6	11.82	0.805
24.10	816.2	81.62	612.1	11.83	0.805
24.12	816.8	81.68	612.6	11.84	0.806
24.14	817.5	81.75	613.2	11.85	0.807
24.16	818.2	81.82	613.7	11.86	0.807
24.18	818.9	81.89	614.2	11.87	0.808
24.20	819.5	81.95	614.7	11.88	0.809
24.22	820.2	82.02	615.2	11.89	0.809
24.24	820.9	82.09	615.7	11.90	0.810
24.26	821.6	82.16	616.2	11.91	0.811
24.28	822.2	82.22	616.7	11.92	0.811
24.30	822.9	82.29	617.2	11.93	0.812
24.32	823.6	82.36	617.7	11.94	0.813
24.34	824.3	82.43	618.2	11.95	0.814
24.36	825.0	82.50	618.7	11.96	0.814
24.38	825.6	82.56	619.3	11.97	0.815
24.40	826.3	82.63	619.8	11.98	0.816
24.42	827.0	82.70	620.3	11.99	0.816
24.44	827.7	82.77	620.8	12.00	0.817
24.46	828.3	82.83	621.3	12.01	0.818
24.48	829.0	82.90	621.8	12.02	0.818
24.50	829.7	82.97	622.3	12.03	0.819

Table D.8. Sea-level (adjusted to) atmospheric pressure conversion chart.

Atmospheric Pressure					
(in. Hg)	(mbar)	(kPa)	(mm Hg [torr])	(lb/in.^{2})	(atm)
29.00	982.1	98.21	736.6	14.24	0.969
29.02	982.8	98.28	737.1	14.25	0.970
29.04	983.4	98.34	737.6	14.26	0.971
29.06	984.1	98.41	738.2	14.27	0.971
29.08	984.8	98.48	738.7	14.28	0.972
29.10	985.5	98.55	739.2	14.29	0.973
29.12	986.1	98.61	739.7	14.30	0.973
29.14	986.8	98.68	740.2	14.31	0.974
29.16	987.5	98.75	740.7	14.32	0.975
29.18	988.2	98.82	741.2	14.33	0.976
29.20	988.9	98.89	741.7	14.34	0.976
29.22	989.5	98.95	742.2	14.35	0.977
29.24	990.2	99.02	742.7	14.36	0.977
29.26	990.9	99.09	743.2	14.37	0.978
29.28	991.6	99.16	743.7	14.38	0.979
29.30	992.3	99.23	744.3	14.39	0.979
29.32	992.9	99.29	744.8	14.40	0.980
29.34	993.6	99.36	745.3	14.41	0.981
29.36	994.3	99.43	745.8	14.42	0.981
29.38	995.0	99.50	746.3	14.42	0.982
29.40	995.6	99.56	746.8	14.43	0.983
29.42	996.3	99.63	747.3	14.44	0.983
29.44	997.0	99.70	747.8	14.45	0.984
29.46	997.7	99.77	748.3	14.46	0.985
29.48	998.3	99.83	748.8	14.47	0.985
29.50	999.0	99.90	749.3	14.48	0.986
29.52	999.7	99.97	749.8	14.49	0.987
29.54	1000.4	100.04	750.3	14.50	0.987
29.56	1001.0	100.10	750.9	14.51	0.988
29.58	1001.7	100.17	751.4	14.52	0.989
29.60	1002.4	100.24	751.9	14.53	0.989
29.62	1003.1	100.31	752.4	14.54	0.990
29.64	1003.8	100.38	752.9	14.55	0.991
29.66	1004.4	100.44	753.4	14.56	0.991
29.68	1005.1	100.51	753.9	14.57	0.992
29.70	1005.8	100.58	754.4	14.58	0.993
29.72	1006.5	100.65	754.9	14.59	0.993
29.74	1007.1	100.71	755.4	14.60	0.994
29.76	1007.8	100.78	755.9	14.61	0.995
29.78	1008.5	100.85	756.4	14.62	0.995
29.80	1009.2	100.92	757.0	14.63	0.996
29.82	1009.9	100.99	757.5	14.64	0.997
29.84	1010.5	101.05	758.0	14.65	0.997
29.86	1011.2	101.12	758.5	14.66	0.998
29.88	1011.9	101.19	759.0	14.67	0.999
29.90	1012.6	101.26	759.5	14.68	0.999
29.92	1013.3	101.33	760.0	14.69	1.000
29.94	1013.9	101.39	760.5	14.70	1.001
29.96	1014.6	101.46	761.0	14.21	1.001
29.98	1015.3	101.53	761.5	14.72	1.002
30.00	1016.0	101.60	762.0	14.73	1.003

Table D.8 (Continued)

Atmospheric Pressure					
(in. Hg)	(mbar)	(kPa)	(mm Hg [torr])	(lb/in.^{2})	(atm)
30.02	1016.7	101.67	762.5	14.74	1.003
30.04	1017.4	101.74	763.0	14.75	1.004
30.06	1018.0	101.80	763.6	14.76	1.005
30.08	1018.7	101.87	764.1	14.77	1.005
30.10	1019.4	101.94	764.6	14.78	1.006
30.12	1020.1	102.01	765.1	14.79	1.007
30.14	1020.7	102.07	765.6	14.80	1.007
30.16	1021.4	102.14	766.1	14.81	1.008
30.18	1022.1	102.21	766.6	14.82	1.009
30.20	1022.8	102.28	767.1	14.83	1.009
30.22	1023.5	102.35	767.6	14.84	1.010
30.24	1024.1	102.41	768.1	14.85	1.011
30.26	1024.8	102.48	768.6	14.86	1.011
30.28	1025.5	102.55	769.1	14.87	1.012
30.30	1026.2	102.62	769.7	14.88	1.013
30.32	1026.8	102.68	770.2	14.89	1.013
30.34	1027.5	102.75	770.7	14.90	1.014
30.36	1028.1	102.81	771.2	14.91	1.015
30.38	1028.8	102.88	771.7	14.92	1.015
30.40	1029.5	102.95	772.2	14.93	1.016
30.42	1030.2	103.02	772.7	14.94	1.017
30.44	1030.9	103.09	773.2	14.95	1.017
30.46	1031.5	103.15	773.7	14.96	1.018
30.48	1032.2	103.22	774.2	14.96	1.019
30.50	1032.9	103.29	774.7	14.97	1.019
30.52	1033.6	103.36	775.2	14.98	1.020
30.54	1034.2	103.42	775.7	14.99	1.021
30.56	1034.9	103.49	776.3	15.00	1.021
30.58	1035.6	103.56	776.8	15.01	1.022
30.60	1036.3	103.63	777.3	15.02	1.023
30.62	1036.9	103.69	777.8	15.03	1.023
30.64	1037.6	103.76	778.3	15.04	1.024
30.66	1038.3	103.83	778.8	15.05	1.025
30.68	1039.0	103.90	779.3	15.06	1.025
30.70	1039.7	103.97	779.8	15.07	1.026
30.72	1040.3	104.03	780.3	15.08	1.027
30.74	1041.0	104.10	780.8	15.09	1.027
30.76	1041.7	104.17	781.3	15.10	1.028
30.78	1042.4	104.24	781.8	15.11	1.029
30.80	1043.0	104.30	782.4	15.12	1.029
30.82	1043.7	104.37	782.9	15.13	1.030
30.84	1044.4	104.44	783.4	15.14	1.031
30.86	1045.1	104.51	783.9	15.15	1.031
30.88	1045.8	104.58	784.4	15.16	1.032
30.90	1046.4	104.64	784.9	15.17	1.033
30.92	1047.1	104.71	785.4	15.18	1.033
30.94	1047.8	104.78	785.9	15.19	1.034
30.96	1048.5	104.85	786.4	15.20	1.035
30.98	1049.1	104.91	786.9	15.21	1.036
31.00	1049.8	104.78	787.4	15.22	1.036

Table D.9. Vertical insolation flux (radiation flux) conversion chart.

Insolation (Radiation)			
(ly/min [cal/cm^2-min])	(W/m^2)	(J/cm^2-min)	(Btu/ft-min)
0.05	34.9	0.21	0.18
0.10	69.8	0.42	0.37
0.15	104.6	0.63	0.55
0.20	139.5	0.84	0.74
0.25	174.4	1.05	0.92
0.30	209.3	1.26	1.11
0.35	244.2	1.47	1.29
0.40	279.1	1.67	1.47
0.45	313.9	1.88	1.66
0.50	348.8	2.09	1.84
0.55	383.7	2.30	2.03
0.60	418.6	2.51	2.21
0.65	453.5	2.72	2.40
0.70	488.3	2.93	2.58
0.75	523.2	3.14	2.77
0.80	558.1	3.35	2.95
0.85	593.0	3.56	3.13
0.90	627.9	3.77	3.32
0.95	662.8	3.98	3.50
1.00	697.6	4.19	3.69
1.05	732.5	4.40	3.87
1.10	767.4	4.60	4.06
1.15	802.3	4.81	4.24
1.20	837.2	5.02	4.42
1.25	872.1	5.23	4.61
1.30	906.9	5.44	4.79
1.35	941.8	5.65	4.98
1.40	976.7	5.86	5.16
1.45	1011.6	6.07	5.35
1.50	1046.5	6.28	5.53
1.55	1081.3	6.49	5.71
1.60	1116.2	6.70	5.90
1.65	1151.1	6.91	6.08
1.70	1186.0	7.12	6.27
1.75	1220.9	7.33	6.45
1.80	1255.8	7.54	6.64
1.85	1290.6	7.74	6.82
1.90	1325.5	7.95	7.00
1.95	1360.4	8.16	7.19
2.00	1395.3	8.37	7.32

Appendix E

Psychometric Charts (Tables E.1 and E.2)

Table E.1 Relative humidity (%) psychometric chart for 23 in. atmospheric pressure.

Dry-Bulb Temp. (°F)	Wet-Bulb Depression (°F)																								
	0	1	2	3	4	5	6	7	8	9	10	11	12	14	16	18	20	22	24	26	28	30	35	40	45
15	91	77	64	50	37	24	11	–	–	–	–	–	–	–	–	–	–	–	–	–	–	–	–	–	–
17	92	79	66	54	41	29	17	5	–	–	–	–	–	–	–	–	–	–	–	–	–	–	–	–	–
19	93	81	69	57	45	33	22	10	–	–	–	–	–	–	–	–	–	–	–	–	–	–	–	–	–
21	94	82	71	60	48	37	27	16	5	–	–	–	–	–	–	–	–	–	–	–	–	–	–	–	–
23	95	84	73	62	52	41	31	21	11	1	–	–	–	–	–	–	–	–	–	–	–	–	–	–	–
25	96	86	75	65	55	45	35	26	16	7	–	–	–	–	–	–	–	–	–	–	–	–	–	–	–
27	97	87	77	67	58	48	39	30	21	12	3	–	–	–	–	–	–	–	–	–	–	–	–	–	–
29	98	89	79	70	61	52	43	34	25	17	9	–	–	–	–	–	–	–	–	–	–	–	–	–	–
31	99	90	81	72	63	55	46	38	30	22	14	6	–	–	–	–	–	–	–	–	–	–	–	–	–
33	100	92	83	74	66	57	49	41	34	26	18	11	4	–	–	–	–	–	–	–	–	–	–	–	–
35	100	92	84	76	68	60	52	45	37	30	23	16	9	–	–	–	–	–	–	–	–	–	–	–	–
37	100	92	85	77	70	63	55	48	41	34	27	20	13	–	–	–	–	–	–	–	–	–	–	–	–
39	100	93	85	78	71	64	58	51	44	37	31	24	18	5	–	–	–	–	–	–	–	–	–	–	–
41	100	93	86	79	72	66	59	53	47	41	34	28	22	10	–	–	–	–	–	–	–	–	–	–	–
43	100	93	86	80	73	67	61	55	49	43	37	31	26	14	3	–	–	–	–	–	–	–	–	–	–
45	100	93	87	81	74	68	62	57	51	45	40	34	29	18	7	–	–	–	–	–	–	–	–	–	–
47	100	94	87	81	75	70	64	58	53	47	42	37	31	21	12	2	–	–	–	–	–	–	–	–	–
49	100	94	88	82	76	71	65	60	54	49	44	39	34	24	15	6	–	–	–	–	–	–	–	–	–
51	100	94	88	83	77	72	66	61	56	51	46	41	36	27	18	10	1	–	–	–	–	–	–	–	–
53	100	94	89	83	78	73	67	62	57	52	48	43	38	30	21	13	5	–	–	–	–	–	–	–	–
55	100	94	89	84	79	73	68	64	59	54	49	45	40	32	24	16	8	–	–	–	–	–	–	–	–
57	100	95	89	84	79	74	69	65	60	55	51	47	42	34	26	18	11	4	–	–	–	–	–	–	–
59	100	95	90	85	80	75	70	66	61	57	52	48	44	36	28	21	14	7	–	–	–	–	–	–	–
61	100	95	90	85	80	76	71	67	62	58	54	50	46	38	30	23	16	10	3	–	–	–	–	–	–
63	100	95	90	85	81	76	72	68	63	59	55	51	47	40	32	25	19	12	6	–	–	–	–	–	–
65	100	95	90	86	81	77	73	68	64	60	56	52	49	41	34	27	21	15	9	3	–	–	–	–	–
67	100	95	91	86	82	78	73	69	65	61	57	54	50	43	36	29	23	17	11	6	–	–	–	–	–
69	100	95	91	87	82	78	74	70	66	62	58	55	51	44	38	31	25	19	13	8	3	–	–	–	–
71	100	96	91	87	83	79	75	71	67	63	59	56	52	46	39	33	27	21	16	10	5	–	–	–	–
73	100	96	91	87	83	79	75	71	68	64	60	57	53	47	41	34	28	23	18	13	8	3	–	–	–
75	100	96	92	87	83	80	76	72	68	65	61	58	55	48	42	36	30	25	20	15	10	5	–	–	–
77	100	96	92	88	84	80	76	73	69	66	62	59	55	49	43	37	32	26	21	17	12	7	–	–	–
79	100	96	92	88	84	80	77	73	70	67	63	60	56	50	44	39	33	28	23	18	14	9	–	–	–
81	100	96	92	88	84	81	77	74	70	68	64	60	57	51	45	40	35	30	25	20	16	11	1	–	–
83	100	96	92	89	85	81	78	74	71	68	64	61	58	52	47	41	36	31	26	22	17	13	3	–	–
85	100	96	92	89	85	81	78	75	71	69	65	62	59	53	48	42	37	32	28	23	19	15	5	–	–
87	100	96	92	89	85	82	78	75	72	69	66	63	60	54	48	43	38	33	29	25	20	16	7	–	–
89	100	96	92	89	86	82	79	76	72	70	66	63	60	55	49	44	39	35	30	26	22	18	9	1	–
91	100	96	92	89	86	82	79	76	73	70	67	64	61	56	50	45	40	36	31	27	23	19	10	2	–
93	100	96	92	89	86	82	79	76	73	70	67	64	62	56	51	46	41	37	33	28	24	21	12	4	–
95	100	96	92	89	86	82	79	76	73	70	68	65	62	57	52	47	42	38	34	30	26	22	13	6	–
97	100	96	92	89	86	82	79	76	73	70	68	65	58	58	53	48	43	39	35	31	27	23	15	7	–
99	100	96	92	89	86	82	79	76	73	70	68	65	63	58	53	49	44	40	36	32	28	24	16	9	2
101	100	96	92	89	86	82	79	76	73	70	68	65	63	58	54	49	45	41	37	33	29	25	17	10	3
103	100	96	92	89	86	82	79	76	73	70	68	65	63	58	54	50	46	41	37	34	30	26	18	11	5
105	100	96	92	89	86	82	79	76	73	70	68	65	63	58	54	50	46	42	38	34	31	27	20	12	6
107	100	96	92	89	86	82	79	76	73	70	68	65	63	58	54	50	46	43	39	35	32	28	21	14	7
109	100	96	92	89	86	82	79	76	73	70	68	65	63	58	54	50	46	43	40	36	33	29	22	15	9

Table E.2 Dew-point (°F) psychometric chart for 23 in. atmospheric pressure.

Dry-Bulb Temp. (°F)	Wet-Bulb Depression (°F)																								
	0	1	2	3	4	5	6	7	8	9	10	11	12	14	16	18	20	22	24	26	28	30	35	40	45
15	13	9	+5	0	−7	−15	−30	—	—	—	—	—	—	—	—	—	—	—	—	—	—	—	—	—	—
17	15	12	8	+3	−3	−10	−21	44	—	—	—	—	—	—	—	—	—	—	—	—	—	—	—	—	—
19	17	14	10	6	+1	−5	−14	−28	—	—	—	—	—	—	—	—	—	—	—	—	—	—	—	—	—
21	20	17	13	9	+5	−1	−8	−18	−38	—	—	—	—	—	—	—	—	—	—	—	—	—	—	—	—
23	22	19	16	12	8	+3	−3	−11	−24	—	—	—	—	—	—	—	—	—	—	—	—	—	—	—	—
25	24	21	18	15	11	7	+1	−5	−15	−31	—	—	—	—	—	—	—	—	—	—	—	—	—	—	—
27	26	24	21	18	14	10	+5	0	−8	−19	−42	—	—	—	—	—	—	—	—	—	—	—	—	—	—
29	29	26	23	20	17	13	9	+5	−2	−10	−23	—	—	—	—	—	—	—	—	—	—	—	—	—	—
31	31	28	26	23	20	17	13	8	+3	−4	−13	−29	—	—	—	—	—	—	—	—	—	—	—	—	—
33	33	31	28	26	23	20	16	12	7	+2	−5	−16	−36	—	—	—	—	—	—	—	—	—	—	—	—
35	35	33	31	28	26	23	19	16	12	7	+1	−7	−19	—	—	—	—	—	—	—	—	—	—	—	—
37	37	35	33	31	28	25	22	19	15	11	+6	0	−9	—	—	—	—	—	—	—	—	—	—	—	—
39	39	37	35	33	30	28	25	22	19	15	11	+4	−1	−25	—	—	—	—	—	—	—	—	—	—	—
41	41	39	37	35	33	30	28	25	22	19	15	10	+5	−12	—	—	—	—	—	—	—	—	—	—	—
43	43	41	39	37	35	33	30	28	25	22	19	15	+10	−3	−33	—	—	—	—	—	—	—	—	—	—
45	45	43	41	39	37	35	33	31	28	25	22	18	15	+4	−14	—	—	—	—	—	—	—	—	—	—
47	47	45	43	42	40	38	35	33	31	28	25	22	18	10	−4	−41	—	—	—	—	—	—	—	—	—
49	49	47	46	44	42	40	38	36	33	31	28	25	22	14	+3	−16	—	—	—	—	—	—	—	—	—
51	51	49	48	46	44	42	40	38	36	33	31	28	25	18	+9	−5	−48	—	—	—	—	—	—	—	—
53	53	51	50	48	46	44	42	40	38	36	34	31	28	22	14	+3	−18	—	—	—	—	—	—	—	—
55	55	53	52	50	48	47	45	43	41	39	36	34	31	26	18	+9	−6	−57	—	—	—	—	—	—	—
57	57	55	54	52	51	49	47	45	43	41	39	37	34	29	22	14	+3	−19	—	—	—	—	—	—	—
59	59	58	56	54	53	51	49	48	46	44	42	39	37	32	26	19	+9	−6	—	—	—	—	—	—	—
61	61	60	58	56	55	53	52	50	48	46	44	42	40	35	30	23	15	+3	−20	—	—	—	—	—	—
63	63	62	60	59	57	55	54	52	50	49	47	45	43	38	33	27	20	10	−5	—	—	—	—	—	—
65	65	64	62	61	59	58	56	54	53	51	49	47	45	41	36	31	24	16	+4	−19	—	—	—	—	—
67	67	66	64	63	61	60	58	57	55	53	51	50	48	44	39	34	28	21	11	−4	—	—	—	—	—
69	69	68	66	65	63	62	60	59	57	56	54	52	50	46	42	37	32	25	17	+5	−16	—	—	—	—
71	71	70	69	67	65	64	63	61	59	58	56	54	53	49	45	40	35	29	22	13	−2	−50	—	—	—
73	73	72	70	69	68	66	65	63	62	60	58	56	55	52	48	43	39	33	27	18	+7	−13	—	—	—
75	75	74	72	71	70	68	67	65	64	62	61	59	58	54	50	46	42	37	31	24	14	0	—	—	—
77	77	76	74	73	72	70	69	68	66	65	63	61	60	56	53	49	45	40	35	28	20	+9	—	—	—
79	79	78	76	75	74	72	71	70	68	67	65	64	62	59	55	52	48	43	38	32	25	16	—	—	—
81	81	80	78	77	76	75	73	72	70	69	68	66	64	61	58	54	50	46	42	36	30	22	−23	—	—
83	83	82	80	79	78	77	75	74	73	71	70	68	67	64	60	57	53	49	45	40	34	27	−3	—	—
85	85	84	83	81	80	79	77	76	75	73	72	70	69	66	63	59	56	52	48	43	38	32	8	—	—
87	87	86	85	83	82	81	79	78	77	75	74	73	71	68	65	62	59	55	51	46	42	36	16	—	—
89	89	88	86	85	84	83	82	80	79	78	76	75	73	71	68	64	61	58	54	50	45	40	22	−33	—
91	91	90	88	87	86	85	84	82	81	80	78	77	76	73	70	67	64	60	57	53	48	43	28	−5	—
93	93	91	90	89	88	87	86	84	83	82	81	79	78	75	72	69	66	63	59	55	51	47	33	8	—
95	95	93	92	90	89	88	87	86	85	84	83	81	80	77	75	72	69	65	62	58	54	50	37	16	—
97	97	95	94	92	91	90	89	87	86	85	84	83	82	80	77	74	71	68	64	61	57	53	41	23	−38
99	99	97	96	94	93	92	91	89	88	87	86	85	84	82	79	76	73	70	67	64	60	56	45	29	−5
101	101	99	97	96	94	93	92	91	90	89	88	87	86	83	81	78	76	73	70	66	63	59	49	34	9
103	103	101	99	97	96	94	93	92	91	90	89	88	87	85	83	81	78	75	72	69	66	62	52	39	18
105	105	103	101	99	98	96	95	94	93	92	91	90	89	87	85	83	80	77	74	71	68	65	55	43	25
107	107	105	103	101	99	98	96	95	94	93	92	91	90	88	86	84	82	80	77	74	70	67	58	47	31
109	109	107	105	103	101	99	98	97	96	95	94	93	92	91	88	86	84	82	79	76	73	70	61	51	36

Appendix F

Wind-Chill-Equivalent Temperature Charts (Table F.1)

Table F.1. Wind-chill-equivalent temperatures.

Wind Speed (mph)	Temperature (°F) (equivalent wind-chill temperature)																			
	45	40	35	30	25	20	15	10	5	0	−5	−10	−15	−20	−25	−30	−35	−40	−45	−50
5	43	37	32	27	22	16	11	6	1	−5	−10	−15	−20	−26	−31	−36	−41	−47	−52	−57
10	34	28	22	16	10	4	−3	−9	−15	−21	−27	−33	−40	−46	−52	−58	−64	−70	−76	−82
15	29	22	16	9	2	−5	−11	−18	−25	−32	−38	−45	−52	−58	−65	−72	−79	−85	−92	−99
20	25	18	11	4	−3	−10	−17	−25	−32	−39	−46	−53	−60	−67	−74	−82	−89	−96	−103	−111
25	23	15	8	0	−7	−15	−22	−29	−37	−44	−52	−59	−66	−74	−81	−89	−96	−104	−111	−119
30	21	13	5	−2	−10	−18	−25	−33	−41	−48	−56	−63	−71	−79	−86	−94	−102	−109	−117	−125
35	19	11	3	−4	−12	−20	−28	−35	−43	−51	−59	−67	−74	−82	−90	−98	−106	−113	−121	−129
40	18	10	2	−6	−14	−22	−29	−37	−45	−53	−61	−69	−77	−85	−93	−101	−108	−116	−124	−132
45	17	9	1	−7	−15	−23	−31	−39	−47	−55	−62	−70	−78	−86	−94	−102	−110	−118	−126	−133
Wind speeds >45 mph have little additional cooling effect.	Little Danger[a]					Increasing Danger[a] (Flesh may freeze within 1 minute.)							Great Danger[a] (Flesh may freeze within 30 seconds.)							

Wind Speed (m/s)	Temperature (°C) (equivalent wind-chill temperature)																	
	6	3	0	−3	−6	−9	−12	−15	−18	−21	−24	−27	−30	−33	−36	−39	−42	−45
2	4	0	−3	−6	−9	−12	−16	−19	−22	−26	−29	−32	−36	−39	−43	−46	−50	−52
4	1	−3	−6	−10	−14	−18	−22	−25	−29	−32	−36	−40	−44	−47	−51	−54	−58	−62
6	−2	−6	−10	−14	−18	−22	−26	−30	−34	−38	−42	−46	−50	−54	−58	−62	−66	−70
8	−4	−9	−13	−17	−21	−25	−30	−34	−39	−43	−47	−51	−56	−60	−64	−68	−72	−76
10	−6	−11	−15	−19	−24	−28	−33	−37	−42	−46	−50	−54	−59	−64	−68	−72	−77	−81
12	−8	−12	−17	−21	−26	−30	−35	−39	−44	−48	−53	−57	−62	−66	−71	−75	−80	−84
14	−9	−13	−17	−22	−27	−31	−36	−40	−45	−50	−55	−59	−64	−68	−73	−77	−82	−86
16	−9	−14	−18	−23	−28	−32	−37	−42	−47	−51	−56	−61	−66	−70	−75	−79	−84	−88
18	−10	−14	−19	−24	−29	−33	−38	−43	−48	−52	−57	−62	−67	−71	−76	−81	−86	−90
20	−10	−15	−20	−25	−29	−34	−39	−44	−49	−53	−58	−63	−68	−72	−77	−82	−87	−91
Wind speeds >20 m/s have little additional cooling effect.	Little Danger[a]					Increasing Danger[a] (Flesh may freeze within 1 minute.)							Great Danger[a] (Flesh may freeze within 30 seconds.)					

[a]Danger of freezing exposed flesh.

Glossary*

absolute humidity	Ratio of atmospheric water vapor mass to moist atmospheric mass (g/kg).
absolute temperature	Temperature scale based on absolute zero, given in degrees kelvin (K = °C + 273).
acid rain	Rain having a pH lower than 5.6, usually because of the presence of sulfuric and nitric acids.
adiabatic process (or assumption)	Expansional cooling or compressional warming of air parcels in which there is no net heat exchange between the air parcels and the surrounding air.
advection	Horizontal transport by wind.
advection fog	Fog caused by transport of a mild, humid air mass over a relatively cool air mass or surface.
aerosols	Various tiny liquid or solid particles that are suspended in the atmosphere.
air density	Mass per unit volume of air, about 0.96 kg/m^3 at Los Alamos and 1.29 kg/m^3 at sea level.
air mass	A large volume of air that is horizontally relatively uniform in temperature and water vapor content.
air-mass advection	Horizontal movement of air or air masses from one place to another.
air-mass thunderstorm	Thunderstorm that develops almost randomly in a mass of maritime tropical air, not associated with a cyclone.
air pollutants	Gases and aerosols in air that threaten the well-being of living organisms or that disrupt the orderly functioning of the environment.
anabatic wind	Upslope flow of warm, light air under the influence of gravity; convective upslope wind.
anemometer	Instrument used to measure wind speed.
aneroid barometer	A portable instrument that uses a flexible metal chamber and spring to measure atmospheric pressure.

*Many of the definitions of terms in this glossary were derived from or were taken directly from *Meteorology: The Atmosphere and the Science of Weather* (Moran and Morgan 1986).

anticyclone	See high-pressure system.
apparent temperature	A calculated air temperature at which the heat loss from exposed skin accounts for the wind-speed and humidity effects at the actual temperature. Warming effect by sunshine is often included.
arctic (A) air	A very cold, dry, and shallow air mass that forms primarily during winter over the arctic basin, Greenland, and the northern interior of North America.
arctic high	Anticyclone that originates in arctic areas associated with cold, dry air.
atmosphere	A thin layer of gases (also containing some aerosols) that covers the earth.
atmospheric pressure	The force per unit area exerted on any surface by air molecules.
atmospheric stability	Property of an air layer encouraging or discouraging buoyancy to air parcels moving vertically in the air layer; depends on temperature profile of the air layer.
aurora borealis	Lights visible at night in the Northern Hemisphere produced by electrical activity in the ionosphere; northern lights.
autumn	Season between autumn equinox and winter solstice, about September 21 to December 21; meteorologically, by convention, September through November.
backing	Counterclockwise shift in wind direction with time or altitude.
barometer	An instrument used to measure atmospheric pressure. See also aneroid barometer and mercury barometer.
blizzard	Falling or blowing snow accompanied by winds greater than 35 mph (55 km).
borq	A violent, cold northerly wind (of the Adriatic).
boundary layer	The part of the atmosphere directly affected by turbulent mixing near the surface. Heat, water vapor, momentum, and pollutants mix through this layer readily. The boundary layer often coincides with mixing height, typically 600 ft (200 m) or less (night) and 3000–6000 ft (1–2 km) (afternoon).
channeled wind	Wind directed parallel to a valley or canyon.
Chinook winds	Strong, downslope winds occurring on the leeward slope of a mountain range, common on the eastern slopes of the Rocky Mountains. Because of adiabatic compression, the winds are warm and dry.

cirrocumulus clouds	High clouds, composed of ice crystals, that appear as a wavelike pattern of small white puffs.
cirrostratus clouds	High, layered clouds, composed of ice crystals, that form a thin white veil over the sky.
cirrus clouds	High clouds occurring as silky strands and composed of ice crystals.
climate	Weather variations of some locality averaged over some time period, plus extremes in weather behavior observed during the same period.
climate normal	Mean weather, plus weather variations, at some locality for some period, usually 30 years. Normal is sometimes defined as the mean ±2 std dev for variables such as temperature, precipitation, and snowfall. Abnormal weather represents extremes >2 std dev from the mean.
climatology	The study of climate.
cold-air advection	Flow of air from relatively cool to relatively warm localities.
cold-air drainage	Downslope flow of cold, dense air, caused by gravity; katabatic wind.
cold-core high (anticyclone)	Shallow, high-pressure system associated with dome of relatively cool, dry air; highs that weaken with height.
cold front	A narrow zone of transition between relatively cold, dense air that is advancing and relatively warm, less-dense air that is retreating.
cold wave	Sudden outbreak of cold weather, or period of extremely cold weather. In Los Alamos, a cold wave can be defined as 2 consecutive days with temperatures dropping to 0°F or below or temperatures dropping to −10°F or lower.
compressional warming	A temperature rise associated with a pressure increase of a volume of air, as when air subsides in the atmosphere.
condensation	Process by which water changes phase from a vapor to a liquid.
conduction	Flow of heat in response to a temperature difference in an object or between objects that are in physical contact. Conduction is important in the transfer of heat in the ground and from the ground surface to the air immediately above.
continental polar (cP) air	Relatively dry air mass that develops over the northern interior of North America; very cold in winter and cool in summer.

continental tropical (cT) air	Warm, dry air mass that forms over the subtropical deserts of the southwestern United States.
convection	Vertical air motion in which warm air rises and cold air sinks.
convergence	A wind pattern whereby there is a net inflow of air over some region.
cooling-degree day	Unit that measures the need for air conditioning when the average daily air temperature [(maximum + minimum)/2] exceeds a specific base, commonly 65°F or 70°F; computed by subtracting the base from the average daily temperature (°F).
Coriolis force	A deflecting force caused by the earth's rotation about its axis. Winds are deflected to the right of the initial direction in the Northern Hemisphere and to the left in the Southern Hemisphere.
cumulonimbus clouds	Thunderstorm clouds that form as a result of deep convection in the atmosphere; often characterized by an anvil top; thunderhead.
cumulus clouds	Clouds that develop as a result of convective air currents; resemble puffs of cotton floating in the sky; fair-weather clouds.
cumulus congestus cloud	An upward-building convective cloud, with vertical development between a cumulus cloud and a cumulonimbus cloud.
cutoff high	Anticyclone (high) that separates from the prevailing westerlies and therefore remains stationary or moves slowly.
cutoff low	Cyclone (low) that separates from the prevailing westerlies and therefore remains stationary or moves slowly.
cyclogenesis	Birth and development of a cyclone, a low-pressure system.
cyclone	See low-pressure system.
design	A value, such as a specific temperature, that occurs with a specific frequency during a year. A 1% winter design temperature, for example, can assist in designing a heating system and determining insulation requirements for a building.
dew	Water droplets formed by condensation of water vapor on a surface.
dew point or dew-point temperature	Temperature to which air must be cooled at constant pressure to reach saturation.

diffuse insolation	Solar radiation that is scattered or reflected by the atmosphere or its components (clouds, for example) to the earth's surface.
dilution	A reduction in concentration through mixing, as when polluted air mixes with cleaner air.
direct insolation (solar beam)	Solar radiation that is transmitted directly through the atmosphere to the earth's surface without interacting with the atmosphere or its components.
dispersion	The horizontal and vertical spreading of air pollution by atmospheric turbulent motions, resulting in lower concentrations.
divergence	A wind pattern whereby there is net outflow of air over some region.
drainage wind	See cold-air drainage.
down burst	A strong and potentially destructive thunderstorm downdraft; also called a microburst.
downdraft	Downward-moving air, usually within a thunderstorm.
drainage basin	A fixed geographical region from which a river and its tributaries drain water.
drizzle	A form of liquid precipitation less than 0.02 in. (0.5 mm) in diameter; falls from stratus clouds.
drought	Prolonged dryness resulting in depleted subsoil moisture.
dry adiabatic cooling (warming)	Expansional (compressional) cooling (warming) of rising (sinking) unsaturated air parcels. No heat exchange occurs between the air parcels and the surrounding air.
dry adiabatic lapse rate	Rising (sinking) unsaturated air parcels cool (warm) at the rate of about 5.5°F per 1000 ft, or 10°C per 1000 m of rise (fall).
dry-bulb temperature	The actual air temperature as measured by a dry-bulb thermometer.
dust devil	Swirling mass of dust caused by intense heating of dry surface areas with a consequent rising air current. Dust devils occur during sunny conditions.
El Niño	An anomalous warming of surface ocean waters off the coasts of Ecuador and Peru and extending westward over the eastern tropical Pacific Ocean. The occurrence can change weather patterns in North America.

equinoxes	The first day of spring (~March 21) and autumn (~September 21) when the sun is directly over the equator. Day and night are of equal length at equinox.
evaporation	The change of water phase from liquid to vapor at a temperature below the boiling point of water.
evapotranspiration	Vaporization of water through direct evaporation from wet surfaces and the release of water vapor by vegetation.
expansional cooling	A temperature drop associated with a pressure decrease of a volume of air, as when air rises within the atmosphere.
extreme value analysis	Plot of annual variable extremes, such as temperature and precipitation, used to estimate expected values such as 50- and 100-year return periods.
F-scale	Tornado intensity scale.
flash flooding	A sudden rise in a river, stream, or normally dry arroyo, causing flooding.
foehn wind	European term for Chinook wind; warm, dry wind that flows into the alpine valleys of Austria and Germany.
fog	A cloud in contact with the earth's surface that reduces visibility to less than 1.0 km (0.6 mile).
freeze	A day in which the minimum temperature is 32°F or below. A hard freeze is a day in which the temperature dips to 28°F or below.
freezing rain	Condition where supercooled raindrops freeze on impact with cold surfaces.
freeze-thaw day	Day in which the maximum temperature exceeds 32°F and the minimum is 32°F or less.
friction layer	Atmospheric layer extending from the ground surface to 1–2 km above, where winds are affected by ground frictional resistance; boundary layer.
front	A narrow transitional zone separating air masses of different densities. The different densities represent different temperatures, absolute humidities, or both.
frontal thunderstorms	Thunderstorms associated with forced lifting of air along fronts.
frost	Ice crystals formed by water vapor deposition on a surface at temperatures of 32°F or below.

frost point Temperature to which air must be cooled (if at 32°F or below) at constant pressure to reach saturation.

funnel cloud A tornadic circulation that does not reach the ground.

gas law Relationship among the variables of state. Pressure is proportional to the product of temperature and density.

Gaussian dispersion model An atmospheric dispersion model that estimates downwind pollutant concentrations, given vertical and horizontal distances of and from the pollutant cloud. Pollutant drop-off is assumed to follow a normal distribution from the cloud center line.

geostrophic wind A steady-state wind that flows in regions of straight isobars (contours) above the friction layer; results from balance between the horizontal pressure gradient force and the force caused by the Coriolis effect.

glory Concentric rings of color about a shadow cast by an observer or an observer's head onto the top of a cloud situated below the observer. The glory is caused by the same refraction and internal reflection as occur in rainbows.

gradient The change in some variable (such as pressure or temperature) with distance.

gradient wind Large-scale, horizontal wind that flows in regions of curved isobars (contours) above the friction layer; results from balance between the horizontal pressure gradient force, Coriolis force, and centripetal force.

graupel Precipitation of ice granules or compact snow.

gravity The force that holds all objects onto the earth and that accelerates them toward the earth's surface. Gravity results from the net effect of gravitation and centrifugal force caused by the earth's rotation.

gravity wind Local wind caused by horizontal air-density differences over sloping terrain; includes cold-air drainage.

greenhouse effect The absorption and reradiation of terrestrial infrared radiation primarily by atmospheric water vapor and carbon dioxide.

Greenwich Mean Time (GMT) A worldwide time reference used for synchronizing weather observations; the time at 0° longitude, the prime meridian, which passes through Greenwich, England.

growing-degree day Same as cooling-degree day (see), except that the growing-degree day is used to measure the growth potential of plants. Common bases are 40°F through 70°F.

gust A quick, sharp, and brief increase in wind speed.

gust front The leading edge of a mass of relatively cool air that flows out of the base of a thunderstorm and spreads along the ground well in advance of a storm; a mesoscale cold front.

haboob A dust storm formed by the downdraft of a desert thunderstorm.

hail or hailstones Precipitation in the form of rounded or jagged chunks of ice, often characterized by internal concentric layering. Hail occurs with thunderstorms that have strong updrafts and relatively great moisture content.

halo Ring of light around the sun or moon caused by light refraction by tiny ice crystals of clouds in the upper troposphere.

haze Aerosols suspended in the atmosphere, which may cause a reduction in visibility.

heat The total molecular energy contained by a given amount of a substance.

heat wave Prolonged hot weather. In Los Alamos, a heat wave can be defined as 3 consecutive days with temperatures reaching 90°F or higher.

heat lightning Light reflected by clouds from thunderstorms occurring beyond the horizon.

heating-degree day Unit that measures the need for space heating when the average daily air temperature [(maximum + minimum)/2] is less than a specific base, usually 65°F. The measurement is computed by subtracting the average daily temperature from the base.

high (pressure system) A dome of air that contains relatively high pressure compared with pressure of the surrounding air; anticyclone. A high-pressure system is associated with a slight downward air motion and, therefore, pleasant, fair weather. Surface winds blow clockwise and outward in the Northern Hemisphere.

hurricane Intense, relatively small warm-core cyclones that originate in the tropics; also called typhoons when occurring over the Pacific Ocean. Sustained winds exceed 74 mph (120 km/h).

hygrothermograph An instrument that continuously records temperature and relative humidity.

ice pellets Frozen raindrops that bounce on impact with the ground; sleet; formed by melted snow or rain falling through a colder layer and freezing before reaching the ground.

Indian summer A period of mild, sunny weather that occurs in autumn over eastern North America after the first freeze.

infrared radiation Radiant heat emitted by most objects at wavelengths longer than those of visible red.

insolation *In*coming *sol*ar radi*ation*. See also diffuse insolation, direct insolation.

isobar Line on a map connecting places reporting the same air pressure.

isothermal Constant temperature; lapse rate with constant temperature.

inversion Lapse rate with temperature increasing with height. Inversions resist vertical motion and tend to suppress turbulence.

jet maximum An area of fastest-moving air along a jet stream.

jet streams Relatively narrow ribbons of strong winds embedded in the large-scale winds aloft.

katabatic winds See cold-air drainage.

langley (ly) An energy flux unit defined as 1 calorie/cm^2 or 1.4 kW/m^2.

La Niña An anomalous cooling of surface ocean waters off the coasts of Ecuador and Peru and extending westward over the eastern tropical Pacific Ocean. The occurrence can change weather patterns in North America.

lapse rate Change of temperature with height.

latent heat transfer Movement of heat from one place (moist soil, for example) to another (the atmosphere) as a consequence of the water phase changes. Heat is required for evaporation and sublimation at the earth's surface, and heat is released in condensation and deposition within the atmosphere.

lightning A flash of light produced from an electrical discharge because of the buildup of electrical potential between cloud and ground, between clouds, or within a single cloud.

long waves Series of long-wavelength troughs and ridges formed by the westerlies as they encompass the earth.

low (pressure system) A weather system characterized by relatively low air pressure compared with pressure of surrounding air; cyclone. A low-pressure system is associated with slight upward air motion and, therefore, clouds and precipitation. Surface winds blow counterclockwise and inward in the Northern Hemisphere.

mammatus cloud	Cloud exhibiting pouchlike, downward protuberances; often accompanies thunderstorms and indicates turbulent air.
maritime polar (mP) air	Cool, humid air mass that forms over the cold ocean waters of the north Pacific and north Atlantic.
maritime tropical (mT) air	Warm, humid air mass that forms over tropical and subtropical oceans.
mercury barometer	A mercury-filled tube used to measure air pressure; a high-precision barometric standard.
meridional flow pattern	Pattern of westerlies with series of deep troughs and sharp ridges; considerable northerly and southerly flow components.
mesoscale convective complex (MCC)	A cluster of many thunderstorms covering an area of many thousands of square miles.
mesoscale systems	Weather phenomena operating at the local scale (1–100 km); includes thunderstorms and drainage winds, for example.
meteorology	Scientific study of the atmosphere and atmospheric processes.
microclimate	Means and extremes in weather over a very small spatial scale.
microburst	A strong and potentially destructive thunderstorm downdraft that strikes the ground and spreads laterally; produces wind shear that may be hazardous to low-flying aircraft.
microscale weather	The smallest scale of weather (<1 km).
millibar (mbar)	A conventional meteorological unit of air pressure. The standard sea-level air pressure is 1013.3 mbar.
mirage	An image formed when the atmosphere acts as a large lens to refract light rays. The refraction usually results from intense ground solar heating, resulting in a large drop-off of temperature with height.
mist	Very thin fog in which visibility is greater than 0.6 mile (1 km).
mixing layer	Surface layer of the atmosphere in which air is thoroughly mixed by convection. Mixing depth is the thickness of the mixing layer, which often coincides with the boundary layer.
mixing ratio	Mass of water vapor per mass of dry air; expressed as grams per kilogram (g/kg).
mock suns	Same as parhelia.

moist adiabatic lapse rate	A variable cooling rate of rising saturated air parcels. This rate is less than the dry adiabatic lapse rate because some of the cooling is offset by the latent heat release from condensation.
monsoon active phases	Showery periods with frequent heavy rains.
monsoon (circulation)	Wind reversal that causes a wet season (summer); specifically, in New Mexico, a flow of moisture from the Gulf of Mexico toward New Mexico.
monsoon dormant phases	Sunny and warm periods that interrupt the rainy monsoon periods.
mountain wave clouds	Stationary clouds, located over or downwind of a mountain range, formed because of the disturbance of the winds by the mountain range.
National Weather Service (NWS)	The agency (see NOAA below) responsible for weather data acquisition and analysis, forecast dissemination, and storm watches and warnings.
neutral atmosphere	An atmosphere that has a lapse rate nearly identical to the dry adiabatic lapse rate, implying no tendency for a displaced air parcel to gain or lose buoyancy; represented by the D stability category.
nimbostratus	Low, gray, layered clouds that resemble stratus clouds but that are thicker and yield more-substantial precipitation.
normal	See climate normal.
NOAA	National Oceanic and Atmospheric Administration, the United States federal administrative unit in the Department of Commerce that includes the National Weather Service.
occluded front	A front formed when a cold front overtakes a warm front at the ground surface; represents the decay stage of a cyclone or low.
occlusion	Final stage in the life cycle of a midlatitude cyclone; occurs when the cold front overtakes the warm front at the ground.
orographic lifting	Rising motion of air forced by topography.
orographic precipitation	Rainfall or snowfall from clouds forced by topographic air uplift.
ozone (layer)	Ozone in stratosphere, which filters out (absorbs) ultraviolet radiation from the sun.

parhelia — Two bright spots of light appearing on either side of the sun, separated from the sun by a 22° angle; same as mock suns and sundogs. Parhelia are caused by refraction of sunlight by ice crystals.

Pasquill-Gifford stability categories and curves — Stability categories, designated A through F, which characterize stability of lower atmosphere, with A most unstable, D neutral, and F most stable. Horizontal (σ_y) and vertical (σ_z) dispersion values have been calculated by stability category and downwind distance, assuming a smooth surface.

persistence — Tendency for weather trends to continue for some period of time (for example, wind-direction persistence).

photochemical smog — A noxious, hazy mixture of aerosols and gases produced when sunlight acts on nitrogen oxides and hydrocarbons from automobile exhaust; includes ozone and PAN (peroxyacetyl nitrate).

polar highs — High-pressure systems originating in the source regions for continental polar air.

precipitation — Water in solid or liquid form that falls to the earth's surface from clouds. Water-equivalent precipitation is a measure of rain and melted snow or ice.

pressure gradient — Change in air pressure with distance.

pressure-gradient force — Force that causes air parcels to move from high-pressure to low-pressure regions.

psychrometer — An instrument used to determine relative humidity, dew point, and dry- and wet-bulb temperatures.

pyranometer — An instrument that measures total insolation (direct and diffuse) received on an area parallel to the ground.

radiation — Energy transport via electromagnetic waves traveling at the speed of light and capable of traveling through a vacuum.

radiation fog — Fog formed by the nighttime radiational cooling of a humid air layer so that its relative humidity approaches 100%.

radiation temperature inversion — Cooling of a surface layer by outgoing infrared radiation, resulting in the coldest air at the surface and air temperatures increasing with altitude.

radiosonde — A small balloon carrying a radio telemetry instrument package that measures vertical profiles of temperature, pressure, and relative humidity in the atmosphere.

rain	Precipitation consisting of liquid water droplets having diameters between 0.02 in. (0.5 mm) and 0.2 in (5.0 mm).
rainbow	An arch of colors formed by refraction and internal reflection of sunlight by raindrops in the direction opposite the sun. The raindrops act as prisms, refracting sunlight into its constituent colors.
rain gauge	A device, usually a cylindrical container, that measures precipitation (rain).
rain shadow	A region of reduced precipitation on the lee side (side away from the wind) of a mountain range.
rawinsonde	A radiosonde tracked from the ground by radar to measure variations of wind direction and speed with altitude.
reduction to sea level	An adjustment applied to surface air-pressure readings to eliminate the influence of station elevation.
refraction	The bending of a light ray as it passes from one medium to another (from air to water, for example). The bending is due to the different speeds of light in the different media.
relative humidity	Percentage of water vapor that air can hold at a specific temperature.
return period (T_R)	Expected time period between occurrences of a specific event—a 100-year return period of a specific daily snowfall, for example.
rime	An opaque, granular layer of ice formed by the rapid freezing of supercooled water.
roll cloud	A low, cylindrically shaped and elongated cloud occurring behind a gust front; associated with, but detached from, a cumulonimbus cloud.
Rossby waves	See long waves.
Santa Ana wind	A hot, dry Chinook-type wind that blows from the desert plateaus of Utah and Nevada toward coastal southern California.
saturation mixing ratio	The maximum concentration of water vapor in a given volume of air at a specific temperature.
saturation vapor pressure	The maximum possible vapor pressure in a sample of air at a specific temperature.
sensible heat transfer	Movement of heat from one place to another from advection, convection, or conduction.

severe weather (systems)	Storms that are potentially destructive and disruptive.
severe thunderstorms	Thunderstorms accompanied by locally damaging winds, frequent lightning, or large hail.
sheet lightning	Bright flashes across the sky caused by cloud-to-cloud lightning.
shelf cloud	A low, wedge-shaped and elongated cloud that occurs along a gust front; associated with and attached to a cumulonimbus cloud.
short waves	Relatively small ripples (troughs and ridges) superimposed on long waves. Short-wave troughs or upper-air disturbances are associated with upward air motion and can cause clouds and precipitation.
sleet	Same as ice pellets.
slope wind	Local wind caused by differential heating or cooling on a slope. Upslope winds during the day and downslope (drainage) winds during the night are common with light, large-scale winds and fair skies.
smog	See photochemical smog.
snow	Precipitation consisting of an aggregation of ice crystals in the form of hexagonal flakes.
snow pellets	Miniature "snowballs" that bounce on impact with the ground; formed by snowflakes falling through a warm layer of air, partially melting, and then refreezing.
solar altitude	The angle of the sun above the horizon.
solar constant	The flux of solar radiational energy falling on a surface at the top of the atmosphere, oriented perpendicular to the solar beam when the earth is at an average distance from the sun, about 2.00 langleys/min.
solstice	Time when the sun is at its maximum poleward location relative to the earth (latitudes 23.5° north and south); first days of summer and winter.
soundings	Continuous altitude measurements that provide profiles of variables such as temperature, humidity, and wind speed.
specific humidity	Ratio of atmospheric water vapor mass to the dry atmospheric mass holding it; approximately equal to absolute humidity (g/kg).
split flow pattern	Westerlies to the north that have a wave pattern different from those to the south.

spring	Season between spring equinox and summer solstice, about March 21–June 21; meteorologically, by convention, March through May.
squall line	A line of intense thunderstorms occurring parallel to and ahead of a cold front or trough line.
stability category	See Pasquill-Gifford stability category and curves.
stable atmosphere	An atmosphere in which the temperature decreases more gradually than does the dry adiabatic lapse rate (5.5°F/1000 ft [1°C/100 m]) or actually increases with height; air parcel that resists vertical motion in stable atmosphere; represented by the E category for slightly stable and the F category for very stable.
standard atmosphere	A theoretical average atmosphere of the variables pressure, temperature, and density.
standard deviation (σ_x)	A statistical indicator of variability of a variable (x) about its mean ($\overline{X}$). In a normal distribution, 68% of the x values are contained within $\overline{X} \pm \sigma_x$ and 95% are contained within $\overline{X} \pm 2\sigma_x$.
σ_w	Standard deviation of vertical wind speed.
σ_x	Along-wind standard deviation of a Gaussian puff.
σ_y	Crosswind standard deviation of a Gaussian plume or puff.
σ_z	Vertical standard deviation of a Gaussian plume or puff.
σ_θ	Standard deviation of horizontal wind direction (degrees).
σ_ϕ	Standard deviation of vertical wind direction (degrees).
stratocumulus clouds	Layered, low clouds consisting of large, irregular puffs or rolls.
stratosphere	The atmosphere's thermal subdivision situated between the troposphere and mesosphere; primary site of ozone formation. Within the stratosphere, air temperature in the lower part is constant with altitude and increases at higher altitudes.
stratus clouds	Low clouds that occur as a uniform gray layer stretching from horizon to horizon. They may produce drizzle, and where they touch the ground they are classified as fog.
subadiabatic	Same as stable atmosphere.
sublimation	Process by which water changes from a solid into a vapor without passing through the liquid phase.

subsistence temperature inversion	An elevated temperature inversion formed by air sinking gradually over a wide area and warmed by adiabatic compression; occurs on the eastern side of high-pressure systems.
subtropical high-pressure systems	Semipermanent warm-core high-pressure systems centered over subtropical latitudes of the Atlantic, Pacific, and Indian oceans.
subtropical jet stream	A zone of peak winds located between the tropical and midlatitude tropopauses.
summer	Season between summer solstice and autumn equinox, about June 21–September 21; meteorologically, by convention, June through August.
sun dogs	Same as parhelia.
sunspots	Relatively large, dark blotches that appear on the face of the sun.
superadiabatic	Same as unstable atmosphere.
supercells	Severe thunderstorm cells.
supersaturation	An air sample having a relative humidity greater than 100%.
surface layer	Lowest part of the atmosphere (50 to 200 m above ground level [AGL]) that has the sharpest variations of weather variables (temperature, humidity, winds) with height.
synoptic-scale weather	Weather phenomena operating at the continental or oceanic spatial scale; includes migrating high- and low-pressure systems, air masses, and fronts.
teleconnection	A linkage between weather trends or events occurring in widely separate regions of the globe.
temperature	A measure of the relative molecular activity of a substance.
temperature gradient	Temperature change with distance.
temperature inversion	See inversion.
thermal low	Example of a warm-core low; develops as a consequence of intense solar heating of the ground and adjacent air, thereby lowering its density.
thermograph	An instrument that continuously records temperature with time.
thermometer	An instrument used to measure temperature.

thunder	The sound that accompanies lightning. Thunder is produced by violent expansion of air caused by the intense heating from a lightning discharge.
thunderstorm	A mesoscale weather system produced by strong convective air currents that extend deep into the troposphere. Thunderstorms are accompanied by thunder and lightning and can feature locally heavy rainfall (or snowfall), gusty winds, and hail. Both updrafts and downdrafts accompany a mature thunderstorm, whereas downdrafts overtake the entire cell in the dissipating stage, causing rainfall to decrease and clouds to vaporize.
thunderstorm day	A day in which thunder is heard or a thunderstorm occurs.
tipping-bucket rain gauge	An instrument that accumulates rainfall, usually in increments of 0.01 in. (0.025 cm), by containers that alternately fill and empty (tip).
tornado	A small mass of air that rotates rapidly about an almost vertical axis extending from the base of a strong thunderstorm to the ground. The tornado is made visible by clouds, dust, and debris sucked into the system.
tornado alley	Region of maximum tornado frequency in North America extending from central Texas into Missouri.
trade winds	Prevailing global-scale surface winds in tropical latitudes. The trade winds blow from the northeast in the Northern Hemisphere and from the southeast in the Southern Hemisphere.
transpiration	Process by which water vapor escapes from plants through leaf pores.
Tropic of Cancer	Latitude 23°27′ N; a solstice position of the sun.
Tropic of Capricorn	Latitude 23°27′ S; a solstice position of the sun.
tropical depression	Initial stage in the development of a hurricane. Winds are less than 37 mph (60 km/h).
tropical storm	A tropical cyclone having wind speeds of 37 to 74 mph (60 to 120 km/h).
tropopause	Zone of transition between the troposphere below and the stratosphere above; top of the troposphere.
troposphere	Lowest thermal subdivision of the atmosphere in which air temperature normally drops with altitude; layer where most weather occurs.
turbidity	Dustiness of the atmosphere.

turbulence	Random, chaotic air motions that occur in scales from inches to thousands of feet (centimeters to kilometers).
twilight	Period of time between sunrise or sunset and total darkness.
typhoons	Hurricanes that form in the western Pacific.
ultraviolet radiation	Short-wave, high-energy solar radiation, much of which is absorbed by ozone in the stratosphere.
unstable atmosphere	An atmosphere in which the temperature decreases more with height than the dry adiabatic lapse rate (5.5°F/1000 ft [1°C/100 m]). An air parcel accelerates away from its original position after upward or downward displacement in an unstable atmosphere.
updraft	Upward-moving air, usually in a thunderstorm cell.
upslope fog	Ground-level cloud formed from the expansional cooling of humid air that is forced to ascend a mountain or plateau slope.
upslope wind	A flow of air that is directed up a slope; often can be a thermally driven, relatively deep local wind that forms over slopes during sunny days with light, large-scale winds (anabatic wind).
vapor pressure	The portion of the total air pressure accounted for by the water vapor in the atmosphere.
variables of state	Temperature, pressure, and air density.
veering	Clockwise shift in wind direction with time or altitude.
vertical pressure gradient	Decrease of air pressure with altitude.
virga	A shaft of rain (or snow) falling from a cloud that evaporates before reaching the ground.
virtual temperature	An adjustment made to the real air temperature to account for a reduction in air density because of the presence of water vapor.
visible light	Electromagnetic radiation having wavelengths in the range of about 0.40 (blue) to 0.70 (red) microns.
vorticity	Rotational tendency of the air.
warm-air advection	Flow of air from a relatively warm locality to a relatively cool locality.
warm front	A narrow zone of transition between relatively warm air that is advancing and relatively cool air that is retreating.

warm-core high (anticyclone)	Deep, high-pressure system associated with an extensive column of warm, subsiding dry air; high that intensifies with height.
warm-core low (cyclone)	A surface, synoptic-scale low associated with relatively warm columns of air; low that weakens with height.
water-equivalent precipitation	The total liquid content of precipitation, including rainfall and melted snow.
watershed	Same as drainage basin.
waterspout	A tornadolike disturbance that travels or forms over a large body of water, usually much weaker than a tornado but associated with a cumulonimbus cloud.
wavelength	Distance from successive crest to crest or from successive trough to trough of a wave.
weather	The state of the atmosphere in terms of variables such as temperature, cloudiness, precipitation, and sunshine.
weather warnings	Issued when hazardous weather is observed or is imminent.
weather watches	Issued when hazardous weather is considered possible based on current or anticipated weather conditions.
weighing-bucket rain gauge	A device that is calibrated so that the accumulated rainfall weight is recorded directly in inches or millimeters.
westerlies	Prevailing, global-scale, west-to-east winds in the troposphere of midlatitudes from about 30° to 60°.
wet-bulb (temperature)	The temperature to which air will cool when brought to saturation by evaporation of water; can be measured by wet-bulb thermometer; used to obtain dew point or relativity by comparing with temperature. The difference from dry-bulb temperature is called dew-point depression.
wind	Air movement caused by horizontal pressure differences.
wind-chill-equivalent temperature	A calculated air temperature that takes into account the cooling effects (heat loss) of wind on exposed skin.
wind direction	Direction *from* which the wind is blowing.
wind rose	A diagram that indicates wind-direction frequencies and sometimes wind-speed categories.
wind shear	A change, sometimes abrupt, in wind speed or direction with height or horizontal distance.

wind vane	An instrument used to measure wind direction by pointing into the wind.
windsock	A large, conical open bag designed to indicate wind direction and relative speed; usually used at small airports.
winter	Season between winter solstice and spring equinox, about December 21–March 21; meteorologically, by convention, December through February.
World Meteorological Organization (WMO)	Agency that coordinates the weather data collection and analysis of more than 145 member countries; based in Geneva, Switzerland.
World Weather Watch (WWW)	International weather-monitoring network coordinated by the World Meteorological Organization.
zonal flow pattern	Flow of the westerlies almost directly from west to east; westerlies that show little amplitude.

References

Berry, F. A., Jr., E. Bollay, and N. R. Beers, *Handbook of Meteorology* (McGraw-Hill Book Company, New York, 1945).

Bowen, B. M., W. A. Olsen, I. Chen, and D. M. Van Etten, "Measurement and Modeling of External Radiation During 1985 from LAMPF Emissions," Los Alamos National Laboratory report LA-11150-MS (November 1987).

Draxler, R. R., "Determination of Atmospheric Diffusion Parameters," *Atmospheric Environment* **10**, 99–105 (1976).

EPA (U.S. Environmental Protection Agency), *Guideline on Air Quality Models—Revisions*, Office of Air Quality Planning and Standards, Research Triangle Park, North Carolina (1981).

Fujita, T. T., "Estimate of Maximum Windspeeds of Tornadoes in Southernmost Rockies," Satellite and Mesometeorology Research Paper No. 105, Department of Geophysical Sciences, University of Chicago (June 1972).

List, R. J., *Smithsonian Meteorological Tables*, 6th revised edition (Smithsonian Institution, Washington, DC, 1951).

Moran, J. M., and M. D. Morgan, *Meteorology: The Atmosphere and the Science of Weather* (Burgess Publishing, Edina, Minnesota, 1986).

Morris, W. S., and K. W. Haggard, *New Mexico Climate Manual: Solar and Weather Data*, New Mexico Energy Research and Development Institute report NMERDI 2-72-4523 (November 1985).

NOAA (National Oceanic and Atmospheric Administration), *Climate of New Mexico*, Climatography of the United States No. 60, National Climatic Center, Asheville, North Carolina (March 1977).

NOAA (National Oceanic and Atmospheric Administration, *Climatic Atlas of the United States*, U.S. Department of Commerce, National Climatic Center, Asheville, North Carolina (reprinted 1979).

NRC (U.S. Nuclear Regulatory Commission), *U.S. NRC Regulatory Guide 1.23*, U.S. Nuclear Regulatory Agency (1972).

Olsen, W. A., and J. M. Dewart, "Meteorological Quality-Assurance Program of the Los Alamos National Laboratory's Environmental Surveillance Group, HSE-8," unpublished data (1986).

Steadman, R. G., "A Universal Scale of Apparent Temperature," *Journal of Climate and Applied Meteorology* 23(12), 1674–1687 (December 1984).

Turner, D. B., "Relationships Between 24-Hour Mean Air Quality Measurements and Meteorological Factors in Nashville, Tennessee," *Journal of Air Pollution Control Association* 11, 483–489 (1961).

Turner, D. B., *Workbook of Atmospheric Diffusion Estimates*, U.S. Environmental Protection Agency, Office of Air Programs Publication No. AP-26 (1969).

U.S. Naval Observatory, *Tables of Sunrise, Sunset, and Twilight* (U.S. Government Printing Office, Washington, DC, 1962).

*U.S. GOVERNMENT PRINTING OFFICE: 1990-0-773-034/20027

This report has been reproduced directly from
the best available copy.

Available to DOE and DOE contractors from
[illegible] Information
P.O. Box 62
Oak Ridge, TN 37831
[illegible]
[illegible]

Available to the public from
[illegible]
U.S. Department of Commerce
5285 Port Royal Rd.
Springfield, VA 22161
[illegible]

Price Code	NTIS Price Code	Price Code	NTIS Price Code	Price Code	NTIS Price Code	Price Code	NTIS Price Code
[illegible]	[illegible]	[illegible]	[illegible]	[illegible]	[illegible]	[illegible]	[illegible]
[illegible]	[illegible]	[illegible]	[illegible]	[illegible]	[illegible]	[illegible]	[illegible]
[illegible]	[illegible]	[illegible]	[illegible]	[illegible]	[illegible]	[illegible]	[illegible]
[illegible]	[illegible]	[illegible]	[illegible]	[illegible]	[illegible]	[illegible]	[illegible]
[illegible]	[illegible]	[illegible]	[illegible]	[illegible]	[illegible]	[illegible]	[illegible]
[illegible]	[illegible]	[illegible]	[illegible]	[illegible]	[illegible]	[illegible]	[illegible]
[illegible]	[illegible]	[illegible]	[illegible]	[illegible]	[illegible]	[illegible]	[illegible]

[illegible]